Structural enhancement of timber framing using hemp-lime

Gross, Christopher

Award date:
2013

Awarding institution:
University of Bath

Structural enhancement of timber framing using hemp-lime

Submitted by

Christopher David Gross

for the degree of Doctor of Philosophy
of the

University of Bath

September 2012

Abstract

The world is facing increasing pressures to reduce the amount of energy and resources that are being used. The UK government has targets to reduce carbon emissions and energy usage. Within the UK buildings are a significant contributor towards both energy and material usage.

One approach to reduce the energy and carbon emissions from construction is to use natural materials that require minimal processing and energy input such as straw, timber, unfired earth and hemp-lime. Hemp-lime is a composite solid wall insulating material made from hemp shiv and a lime based binder and water which can be cast between shutters or spray applied. Hemp-lime is typically used with a load bearing timber studwork frame. Current design practice assumes that hemp-lime is a non-structural material and only provides the insulation to the wall construction. However, as it encapsulates the studs it has to potential to enhance their load capacity by preventing buckling and resisting in-plane forces.

This study aimed to establish the contribution of the hemp-lime to the structural performance of composite hemp-lime and studwork frame walls under three loading conditions; vertical compression, in-plane racking and out-of-plane bending. Both theoretical analysis and experimental testing were undertaken in order to establish the contribution. Tradical HF hemp shiv and Tradical HB binder were used to mix hemp-lime with a density of 275kg/m^3. The wall constructions were initially theoretically analysed using existing approaches and both the stiffness and strength of the wall panels were calculated.

Experimental testing was undertaken on 24 full size wall panels. Fifteen were tested with compressive loads, five with in-plane racking loads and four with out-of-plane bending loads. Initially two walls were tested with a concentric compressive load applied to the top of the encapsulated timber studs. The studs were shown to be restrained by the hemp-lime preventing buckling and increasing the failure load by over 500%. Four walls were tested with eccentrically applied compressive loads to investigate bursting of the studs through the hemp-lime surface. On three walls the studs

burst through the hemp-lime showing that bursting is dependent upon the hemp-lime cover over the studs. In addition unrestrained studs were tested and shown to buckle at much lower loads than the hemp-lime lime encapsulated studs.

Under in-plane racking loads two walls were initially tested and found to have increased stiffness and strength over an unrestrained studwork frame. The leading stud joints were found to be a weak point. These joints were improved and two further walls were tested, one with a sheathing board attached to the studwork frame and one without. The strengthened joints were found to improve the stiffness and strength of the wall panels. The wall panel with sheathing was also found to have a higher stiffness than the un-sheathed walls.

Two walls were initially tested with applied out-of-plane loads. One wall was hemp-lime with rendered surfaces and the other included a studwork frame. The studwork frame was found to provide continued load capacity once the render and the hemp-lime had failed. Two further wall panels were tested with a sheathing board attached to the studwork frame and render on the other face of the hemp-lime. Again the studwork frames were found to provide post crack load capacity. The walls were also found to perform with differing stiffness according to the load direction.

Following experimental testing the theoretical results were compared with the experimental results. Generally good correlation is seen between the results. Prior to the experimental testing it was not possible to predict the bursting of the hemp-lime when the studs were loaded in compression, however following testing a technique was developed to allow this prediction to be made.

In conclusion this study has shown that hemp-lime does enhance the load capacity of studwork framing under both compressive and in-plane racking loads. Under out-of-plane bending loads the studwork frame allows continued load capacity after the hemp-lime and render have cracked. This study has shown that material savings can be made when using this type of construction as a sheathing board is not necessary as the hemp-lime can fulfil its structural function. This will contribute towards a more efficient construction system and reduced energy and resource use.

Acknowledgements

Firstly I would like to thank Pete Walker and Richard Harris for their advice and supervision throughout this project. I would like to thank Ian Pritchett and Mark Patten for their support, technical advice and supplying materials for the experimental study. For his technical knowledge of hemp-lime I would like to thank Mike Lawrence. For their help in the labs with experimental testing I would like to extend my thanks to Will Bazeley, Sophie Hayward, Graham Mott, Neil Price and Brian Purnell. For all of their help in constructing the large scale experimental specimens I would like to thank Max Burbidge, Dave Mayle, Piers Ashley-Carter and Richard Hartley. Finally I would like to thank my friends and, particularly Phil, Pete and Dan. I would like to extend particular thanks to my parents and Ellie for all of their support over the last three years.

Table of contents

List of figures

List of tables

List of symbols

Latin upper case letters:

A	Cross sectional area (mm^2).
D_1, D_2	Factors dependent upon α and β.
E	Elastic modulus (N/mm^2).
EI_{ef}	Effective EI (Nmm^2).
F_{burst}	Force required to burst hemp-lime (kN).
F_i	Force on sheathing connector (kN).
F_{xi}	Force in x direction on sheathing connector (kN).
F_{yi}	Force in y direction on sheathing connector (kN).
G	Shear modulus (N/mm^2).
H_1, H_2	Factors dependent upon α and β.
I	Second moment of area (mm^4).
J_i	Slip modulus of connector (N/mm).
K_c	Carbonation constant.
M	Bending moment (kNm).
M_{max}	Maximum bending moment (kNm).
M_p	Applied moment due to eccentric load (kNm).
P	Applied compressive load (kN).
$P_{bearing}$	Bearing failure load (kN).
P_{bu}	Critical buckling load on elastic foundation (kN).
P_{burst}	Axial load to cause F_{burst} (kN).
P_{con}	Concentric buckling load (kN).
P_{crit}	Critical load for column on elastic supports (kN).
$P_{crushing}$	Crushing failure load (kN).
P_{burst}	Axial load to cause F_{burst} (kN).
P_E	Euler buckling load (kN).
P_{ecc}	Eccentric buckling load with no restraint (kN).
R	Racking load (kN).
R_{up}	Racking load to cause separation of leading stud joints (kN).
S	Shear force (kN).
V	Shear force at connector plane (kN).

Latin lower case letters:

a_i	Factor for partial interaction theory (mm).
b	Width of area of burst hemp-lime (mm).
c	Depth of hemp-lime cover to stud (mm).
d	Depth of carbonation (mm).
e	Eccentricity of compressive load (mm).
h	Height of wall panel (mm).
h_i	Height of section for partial interaction theory (mm).
j	Hemp-lime bursting failure surface width (mm).
k	Modulus of elastic restraint (N/mm^2).
$k_{connector}$	Stiffness of leading stud connections (N/mm).
k_{nail}	Equivalent elastic restraint modulus for group of nailed connections (N/mm).
k_{screw}	Equivalent elastic restraint modulus for group of screwed connections (N/mm).
l	Length of member (mm).
m	Number of half sine waves in buckled shape on elastic restraint.
n	Number of spans of beam column.
q	Factor dependent upon cross section shape for shear deflection.
r	Factor dependent upon number of spans n.
s_i	Spacing of connectors (mm).
t	Time in days.
u	Factor dependent upon k (N/mm).
w	Uniformly distributed load (kN/m^2).
x	Distance along member (mm).
y	Deflection in y direction (mm).
y_{max}	Maximum deflection (mm).

Greek lower case letters:

α, β	Factor dependent upon k.
γ_i	Factor for partial interaction theory.
δ	Deflection (mm).
δ_b	Bending deflection (mm).

δ_v	Shear deflection (mm).
θ	Slope of stress displacement plot for hemp-lime (N/mm).
λ	Factor dependent upon k.
μ	Elastic support stiffness (N/mm).
μ_{rigid}	Stiffness at which elastic support appears rigid (N/mm).
ν	Poisson's ratio.
σ	Stress (N/mm^2).
σ_s	Hemp-lime shear stress (N/mm^2).
ϕ	Slope of stress displacement plot for sheathing connections (N/mm).
ω	Modulus of elastic restraint (N/mm^2).
ω_{minor}	Modulus of elastic restraint for buckling about the minor axis (N/mm^2).
ω_{major}	Modulus of elastic restraint for buckling about the major axis (N/mm^2).

1 Introduction

1.1 Background

The Kyoto Protocol has shown that there is a global consensus that energy consumption and carbon emissions need to be reduced (UNFCCC, 2012). Within the UK the domestic housing sector is accountable for 27% of the total carbon emissions, with 53% of this coming from space heating alone (DCLG, 2007). Across the world 5% of CO_2 emissions and an estimated 2% of primary energy consumption are from cement production alone (Hendriks *et al.*, 1998). In 2010 DEFRA (2012) estimated that 77.4 million tonnes of construction waste was produced in England. In 2007 it was estimated that 13% of this waste is new material that is never used on site (DEFRA, 2007).

Over recent years the construction industry and the general public have become increasingly aware of this environmental pollution and the interest in low and zero carbon design and methods of construction has grown (Bevan *et al.*, 2008). The DBERR (2008) published a strategy for sustainable construction with its key themes being to design buildings that are sustainable, resource efficient, fit for purpose and adaptive. Minimising the energy used in construction and running of buildings is key to meeting the UK Governments targets of reducing greenhouse gas emissions to 80% of 1990 levels by 2050 (DFT, 2009).

Hemp-lime composites are one of the many natural, sustainable low energy materials that satisfy the key themes of the DBERR (2008) report. Hemp-lime composites have been used in construction for around 20 years. The use of this lightweight composite, comprised of the woody core of the hemp plant (shiv) and lime binder with water to mix, originated in France (Bevan *et al.*, 2008) and its use has become increasingly widespread across continental Europe and in recent years within the United Kingdom (Lawrence, 2009).

Hemp-lime was initially used in the restoration of historic timber buildings as a replacement for wattle and daub that had deteriorated. It was found that it provided a long lasting natural infill material that was stable, did not shrink and allowed the buildings to breathe which is vital if their condition is to be maintained (Bevan *et al.*,

2008). Hemp-lime is now used in new construction as a natural, sustainable and carbon neutral (Hemp Technology, 2010) infill wall material around timber framed construction. It is typically used in domestic scale construction and a demonstration house, The Renewable House, has been constructed at the Building Research Establishment (BRE) to showcase the material (Figure 1.1).

Figure 1.1 The Renewable House at BRE

It has been shown to provide good insulating properties that keep the internal space at a constant temperature regardless of the external temperatures with very little heat input (Pritchett, 2009). The use of hemp-lime within the UK construction industry is still in its relative infancy and there are many issues with this material that are not yet fully understood. Research is on-going both at a materials scale and larger whole building scale using test structures such as the Hempod (Figure 1.2) at the University of Bath.

Figure 1.2 Hempod experimental building at the University of Bath

1.2 The need for research

In current UK design practice hemp-lime is used as a solid wall insulation material in conjunction with a structural studwork frame which is normally timber (Figure 1.3). Within this type of construction the hemp-lime is currently considered to have no contribution to the structural capacity of the frame. Therefore the frames are designed to withstand the applied vertical and lateral wind loads independently from the hemp-lime.

However hemp-lime does have modest structural strength. It has been shown to have compressive strengths of between 0.05 N/mm^2 and 2.44 N/mm^2 depending upon density, binder and mix ratio (Hustache and Arnaud, 2008) and increases in compressive strength as the density increases (Elfordy *et al.*, 2008). Therefore as the hemp-lime has been proven to have some structural strength of its own, by encapsulating the studs in hemp-lime it may be possible to enhance the structural capacity of the frame around which it is cast.

Figure 1.3 Timber studwork with cast hemp-lime

If the hemp-lime could be used to enhance the structural capacity of the frame, then it may be possible to construct larger structures using this technique, or reduce the quantity of framing used and hence save materials and make the system more efficient. Further research is needed to establish if hemp-lime can contribute structurally, if it can to what extent, and how the enhancement could be predicted and calculated during the design phase of a building.

1.3 Aims and objectives

The main aim of this study is to investigate the structural contribution of hemp-lime to the load bearing capacity of the studwork framing.

The enhancement hemp-lime provides will be studied in three aspects;

- compressive loading of studs;
- in-plane racking loading of studwork framing;
- out-of-plane bending.

When a stud within a typical framework is loaded in compression it will generally fail by minor axis buckling if there is no intermediate support. Intermediate support is conventionally provided by horizontal noggins or sheathing boards. The aim of this research is to establish if, when hemp-lime is cast around a stud it provides sufficient confinement to prevent minor axis buckling failure in the same way sheathing boards or noggins do. The research aims to establish how failure will occur if minor axis buckling is prevented and whether major axis buckling becomes critical.

As with compressive loading, when an in-plane racking load is applied typically noggins, sheathing boards or diagonal bracing help to resist it. Again the aim is to establish if hemp-lime provides resistance to in-plane racking loads when it is cast around a studwork frame.

In a conventional studwork framed building out-of-plane (bending) loads are resisted by the cladding which transfers the load into the frame and then in turn into the foundations. When hemp-lime is used only as the insulation, this will also be the case. However if the hemp-lime is to be used structurally then it will have to withstand the out of plane loads and transfer them into the studwork framing. This study aims to investigate the flexural strength of hemp-lime, which is currently not well known, and how the hemp-lime and studwork framing behave compositely when subjected to out-of-plane bending loads.

The structural contribution of hemp-lime will be investigated through theoretical analysis and laboratory based experiments. The theoretical analysis will aim to predict the performance of the composite wall structures under the three load cases by using existing structural theories. The laboratory based experimental work aims to establish exactly how the composite walls behave under the three load cases and check the accuracy of the theoretical analysis.

1.4 Layout of thesis

This thesis starts by reviewing the structural properties of hemp-lime that have currently been established and highlighting where there is a lack of data available. The use of hemp-lime with structural studwork framing will also be reviewed. The testing and performance of timber studwork framing and the testing methods set out in BS 5268 (1996) and BS EN 594 (1996) for in-plane racking will be reviewed.

The properties of the materials used throughout this study are then presented along with the performance of the connections used within studwork framing. Following this the theoretical analysis and predicted performance for each of the loading cases is presented.

The specimens used for the laboratory based testing are then detailed. The experimental testing has been split into the three load cases with separate chapters presenting the methodology, results, analysis and discussion for the test specimens. The results are then compared to the theoretical predictions.

Finally conclusions from both the experimental testing and theoretical analysis are presented along with recommendations for further research.

2 Literature review

2.1 Introduction

This section of the thesis presents a comprehensive review of literature that has provided a background for this study. As the use of hemp-lime in construction is still in its infancy there has only been a limited amount of published research into its properties. The thermal and environmental performance of hemp-lime has been the subject of numerous studies at a material properties scale (Collet *et al.*, 2008; Elfordy *et al.*, 2008; Evrard, 2006; Evrard and De Herde, 2005, 2010; Evrard *et al.*, 2006). In addition de Bruijn (2012) has studied the moisture transfer properties of large scale wall panels and Shea *et al.* (2012) and BRE (2002) have studied the thermal performance of experimental buildings. The studies relating to mechanical properties will be reviewed in this chapter. There is no published literature on the use of hemp-lime structurally, however some work has been undertaken as undergraduate and postgraduate research but has not been published in peer reviewed publications. As a result it is difficult to obtain copies of some research papers or assess their reliability. For this reason the literature review in this chapter is concise, but it does cover the most significant structural testing undertaken to date.

In this chapter the currently known material properties of hemp-lime will be reviewed. These properties can vary greatly as the mix proportions, binder composition and density vary. The compressive, flexural and shear properties will be reviewed as these are the most significant for this study. There has been generally more research into the thermal, acoustic and moisture properties of hemp-lime, however these will not be reviewed in detail here as they are outside the scope of this research.

The available undergraduate and postgraduate research studies into the structural use of hemp-lime with studwork walling will be reviewed. The research undertaken into the structural capacity of ModCell straw bale panels will be briefly reviewed as these combine timber with a low stiffness material in a similar way to timber framing and hemp-lime. Additionally structural performance of conventional studwork walling will be reviewed, with particular interest in the buckling of studs and the sheathing of frames to stiffen them for in-plane racking and buckling. The procedure for design and testing

of studwork walling to resist in-plane racking forces as set out in BS EN 1995 (2004), BS 5268 (1996) and BS EN 594 (1996) will also be reviewed.

2.2 Mechanical properties of hemp-lime

There are a limited number of studies on the mechanical properties of hemp-lime and therefore these will be reviewed project by project. There are many parts to the stalk of the hemp plant (Figure 2.1) and generally only the shiv is used for hemp-lime, however De Bruijn et al. (2009) also used the fibres. Compressive strength has been the focus of the majority of the studies on the mechanical properties of hemp-lime composites. Only Elfordy et al. (2008) and Murphy et al. (2010) have included flexural strength. In addition to the studies reviewed in the following section Eires and Jalali (2005) have investigated the used of hemp shiv and fibre and Nguyen et al. (2009) investigated the effects of compaction during specimen casting on the mechanical performance.

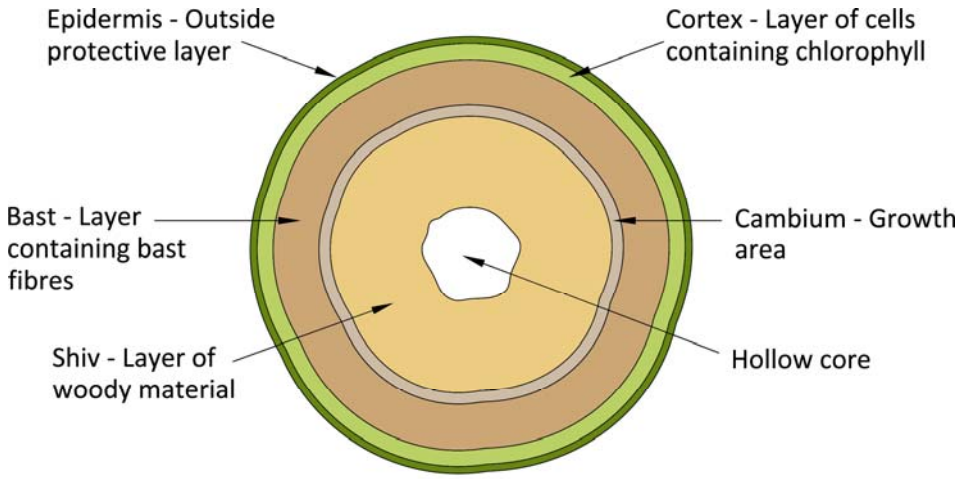

Figure 2.1 Cross section through hemp plant stem

2.2.1 Arnaud (2000, 2012)

Arnaud (2000) studied the mechanical properties of hemp-lime under compressive loading. During the study hemp shiv from La Chanvriere de l'Aube was used and two different binders, Strasservil Tradical 70 and Strasservil Tradical 80, were compared. Four different mixes with varying proportions of hemp shiv, binder and water were produced with each binder. In this paper Arnaud (2000) compares two mixes, A4 (19.6% shiv, 34% Tradical 70 binder, 46.4% water by mass) and B4 (16.8% shiv, 29%

Tradical 80 binder, 54.2% water by mass) as well as specimens consisting of only hemp- shiv.

Compressive testing was carried out on the hemp shiv only specimens. The specimens were 160mm diameter by 320mm high cylinders. The method of manufacture is not detailed. The testing found that there was an elasto-plastic adhesive behaviour of the specimens provided by the contact between shiv particles. The specimens were loaded in compression at a rate of 5mm/min. The maximum compressive stress recorded was 0.25N/mm^2 (5000N) at a displacement of 128mm when the specimens lost their integrity. At the time of failure the elastic modulus was 0.6N/mm^2 although the range over which the elastic modulus was calculated is not clear. Additionally the strain of the specimens at maximum stress is not given; therefore it is difficult to compare these results with those from other studies.

Arnaud (2000) also tested 160mm diameter by 320mm high cylindrical A4 and B4 hemp-lime specimens in compression. The method of manufacture and drying conditions for the specimens is not given. However Arnaud (2000) notes that the specimens were tested at an age of seven months which indicates that they were likely to be at a stable moisture content. With a strain of $\varepsilon \leq 0.05$ the specimens displayed linear although not elastic behaviour. Arnaud (2000) notes that this stage represents the response of both the hemp shiv and binder matrix and following this stage the binder matrix ruptures and only the hemp shiv is loaded. The results obtained are shown in Figure 2.2.

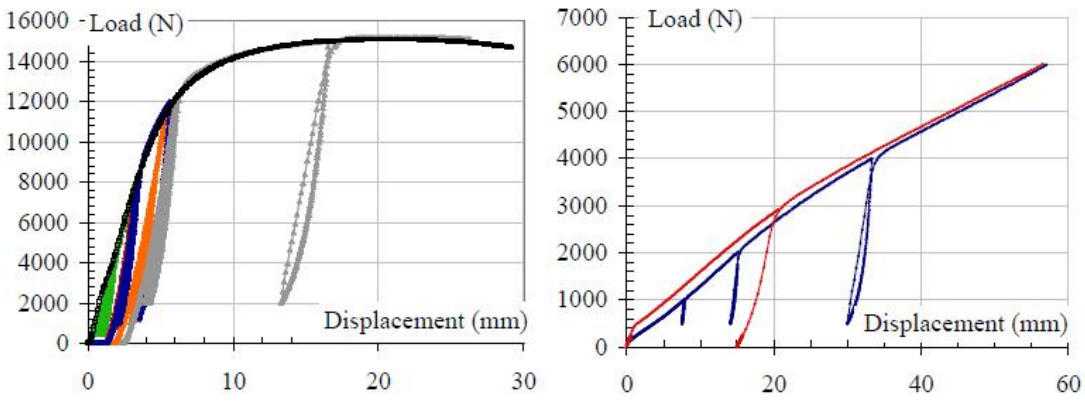

Figure 2.2 Load against displacement for A4 (left) and B4 (right) hemp-lime specimens tested at 7 months (Arnaud, 2000)

At an age of seven months Arnaud (2000) reports that A4 had a maximum compressive strength of 0.75N/mm^2 and elastic modulus of 37N/mm^2 . At the same age B4 had a compressive strength of 0.15N/mm^2 and elastic modulus of 2.4N/mm^2. From Figure 2.2 it can be seen that the displacement at maximum stress is much higher for B4 and this is confirmed by the fact that the elastic modulus is 15 times smaller. Arnaud (2000) does not give reasons for the large difference in strength and elastic modulus between the two specimen types, there is 5% more binder in A4 which may have contributed to the difference although it is unlikely that this is the sole reason. However the densities of the specimens are also not given and therefore a difference in these could also have influenced the results.

Arnaud and Gourlay (2012) continued to investigate the performance of different binders, but in this study also varied the hemp shiv and curing conditions to establish their effect on the mechanical performance of hemp-lime. Arnaud and Gourlay (2012) used four binders; A (NHL 3.5), B (NHL 3.5Z), C (NHL 2) and D (formulated, 75% air lime, 15% hydraulic lime, 10% pozzolanic lime). Three types of shiv were also tested and their properties are shown in Table 2.1. Cylindrical specimens, 160mm diameter by 320mm high, were used and filled in 50mm layers that were compacted with a force of 0.05N/mm^2.

Table 2.1 Shiv properties (Arnaud and Gourlay, 2012)

Hemp shiv	**No.1**	**No.2**	**No.3**
Bulk density (kg/m^3)	112	114	119
Average length (mm)	8.9	7.6	3.1
Average width (mm)	2.0	1.8	1.0
Average thickness (mm)	0.5	0.5	0.5

Initially Arnaud and Gourlay (2012) compared the different binders and curing conditions by using one type of shiv (No.2). The curing conditions were all 20^{o}C and four different relative humidities (RH) were used, 30%, 50%, 75% and 98%. The cylinders from each type of binder were kept in their moulds prior to testing and were tested at an age of 28 days. They cylinders ranged in dry density from 460kg/m^3 to 480kg/m^3. The results are summarised in Table 2.2.

Table 2.2 Compressive strength test results (Arnaud and Gourlay, 2012)

	Compressive strength, σ_c (N/mm^2)			
RH	50%	30%	75%	98%
A	0.18	<0.11		
B	0.31	0.17	0.19	0.17
C	0.10 to 0.22			
D	0.31	0.31	0.18 to 0.24	

Arnaud and Gourlay (2012) found that binder C gave the lowest compressive strength in all conditions and binder D gave the highest compressive strength and elastic modulus in all conditions. It was also noted that the cylinders cured at 50% RH showed the highest compressive strengths and elastic modulus. The cylinders cured at high RH (75% and 98%) showed the lowest strength and this has been attributed to the high moisture content preventing the hemp-lime from drying sufficiently to allow CO_2 to penetrate the specimens as their pores remain saturated. Therefore the air lime in the binder does not set (Arnaud and Gourlay, 2012).

As the best performance was achieved with binder D and 50% RH curing conditions Arnaud and Gourlay (2012) investigated the effects of curing time on strength and elastic modulus. Cylindrical specimens were used again and were tested at 21 days, 3 months, 6 months, 15 months and 24 months. Arnaud and Gourlay (2012) found that at young ages the compressive failure of the specimens was ductile and there was a post peak plateau as the binder had not developed its strength. Tests of the older specimens showed that with age the strength of the binder becomes more dominant. At 21 days the average compressive strength was 0.35N/mm^2 and at 24 months it was 0.85N/mm^2. Similarly Arnaud and Gourlay (2012) found that the strains at peak stress changed from 11% at 21 days to 4% at 24 months.

Finally Arnaud and Gourlay (2012) investigated the effects of shiv type on the compressive strength. The longer particle lengths in shiv type No.1 resulted in a lower density and lower compressive strength than when shiv type No.2 was used. Shiv type No.3 was finer and as a result Arnaud and Gourlay (2012) found that the hemp-lime specimens made with this shiv were less porous and therefore the strength developed

more slowly. However at 4 months old the specimens had a higher strength as there was more interaction between the particles.

From this work by Arnaud and Gourlay (2012) several important considerations can be concluded that will apply to this study. Firstly the type of binder affects the performance of the hemp-lime and therefore this should be kept constant if other properties are to be studied and compared. The same can also be said of the hemp shiv and therefore this should also be kept constant. Secondly the curing conditions can affect the mechanical properties, so again these should be kept constant in order that comparisons can be made. Finally the age of the hemp-lime greatly affects its performance, and therefore this should be considered when planning experimental work. The specimens that Arnaud and Gourlay (2012) tested were generally of a higher density than will be used during this study and therefore a direct comparison between the two investigations will be difficult.

2.2.2 Evrard (2002)

Evrard (2002) investigated both the environmental (thermal, moisture, acoustic) and mechanical properties of hemp-lime composites. Only the work on mechanical properties will be reviewed here. Three different hemp-lime mixes were prepared and cast into cylindrical moulds 160mm in diameter and 320mm high. The proportions of the mixes are shown in Table 2.3. Evrard (2002) assigns the different mixes to particular uses within a building, roof (low density), wall (medium density) and floor (high density).

Table 2.3 Mix proportions by weight (Evrard, 2002)

	Hemp shiv (%)	**Binder (%)**	**Water (%)**
Low density	28	24	48
Medium density	19	31	50
High density	14	30	55

The hemp shiv used was Chanvribat and the binder used was Stasservil Tradical 70 which Evrard (2002) reports to contain 75% aerated lime, 15% hydraulic binders, 10%

pozzolanic binders and <5% additives. The specimens were allowed to dry and cure in a constant environment at 50% RH and 20°C for six months prior to testing. Evrard (2002) notes that the specimens were allowed to dry from two edges rather than over their whole surface area.

The specimens were tested in compression and the results in Table 2.4 were obtained. The rate of loading is not given. Evrard (2002) found that increasing the binder and density of the specimens increased the compressive strength and increased the stiffness. During compressive testing the matrix of lime surrounding the particles breaks but the hemp-lime retains some cohesion which allows for the specimens to continue carrying load even at high strains. Drying lasts longer than the six months the specimens were left prior to testing and the conditions in which the hemp-lime was dried affected its structural performance.

Table 2.4 Compression test results (Evrard, 2002)

	Density (kg/m^3)		**Moisture Content (%)**	**Elastic modulus (N/mm^2)**	**σ_c (N/mm^2)**	**Strain (%)**
	Bulk	**Dry**				
Low	285	265	6.9	3	0.2	14.0
Medium	445	420	6.0	24	0.4	6.0
High	530	500	5.7	26	0.5	5.5

Evrard (2002) notes that these results indicate that hemp-lime cannot be considered as a load bearing material, but that it may one day play a part in load bearing structures. The medium density mixture used has similar proportions to the hemp-lime mix that has been selected for use during this investigation (see Chapter 3); however the density will be similar to that used for the low density mix. Therefore a direct comparison will not be possible.

2.2.3 Elfordy, Goudet, Lucas, Scudeller, Tancret (2008)

Elfordy et al. (2008) studied the mechanical properties of sprayed hemp-lime. The rationale behind spraying the hemp-lime was to increase its density as in the view of the study the low density of cast hemp-lime is a significant problem. Spraying the hemp-lime allowed for higher densities without additional binder or excessive compaction by

hand. Hemp shiv can absorb up to five times its weight in water and as a result during conventional mixing more water needs to be added than is necessary for hydration of the lime in the binder. With the spraying process Elfordy et al. (2008) was able to add the water immediately before the hemp and binder mixture was projected and therefore minimise absorption by the hemp shiv. As a result it was possible to use only the amount of water required for the lime and no more.

The proportions of hemp shiv, binder and water were kept constant throughout, using 34% binder, 16% hemp and 50% water by weight. The binder used was Tradical 70 (70% hydrate lime, 15% pozzolanic material, 15% hydraulic lime by weight) and the hemp shiv used was produced by Chanvribat. In comparison this mix ratio is very similar to that used for cast hemp walls (32% binder, 19.4% hemp shiv, 48.6% water by mass (Lime Technology 2010a)).

Elfordy et al. (2008) filled moulds with a cross section of 300mm by 600mm and a height of 200mm and controlled the densities by varying the projection distance. The specimens were left to cure for one month. The curing conditions are not reported. After one month the specimens were de-moulded and cut into 50mm cubes for compression testing. The specimens were loaded in compression at a rate of 5mm/min. The direction the specimens were loaded is not recorded, this is potentially important as the properties of hemp-lime can vary depending upon the orientation of the specimen. The maximum compressive strength recorded was 0.850N/mm^2 with a density of 650kg/m^3 and the minimum was 0.180N/mm^2 with a density of 291kg/m^3 (Figure 2.3).

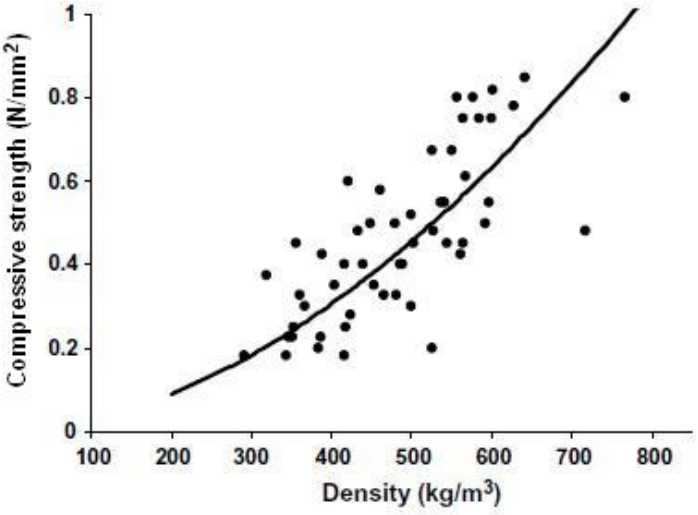

Figure 2.3 Density against compressive strength (Elfordy *et al.*, 2008)

The strains at which these compressive strengths were recorded are not given. When testing hemp-lime the strain is important as the material is highly compressible and the maximum strength may not occur until strains of 6 – 10%. Figure 2.4 shows a general plot of compressive stress against strain from the testing by Elfordy et al. (2008). This figure highlights the problems of using prismatic compression specimens where the stress continues to increase with strain. From these types of results it is difficult to determine a maximum stress and therefore it is not possible to know where the maximum stresses were recorded during this study. It is preferable to use 1:2 (diameter : height) ratio cylindrical specimens as they generally provide a clear maximum load peak during compressive testing.

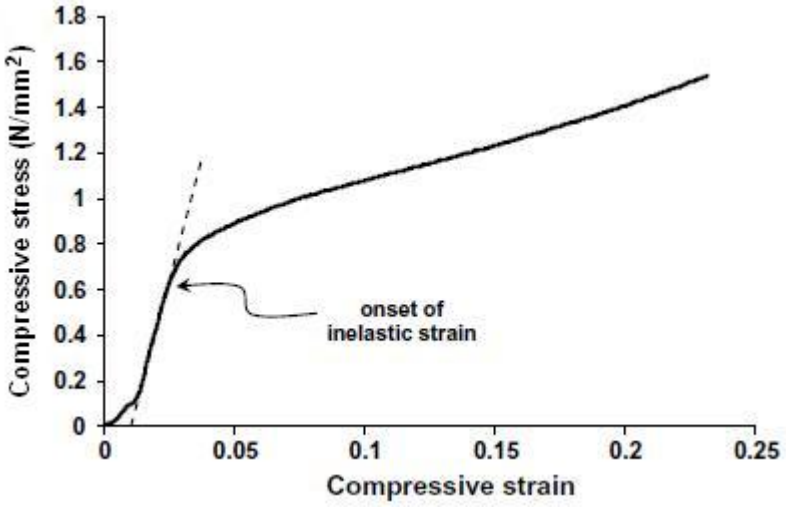

Figure 2.4 Plot of compressive strain against compressive stress (Elfordy *et al.*, 2008)

The authors conclude that as the density of the hemp-lime is increased the compressive strength increases. However from Figure 2.3 it can be seen that there is up to 300% variation in compressive strengths for given densities. While generally the highest density specimens had higher compressive strengths and elastic modulus than the lower density ones, there is a large variation. Unfortunately the authors do not give any statistical analysis of the results. The authors also conclude that the use of the spraying process, and hence less water, allowed the specimens to be fully dry in less than one month. The reduction in drying time reported when using the projection process is significant. When mixing and casting hemp-lime drying times vary from 18 weeks (de Bruijn *et al.*, 2009) to over one year (Arnaud, 2000), however when projecting the hemp-lime the drying time has been reduced to one month (Elfordy *et al.*, 2008). As

previously noted the curing conditions are not given for this study. Additionally the moisture content of the specimens at testing is not given and therefore it is not possible to compare or verify any of the claims about curing and drying times.

Elfordy et al. (2008) also comment that when hemp-lime is used within the building industry a compromise will have to be struck between using a low density highly insulating mix and a high density higher strength mix depending upon intended use. This is very relevant and will always be a key consideration when using hemp-lime, particularly in structural applications.

Elfordy et al. (2008) also investigated the flexural strength of hemp-lime. The bending strength of hemp-lime composites has been subject to very limited study; Hustache and Arnaud (2008) only note five studies into bending performance. Bevan et al. (2008) comment that there is no direct data published on the bending resistance of hemp-lime. They do however suggest possible values for flexural strength of 0.3 to 0.4N/mm^2 which are based on the properties of lime renders. Bevan et al. (2008) also suggest that the flexural strength of hemp-lime walls could be enhanced when rendered, however there is a need for further research in this area.

Elfordy et al. (2008) made and cured specimens using the same process as for the compression tests and the dimensions were 100mm x 150mm x 300mm. As with their work on compressive strength, the short drying and curing time must be questioned as the moisture content of the specimens is not stated at the time of testing. Additionally any strength from the lime content of the binder is unlikely to have developed after only a month as full carbonation of lime based binder and mortars can take several months or even years (Holmes and Wingate, 1997).

Once cured the specimens were tested in three point bending with the load applied normal to the shiv alignment over a span of 250mm. The specimens tested ranged in density from 430kg/m^3 to 607kg/m^3 and their flexural strengths varied from 0.832N/mm^2 to 1.209N/mm^2 with the strengths generally increasing with density (Figure 2.5).

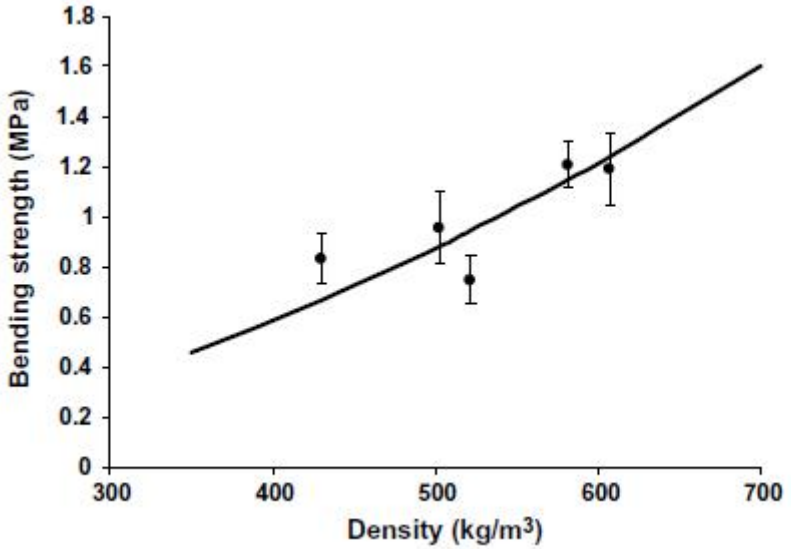

Figure 2.5 Bending strength and density of hemp-lime (Elfordy *et al.*, 2008)

Finally Elfordy et al. (2008) only studied the flexural strength of hemp-lime by bending it about one axis. If hemp-lime were to be used as a walling material it is likely to experience bending in two directions (depending on support conditions). They applied the load normal to the direction of the hemp shivs, which one would assume to be the strongest direction as there will be fewer planes of weakness due to overlapping of the shivs. Therefore the bending strength of hemp-lime may be weaker than is suggested in this work when bending in both directions is considered.

Murphy et al. (2010) also studied the flexural strength of hemp-lime and reported similar results to Elfordy et al. (2008). Three hemp-lime mixes of different ratios of hemp shiv to binder were produced and flexural strength was shown to increase with increasing binder content between 25% and 50%, however there was little strength gained when it was increased to 90% (Murphy *et al.*, 2010). The amount of hemp shiv was found to alter the failure from brittle (10% shiv) to ductile (50% and 75% shiv) and that the type of binder used affected the stiffness (Murphy *et al.*, 2010).

2.2.4 De Bruijn, Jeppsson, Sandin and Nilsson (2009)

De Bruijn et al. (2009) studied the mechanical properties of hemp-lime made with both shiv and fibre. This work used both shiv and fibres as there was no facility in Sweden, where the work was undertaken, to separate them and the main aim was to establish if hemp-lime with both shiv and fibre could be used in load bearing construction.

The hemp used consisted of 35% fibre, 62% shiv and 4% dust with a moisture content prior to mixing of 13.3%. Different binders were used to make five mixes with a hemp to binder ratio of 3:1 by volume and with 250ml of water for every 100g of hemp. The binders were made up of differing quantities of hydrated lime, hydraulic lime (NHL 5) and cement (CEM II/A-L). De Bruijn et al. (2009) filled 150mm diameter, 300mm long cylindrical moulds in 50mm layers, tamped the layers and once full placed the moulds on a vibration table at 50Hz for 1 minute.

Following casting an elaborate process was used in an attempt to speed up the drying and carbonation process. The specimens were removed from their moulds after two days and kept in an indoor climate for 12 weeks (average temperature of 19.7^{o}C, relative humidity (RH) 75% - 95%), following this they were stored in a carbonation room with 4.5% CO_2 and RH of 50% for 40 days, then prior to testing they were stored at atmospheric CO_2 levels and a RH of 50%. While this process may have sped up the drying and carbonation it is unlikely to have had any effect on the material properties as elevated temperatures were not used and therefore the specimens will not have dried too quickly.

Prior to compressive testing the densities of the specimens ranged from 587kg/m^3 to 733kg/m^3. The density of these specimens is high when compared to those used in other studies and are almost three times higher than the hemp-lime being used during this investigation (dry density 275kg/m^3). It should be noted however that the moisture content at the recorded densities is not given and the moisture content of the specimens at the time of testing is not given. This information would have been useful in assessing how much the specimens had dried during curing. The moisture content of the specimens at testing will have an effect on their structural performance and carbonation, and therefore could change the outcome of the work, particularly if different specimens are at different moisture contents.

The loading rate used during compressive testing was not given. The average compressive strengths recorded during testing ranged from 0.15N/mm^2 to 0.83N/mm^2, with the lowest having binder ratios of 2:3:0 hydrated lime, hydraulic lime, cement and the highest having a ratio of 2:3:5. The strains at which these stresses occurred are not

given. The strain at which the maximum stress occurs is important with hemp-lime, particularly when investigating structural performance, as the maximum stress often occurs at very high strains of 6% to 10%. Figure 2.6 shows the stress strain plot for one particular specimen tested by De Bruijn et al. (2009) and at maximum stress the strain is roughly 6%. The elastic modulus was calculated using the tangent to the stress .v. strain curve between 15% and 50% (Figure 2.6) of the maximum compressive strength. The elastic modulus ranged from 12.65N/mm^2 to 49.40N/mm^2 with the lowest having the binder ratio of 2:3:0 (as above) and the highest having 0:0:1 (totally cement).

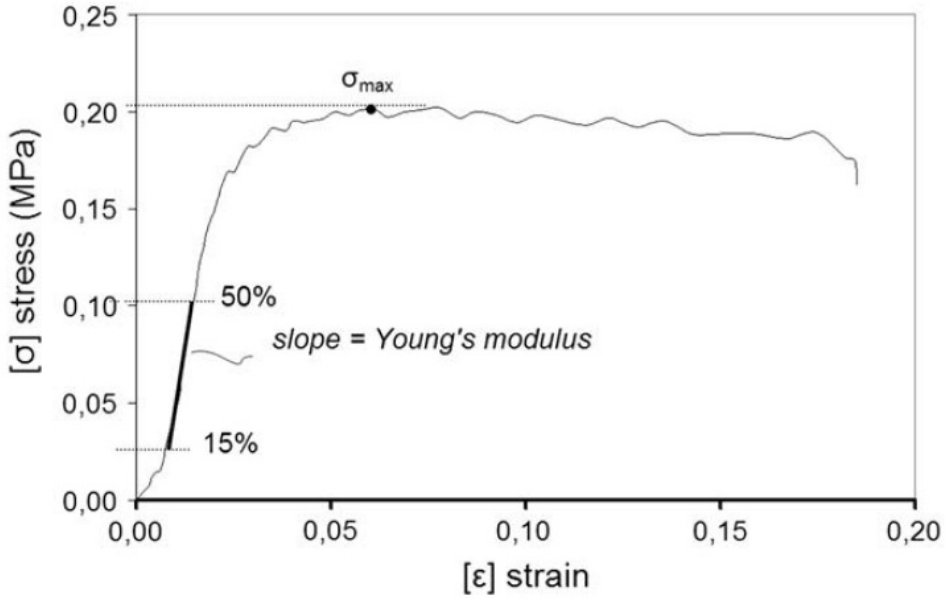

Figure 2.6 Typical stress strain curve for hemp-lime specimen (de Bruijn *et al.*, 2009)

De Bruijn et al. (2009) noted that the cement had an impact on both the compressive strength and elastic modulus by increasing them when used in conjunction with hydrated and hydraulic lime, however a purely cement binder did not produce the highest compressive strength. This work concluded that use of hemp shiv and fibre does not increase the strength of the composite, but it also does not cause any adverse effects. Finally De Bruijn et al. (2009) concluded that currently hemp-lime is not a load bearing material as it is not strong or stiff enough, and suggested that in order to be load bearing a compressive strength of 3.0 to 5.0 N/mm^2 would be required. This figure is quite high, particularly when the compressive strength of straw bale is around 0.05N/mm^2 (King, 2006) and is considered to be a load bearing material.

2.2.5 Hirst, Paine, Walker, Yates (2012)

Hirst et al. (2012) studied the mechanical and carbonation properties of low density hemp-lime composites. Initially three different formulated binders were compared, Tradical HB-B (THB-H), Tradical HB-A (THB-A) and St Astier Batichanvre (BC). The Tradical HB-A binder is a derivative of the HB-B binder that has a faster initial set time and has been specially developed for colder climates. Hirst et al. (2012) noted that the constituent ratios are not publically known for any of the binders. The hemp shiv used was Tradical HF and was consistent throughout the study. Three different densities of hemp-lime were studied, 330kg/m^3, 275kg/m^3 and 220kg/m^3.

Initially the strength of the binders were measured on their own. Specimens were made in accordance with BS EN 196-1:2005 with two parts binder to one part standard graded sand. The binders were tested at 28 days and Hirst et al. (2012) reported that BC had the highest average compressive strength at 30.1N/mm^2 with 13.9N/mm^2 for THB-B and 9.3N/mm^2 for THB-A. The additional strength of the BC was believed to be due to a higher proportion of hydraulic material in the binder.

Hirst et al (2012) decided to use the THB-A binder for the majority of the mechanical properties testing on hemp-lime specimens as it is the most commonly used binder within the UK. Three different densities were studied, 220, 275 and 330 kg/m^3 which correspond to three different mix ratios (by weight) of 1:1, 1:1.5 and 1:2 hemp shiv to binder. The hemp-lime was mixed as it would be on a construction site in order to achieve a representative material. First the binder and water was mixed in a pan mixer in order to create a slurry. Then the hemp shiv was added and mixed until all the shiv particles were evenly coated. The specimens were cast in 150mm diameter by 300mm long cylindrical moulds and placed in a conditioning room with a temperature of 20^oC and RH of 60%. They were de-moulded at 7 days and continued to be stored in the same conditions until testing. This mixing procedure and storage conditions are similar to those that will be used during this study and therefore the results can be easily compared.

The mixing process, specimen casting and storage described by Hirst et al. (2012) is a good precedent for the testing being carried out during this study. The mixing process is based on site mixing and the de-moulding procedures are based on what a cross section

of hemp-lime wall in a building might experience during construction. As this study is primarily investigating aspects of hemp-lime when used in structures the procedures will be adapted and followed as they produced good repeatable results for Hirst et al. (2012).

The specimens were tested in compression by Hirst et al. (2012) at ages of 14, 28, 91 and 180 days. The specimens were capped with dental plaster to provide flat parallel ends for even spreading of the compressive load. They were loaded at a rate of 3mm of vertical displacement per minute. Hemp-lime specimens made with THB-B and BC binders at a density of 275kg/m^3 were also prepared and tested in the same way. The results from Hirst et al. (2012) for the 180 day compressive tests are displayed in Table 2.5.

Hirst et al. (2012) commented that from the results it is clear the compressive strength is related to the density of the material. It was found that while there was little difference in strength between the 220kg/m^3 and 275kg/m^3 specimens at early ages, but by 180 days the 275kg/m^2 specimens were nearly twice the strength. Hirst et al. (2012) commented that the 220kg/m^3 specimens were notably more fragile than the higher density specimens and some even broke when being handled gently within the laboratory. While the compressive strengths were found to be low and therefore potentially unsuitable for load bearing construction, an amount of structural integrity is required for the material to be used effectively for non-load bearing applications. Additionally the strength of the binder does not directly affect the strength of the hemp-lime composite as the specimens made with THB-B are stronger than those made with BC whereas with the binder specimens showed the opposite result.

Table 2.5 Compressive testing results (Hirst *et al.*, 2012)

Binder	**Density (kg/m^3)**	**Max Stress σ_c (N/mm^2)**	**Strain at max σ_c (%)**	**Elastic modulus (N/mm^2)**
THB-A	220	0.03	4	3.3
THB-A	275	0.06	8.5	2.8
THB-A	330	0.21	5.3	16.5
THB-B	275	0.11	9.5	4.7
BC	275	0.06	3.3	5.0

In addition to compressive strength testing Hirst et al. (2012) studied the carbonation progression through hemp-lime. Smaller 100mm diameter by 200mm tall cylindrical specimens were made and stored using the same process as for the compressive test specimens. The specimens were split at mid height at 14, 28, 91 and 180 days and phenolphthalein solution was sprayed onto the freshly broken surfaces with the depth of carbonation being measured. The progress of carbonation was found to follow a simple square root rule where the depth is equal to the square root of time multiplied by a constant. The results of this testing were input into the equation by Hirst et al. (2012) and the resulting carbonation times are shown in Table 2.6.

Table 2.6 Carbonation times (Hirst *et al.*, 2012)

Binder	**Density (kg/m^3)**	**Time to carbonate 50mm depth**	**Carbonation constant, k_c**
THB-A	220	36	8.4
THB-A	275	55	6.7
THB-A	330	188	3.7

This work on carbonation by Hirst et al. (2012) has the potential to be particularly useful and relevant to this study. Both the binder and hemp shiv used are the same as those that will be used throughout this study and therefore direct comparisons can be made. The calculation of carbonation times from the carbonation constants established will help in determining the length of time specimens should be left before testing. From this it is possible to assess the extent of carbonation without using destructive testing methods such as phenolphthalein solution testing. Additionally as the same binder and shiv are used the compressive strengths resulting from this study will be able to be compared with those from the work by Hirst et al. (2012).

2.2.6 Other mechanical properties

There are currently no published data on the shear resistance of hemp-lime. This is likely to be due to the fact that in its current use, hemp-lime does not need any significant shear resistance as these forces will be carried by the timber framing and

sheathing that is typically used. However if hemp-lime is to be used structurally it may be necessary to know the shear resistance.

The influence of binder type, mix proportions, density, curing conditions and moisture content are all important considerations when using hemp-lime, but also while reviewing previous studies. The literature reviewed has shown the effects of these on the compressive strength and elastic modulus. They must also be kept in mind when comparing the results from different studies and this is something that will be done throughout this investigation. Another important consideration is the strain at which the maximum compressive stress occurs. In hemp-lime it is often high at between 6% and 10%, but as shown in the literature it does alter depending upon the variables listed above. This again must be kept in mind when comparing results. It is also particularly important for this study as if hemp-lime is to be used in a structural capacity the full strength may not be available at serviceability limits of deflection.

2.3 Hemp-lime composite studwork walling

There is no published research on the structural performance of studwork walling with hemp-lime composites. There are three university based studies on the compressive performance, and one study on the racking performance by Lime Technology, all of which are unpublished. The first piece of work on compressive performance is an undergraduate study from the University of Bath. The second study of compressive performance of hemp-lime and studwork walling was undertaken at Queen's University in Kingston, Canada and the third is from a Masters dissertation also from Queen's University. Research by Lawrence et al. (2009) and Gross et al. (2009) into the racking performance of ModCell prefabricated straw bale panels will also be discussed as there are some similarities to timber studwork framing and hemp-lime composite construction.

2.3.1 Helmich (2008)

Helmich (2008) studied the effects on structural performance under compressive loading of cold formed lightweight steel studwork with and without hemp-lime cast

around it. Two studwork frames were constructed, 2.5m high by 1.2m wide, comprising of three studs at 600mm centres with a header and footer rail. One frame was tested as it was (unrestrained) and the other had hemp-lime cast around it (restrained) to create a solid wall 2.5m high by 1.2m wide by 0.3m thick with the frame at the centre of it. The binder used was Tradical HB which is a formulated binder specifically developed for use with hemp. Tradical HF hemp shiv was also used.

The unrestrained frame was loaded with a single compressive load on the centre stud through its centroidal axis. Failure occurred when the central stud suffered global buckling at a load of 38.5kN. The second restrained frame was tested 28 days after the hemp-lime had been cast. During this time the hemp-lime was left to dry in the laboratory environment and the temperature and humidity was not recorded. The restrained frame was tested in compression by loading the central stud as with the first frame. The frame was deemed to have failed at 75kN and upon deconstruction it was found that the central stud had crushed (local buckling) at its head (Figure 2.7). At the time of testing the hemp-lime had a dry density of 466kg/m^3 and moisture contents ranging from 48% to 75%. The moisture content is high due to the young age of the specimen and the high density.

Figure 2.7 Crushed stud (Helmich, 2008)

The hemp-lime cast by Helmich (2008) is of a much higher density than currently used in the United Kingdom by manufacturers such a Lime Technology. It is also much higher than is to be used during this investigation. Therefore it will be interesting to see if the same enhancement in strength can be achieved when using a lower density hemp-lime composite. Additionally it is unfortunate that Helmich (2008) was unable to investigate the full potential of the hemp-lime containment due to the high moisture content of the hemp-lime at testing. At such high moisture contents carbonation of the lime content of the binder would have been limited and therefore its strength influence upon the results limited. Figure 2.8 shows a section of hemp-lime taken from the wall following testing and sprayed with phenolphthalein solution. The pink colouration indicates a high PH and therefore that carbonation has not yet occurred.

Figure 2.8 Extent carbonation of hemp-lime (Helmich, 2008)

Helmich (2008) concludes that the addition of hemp-lime significantly increases the structural load bearing capacity of the frame and that hemp-lime should now be considered as a possible intermediate restraint from lightweight steel studwork walling. Additionally Helmich (2008) comments that the increase in compressive strength could have been greater if the hemp-lime had been allowed to dry and cure for longer.

Helmich (2008) also analysed the results numerically and found that the failure loads could be predicted using existing analysis methods for lightweight cold formed steel sections as detailed in BS 5950 Part 5 (1998). For the unrestrained frame global

buckling methods were used and for the restrained frame the short stud section capacity was used. Helmich (2008) found that both gave good predictions of the failure loads of the studs.

2.3.2 Dutton (2009)

Dutton (2009) tested timber studwork frames loaded in compression with and without hemp-lime restraint. As there are no proprietary hemp-lime binders available in Canada, a mix and binder was designed with the following proportions by weight, 14.5% hemp, 14.5% lime, 24.1% cement and 46.9% water.

Initially Dutton (2009) tested a small timber studwork frame 0.6m high by 0.46m wide with four 50mm by 100mm timber studs evenly placed (Figure 2.9). The frame was loaded with an evenly spread compressive load and failed at a load of 215kN when one of the outer timber studs split and the header and footer rails crushed. Dutton (2009) comments that it is surprising that the studs did not buckle. This is not too surprising however as the studs were of such a short length that global buckling is unlikely to occur. An identical frame with hemp-lime cast around it to create a solid wall was then tested. The wall was tested with an evenly spread compressive load and failed at a peak load of 202.3kN when the outer studs buckled. Upon deconstruction it was found that the inner stud had crushed locally. There is no explanation for this result within the paper.

Dutton (2009) then went onto test larger scale specimens with three studs; the dimensions of these frames are not given. The outer two studs were ‘braced’ by screwing an additional stud to each in order to ensure failure occurred in the inner stud. Enhancing the strength of the outer studs in order to induce failure in the central stud has the potential to influence the results particularly as the frames are loaded with a spread compressive force. The stiffer outer studs will attract more of the load and therefore significantly alter the loading on the central stud. Two timber only frames were tested with a compressive load spread evenly across the top of the frame and maximum loads of 92.72kN and 90.67kN were recorded at displacements of 11.13mm and 11.87mm respectively when the central studs buckled about their minor axis.

Figure 2.9 Timber studwork frame (Dutton, 2009)

Dutton (2009) then tested two identical frames with hemp-lime cast between the studs only (not surrounding them) so that the behaviour of the studs could be observed during testing (Figure 2.10). Again the outer studs were braced so that failure would occur within the inner stud that was in contact with the hemp-lime on both sides. The two frames achieved maximum loads of 106.64kN and 114.70kN at displacements of 23.29mm and 17.43mm respectively. Both specimens failed due to buckling of the outer studs not the inner one which was being restrained by the hemp-lime. Dutton (2009) concludes by stating that hemp-lime does increase the compressive capacity of the studwork frames, but that the tests are inconclusive as local buckling failure of the central stud was not achieved.

Figure 2.10 Timber studwork frame with hemp-lime (Dutton, 2009)

2.3.3 Mukherjee (2012)

A masters project was undertaken at Queen's University in Canada by Mukherjee (2012) investigating timber studwork framing under compressive loading both with and without hemp-lime. Three different mixes of hemp-lime were used to create different final densities of 715kg/m^3, 430kg/m^3 and 313kg/m^3, it is not stated if these are bulk or dry densities. The binder used was mixed from hydrated lime and cement and the mix proportions are shown in Table 2.7.

Table 2.7 Mix proportions (Mukherjee, 2012)

	Proportions by weight (%)		
	Mix 1	**Mix 2**	**Mix 3**
Cement	24.0	22.4	22.4
Lime	14.4	13.4	13.4
Hemp shiv	14.4 (5mm shiv)	20.2 (20mm shiv)	20.2 (12mm shiv)
Water	47.2	44.0	44.0

Mukherjee (2012) constructed and tested eight studwork frames in compression, two without hemp-lime infill and 6 with hemp-lime infill. Three walls were 1200mm high and five walls were 2133mm high. The different heights were used to investigate height effects. Two sizes of timber studs were used, 38mm by 89mm and 38mm by 235mm. Mukherjee (2012) cast the hemp-lime with the frames laying down and only between the studs, not entirely surrounding them. The hemp-lime was allowed to dry for one and a half to three months until it was dry to the touch (Mukherjee, 2012).

Mukherjee (2012) loaded the central stud of all of the frames in compression and found that the two frames (one 1200mm high and one 2133mm high, with 38mm by 89mm stud) without hemp-lime failed by minor axis buckling of the central stud. Two 1200mm high frames, one with 715kg/m^3 hemp-lime and one with 313kg/m^3 hemp-lime, were tested. The frame with higher density hemp-lime experienced bearing failure of the header and footer timber plates, while the other frame failed by major axis buckling. Mukherjee (2012) comments that these frames achieved higher loads than the two without hemp-lime and minor axis buckling was prevented , however on one frame failure was not within the studs. In order to force failure in the studs Mukherjee (2012) replaced the header and footer timber elements with steel and aluminium and following this two 2133mm high walls were tested with 313kg/m^3 hemp-lime with both walls failing by major axis buckling. Finally Mukherjee (2012) tested two frames with increased stud size of 38mm by 235mm in order to force minor axis buckling. One frame had 313kg/m^3 and 430kg/m^3 hemp-lime while the other had 430kg/m^3 hemp-lime on one side of the stud and solid foam on the other side. Mukherjee (2012) comments that this was to force the stud to fail into the hemp-lime. The first frame failed by bearing on the header and footer timbers while the second failed by minor axis buckling into the hemp-lime.

Mukherjee (2012) found that all of the frames with hemp-lime failed at higher loads than those without. Following testing predictions were made using analytical methods to try and match the test results. Bearing, major axis buckling and minor axis buckling into the hemp-lime were checked and the lowest strength was taken as the prediction. Mukherjee (2012) predicated the bearing strength and major axis buckling using timber design codes and the minor axis buckling strength using a combination of the design

codes and the theory of a buckling strut on an elastic foundation. The accuracy of the predictions ranged from 12% to 102% with some stronger and some weaker.

The work by Mukherjee (2012) is significant as it focuses on the use of hemp-lime to add to the structural capacity of studwork frames. The works shows that minor axis buckling can be prevented in certain situations. However this work shows that major axis buckling can be a mode of failure and due to the positioning of the hemp-lime on each side of the studs rather than around them the role of the hemp-lime in preventing this failure mode has not been investigated. Additionally the method of loading was not described in sufficient detail to determine if the tops of the stud were being restrained in either direction and therefore this could have had an effect on the failure modes observed. The density and moisture content of the hemp-lime at the time of testing are not presented and this could have a significant effect on the results. It is unlikely that the hemp-lime was fully dry after one and a half to three months that Mukherjee (2012) left the specimens prior to testing as drying can take up to six months or even a year (Arnaud, 2000; Evrard, 2002). Finally while some comparisons will be able to be made between the work by Mukherjee (2012) and the investigation being undertaken here, the use of higher density hemp-lime and hemp-lime cast around the studs will limit this.

2.3.4 CERAM (2009)

Two racking tests have been carried out at CERAM for Lime Technology Ltd (CERAM, 2009b, a) on timber studwork walling both with and without hemp-lime. The two studwork frames consisted of five 38mm by 140mm C16 timber studs, header and footer rails and the connections were made by two 89mm long by 3mm diameter wire nails into the end of the studs. One frame had Resistant Multi-pro XS sheathing board fixed to it with 42mm drywall screws at 200mm centres on the sheet perimeter studs and 300mm centres on the inner studs (CERAM, 2009b), while the other had hemp-lime cast between the studs to a depth of 200mm (CERAM, 2009a).

Both wall panels were loaded in accordance with BS EN 594 (1996) and had 5kN vertical point loads continuously applied to the top of each stud throughout the test. The studwork frame with the Multi-pro sheathing board achieved a maximum load of 20.9kN (CERAM, 2009b) while the studwork frame with hemp-lime achieved a

maximum load of 16.6kN (CERAM, 2009a). As these tests were carried out in accordance with BS EN 594 (1996) it will be possible to compare them with any tests undertaken during this study following the same test standard.

2.3.5 ModCell

The racking resistance of ModCell straw bale panels has been the subject of research by Lawrence et al. (2009) and Gross et al. (2009). ModCell is a prefabricated straw bale panel system for use as load bearing walls and cladding panels. The panels consist of a glulam frame, in-filled with straw bales and rendered on both the internal and external faces. Figure 2.11 shows the build-up of a typical panel. ModCell panels are being reviewed as they are similar in some aspects to studwork walling with hemp-lime. Both construction systems consist of structural timber framing elements with a low stiffness plant based material infilling between. Additionally ModCell panels are typically rendered and so are hemp-lime walls.

Figure 2.11 ModCell panel (Gross *et al.*, 2009)

Lawrence et al. (2009) investigated the racking shear resistance of non-load bearing ModCell panels. Tests were carried out on corner joints to investigate the resistance offered to racking shear. This work found that even with corner bracing the joints were not sufficient alone to resist the required racking forces. Lawrence et al. (2009) then confirmed this by testing a two metre by two metre ModCell timber frame, timber frame

with the straw bales and finally a fully rendered panel. The rendered panel was 3.5 times stiffer than the straw filled panel. Racking shear load resistance tests were then performed on full size ModCell panels measuring 3.08 metres wide, by 3.34 metres high, by 0.48 metres thick. Panels reinforced with steel bracing as well as unreinforced panels were tested. Cracks developed in the render of the reinforced panel at 1.25 times the load in the unreinforced panels and failure occurred at nearly three times the load. It was observed that load capacity and lateral stiffness of the frame is significantly influenced by the joint and reinforcement details. In addition Lawrence et al. (2009) also observed that the render is a key contributor to the shear resistance of the panels. This observation is in keeping with other straw bale building techniques. Mesh reinforcement was not used in any of the render, but Lawrence et al. (2009) points out that the vertical reinforcing bars have the same effect by adding some tensile strength to the render.

Gross et al. (2009) investigated the racking shear resistance of load bearing ModCell panels. These panels were a development of those tested by Lawrence et al. (2009). The timber frame was increased in thickness from 80mm to 100mm. Initially three different types of joint, screwed, dowelled and dove tailed, were tested in vertical pull out. The screw connected joints were deemed to be most suitable as they had the highest load capacity and stiffness. Gross et al. (2009) then tested two full panels (3 bale) and two panels with a door opening (2 bale) with these joints in racking shear. One panel had diagonal corner bracing and the other had cross bracing across the entire panel. The panels were 3.2m long by 2.6m high and 0.49m thick. Serviceability deflection limits of height/500 and height/300 were set.

At these deflection limits the 3 bale panels carried three times the load that the two bale panels carried (Figure 2.12). The cross braced and corner braced panels both performed similarly, with the two bale corner braced panel outperforming the two bale cross braced panel. Gross et al. (2009) notes that as the panel racks the top and bottom frame elements move closer together putting the render into compression and that as shown by Lawrence et al. (2009) the render plays a key role in the strength of the panels. This comment is useful for this investigation as often hemp-lime walls are rendered. The render or other surface coverings may also increase the strength of hemp-lime walls and this should be taken into consideration when designing test walls and analysing results.

The walls may behave in a similar way to sandwich panels with a low stiffness core and high stiffness membrane skins that are prevented from buckling by the core.

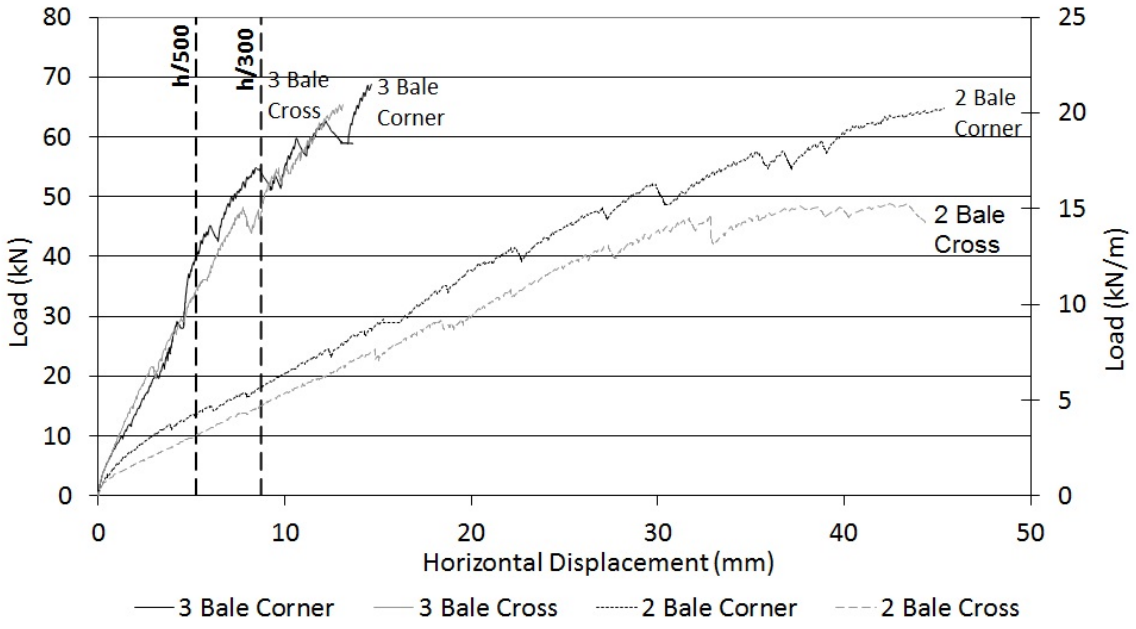

Figure 2.12 Racking test results (Gross *et al.*, 2009)

2.4 Previous work on performance of timber studwork framing

The timber studwork framing used in hemp-lime composite construction will have a large effect on the structural performance of walls constructed in this way. Therefore it is necessary to consider the design and structural performance of conventional timber studwork framing. There is guidance on the design of structural studwork framing in *BS EN 1995 (2004) Eurocode 5 - Design of timber structures - Part 1-1: General – Common rules and rules for buildings* (EC5) and *BS 5268 (1996) Part 6.1 – Structural use of Timber – Part 6: Code of practice for timber frame walls – Section 6.1: Dwellings not exceeding seven storeys.*

There are many studies on the structural performance of studwork walling. A large number of these focus on in-plane racking performance as these types of structures work in a complex manner. Additionally a large number of the studies on studwork walling concentrate on lightweight steel studs. The key pieces of research focussing on timber studwork framing will be reviewed as they are relevant to this study.

2.4.1 Timber design codes

The design of structural studwork walling is covered in detail in Chapter 9 of BS EN 1995 Part 1.1 (2004). Both resistance to vertical compressive loads and in-plane racking loads are covered. With vertical compressive loads several design checks are performed. Firstly the compressive stress in the column from the applied loads is checked against the compressive strength. The column is also checked for buckling under the applied loads. Finally any combined load effects, such as out-of-plane bending and compression, are considered.

Two methods for calculating the design racking resistance of a wall assembly are set out. The National Annex for the United Kingdom, NA to BS EN 1995 Part 1.1 (2004), states that Method B should be used. Both Method A and Method B use similar process for calculating the racking resistance. In both cases the racking resistance is based on the lateral design capacity of individual fasteners through the sheathing board material into the timber framing elements. Alternatively BS EN 1995 (2004) states that the racking resistance can be determined by testing following the procedures set out in *BS EN 594 (1996) Timber Structures – Test Methods – Racking strength and stiffness of timber frame wall panels.*

The compression resistance is covered in differing ways as well. Within Chapter 9 of BS EN 1995 Part 1.1 (2004) clause 9.2.5.3 allows for the calculation of the design stabilising force required in restraints at intermediate distances along a member subjected to axial compression. This approach calculates the required stabilising force and the required spring stiffness in the lateral supports to prevent buckling. Clause 9.2.4.3.2 Part 6 states that studs subjected to vertical compressive forces should also be checked for buckling in accordance with clause 6.3.2 of BS EN 1995 Part 1.1 (2004). In clause 6.3.2 the stability of compression members is checked taking into consideration the effective length and slenderness ratio of the members to calculate modification factor by which the compressive and bending stresses are multiplied. This approach ignores any finishes, such as render. Therefore this approach could be unsuitable for hemp-lime walls with rendered faces if the render is being included as a resisting element. In addition BS EN 1995 Part 1.1 (2004) states that the bearing capacity of the footer and header rails perpendicular to the grain must be checked.

The approaches of design for both racking and compression resistance BS EN 1995 Part 1.1 (2004) assume that there are discrete points of fixing between the timber framing elements and the lateral restraints, such as sheathing boards or noggins. This approach may not be entirely applicable to hemp-lime and timber studwork frame composites as the hemp-lime forms a continuous restraint against the studs along their entire length. For these reasons the approaches followed in BS 5268 Part 6.1 (1996) will be reviewed as they may offer a more applicable approach.

The design of timber studwork walling is covered extensively in BS 5268 Part 6.1 (1996). The parts of BS 5268 Part 6.1 (1996) that are relevant to timber studwork walling where composite action occurs between the studs and other material in the wall construction and whether these can be applied to the design of walling with structural hemp-lime.

BS 5268 Part 6.1 (1996) was drafted specifically for use with timber frame walls sheathed with sheet material on one or two faces. This is a result of the timber framing industry supporting the code and not wanting to give their competitors using other materials a helping hand (Griffiths, 2010). The code firstly states that when timber studs are being used compositely with other materials to resist the loads applied to the walling the appropriate composite action for that system should be established through testing or by calculations.

The design of compression members within the wall system is covered. Lateral restraint should be provided by either noggins or sheathing boards (BS 5268 Part 6.1, 1996). BS 5268 Part 6.1 (1996) also notes that where sheathing boards are used as an intermediate restraint for the stud when resisting compression the relative stiffnesses of the stud and sheathing should be considered. If the stud is relatively much stiffer than the sheathing then the sheathing will have very little effect in providing an intermediate restraint.

BS 5268 Part 6.1 (1996) also sets out how the racking resistance of timber stud work walls should be provided. The resistance to in-plane racking loads should be provided by sheathing, diagonal bracing or moment connections. The capacity of these should be determined in one of four ways:

1. By the calculation assessment method outlined in BS 5268 (1996) Part 6;
2. By laboratory testing as outline in BS EN 594 (1996), and the results should then be analysed in accordance with BS 5268 (1996);
3. By testing of full scale wall structures;
4. By other analytical methods not covered in BS 5268 (1996).

Both BS EN 1995 (2004) and BS 5268 (1996) allow the use of laboratory testing to determine the racking resistance of wall panels. For the purposes of this investigation this is something that will be closely followed. BS EN 594 (1996) sets out very specific criteria to fulfil and follow when testing timber studwork wall panels for racking stiffness.

BS EN 594 (1996) was also specifically drafted for use with timber frame walls with sheet material sheathing on one or two faces (Griffiths, 2010). The code was introduced in order to align UK test standards with those used in Europe. However since the adoption of the code in 1996 a wide range of panels, including steel framed panels, nail-plated panels and sandwich panels, have been tested following its guidance. This can give confusing and incorrect results and engineering judgement needs to be used to apply the test method and interpret the results (Griffiths, 2010). BS EN 594 (1996) is currently going through the BSI Code Committee with revisions that will encompass a wider range of constructions.

BS EN 594 (1996) states that the principle of the testing method outlined is to measure the resistance to racking loads of timber studwork wall panels which can deform both horizontally and vertically in the plane of the panel. The panel tested must be 2.4m long by 2.4m high with studs at 600mm centres. The panel dimensions and details are shown in Figure 2.13 (BS EN 594, 1996).

During testing the bottom rail of the panel must be fixed to the floor or supporting structure in such a way to prevent uplift when loaded. Vertical point loads are applied to the top rail above the stud heads equally and their total load will be equal to that which the wall panel must support within its design application (BS EN 594, 1996). A horizontal racking load is also applied to the top rail at the leading stud side of the panel

(BS EN 594, 1996). The loading positions and requirements recording displacements and loads are shown in Figure 2.14.

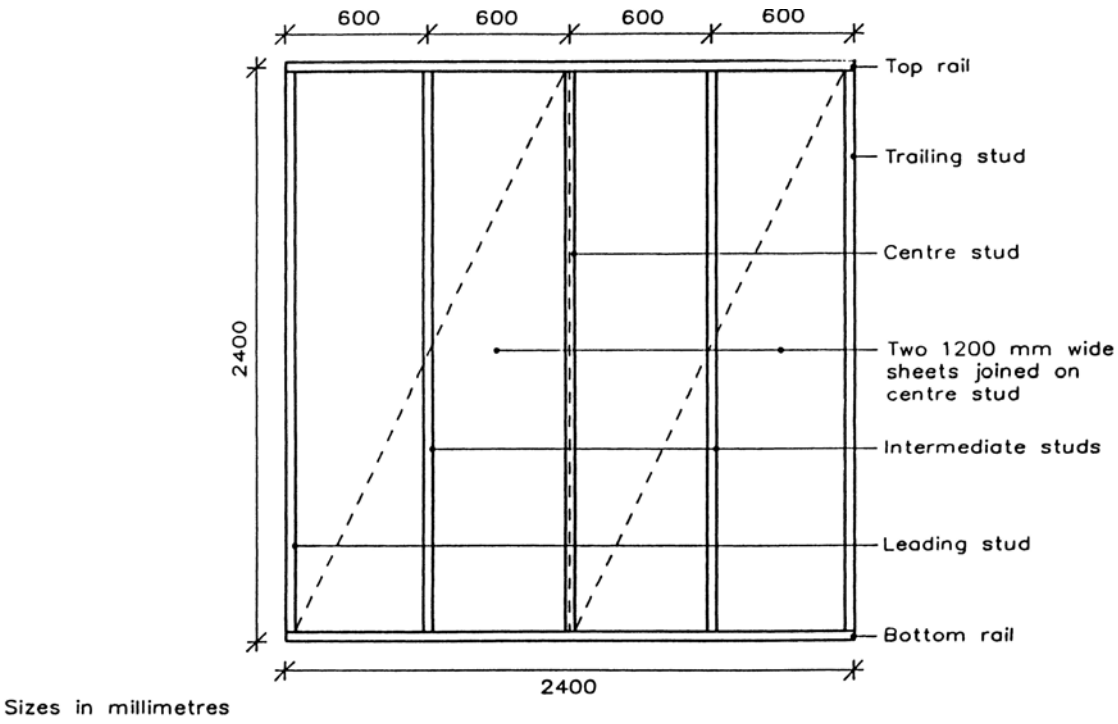

Figure 2.13 Racking test panel dimensions (BS EN 594, 1996)

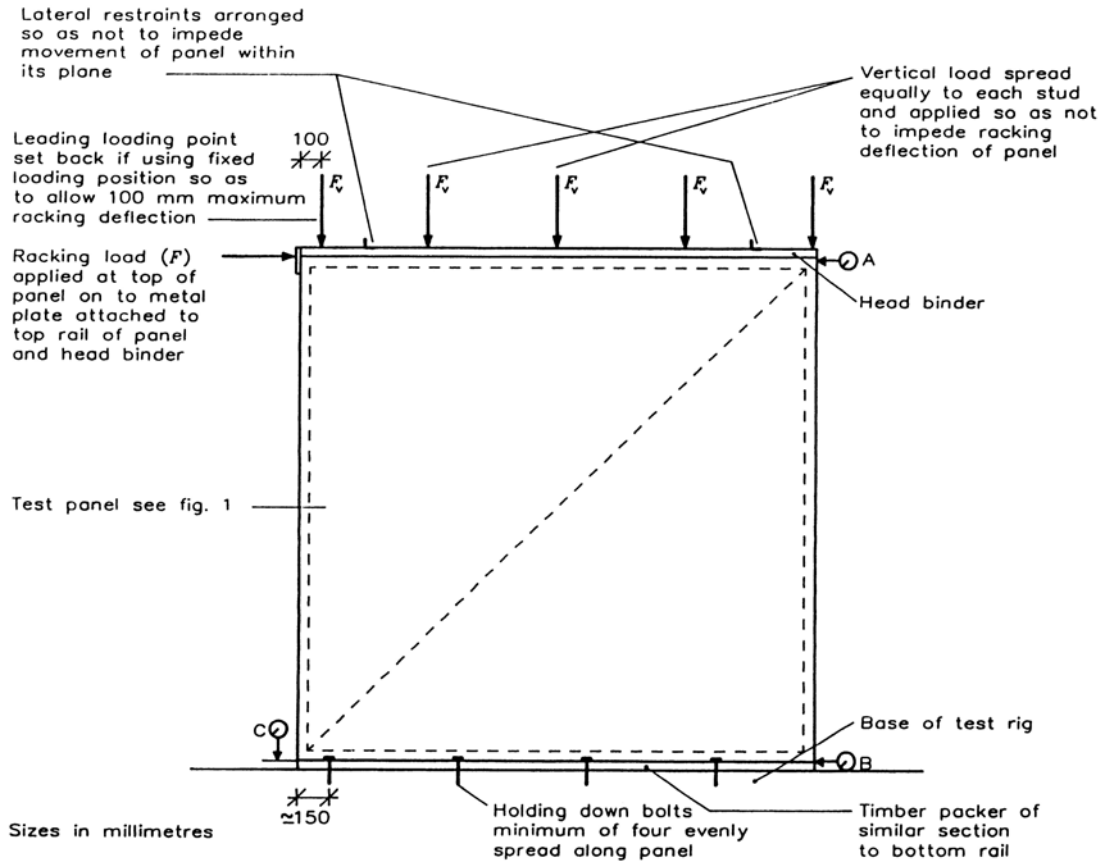

Figure 2.14 Racking test set up (BS EN 594, 1996)

BS EN 594 (1996) also sets out the testing procedure for wall panels and the magnitude of the vertical and horizontal loads. When the test is being used to establish the basic racking resistance of a combination of materials the vertical loads on each stud (F_v) should be within the range 0kN to 5kN (BS EN 594, 1996). The application of the horizontal racking load is based on the estimated horizontal failure load of the wall panel, $F_{max,est}$. BS EN 594 (1996) breaks down the testing procedure into four sections:

1. Vertical preload – when the vertical loads, F_v, are lower than 1kN a vertical preload of 1kN must be applied to each stud for 120 seconds and then released. The panel should be allowed to recover for 300 seconds.
2. Stabilising load cycle – the vertical loads F_v are applied and then $0.1F_{max,est}$ is applied for 120 seconds. The panel should be allowed to recover for 600 seconds.
3. Stiffness load cycle - the vertical loads F_v are applied and then $0.4F_{max,est}$ is applied for 300 seconds. The deformations and loads should be recorded. The panel should be allowed to recover for 600 seconds.
4. Strength test - the vertical loads F_v are applied and then $0.4F_{max,est}$ is applied for 300 seconds. Then the horizontal load is increased until failure occurs.

This testing procedure is shown graphically in Figure 2.15.

All of the testing procedures and design guidance in BS EN 1995 Part 1.1 (2004), BS 5268 Part 6.1 (1996) and BS EN 594 (1996) relate specifically to commonly used studwork walling materials and sheathing boards. As a result the guidance and procedures are prescriptive and do not allow for any deviation from the standard materials. Therefore the procedure for establishing the racking resistance of a timber studwork wall does not apply to the use of hemp-lime as BS 5268 Part 6.1 (1996) states specific values of resistance for known sheathing boards such as plywood and plasterboard and BS EN 1995 Part 1.1 (2004) uses fastener capacities. A more complex design procedure will be necessary when using hemp-lime which will result from this piece of research.

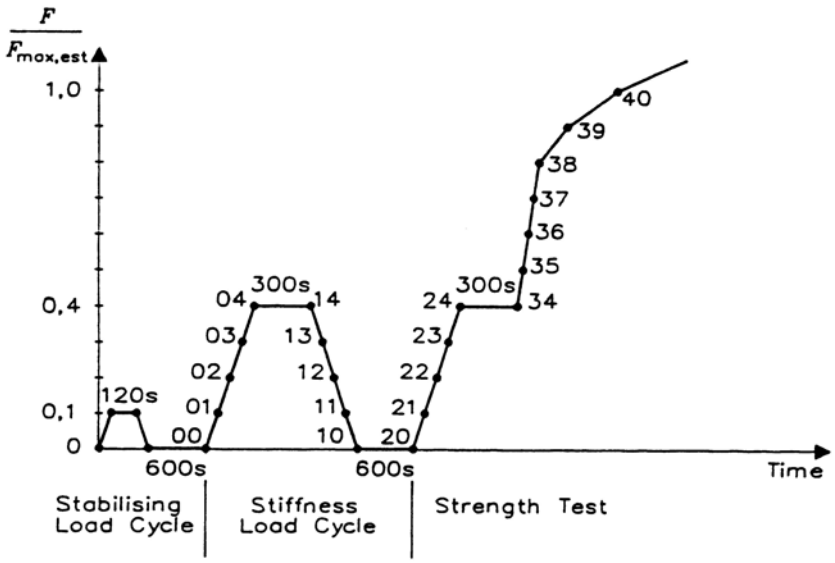

Figure 2.15 Graphical representation of testing procedure (BS EN 594, 1996)

Despite the fact that the racking test procedures set out in BS EN 594 (1996) are very prescriptive the general process and reasoning behind them is still relevant to hemp-lime. The testing procedure sections 3 (stiffness) and 4 (failure) mentioned above are relevant as establishing both of these parameters will be part of the aims of any racking testing. The level of load applied to establish the stiffness could be altered to the serviceability loading of the wall panel as its behaviour under these conditions may be critical. Alternatively an additional loading cycle loading the wall to serviceability conditions could be added. The strength or failure load cycle is also relevant as the ultimate capacity of the wall panel needs to be established.

Section 1 (preload) and 2 (stabilizing) are less relevant. BS EN 594 (1996) states that a vertical preload should be applied where the design vertical loads are less than 1kN per stud. This is in order to bed in the construction. This may not be necessary as the vertical and racking loads will do this during the actual load testing. The same is true of the stabilizing load cycle where racking loads are applied.

An update to BS EN 594 (1996) was published in 2011. The new BS EN 594 (2011) is very similar to the previous revision of the standard. There is a slight change in loading procedure and therefore in the calculation for determining the racking stiffness of the test panel. The stiffness cycle has been removed from the testing procedure and as a result the racking stiffness is determined from the stiffness over the initial part of the strength test. In BS EN 594 (1996) the racking stiffness was an average of the

stiffnesses from the stiffness test and the initial part of the strength test. Throughout this investigation BS EN 594 (1996) will be followed as the majority of the work was undertaken prior to the change in the test standard and additionally it allows easy comparison with previous test results.

BS EN 1995 Part 1.1 (2004) may not be entirely applicable when using hemp-lime as the calculation methods are based on the sheathing board fastener resistance. In hemp-lime construction a sheathing board may not be used, but a brittle finish, such as a render, will be applied. This will behave in a different manner. Similarly BS 5268 Part 6.1 (1996) may not be suitable, however racking tests undertaken according to BS EN 594 (1996) can be used to calculate design racking loads in BS 5268 Part 6.1 (1996) which will allows a comparison to be made between hemp-lime composite walling and other sheathing materials that are set out in BS 5268 Part 6.1 (1996).

2.4.2 Conventional timber studwork framing

There have been many studies on the performance of timber studwork frames under different loading conditions (Enjily, 2001; Kallsner and Girhammar, 2009b, a; Kermani and Hairstans, 2006; Robertson and Griffiths, 1981; Winkel and Smith, 2010). The majority of these studies relate to very specific constructions and there have been very few studies on the compression loading of timber studs within studwork framing. In the United Kingdom it is assumed that as long as the sheathing boards and fixings comply with the specifications given in the design standards (BS EN 1995, 2004 and BS 5268, 1996), minor axis buckling will be prevented under the design loading (IStructE and TRADA, 2007). Assuming minor axis buckling is controlled by the sheathing board, major axis buckling could lead to stud failure.

Marxhausen and Stalnaker (2006) investigated the use of different sheathing boards as a means of restraint to prevent minor axis buckling in timber stud work walling and found that major axis buckling was the dominant failure mode. The results were compared to the minimum required performance outlined in the American Forest and Paper Association's (AFPA) guidelines. Timber studwork walls 2.44m high by 1.22m wide with 38mm by 89mm studs at 406mm centres were constructed and tested with the following combinations of sheathing boards attached:

1. Oriented Strand Board (OSB) on both sides;
2. OSB on one side;
3. Drywall on both sides;
4. Drywall on one side;
5. No sheathing.

From the AFPA guidelines Marxhausen and Stalnaker (2006) calculated that an un-sheathed wall made to the same specifications as the test walls must sustain a minimum load of 8.67kN and 42.5kN for a sheathed wall.

Prior to testing, the wall specimens were handled as if they were being transported to a real construction project as previous research of this type had been discounted by the U.S. Department of Agriculture Forest Products Laboratory as the specimens had been kept in pristine conditions prior to testing. The studies this comment relates to are not mentioned. While valid reasons are given for handling the specimens tested as though they were on a construction site, this is not a very easily controlled method of testing. It is possible that each specimen could have been subjected to different amounts of handling and rough treatment. This could have affected the results, although there is no suggestion it did.

A uniformly distributed compressive load was applied to the header of the panels. All of the sheathed specimens tested failed by major axis buckling (Figure 2.16) of the studs except for the one with drywall on one side. Upon failure the nails attaching the OSB to the studs bent and the screws attaching the Drywall pulled through. Marxhausen and Stalnaker (2006) concluded that all of the sheathed walls achieved the requirements of the AFPA guide with a factor of safety of 2.8 or higher and that some ductility was present in all specimens as the header and sole plates crushed during testing.

Figure 2.16 Major axis buckling (Marxhausen and Stalnaker, 2006)

It will be possible to make comparisons between the research by Marxhausen and Stalnaker (2006) and compressive testing carried out during this investigation. Conventional timber framing timber stud sizes and spacings were used along with conventional sheathing boards and fixing methods. However there are difference in specimen construction and test procedure when compared to those that will be used during this investigation. The specimens used by Marxhausen and Stalnaker (2006) have a smaller centre to centre spacing of 406mm whereas in this investigation the studs will generally be spaced at 600mm centres to fit with current UK construction practice. Despite this it will still be possible to make comparisons with hemp-lime surrounded specimens constructed during this investigation.

Racking of timber studwork frames has been studied in more detail than compressive loading. Doudak and Smith (2009) investigated wall panels under in-plane racking with oriented strand board (OSB) sheathing with and without window and door openings. Winkel and Smith (2010) investigated timber studwork walls panels with in-plane racking loading and then combinations of in-plane loads as well as out of plane loads. Rosowsky et al. (2005) also studied the effects of load combinations on the strength and stiffness of timber studwork wall panels.

Doudak and Smith (2009) initially compared a timber studwork frame with no sheathing to one with OSB sheathing on one side under in-plane racking loading. All of the frames tested used 38mm by 89mm studs at 400mm centres and were 2.4m long by 2.4m high. 11.1mm OSB was used throughout the investigation with nailed fixings at 150mm centres around the perimeter of the sheets and 300mm centres along the interior studs.

Doudak and Smith (2009) initially tested a frame without sheathing with 5kN total vertical load and found that it had an initial racking stiffness of 8.7N/mm and ultimate racking load of 0.3kN. The frame with OSB sheathing and no openings was tested with 10kN total load and was found to have an initial racking stiffness of 558N/mm and ultimate racking load of 20.8kN. Doudak and Smith (2009) discuss how each wall panel failed but do not compare the two results. Doudak and Smith (2009) note that the wall with no sheathing behaved differently from all the other walls as it only exhibited sway deformation while the stud to header and footer joints remained intact. The wall with OSB sheathing was observed to exhibit both racking deformations and rigid body rotation with large amounts of slip between the OSB sheathing and framing elements at failure (Doudak and Smith, 2009). Comparing the two results it can be seen that the OSB sheathing has the effect of significantly stiffening the frame and increasing the ultimate load.

Doudak and Smith (2009) then went on to test wall panels with a door opening or a window opening either with or without additional anchoring connections. All of the wall panels had a 5kN vertical load applied. All of the walls with openings were less stiff and had a lower ultimate racking strength than the wall with no openings. It is noted however that the improved connections helped to lessen this effect by reducing the rigid body rotation and increasing overall strength (Doudak and Smith, 2009).

This work by Doudak and Smith (2009) is useful as it compares the performance of studwork frames with and without sheathing boards. Studwork frames with and without hemp-lime will be compared during this investigation and therefore comparisons can be made. Additionally Doudak and Smith (2009) have shown that the base connections and anchoring can affect the performance of a wall panel which may be something that should be considered during this study.

Winkel and Smith (2010) investigated 2.44m high by 2.44m long timber studwork frames with OSB sheathing subjected to in-plane racking loads or a combination of in-plane and out of plane loads. The wall panels were constructed using 38mm by 89mm stud grade timber at 0.61m centres with 11.1mm OSB nailed at 152mm centres around the edges of the sheets and 305mm centres on interior studs. 14 wall panels were tested in total (see Table 2.8) and some had reinforced joints between the studs and the footer rail (Winkel and Smith, 2010). Winkel and Smith (2010) reinforced the joints with 3mm steel plates screwed to the studs and footer rails. Standard connections were made with two nails.

Table 2.8 Test schedule (Winkel and Smith, 2010)

Force applied	Number of specimens	
	Standard	Reinforced
In-plane racking	2	2
Uplift	2	2
Out-of-plane bending	2	-
Racking and uplift	1	1
Racking and bending	-	2

Winkel and Smith (2010) found that with only an in-plane racking load applied failure occurred with the OSB to timber connections failing from the bottom corners followed by the stud to footer and header plate connections failing with the maximum load of 5.6kN/m being achieved. When the connections were reinforced it was found that failure was similar, but the frame connections remained intact and a maximum load of 6.7kN/m was achieved. Under uplift loading Winkel and Smith (2010) found that the failures were similar with the connections between the OSB and framework failing followed by failure of the stud to header connections. The maximum uplift load at failure was 10.1kN/m. The reinforced connections had no effect as only the bottom joints were reinforced. With the panels loaded in out of plane bending full failure was not achieved, however there was local pull out of some of the nailed fixings of the OSB to interior timber studs (Winkel and Smith, 2010).

With combined in-plane racking and uplift Winkel and Smith (2010) found that the panels failed at a lower racking load as the forces accumulated in critical areas such as the bottom corner OSB to timber connections and failure was initiated from these points. Again it was found that the reinforced connections made an improvement. The maximum racking load achieved with uplift was 5.8kN/m. Finally Winkel and Smith (2010) found that the combination of in-plane racking loads and out of plane bending has no effect to the overall load carrying capacity of the studwork frames.

In conclusion Winkel and Smith (2010) note that improving the stud to footer connections has a large effect on the strength and stiffness of the frames, increasing the in-plane racking strength and stiffness by up to 25%. Racking peak loads were at high deformations, applied uplift loads have a negative impact on the racking performance and finally there is no negative effect when combining in-plane racking and out of plane bending.

This investigation is useful as it again shows that improvement of connections can have a significant effect on the performance of studwork frames. It also highlights the effects of multiple load combinations on timber studwork frames. Multiple loads combinations will not be investigated during this study and therefore Winkel and Smith (2010) give a good indication of the possible effects of multiple load combinations on timber studwork wall panels.

2.5 Conclusions

This literature review has highlighted that there is still only limited work on the material properties of hemp-lime and that within this small amount of published work the densities, binder type and mix proportions vary greatly. Therefore it will be necessary within this investigation to establish all the material properties required by laboratory testing in order that they are correct and accurate for the exact binder and mix proportions being used.

This review has also shown that there is very minimal research onto the use of hemp-lime structurally in combination with studwork walling. There were only three pieces of research, all of which are unpublished. There is only limited information available on

the studies by Dutton (2009) and Mukherjee (2012) however more in known about the study by Helmich (2008) as it was undertaken at the University of Bath. All of these investigations used different testing procedures and as a result these will have to be established throughout this investigation.

However the review has shown that there are strict guidelines to follow when carrying out racking tests on stud wall panels as set out in BS EN 594 (1996). These should be followed when undertaking racking tests in order that the tests are credible and can easily be compared to other studwork walling racking tests. While they are not entirely applicable to studwork framing with hemp-lime it will be possible to follow them.

Finally the review has shown that there has been some research into the buckling of timber studs within sheathed frames, but that this has been limited as the design standards assume that minor axis buckling will be prevented by sheathing boards and major axis buckling is not an issue. The review has also highlighted some useful research into the behaviour of timber studwork frames under in-plane racking loads where it has been shown that sheathing plays an important role in the strength and stiffness of wall panels as do the stud to footer and header connections.

3 Experimental Materials and Testing

3.1 Introduction

This chapter will describe the constituent materials used during the study. The material properties of hemp shiv, lime based binder and render, timber and steel studwork, and sheathing board will be outlined.

3.2 Hemp

Hemp (*Cannabis Sativa*) is a fast growing plant that can achieve a height of up to four metres from seed in 14 weeks and is resistant to most diseases (Pritchett, 2009). It has been used for centuries for making ropes, sails and clothing. More recently hemp has been grown in mainland Europe for use in high quality paper manufacture and car interior body panel mouldings. The modern use of hemp in construction developed in Europe as a by-product from the paper production industry (Woolley, 2004).

Hemp is currently grown under license within the United Kingdom. In 2010 10,600 ha of hemp were grown within the EU with 1100 ha grown in the UK (EU DGARD, 2012). The hemp grown in the UK is referred to as 'industrial hemp', which defines *Cannabis Sativa* plants that have been selectively bred to contain less than 0.2% tetra hydro cannabinnol (THC) (Bevan *et al.*, 2008). It is these plants that are used for hemp-lime construction and are shown being harvested in Figure 3.1. Modern industrial hemp has generally been grown for its fibres which are used in the automotive industry for interior body panels and the shiv has been seen as a low value by product of this process which is chopped up and sold for animal bedding (Bevan *et al.*, 2008). However the increasing demand for hemp-lime composites is starting to change this attitude to hemp end use.

Once the hemp plant has been harvested it is often left on the ground to dry. This allows for the outer fibres to be easily separated from the inner woody core (shiv) in a process known as retting. Once the fibres and any dust have been removed the woody core is chopped into small chips ranging in size from 5mm to 30mm. It is the shiv that is used in hemp-lime construction and is shown in Figure 3.2.

Figure 3.1 Harvesting hemp crop in the UK (Bevan *et al.*, 2008)

Figure 3.2 Hemp shiv

Bevan et al. (2008) set out several criteria that should be considered when selecting hemp shiv to use in a construction project. The shiv should be dry, free from fibre, dust and other foreign matter and should be chopped into lengths of roughly 25mm. However in the UK hemp shiv for construction is generally sourced from a manufacturer as a proprietary product, such as Tradical HF, and in this case all of these criteria should be fulfilled. As long as the hemp shiv is being used as hemp-lime and therefore is being mixed with a lime based binder there is no need to treat the shiv to prevent decay, insect attack or resist fire as the lime binder fulfils this function (Bevan *et al.*, 2008).

Tradical HF shiv will be used throughout this study. The particle size distribution for the hemp shiv is shown in Figure 3.3. The distribution was plotted from a sample of 5kg of hemp shiv passed through 14mm, 10mm, 6.3mm, 4mm and 2mm sieves. The shiv was passed through the sieves starting with the largest size first. All the material that passed was collected, weighed and then passed through the next size of sieve. This was repeated for all sieves and all of the shiv that did not pass through was also weighed. The elongated shape of hemp shiv particles is not ideal for sieving as when lying flat they do not readily pass through the mesh. Nguyen *et al.* (2009) encountered similar problems when sieving hemp shiv and found 27% of the particles to be less than 2mm and 76% less than 4mm. In comparison the results in Figure 3.3 show 17% less than 2mm and 70% less than 4mm. Both sets of results show a similar profile with the percentages passing through the sieves differing slightly. This is a result of natural variation within the material.

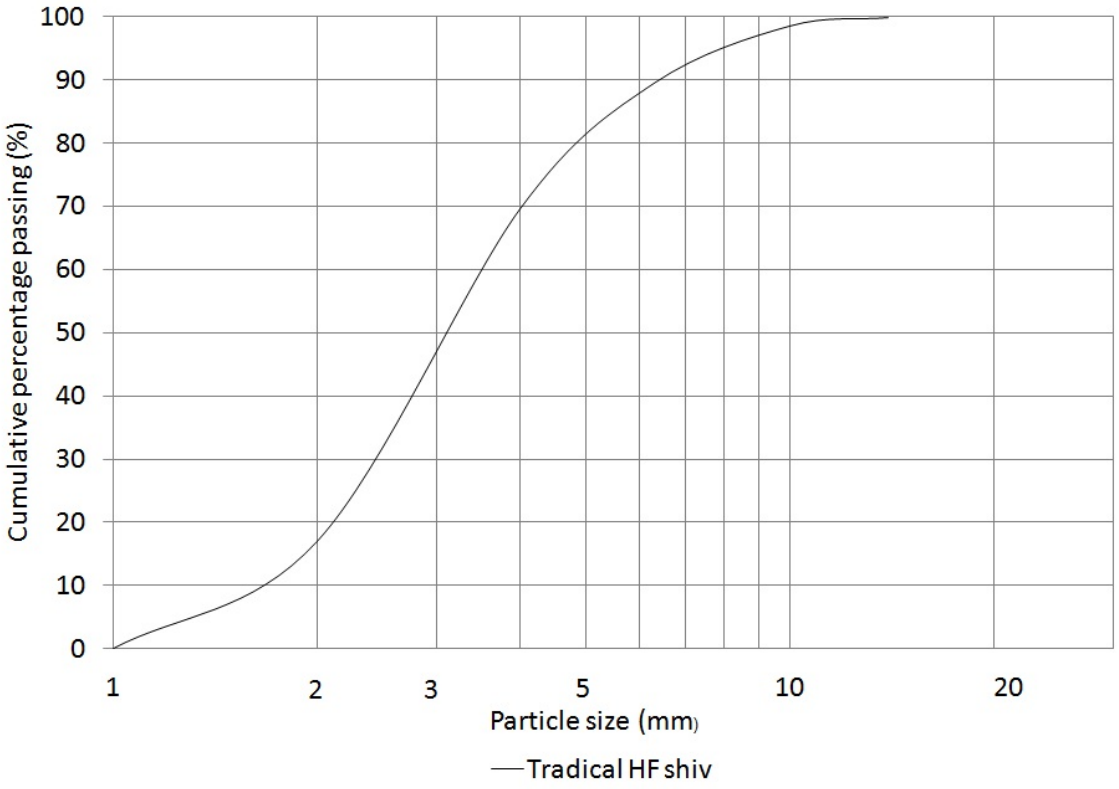

Figure 3.3 Hemp shiv particle size distribution

3.3 Lime binders

Lime has been used as a binder in construction for thousands of years due to its versatility and favourable properties such as its flexibility and durability (Holmes and Wingate, 1997). Its use has declined in many countries due to the development of Portland cement as a binder in 1824 which is stronger and easier to work with. However, the British Lime Association (2012) comment that over recent years there has been a revival of its use due to increased awareness of its benefits of increased flexibility, breathability and sustainability.

Lime is produced from limestone (calcium carbonate, $CaCO_3$ or dolomitic limestone, $CaCO_3.MgCO_3$). Whether using calcium carbonate or dolomitic limestone the process of producing lime is the same and is described here for calcium carbonate. The limestone is heated in a kiln which causes it to give off carbon dioxide (CO_2) and forms calcium oxide (CaO). Calcium oxide, also known as quicklime, is highly reactive with water and therefore must be stored and handled carefully. When water is added to quicklime a reaction takes place combining the water and quicklime to form calcium hydroxide ($Ca(OH)_2$) and heat. Calcium hydroxide is known as hydrated or slaked lime and it is at this point that it is used within construction. Calcium hydroxide will absorb carbon dioxide from the atmosphere to form calcium carbonate ($CaCO_3$) which is chemically the same as the original limestone. This cycle is shown in Figure 3.4.

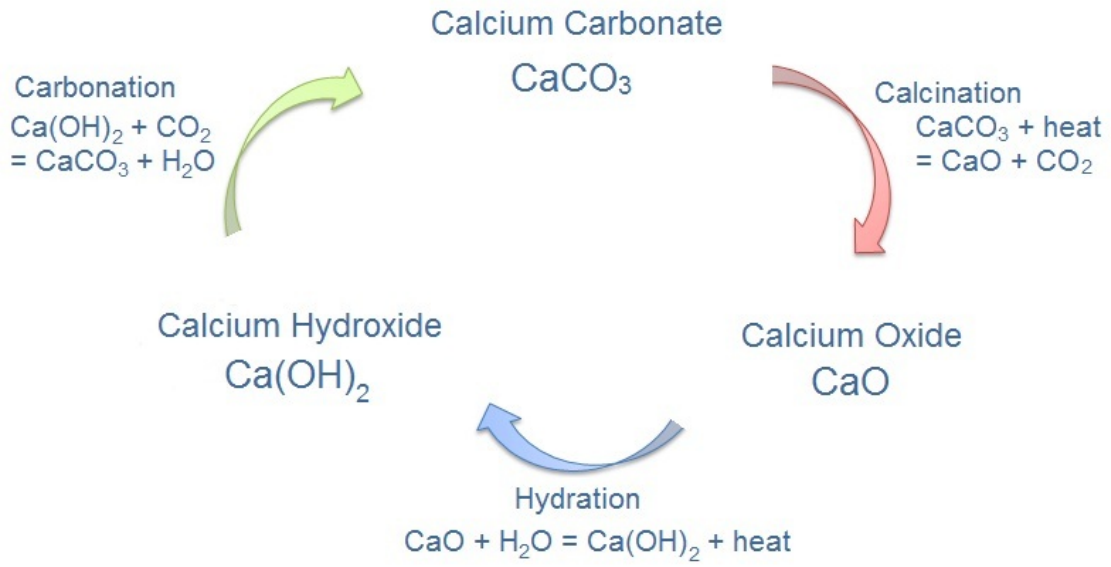

Figure 3.4 Lime cycle

There are two general types of building limes, air limes and hydraulic limes. Air limes, also known as pure lime, set by absorption of carbon dioxide in a process called carbonation. As they require carbon dioxide they will not set underwater. It was found that lime produced from certain types of limestone set underwater and as a result these limes became known as hydraulic limes (Holmes and Wingate, 1997). The limestones that hydraulic limes are produced from contain clay materials which combine with the lime to form active compounds when fired in a kiln. It is these compounds that form a chemical set and therefore the lime will harden underwater (Holmes and Wingate, 1997). Additionally, pozzolanic material can be added to limes in order to produce a reaction similar to that in hydraulic limes (Holmes and Wingate, 1997). Pozzolans can come from a variety of sources such as certain volcanic ashes, Pulverised Fuel Ash (PFA) from coal powered power stations and brick dust.

When using a lime based binder for hemp-lime construction there are two options. Either the binder can be designed by the person using or specifying the mix as done by De Bruijn et al. (2009) and Dutton (2009), or a binder specifically formulated for use with hemp can be used. Within the UK there are two commercially available binders specifically designed for use with hemp shiv: Tradical HB produced by Lime Technology Ltd; and Batichanvre produced by St Astier in France.

Tradical HB binder will be used throughout this study (Figure 3.5). Tradical HB contains hydrated air lime blended with selected cementitious, hydraulic and inorganic materials (Lime Technology, 2010b). Bevan et al. (2008) state that Batichanvre binder also contains lime, cement and other additives. The exact proportions of both mixes are not publicly known as both companies are not keen to reveal such details. The flexural and compressive strength of the binder are shown in Table 3.1[1]. These were tested by Kirton Concrete Services Limited in accordance with BS EN 1015-11 (1999).

[1] Data provided by DEFRA Link Project 'Developing hemp-lime low-carbon construction for mainstream uptake through innovation and optimisation'.

Figure 3.5 Tradical HB binder

Table 3.1 Tradical HB properties[1]

Age (days)	Flexural strength (N/mm^2)	Compressive strength (N/mm^2)
7	0.6	1.1
14	1.1	2.1
28	1.5	2.5
91	1.8	4.4

The lime based binder in hemp-lime composites fulfils several functions. It combines the hemp shiv particles into a continuous matrix with structural integrity. This allows for solid walls to be formed either by casting or by forming into blocks. As lime is alkaline and forms a continuous matrix around the hemp shiv it protects the shiv from fungal decay and insect attack. This is also true for any timber that has been cast into the hemp-lime, such as studwork framing, as the hemp-lime often surrounds these structures and therefore protects them. Additionally the binder improves the fire

resistance of hemp shiv. Any binder used with hemp should be breathable to allow moisture to be absorbed and desorbed from the hemp-lime.

Hemp shiv is highly absorbent and studies have shown that it can absorb as much as 250% to 400% of its own weight in water in a very short space of time (Magniont *et al.*, 2012; Nguyen *et al.*, 2009). 95% of the absorption occurs within 10 minutes of submersion in water (Arnaud and Gourlay, 2012). This can present problems when mixing with binder as the hemp shiv and binder compete for water. Dewatering of the binder by the hemp shiv can occur and as a result the binder may not be fully hydrated. Therefore more water than is necessary for hydration of the binder may be required which can increase the drying time. The Tradical HF shiv and Tradical HB binder have been specifically designed to be used together and the amount of water added to the mix will be based upon advice from the manufacturers to minimise any problems and drying time.

3.4 Hemp-lime

Hemp-lime is produced by mixing the hemp shiv with the binder and water. Varying the proportions of the binder and hemp shiv can affect the properties of the final material (Bevan *et al.*, 2008). Generally the higher the proportion of binder the higher the density of the hemp-lime once it has set although this is also affected by the amount of compaction of the wet mix.

Hemp-lime can either be cast between shuttering (Figure 3.6) or it can be spray applied against one permanent or temporary shutter (Figure 3.7). Both techniques encapsulate the studs and achieve similar results. Bevan et al. (2008) note that spraying leads to a more consistent material as hand cast hemp-lime can be over tamped leading to varying densities. However spraying is generally only suitable for larger projects where more than 70m^3 is being used (Bevan *et al.*, 2008) and is still not widely used in the UK. Spraying requires specialist machinery and trained operatives which can be costly. With both casting and spraying the shuttering can be removed after 24 hours.

Figure 3.6 Casting hemp-lime

Figure 3.7 Spraying hemp-lime (Bevan *et al.*, 2008)

Cast hemp-lime is used throughout this study. Casting was chosen for several reasons. It is the most commonly used for hemp-lime construction in the UK and therefore its use will allow this study to be representative. Additionally on a laboratory scale it is much easier to produce specimens by casting. Often the small size of the specimens would not allow for spraying to be used. The need to use costly specialist spraying equipment is

also a prohibiting factor. The hemp-lime mix used for this study was kept constant throughout, as was the target dry density. The hemp shiv used was Tradical HF and the binder was Tradical HB, both sourced from Lime Technology Ltd. The mix proportions used are as follows: 19.5% hemp shiv, 32% binder and 48.5% water by weight. This is equivalent to using one bale of Tradical HF hemp shiv with 1.5 bags of Tradical HB binder and 50 litres of water. The hemp-lime was cast to achieve a target dry density of 275kg/m^3. This is the current Lime Technology standard mix and therefore is representative of current construction practice.

The material properties of the hemp-lime were established by laboratory testing. Compressive strength is used to compare different specimens as it can be easily and reliably established via testing. In addition to compressive strength, bending strength and the effects of casting direction were also tested.

3.4.1 Hemp-lime compressive strength

Compressive testing was carried out on cylindrical specimens. Cylindrical specimens with height : diameter ratio 2:1 were used because when loaded in compression they generally exhibit a clear peak stress as well as providing an 'unconfined' strength. Cubes tend to show increasing stress with increasing strain and a peak resistance is often not clearly defined. The precedent for using cylindrical specimens has been set by previous studies (Arnaud, 2000; de Bruijn *et al.*, 2009; Evrard, 2002; Hirst *et al.*, 2012). The cylindrical specimens were cast during construction of the large scale test panels. The large scale test panels were constructed in three groups, Initial, LS1 and LS2. The cylinders have been named with reference to the group they were constructed with. Hemp-lime was taken directly from the wet mix and used to cast the cylindrical specimens.

All of the cylindrical specimens were made using the same method. The cylindrical specimens were cast in paraffin wax covered cardboard moulds. The specimens were 150mm diameter and 300mm long. The moulds were filled on a balance so that the correct amount of wet hemp-lime mix was added to ensure the correct dry density of 275kg/m^3. The hemp-lime mix was lightly levelled and tamped so that the hemp-lime was level with the top of the mould. The moulds were then capped with plastic lids

(Figure 3.8). The cylinders were then either stored with the large scale wall panels they were cast alongside or in a conditioning room (Figure 3.9) which had a constant temperature of 20^{o}C and relative humidity of 60%.

Figure 3.8 Cylinder immediately after casting

Figure 3.9 Hemp-lime cylinders in conditioning room

After 24 hours the caps were removed. This process replicated the process of removing the shuttering on site once a hemp-lime wall has been cast. The cylinders were removed from their moulds after seven days as at this point they were robust enough to be

handled. Removing them from their moulds accelerated the drying process which ensured the moisture content was at equilibrium when they were tested.

Compressive testing of the cylinders was carried out using a Dartec 100kN testing machine. The specimens were loaded under displacement control, at a rate of 3mm per minute. Prior to testing the diameter, length and weight of each specimen was recorded. Compressive stress was taken as load divided by original cross-sectional area; compressive strength as maximum (peak) compressive stress. Compressive strain was taken as change in height of the entire cylinder (platen movement) divided by original height. This is seen as a valid method for measuring strain as work undertaken at the University of Bath by Hirst (unpublished) as part of a doctoral research project compared surface mounted strain devices with platen movements and found no difference in recorded strain.

The compressive strengths and elastic moduli are shown in Table 3.2. The elastic modulus was calculated between 25% and 50% of the maximum load (Figure 3.10). Cylinders Initial (from initial wall test) A, B and C were tested at an age of 28 days from casting, whereas all of the LS1 (large scale tests No.1) and LS2 (large scale tests No.2) cylinders were tested after 90 to 100 days. All Initial and LS1 cylinders were capped with dental plaster prior to testing (Figure 3.11).

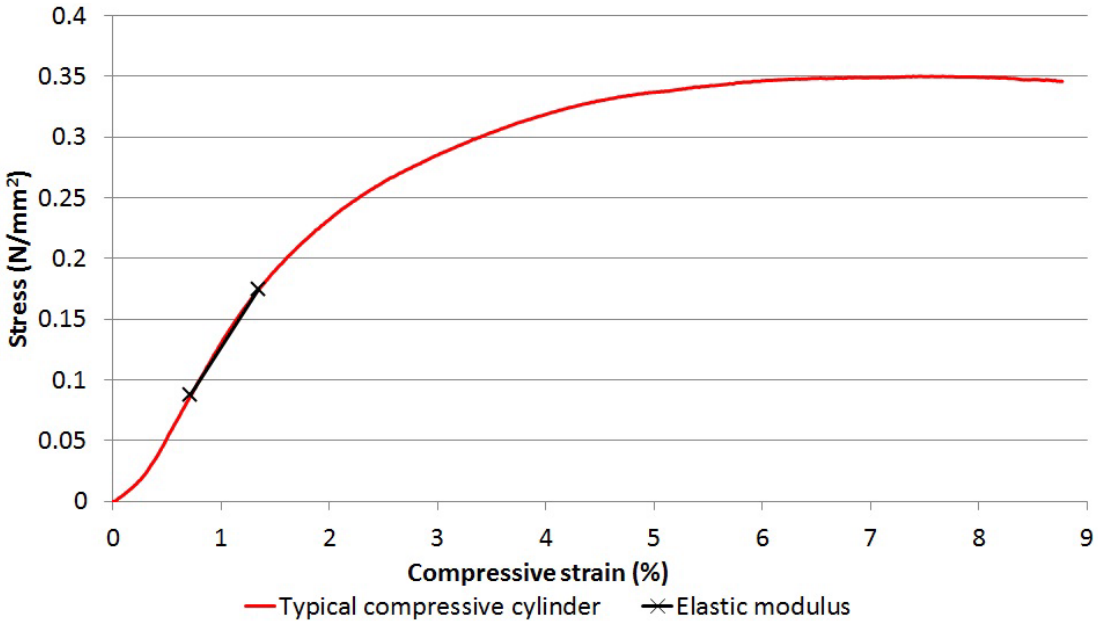

Figure 3.10 Stress .v. strain characteristic with indication of elastic modulus calculation range

Capping ensures that the top and bottom surfaces of the hemp-lime are flat and level and therefore the load is applied evenly to the entire cross section of the specimen. It also allows the axial strain in the specimen to be accurately measured using the loading platen displacement. Capping was carried out immediately before testing to minimise the possibility that moisture in the wet dental plaster would migrate into the hemp-lime and affect its performance.

The LS2 cylinders were not capped. It had been observed in a few cases on previously tested cylinders that the dental plaster on cylinders that had been capped had curved into a slight concave shape. It is likely that this was due to moisture absorption by the hemp-lime. For this reason they were not capped. During casting particular attention was paid to making sure the top and bottom surface of the cylinders were as flat and parallel as possible. When testing in this manner without capping the compressive strength is unaffected.

Figure 3.11 Compression testing of capped hemp-lime cylinder

Table 3.2 Hemp-lime compressive strength

Cylinder	Compressive strength σ_{chl} (N/mm^2)	Elastic modulus, E (N/mm^2)	Average moisture content (%)
Initial A	0.06	3.10	-
Initial B	0.06	3.70	
Initial C	0.05	4.28	
Initial average	**0.06**	**3.69**	
LS1 A	0.37	18.55	**7.7**
LS1 B	0.34	31.41	
LS1 C	0.33	27.29	
LS1 D	0.35	25.80	
LS1 E	0.75	40.08	
LS1 F	0.37	46.29	
LS1 G	0.57	52.93	
LS1 H	0.55	67.86	
LS1 average	**0.45**	**39.73**	
Standard deviation	**0.14**	**15.55**	
LS1 J	0.41	47.36	**8.6**
LS2 A	0.42	14.58	
LS2 B	0.36	13.78	
LS2 C	0.29	10.00	
LS2 D	0.42	16.74	
LS2 E	0.33	13.92	
LS2 F	0.37	14.06	
LS2 G	0.37	13.49	
LS2 H	0.31	6.57	
LS2 J	0.35	9.16	
LS2 K	0.31	12.11	
LS2 L	0.36	12.91	
LS2 M	0.33	13.26	
LS2 N	0.34	12.22	
LS2 average	**0.35**	**12.52**	
Standard deviation	**0.04**	**2.63**	

The compressive strengths and elastic moduli of the cylinders Initial A, B and C are much lower than the LS1 or LS2 cylinders. The Initial cylinders were tested 28 days after casting and consequently were not fully dry and only a small amount of carbonation had taken place. The standard deviation of the elastic modulus for the LS1 cylinders is very high. This is due to variations in the density of the hemp-lime throughout the cylinder height formed during casting. The 5% characteristic compressive strength of the LS1 and LS2 cylinders is 0.22N/mm^2 and the 5% characteristic elastic modulus of the LS1 cylinders is 14.16N/mm^2. These characteristic values will be used during theoretical predictions of wall panel test specimen performance. The characteristic strength has been calculated from LS1 and LS2 cylinders as the materials and mix proportions that were used for these cylinders will also be used for the wall panels. The characteristic elastic modulus has only been taken from LS1 cylinders as the LS2 cylinders were not capped and therefore the elastic modulus calculated from these test results is not as accurate due to crushing of the ends of the cylinders during testing.

The Poisson's ratio of the hemp-lime cylinders has not been measured due to difficulty in accurately recording it. However from the literature the Poisson's ratio for hemp-lime ranging in density from 256kg/m^3 to 460kg/m^3 is between 0.05 and 0.16 (Cerezo, 2005). Therefore by assuming isotropic properties and a Poisson's ratio of 0.05 for 275kg/m^3 hemp-lime the shear modulus can be calculated as:

$$G = \frac{E}{2(1+\nu)} = \frac{39.73}{2 \times (1+0.05)} = \underline{18.9N/mm^2}$$

Equation 3.1

The cylinders were split immediately following testing and sprayed with phenolphthalein solution to evaluate the extent of carbonation through the section. Figure 3.12 shows one of the Initial cylinders and one of the LS2 cylinders after spraying with phenolphthalein solution. The Initial cylinder was tested at an age of 28 days whereas the LS2 cylinder was tested at between 90 and 100 days age. There is a difference in carbonation penetration which can clearly be seen. The average carbonation penetration for the Initial, LS1 and LS2 cylinders is shown in Table 3.3 along with the age of testing.

Table 3.3 Average carbonation penetration

	Average carbonation penetration (mm)	Carbonation rate (mm/day)	Age tested (days)
Initial	27	0.96	28
LS1	50	0.53	90 to 100
LS2	47	0.49	90 to 100

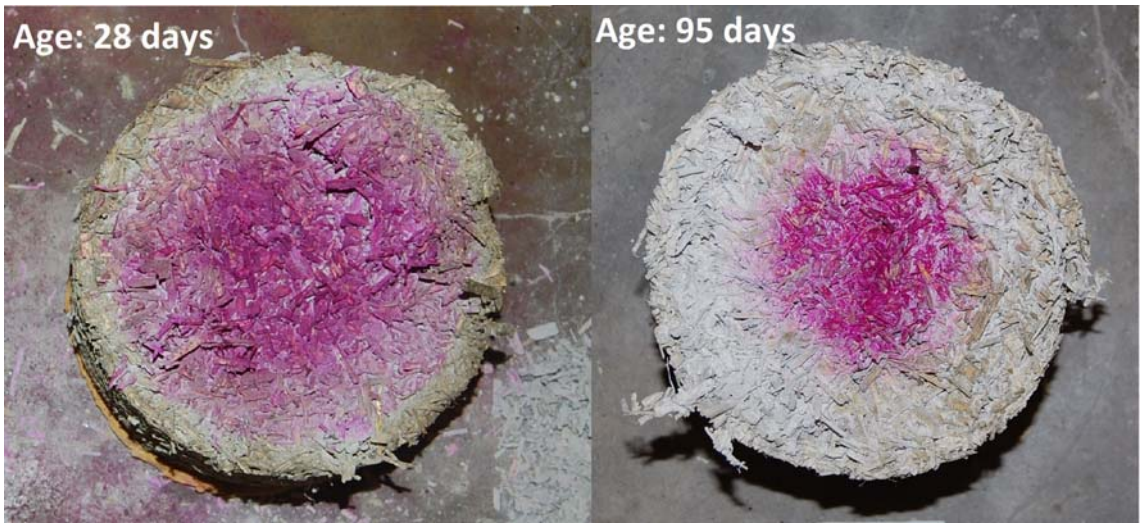

Figure 3.12 Initial (left) and LS2 (right) cylinders showing carbonation penetration

Hirst et al. (2012) proposed that the rate of penetration of carbonation could follow a square root law that is typically used for cement materials in the form:

$$d = K_c\sqrt{t}$$

Equation 3.2

where d is the depth of carbonation, K_c is the carbonation constant and t is the time in days. Hirst et al. (2012) found the carbonation constant, K_c, for several different binders by laboratory testing. One of the binders used was Tradical HB, the same binder as used during this investigation. For hemp-lime cast at a density of 275kg/m^3 using Tradical HB, K_c is 6.7 (Hirst *et al.*, 2012). From Equation 3.2 and using K_c = 6.7 the depth of carbonation penetration for the Initial cylinders at 28 days is 35mm and for the LS1 and LS2 cylinders at 95 days is 65mm. Both of these predicted carbonation penetrations are 30% higher than the actual results. The cause of this difference is likely to be a result of different mix proportions. Hirst et al. (2012) used 43% water, 36% binder and 21% hemp shiv by mass whereas the mix used in the all of the cylinders in this investigation

was 48.5% water, 32% binder and 19.5% hemp shiv by mass. The additional water in the mix will have increased the initial moisture content of the cylinders and may have reduced the rate at which carbonation was penetrating the hemp-lime. Additionally the difference could be as a result of differing curing conditions. LS1 and LS2 cylinders were left to cure indoors in the natural environment to ensure that they were representative of the large scale specimens used in the experimental study whereas the Initial cylinders and those tested by Hirst et al. (2012) were cured in a conditioning room kept at constant temperature and relative humidity of 20^{o}C and 60%.

All of the LS1 and LS2 cylinders performed in a similar manner. All of these cylinders were at moisture content equilibrium when they were tested and all had moisture contents between 7% and 10%. From these results the average compressive strength of the hemp-lime used was 0.39N/mm^2 and the 5% characteristic compressive strength is 0.22N/mm^2. The average and 5% characteristic values for the elastic moduli of the hemp-lime are 39.73N/mm and 15.55N/mm respectively. These are calculated from the LS1 tests as the elastic modulus in the LS2 tests was affected by crushing of the ends of the cylinders as they were not capped. Therefore in future work if the initial modulus is required the specimens should be capped.

The moisture content and compressive strength can be directly compared with those reported by Hirst et al. (2012) as the same binder (Tradical HB), shiv (Tradical HF) and density (275kg/m^3) were used. The hemp-lime tested by Hirst et al. (2012) had compressive strengths of 0.05N/mm^2 at both 28 days and 91 days and moisture contents of 9.2% at 28 days and 6.2% at 91 days. Helmich (2008) also used the same binder and shiv but produced hemp-lime with a density of 486kg/m^3 with a compressive strength of 1.4N/mm^2 at 28 days. Elfordy et al. (2008) used similar mix proportions and produced hemp-lime with a density of 300kg/m^3 with a compressive strength of 0.2N/mm^2.

The results from the Initial cylinders in the investigation and the 28 day results from Hirst et al. (2012) are similar, as would be expected. However the difference in compressive strength between the LS1 and LS2 and the 91 day results from Hirst et al. (2012) are unexpected. The only significant difference between the cylinders tested is the storage conditions while curing was taking place. LS1 and LS2 were stored indoors at uncontrolled temperature and relative humidity, whereas Hirst et al. (2012) stored the

cylinders at a constant temperature of 20°C and 60% relative humidity. The two other potential differences are in the composition of the binder, as its exact details are not released by its producer Lime Technology, and the density of the hemp-lime. Hirst et al. (2012) used the air dry density, whereas in this investigation the oven dry density is used. However with a moisture content of 6.2% this only makes a difference of 17.0kg/m^3 in density and this is unlikely to have such a significant effect on the compressive strength. A combination of all three possible causes may amount to the difference seen in the results. The compressive strengths reported by Elfordy et al. (2008) show the closest correlation. From the literature for hemp-lime at densities between 256kg/m^3 and 391kg/m^3 the compressive strength can vary between 0.06N/mm^2 and 0.45N/mm^2 and the elastic modulus between 2.5N/mm^2 and 55N/mm^2 (Hustache and Arnaud, 2008). Comparing these and the compressive strength of the hemp-lime being used in this study, the results from this investigation are not outside what is the norm for cast hemp-lime.

3.4.2 Hemp-lime bending strength

The bending strength of the hemp-lime was established from four point bending tests. Prismatic specimens were used. Moulds were constructed from phenolic coated plywood. They were filled using the same process at the cylindrical specimens with the wet hemp-lime mix weighed out so that a dry density of 275kg/m^3 was achieved. The size of the specimens and the test method were based on flexural strength tests for masonry set out in BS EN 1052-2 (1999) as hemp-lime is similar is to masonry with a low flexural strength. Cast hemp-lime is not a uniform material as it is built up in layers the orientation of the pieces of shiv are not random. Therefore its bending properties will vary depending upon which axis it is stressed. Prisms were cast from two different directions (Figure 3.13), and tested at 90 days after casting.

The test set up is shown in Figure 3.14. Linear Variable Differential Transformer (LVDT) were used to measure displacements and a load cell to measure the load. Both the load and displacements were recorded by a System 5000 data logger at 10 times a second. Displacements were measured at the two supports and two loading points in order to record any crushing of the hemp-lime. Displacement of the actual loading rig was also recorded. The load was applied using a hydraulic jack and hand pump. The

load was applied as slowly and evenly as possible due to the potentially weak nature of the specimens. The specimens failed within two to three minutes of testing commencing. The bending strength is shown in Table 3.4.

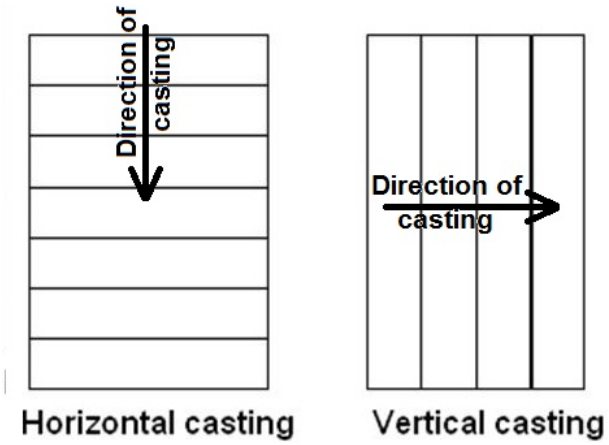

Figure 3.13 Wall specimen casting directions

Figure 3.14 Four point bending test set up

Table 3.4 Bending test results (90 days)

Specimen number	Density (kg/m^3)	Max σ_{bhl} (N/mm^2)	Moisture content at test (%)
V1	297	0.07	11.9
V2	293	0.06	10.7
V3	297	0.09	12.0
H1	308	0.03	15.3
H2	295	0.03	11.4
H3	294	0.04	11.2

All six specimens failed between the two points of load application. From the results average flexural strengths can be calculated. These are 0.07 N/mm^2 for the vertical cast specimens and 0.04 N/mm^2 for the horizontally cast specimens. It is clear from the bending strengths that the casting direction had a large effect on the performance of the specimens with the vertically cast specimens having roughly twice the bending strength of the horizontally cast specimens. Statistically analysing these results with a t-test and a null hypothesis of the results being the same, it is shown that the results will only be the same in 2.6% of cases with a certainty of 95%. As the percentage of results that will be the same is less than 5% it can be safely assumed that the bending strengths in each direction differ. These bending strengths are lower than those found by Elfordy et al. (2008). This is likely to be due to the lower density of hemp-lime used in this study.

The vertically cast specimens showed a small amount of post peak ductility during failure with the two halves of the specimens slowly breaking away from each other as the bond broke on each individual piece of shiv. This behaviour is largely caused by using a hydraulically applied load which decreases as the deflection increases if no further pressure is being applied. If static masses were used it is likely that this phenomenon would not occur. The horizontal specimens failed along their lines of casting in a similar manner to masonry failing along its bed joints.

3.4.3 Effect of casting direction on compression performance

The compressive strength of the hemp-lime will also vary according to which axis it is being compressed. Six prism specimens of hemp-lime were cast in moulds measuring

300mm high by 150mm square. The specimens were cast in two different directions, vertically and horizontally, as with the bending specimens. They were tested 90 days after casting. They were removed from the conditioning room (constant 20^{o}C, 60% RH) an hour before testing and the top and bottom of the specimens were capped with dental plaster to give level and uniform loading surfaces. The prisms were loaded in compression using the Dartec 100kN loading frame under displacement control (Figure 3.15) at a rate of 3mm/min. The properties of the prisms are shown Table 3.5.

Figure 3.15 Prism specimen in Dartec testing frame

Table 3.5 Prism dimensions and initial modulus

Specimen	**Density (kg/m^3)**	**Moisture content at test (%)**	**Compressive strength (N/mm^2)**	**Strain at peak stress (%)**	**Elastic modulus (N/mm^2)**
Vertical 1	294	6.8	0.07	7.4	7.89
Vertical 2	293	6.8	0.07	5.2	8.73
Vertical 3	294	7.0	0.07	8.3	10.44
Horizontal 1	294	6.8	0.14	1.0	14.29
Horizontal 2	296	7.6	0.11	1.1	15.66
Horizontal 3	293	6.5	0.14	1.0	12.75

These results did not display the phenomenon of indefinite increases in stress with strain usually associated with prismatic specimens (specimens had a height to width ratio of 2:1). From the results shown in Table 3.5 the average compressive strength of the horizontal (compressive force perpendicular to casting layers) specimens is 0.13 N/mm^2 and the average for the vertical (compressive force parallel to casting layers) specimens is 0.07 N/mm^2. Comparing with the cylindrical specimens the compressive strength and the elastic modulus are lower. With the horizontal specimens this has been caused by the testing direction with the layers parallel to the load. With the vertical specimens it could be due to the shape of the specimens, however further investigation would be required to confirm this. This result indicates significant orthogonality in the material. This will have implications when using hemp-lime to enhance the structural capacity of studwork framing as the direction of loading and stressing of the hemp-lime will have to be carefully considered to ensure that the difference in compressive and flexural strength about each axis is taken into account during the analysis of results and design of this type of composite wall.

3.4.4 Effect of accelerated drying on compressive strength

Cast hemp-lime can take a long time to dry due to the high proportion of water in the mix. In order to reduce the drying time and therefore speed up the testing programme the drying process can be accelerated by placing the hemp-lime specimens in a heated chamber where the air is regularly extracted and circulated. However, rapid drying could affect the mechanical properties of the hemp-lime. Therefore the effects of different temperatures on hemp-lime were studied to find out if this drying process altered the material's mechanical properties.

Cylinders of hemp-lime were cast using the same process as for previous cylindrical specimens. The cylinders were placed into ovens at four different ages after casting (4, 7, 14 and 28 days) and three different oven temperatures as detailed in Table 3.6. All of the cylinders, apart from those in the 50^{o}C vented oven, were in sealed containers for the first 48 hours in the ovens to prevent moisture evaporating during this time as this is representative of the drying process used in industry. The 50^{o}C vented specimens were not sealed to allow comparisons to be made with the sealed specimens. The cylinders were removed from the oven when their moisture content, measured by weighing,

reached 12%. Two cylinders were allowed to dry naturally in the conditioning room at 20°C and 60% relative humidity.

Table 3.6 Number of specimens at each temperature and age

Cylinder age (days) into oven	**Oven temperature (°C)**			
	30	**50**	**50 (vented)**	**70**
4	3	3	3	3
7	3	3	2	3
14	3	3	3	3
28	3	3	2	3

The cylinders were tested un-capped in compression using a Dartec 100kN testing frame in displacement control at a rate of 3mm per minute 90 days after casting. The average compressive strength and elastic modulus for each age and temperature are shown in Figure 3.16 and Figure 3.17.

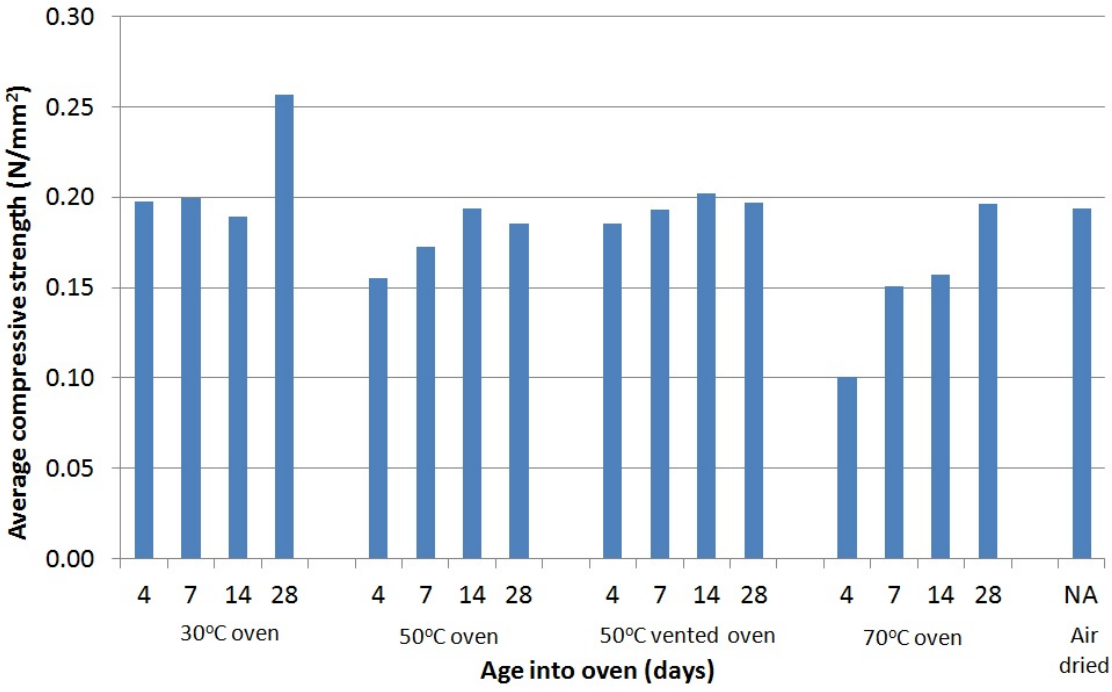

Figure 3.16 Accelerated drying cylinder compressive strength

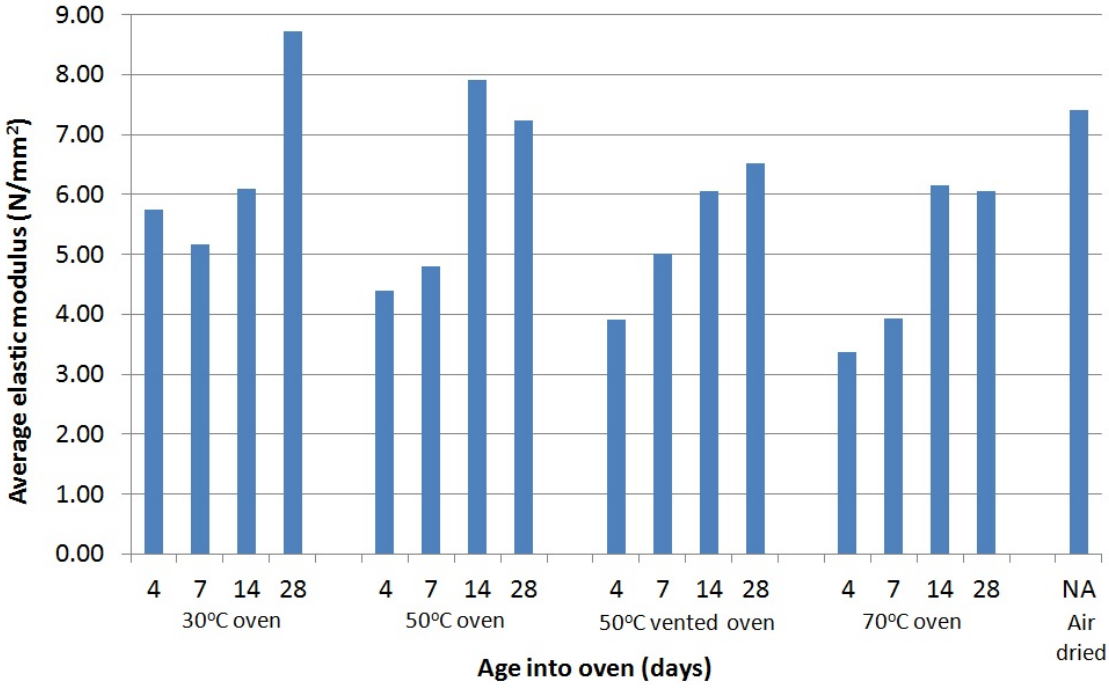

Figure 3.17 Accelerated cylinder drying elastic modulus

From Figure 3.16 comparing the air dried specimens with the 30°C oven specimens there is very little difference in compressive strength. With both 50°C oven specimens there is 0.01N/mm^2 to 0.04N/mm^2 difference in strength between the air-dried specimens and the oven dried four day and seven day specimens. The 70°C specimens show the greatest difference in compressive strength at four days, seven days and 14 days. Similar patterns can be seen in the elastic modulus results shown in Figure 3.17. Following compressive testing the cylinders were split and the freshly broken surfaces were sprayed with phenolphthalein solution. Figure 3.18 shows the extent of penetration of carbonation. The specimens are labelled with their age into the over first, followed by the oven temperature. For example, 7 day 30°C was placed into a 30°C oven at 7 days after casting.

The extent of penetration of carbonation as shown by phenolphthalein solution is similar in all of the cylinders apart from the 4 day, 7 day and 14 day 70°C specimens which showed more carbonation. This result is unusual as the opposite might be expected because the cylinders were dried very quickly and therefore they may have been too dry for carbonation to take place. As spraying with phenolphthalein solution showed these unusual results specimens of the binder from each of the cylinders were taken for Thermo Gravimetric Analysis (TGA). The specimens were tested in a Setaram TGA 92 machine.

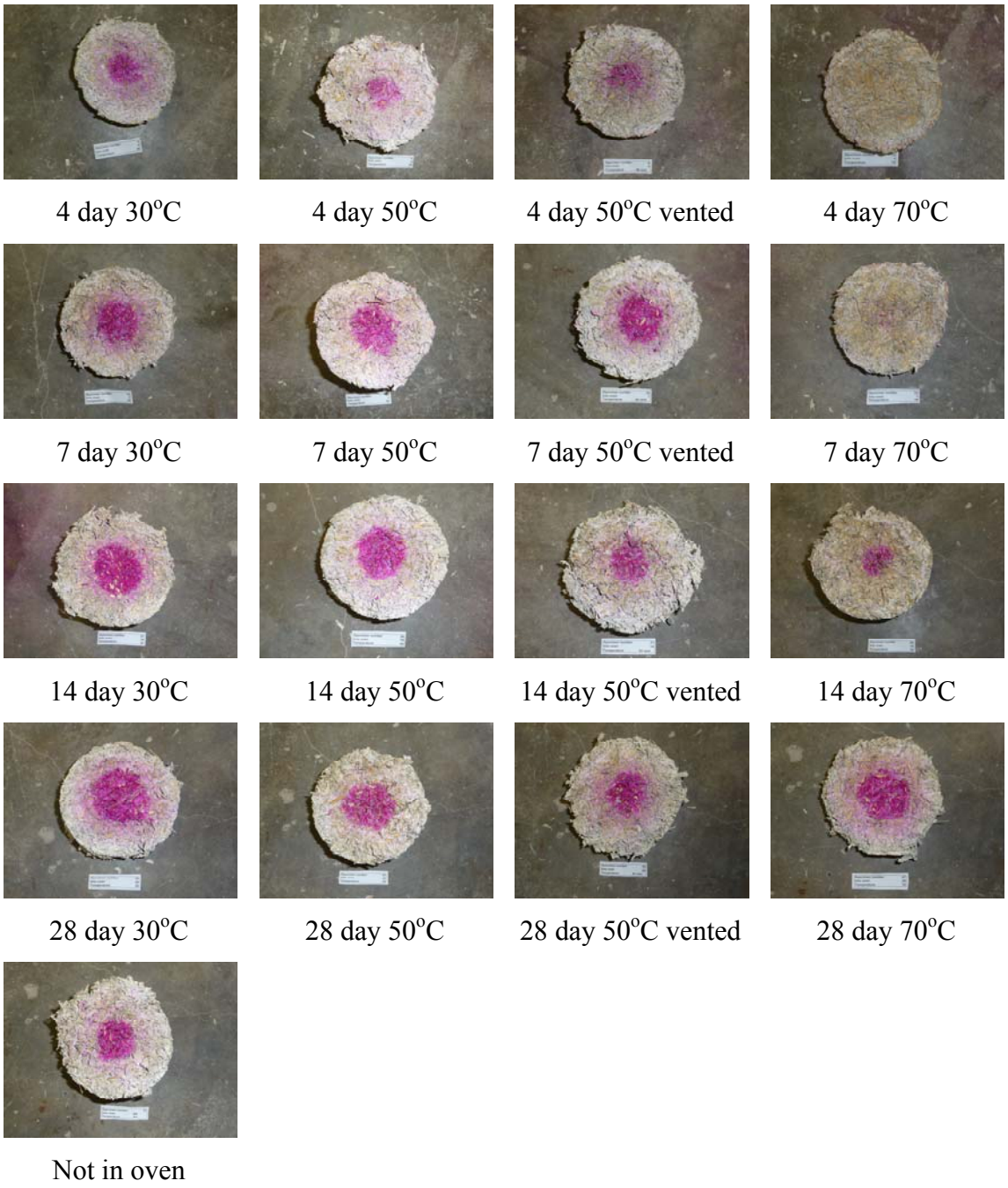

Figure 3.18 Extent of carbonation penetration

In TGA a small specimen of the binder is heated under controlled conditions within a furnace up to a temperature of 900°C. During the heating process the weight, temperature and change in temperature are all very carefully monitored and recorded. Different compounds within the binder burn off at different temperatures and therefore if these temperature compound relationships are known the quantity of each compound in the specimen can be established. In the specimens of binder from the cylinders at 450°C calcium hydroxide ($Ca(OH)_2$) burns off to calcium oxide (CaO) and water (H_2O)

and at 800°C calcium carbonate ($CaCO_3$) burns off to calcium oxide (CaO) and carbon dioxide (CO_2).

Specimens of the binder were taken from the centre of a cylinder from each temperature and age into the oven. The 17 specimens were collected by crushing the hemp-lime between hands into a 125 micron sieve and brushing it around the sieve until enough binder had passed through. The collected binder was then placed into a small glass pot which was transferred to a 100°C oven to thoroughly dry the specimen. Once dry the lids were tightly placed on the glass pots while still in the oven. This process ensured there was no moisture in the specimens and therefore further carbonation could not take place between specimen collection and testing. Only one specimen from each cylinder was tested as each TGA run is very time consuming and costly.

The results from the TGA for percentage calcium hydroxide ($Ca(OH)_2$) and calcium carbonate ($CaCO_3$) are shown in Figure 3.19.

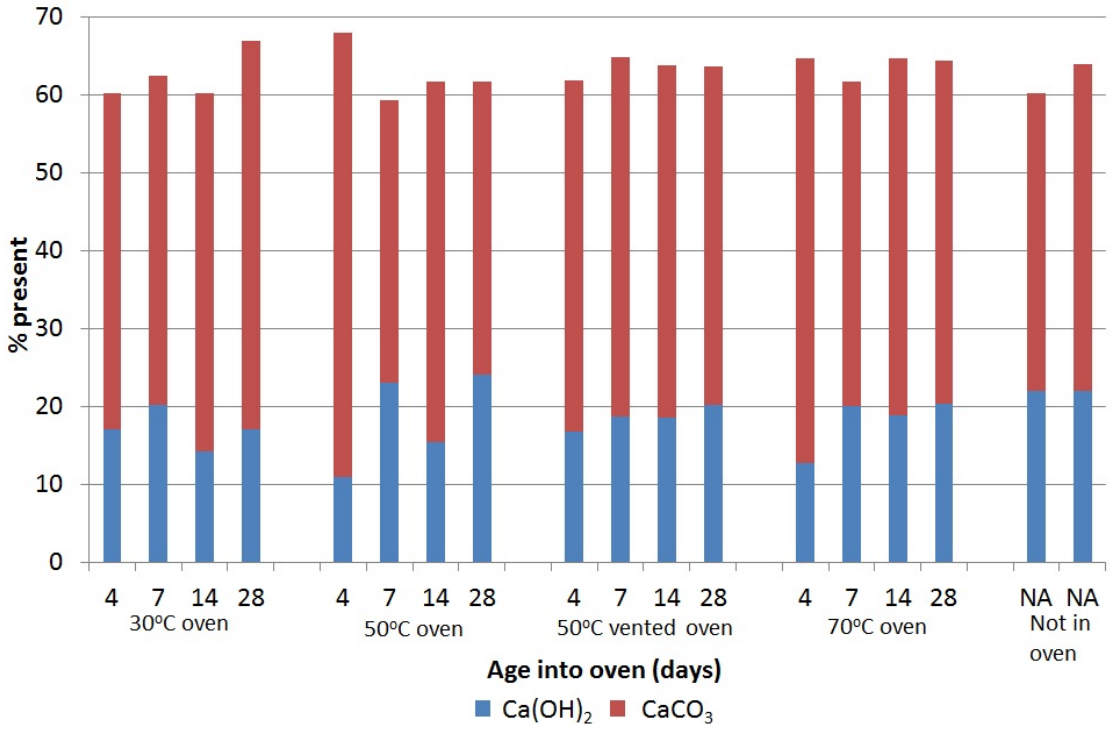

Figure 3.19 Relative calcium hydroxide and calcium carbonate contents from TGA tests

The total percentage of calcium hydroxide and calcium carbonate should be the same for all of the specimens as calcium hydroxide is changed into calcium carbonate during the process of carbonation. This is generally shown in Figure 3.19 and the variations in

total percentage result from the limited number of tests undertaken. The same can be said of the separate results for both calcium hydroxide and calcium carbonate, particularly the calcium hydroxide results for the 50^{o}C oven. The main point shown in Figure 3.19 is that the 4 day, 7 day and 14 day 70^{o}C cylinders do not appear to be any more or less carbonated than the other cylinders. This is in contradiction to the results shown in Figure 3.18 when using phenolphthalein solution. It is possible that the aggressive drying of the cylinders caused a casing of calcium carbonate to form around the calcium hydroxide. As a result the phenolphthalein solution could not detect the calcium hydroxide as it was not exposed. This is only one possible explanation and further research is required here.

From the results of both the compressive properties of the hemp-lime and the TGA, hemp-lime should not be detrimentally affected if it is placed into the accelerated drying environment at an age greater than 14 days and at a temperature lower than 50^{o}C. These conditions will be followed for accelerated drying of large scale test specimens.

3.5 Studwork materials

The choice of stud material is important as it has the potential to affect the behaviour of the composite hemp-lime and studwork walls during testing. There are three different stud walling materials that could be used within this study and they will each have a different effect on the testing carried out. The three materials considered for this study were sawn timber, Laminated Veneer Lumber (LVL) and cold formed lightweight steel sections (Figure 3.20).

Figure 3.20 Stud materials (lightweight steel, LVL, sawn timber)

Within the UK two sizes of C16 standard timber are commonly used within structural studwork walling, 38mm by 89mm and 38mm by 140mm. Therefore it would be more representative to utilise one of these sizes and grade of timber during this investigation as it is the type of construction that hemp-lime is currently cast around (Bevan *et al.*, 2008). Within the research environment there are however some disadvantages to using sawn timber. As timber is a natural material it is inherently variable. There are knots, splits or other variable natural features that affect performance. Within large pieces of walling these are not a problem as the overall composite performance of the wall will be unaffected. However in smaller laboratory test specimens any variability will be more apparent. This therefore could cause anomalies in performance.

Engineered timber such as LVL or glulam would significantly reduce variation due to these problems. With an engineered timber it is possible to get a more consistent material and therefore properties as there are no knots or other serious flaws in the material. Engineered timber is also significantly stronger and stiffer than standard timber, LVL has over twice the bending strength of normal C16 timber ($44N/mm^2$ compared to $16N/mm^2$ (IStructE and TRADA, 2007)). There is however a disadvantage to using engineered timber. It is not generally used in timber studwork walling as it is more expensive than normal timber, less widely available and is stronger and stiffer than necessary for this type of construction. For use in test specimens the main problems are the increased strength and stiffness. As this study will be investigating the composite behaviour of the studwork elements and hemp-lime their performance and how they share load will be partly influenced by their relative stiffness. The studs used in this study need to be representative of the studs used in buildings. Therefore LVL will not be used for test specimens as it is unlikely that it will be used with hemp-lime in the future.

Lightweight steel studwork is even more consistent in strength and stiffness than engineered timber. Helmich (2008) used lightweight steel studs for the reasons of consistency. Lightweight steel studwork is used in walling, but usually of larger commercial type buildings. Steel studs could be applicable in all studwork building types however where there is a potential issue of insect attack, such as termites, on the timber. If steel were to be used with hemp-lime it would need protection from corrosion as initially the hemp-lime has a high moisture content, but also because hemp-lime

absorbs and desorbs moisture in the atmosphere and therefore the steel would constantly be in an environment that could promote corrosion. Most lightweight steel studwork is galvanised, this however is not appropriate for use with lime as the galvanising and the lime react and the protective layer is diminished. Paint finishes would also not be appropriate as they could not be renewed once the stud was encased in hemp-lime. Usually any steelwork used in conjunction with lime, such as wall ties in lime mortar, is stainless steel as it is resistant to the corrosive effects of moisture and lime. This is very expensive and therefore not practical for use in studs. As a result it is considered inappropriate to use lightweight steel studwork with hemp-lime in practice and therefore it will not generally be used during this study.

Sawn C16 graded timber will be used for all of the studwork framing tested in this study with the exception of one initial wall test which will use lightweight steel studwork. The compressive strength parallel to the grain and the bending strength of the timber used were established from laboratory testing. The test procedures for both properties followed BS 373 (1957) and were undertaken on small clear specimens. The bending tests were carried out with the timber at a moisture content that was at equilibrium with the surroundings. The compression tests were carried out on specimens of varying moisture contents to allow the change in strength with relation to moisture content to be studied as this may be critical in full size wall panels.

The sizes of the test specimens conformed to BS 373 (1957). The bending test specimens were 2cm by 2cm in cross section and 30cm long (for a 28cm span, Figure 3.22) and the compression test specimens were 2cm by 2cm in cross section and 6cm long (Figure 3.21). The testing of the compression specimens is shown in Figure 3.23 and the bending specimens in Figure 3.24. The specimens were tested in an Instron 3369 50kN testing frame. The compression specimens were loaded at a rate of 0.635mm/min and the bending specimens at 6.6mm/min in accordance with BS 373 (1957).

Figure 3.21 Compression specimen specification (BS 373, 1957)

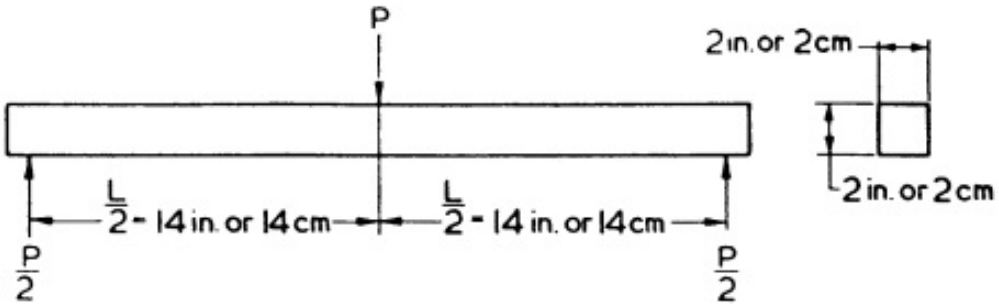

Figure 3.22 Bending specimen specification (BS 373, 1957)

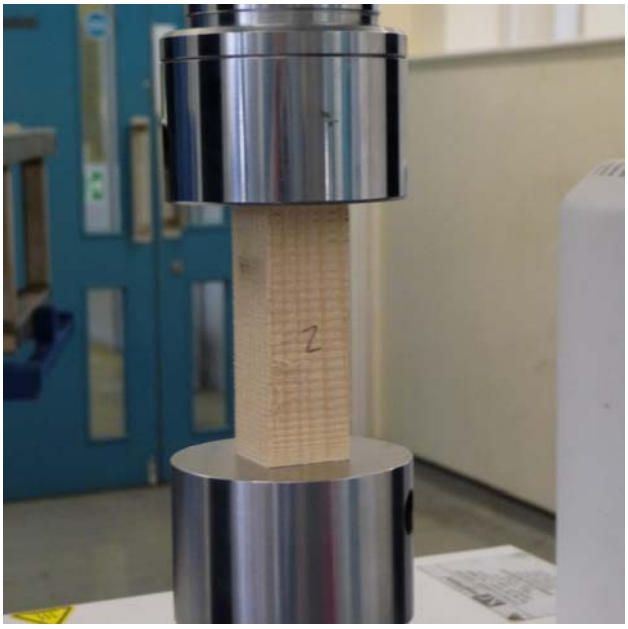

Figure 3.23 Compression small clear testing

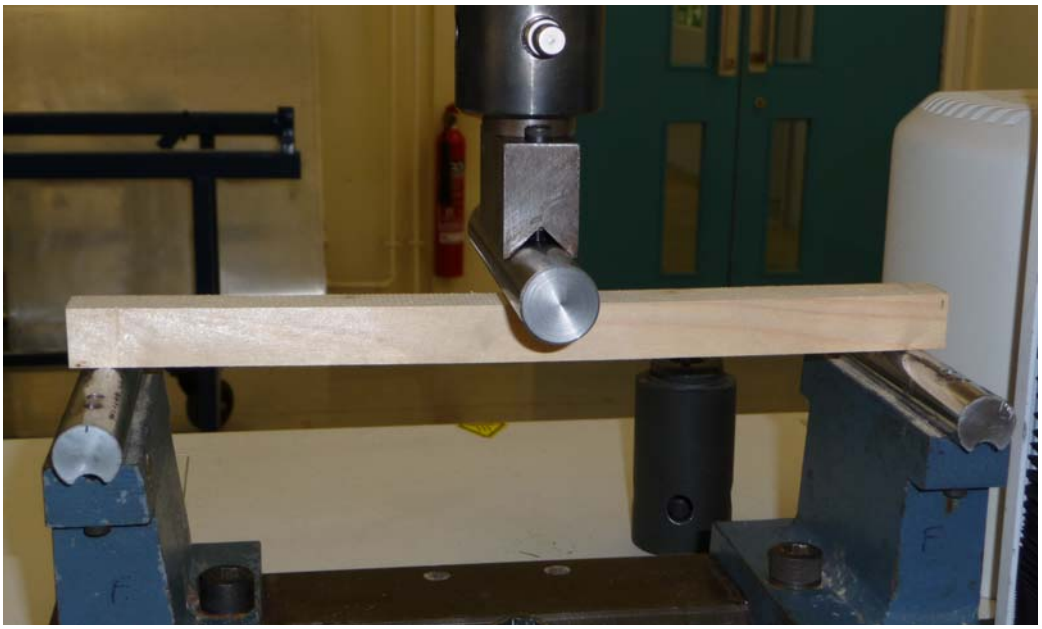

Figure 3.24 Bending small clear testing

Ten small clear specimens were tested in bending. The results are shown in Table 3.7. The average bending strength was 71.7N/mm^2 and the 5% characteristic bending strength was 64.6N/mm^2. These values will be used for theoretical predictions of performance of full scale hemp-lime and studwork frame wall panels.

Table 3.7 Small clear bending specimen test results

Specimen	**Flexural strength (N/mm^2)**	**Flexural modulus (N/mm^2)**
1	68.1	9,253
2	74.5	10,474
3	66.6	8,867
4	71.9	9,567
5	79.5	11,059
6	71.4	9,639
7	71.1	9,625
8	77.7	10,602
9	69.7	9,749
10	67.1	9,536
Average	71.7	9837
Standard deviation	4.3	668

The results from the 35 compression small clear specimens are shown in Figure 3.25 with compressive strength plotted against moisture content. A third order polynomial trend line has been fitted to the results. The timber design service classes as defined by BS EN 1995 (2004) are also shown. Service class 1 relates to timber that is used in an internal environment which will not exceed a moisture content of 12% during its life. Service class 2 if for timber that is in a protected environment and will not exceed a moisture content of 20% during its life. Service class 3 is for timber used externally. The timber in a hemp-lime wall is likely to be in service classes 1 or 2 once the wall has reached equilibrium. The exact moisture content will be dependent upon the atmospheric conditions. Figure 3.25 has been plotted to allow the strength of the timber used to be easily determined throughout a range of moisture contents.

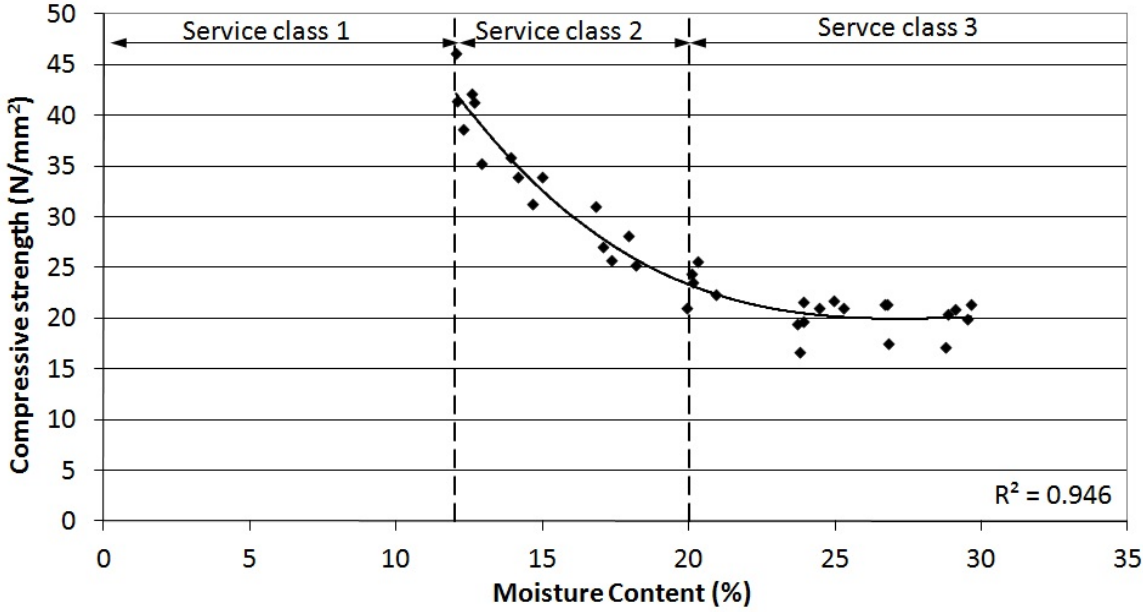

Note: Service classes as defined by BS EN 1995 (2004)

Figure 3.25 Timber compressive strength

From Figure 3.25 it is clear that as the moisture content of the timber increases the compressive strength reduces. The compressive strength is around 20N/mm^2 at moisture contents greater than 25%. At moisture contents less than 20% the compressive strength increases rapidly to a maximum of 46.1N/mm at 12% moisture content. As the timber studs in hemp-lime construction are cast into the wet hemp-lime mix, their moisture content will increase when the hemp-lime is cast and slowly dry out with the hemp-lime. As the wall is drying out the strength of the studs will change, therefore it is

important to know the strength of the timber at different moisture contents. The average density of all of the small clear specimens is 479.6kg/m^3.

The bearing strength of the timber perpendicular to the grain was tested. The test set up is shown in Figure 3.26. Sections of C16 timber 150mm long by 89mm wide by 38mm thick were loaded with a steel block 38mm wide. The loading block was chosen as it was representative of a 38mm by 89mm stud bearing onto the header or footer rails being used throughout this study. From these tests the average bearing strength perpendicular to the grain was 9.3N/mm^2.

Figure 3.26 Timber bearing strength testing

The strengths of the timber detailed above will be used during theoretical analysis of hemp-lime and timber studwork composite walling during this study.

3.6 Lime render

Weather protection to the external face of hemp-lime walls is essential. This can be provided as rain screen cladding or render. The finishes must allow the hemp-lime to breathe so that it can absorb and desorb moisture as atmospheric moisture levels change. Lime based renders are used as they are vapour permeable. When external finishes are applied in this study render will be used.

The render used in this study is Baumit FL68. This is a formulated lightweight fibrous lime based render. The render is comprised of sand, cement, lime, mineral and organic lightweight aggregates, fibres and additives (Lime Technology, 2010a). The material properties of the render have been established via laboratory testing. The flexural strength and the compressive strength were tested following the procedures set out in BS EN 1015-11 (1999) using prisms of render 40mm by 40mm in cross section and 160mm long. The prisms were loaded using a Dartec 100kN testing frame under displacement control at a rate of 0.5mm per minute (Figure 3.27 and Figure 3.28). The average flexural strength of the render is 0.93N/mm^2 and the 5% characteristic flexural strength is 0.66N/mm^2. The average compressive strength of the render is 2.22N/mm^2 and the 5% characteristic compressive strength is 1.42N/mm^2. All of the prisms were tested between ages of 90 days and 100 days after casting.

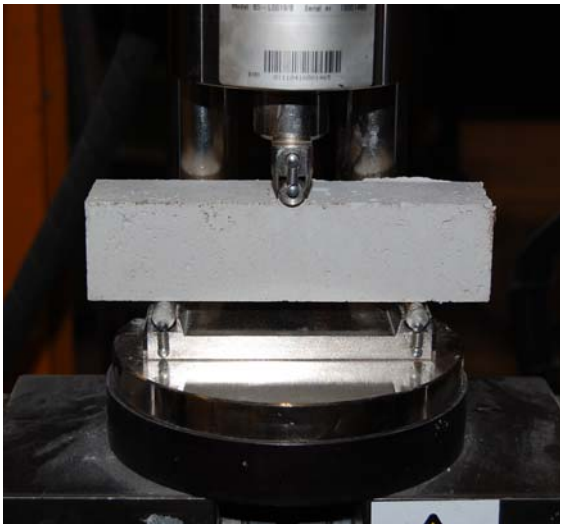

Figure 3.27 Render flexural testing

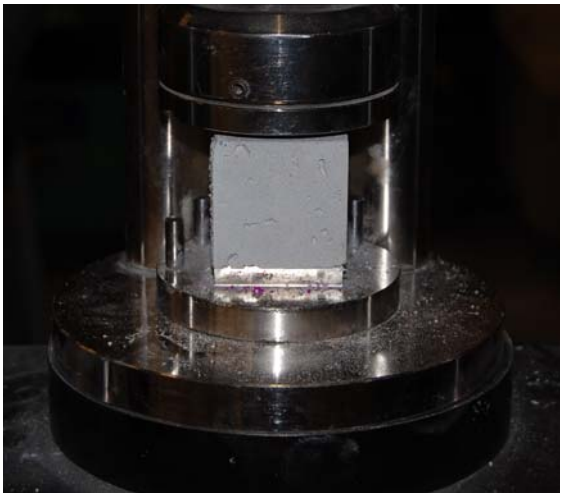

Figure 3.28 Render compressive testing

The elastic modulus of the render was measured by loading 40mm by 40mm cross section by 160mm long prisms in compression along their long axis and recording the stress and the strain. The prisms were tested using the Dartec 100kN testing frame. The stress was recorded via the load cell on the testing frame and the strain was measured using a 100mm long DeMec gauge (Figure 3.29). DeMec studs were attached to each of the four long sides of the prisms. The load was increased in increments of 0.25kN and held while the stress and strain were recorded. The load was held for 60 seconds while the DeMec readings were taken and varied by an average of 0.01kN during this time. Figure 3.30 shows the stress strain plot for each render specimen.

Figure 3.29 Render elastic modulus testing

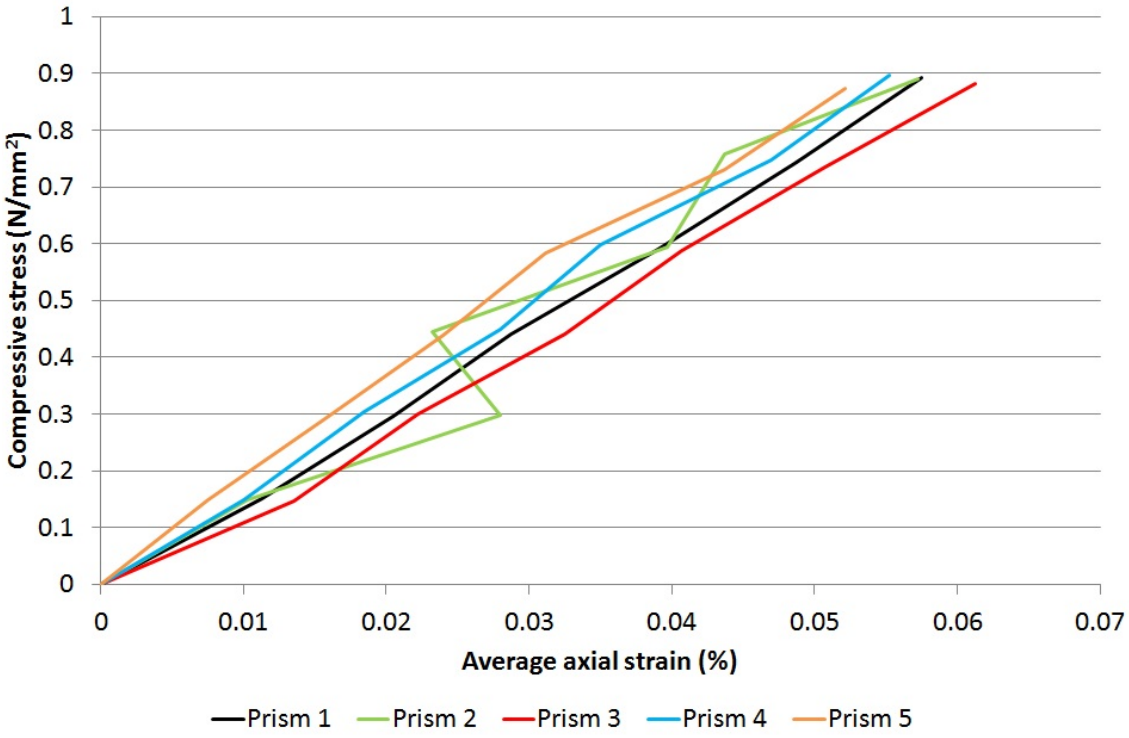

Figure 3.30 Render prism stress strain curves

All of the specimens except for Prism 2 show linear stress strain curves. With Prism 2 the curve varies with the gradient becoming negative at times. The loading platens on the testing frame may not have been properly bedded on the specimen ends or there may have been some contamination on the ends of the specimen causing uneven loading. For this reason it has been discounted when calculating the average elastic modulus. This elastic modulus was calculated for each specimen between stresses of 0.15N/mm^2 and the maximum recorded stress to remove any initial settling of the loading platens on the specimens. The elastic modulus for each specimen is shown in Table 3.8.

Table 3.8 Render elastic modulus

Specimen	**Elastic modulus (N/mm^2)**
Prism 1	1551
Prism 3	1441
Prism 4	1625
Prism 5	1673
Average	**1573**
Standard deviation	**101**

3.7 Sheathing board

A sheathing board is used on some of the wall panels tested during this study. The sheathing board performs two functions. It provides permanent formwork for the hemp-lime to one side of the wall and it provides some racking resistance to the studwork framing. The sheathing board must have properties that allow it to remain rigid when wet hemp-lime is being cast, but also be vapour permeable once the wall is constructed.

One sheathing board that satisfies these criteria is Resistant Multi-pro XS. This is a 9mm thick magnesium silicate fibreglass mesh reinforced sheathing board. It has been used during this study as it is representative of what is currently used with hemp-lime construction. The properties shown in Table 3.9 are taken from the manufacturer's data.

Table 3.9 Multi-Pro XS properties

Property	**Value**
Tensile strength	2.72 N/mm^2
Modulus of rupture	12.4 N/mm^2
Modulus of elasticity	6503 N/mm^2
Density	1050 kg/m^3
Moisture content	8.6 %
All values from manufacturer (Resistant, 2012)	

The only property that remained to be tested in the laboratory was the slip modulus between the sheathing board and the 38mm by 89mm C16 timber studs used in the test wall panels. This was tested by fixing a piece of Multi-pro XS sheathing board to each side of a section of stud with one 3.5mm diameter by 38mm long black phosphate drywall screw and performing a push out test as shown in Figure 3.31 and Figure 3.32. The specimens were tested in the Dartec 100kN testing frame at a displacement rate of 3mm/min. The results are shown in Figure 3.33.

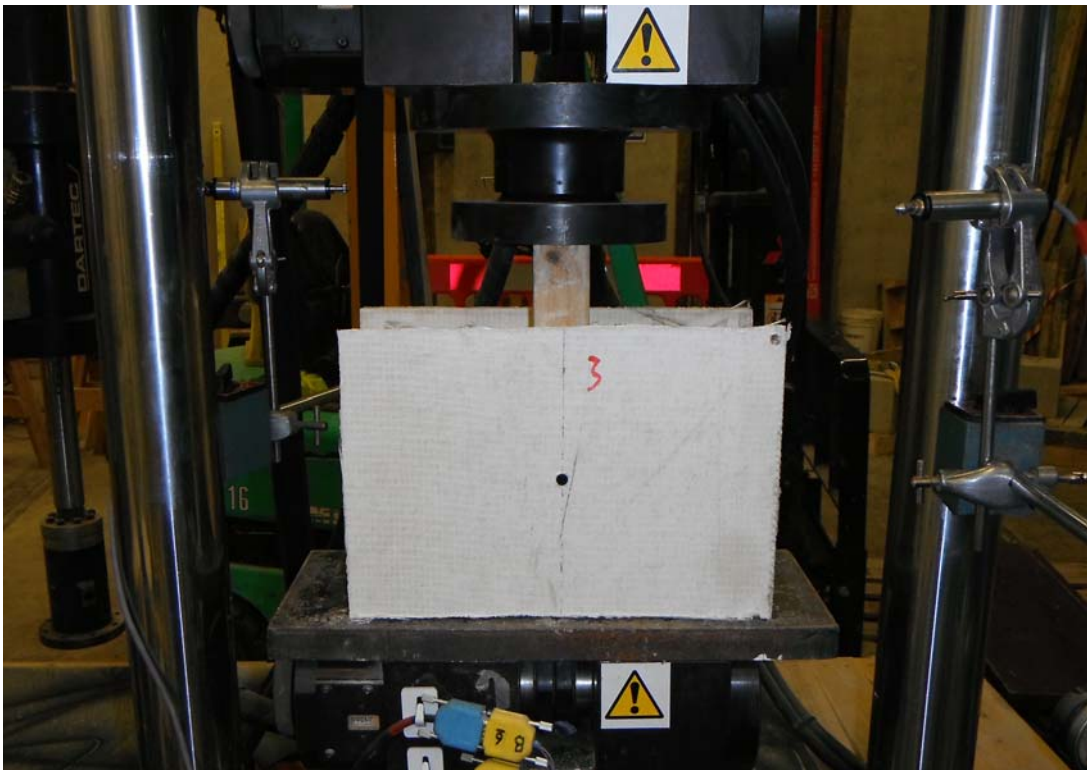

Figure 3.31 Multi-pro XS to timber slip modulus testing

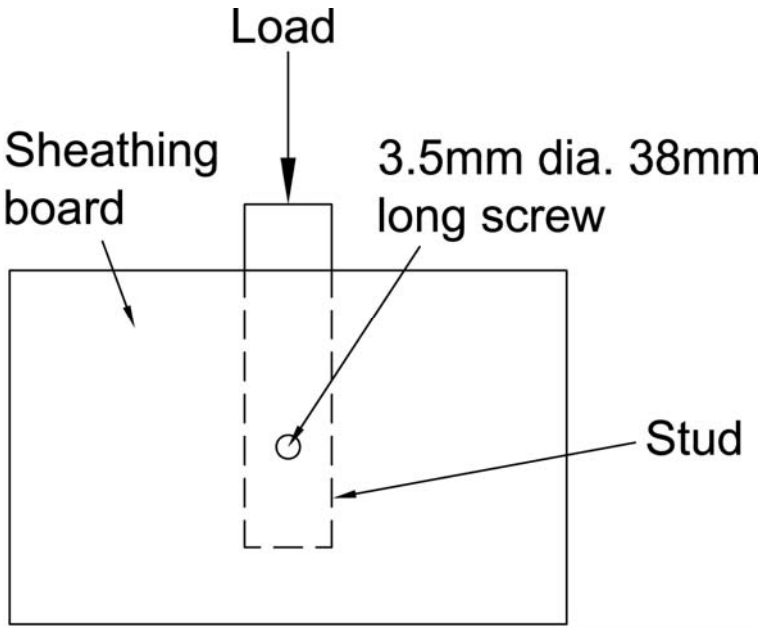

Figure 3.32 Multi-pro XS to timber slip modulus test set up

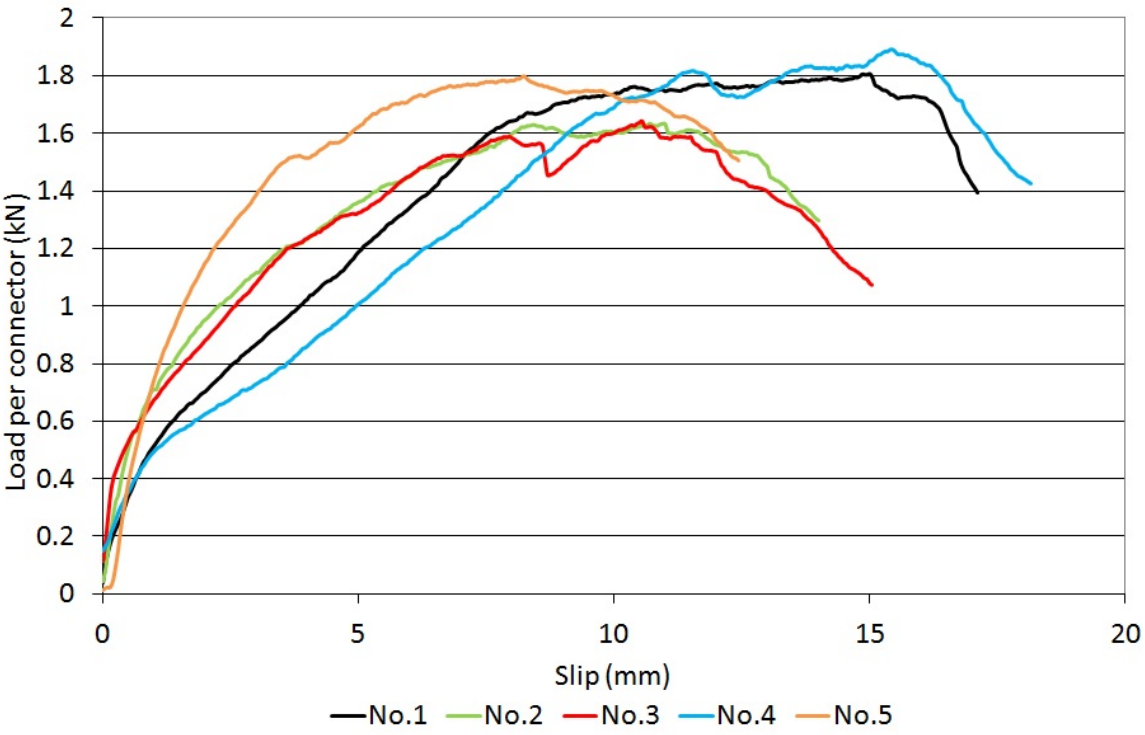

Figure 3.33 Multi-pro connection slip test results

The slip modulus for each connector was calculated between loads of 0.2kN and 0.4kN as only very small movements will be expected in the sheathing to stud connections. The slip modulus and strength are shown in Table 3.10. The large differences in slip modulus are caused by natural variations in the timber studs.

Table 3.10 Multi-pro connector slip modulus

Specimen	**Slip modulus (N/mm^2)**	**Strength (kN)**
No.1	440	1.80
No.2	890	1.64
No.3	1052	1.64
No.4	402	1.89
No.5	1038	1.80
Average	764	1.75

3.8 Connectors

The stiffness and strength of the two timber to timber connections in the timber studwork framing to be used during this study were tested. These were the stud to header and footer connections and the horizontal rail to stud connections. The horizontal

rails are used when the studwork frame is cast on the edge of the hemp-lime and prevent separation of the two elements.

3.8.1 Stud to header and footer

Five different mechanical connectors were tested in the stud to header and footer joints. The connectors used are shown in Table 3.11. Small sections of joint were constructed with two connectors per joint. The joints were tested in the Dartec 100kN testing frame. The base of the joint was fixed to the bottom jaw of the testing frame and the vertical section of the joint (representing the stud) was loaded in tension via the top jaw as shown in Figure 3.34. Five specimens for each connector type were tested.

Table 3.11 Joint test fixing details

Fixing type	
3.75mm x 75mm long nails (**N**)	
No.8 x 75mm long screws (**No.8**)	
No.12 x 100mm long screws (**No.12**)	
6.5mm dia. x 150mm long Double Thread screws (**DT**)	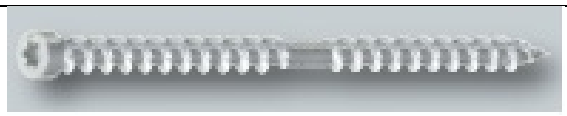
6mm dia. x 140mm long Washer Head screws (**WH**)	

Figure 3.34 Joint test set up

The average stiffness and average maximum load for each connector type are shown in Table 3.12 and typical results are shown in Figure 3.35. The stiffness was taken between 15% and 30% of the maximum load.

Table 3.12 Joint stiffness and maximum load

	Stiffness		**Load applied**	
Connector type	**Average (N/mm)**	**Coefficient of variation (%)**	**Maximum (kN)**	**Coefficient of variation (%)**
Nail	433	77.6	0.55	11.8
No. 8 screw	485	26.8	3.06	3.2
No. 12 screw	1137	20.2	5.49	10.0
Double thread screw	2710	15.6	9.89	5.0
Washer head screw	2155	15.7	13.16	12.9

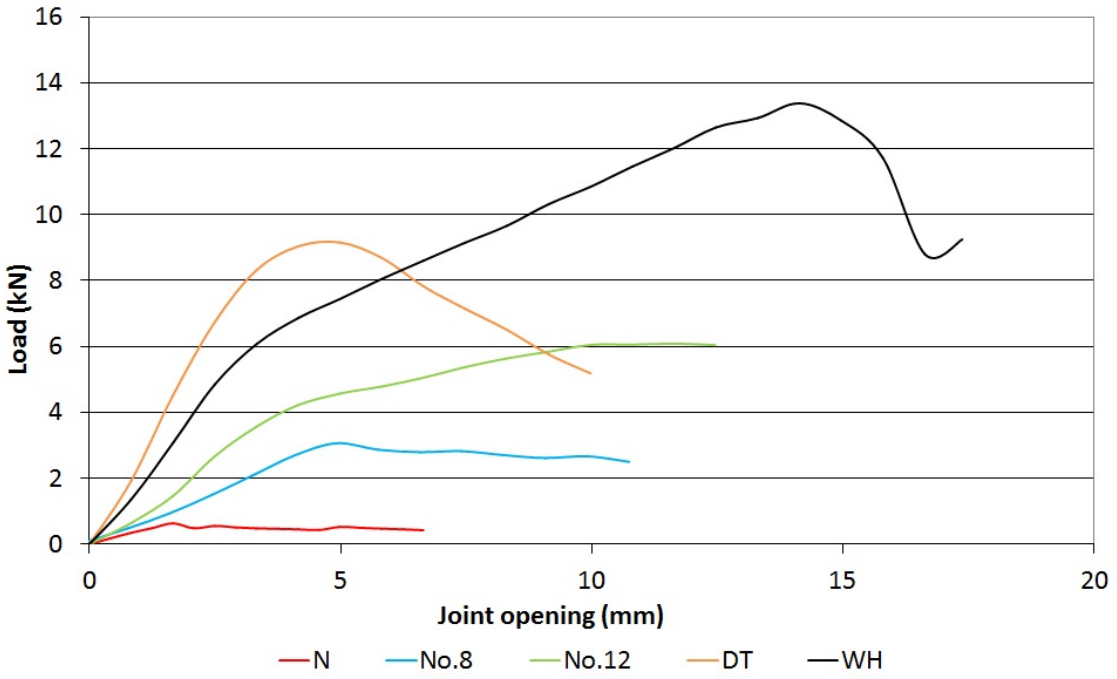

Figure 3.35 Joint testing results

From the result shown in Table 3.12 it is clear that the nailed connections are both the least stiff and they have the lowest maximum load. The double thread screwed connections are the stiffest and the washer head screwed connections have the highest load capacity. From Figure 3.35 it can be seen that while the washer head screwed connections did have the highest capacity, they achieved their maximum load at a high displacements. The variation in the stiffness of the nailed connections is very high at 77.6%. Two of the specimens displayed a large amount of slip as the load reached 0.1kN which may have been as a result of the loading rig slipping. If these results are removed then the variation is significantly reduced to 34%. The maximum loads achieved were however all similar with a coefficient of variation of 11.8% which will account for the natural differences in the timber. The other connectors have lower values of coefficient of variation for stiffness and maximum load. All of the screw connectors failed by pull through of the heads of the screws. This may have produced less variation in the results compared to the nailed connections where failure occurred by pull out of the nail rather than pull through of the head.

The stiffness and maximum load established through these tests will be used during prediction of the performance of full size wall panels prior to testing as well as in analysis following testing.

3.8.2 Horizontal rail to stud

Three different mechanical connectors were tested on the horizontal rail to stud connections. The details of the connectors are shown in Table 3.13. The connections were made using a single connector with the section of rail (25mm by 50mm) perpendicular to the section of stud (38mm by 89mm C16). The timber used for the rails during the second series (LS2) of large scale wall panels differed from the first series (LS1) as it was 19mm by 38mm in cross section. This was because the 19mm by 38mm timber is more suitable for construction use as it is more easily available and treated to prevent decay. As a result the connection tests were repeated with the No.8 screw using this rail timber. Five specimens of each connection were initially tested followed by a further 10 specimens using the No.8 screw (No.8 LS2). The connections were tested in the Dartec 100kN testing frame by supporting the rail ends and loading downwards on the stud ends as shown in Figure 3.36 and Figure 3.37.

Table 3.13 Rail connection connector details

Fixing type	
2.65mm x 50mm long nails	
No.8 x 50mm long screws	
No.10 x 50mm long screws	

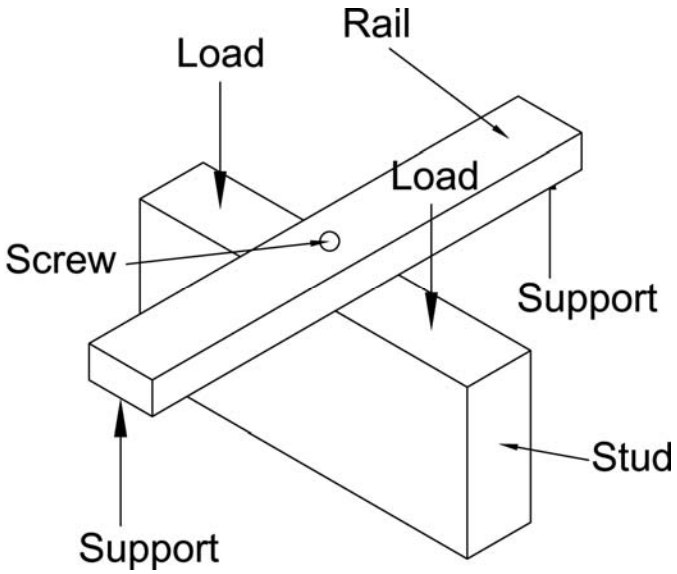

Figure 3.36 Rail connection test set up

Figure 3.37 Rail connection testing

The average stiffness and average maximum load for each connector type are shown in Table 3.14 and average results for each connector type are shown in Figure 3.38. The stiffness was taken between 20% and 40% of the maximum load.

Table 3.14 Rail connection average stiffness and strength

	Stiffness		**Load**	
Connector type	**Average (N/mm)**	**Coefficient of variation (%)**	**Maximum (kN)**	**Coefficient of variation (%)**
N	2216	17.5	0.80	25.2
No. 8	2195	33.9	2.19	17.5
No. 10	2339	28.3	2.56	5.1
No. 8 LS2	1410	32.9	1.66	17.0

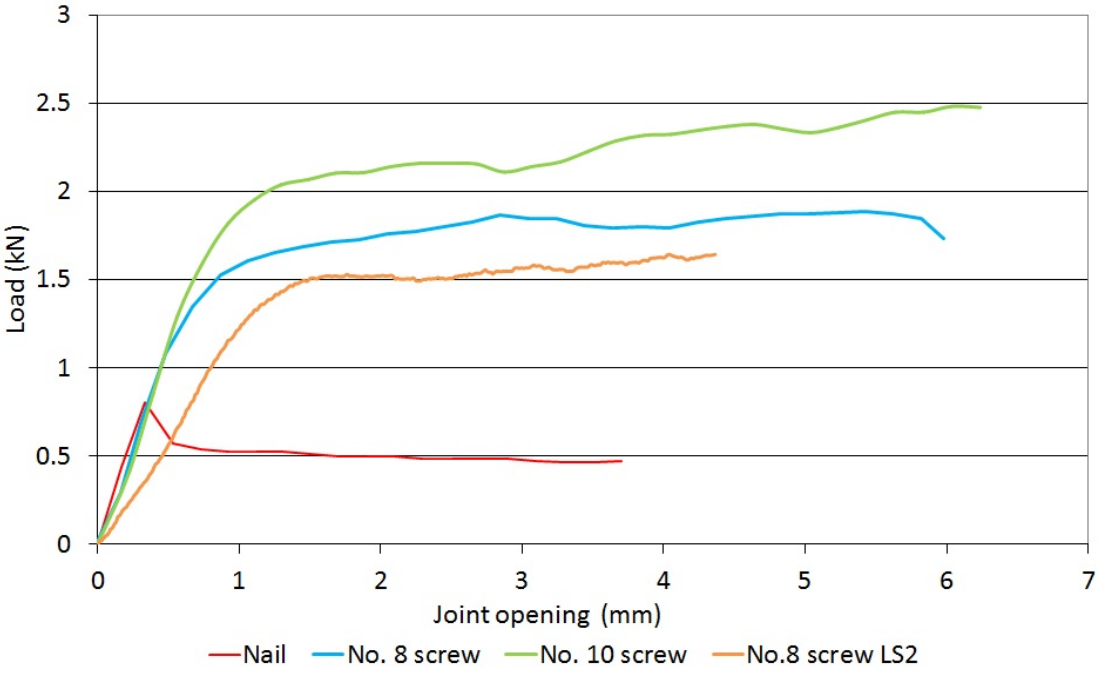

Figure 3.38 Rail connection test results

Ignoring No.8 LS2 initially, the results shown in Table 3.14 and Figure 3.38 the initial stiffness of the different types of connector are all similar only varying by 6%. However the two screwed connections are much stronger than the nailed connection. This is to be expected as screws have higher withdrawal loads than nails and failed by head pull through rather than shank withdrawal. The difference in strength between the No.8 screwed connection and the No.10 screwed connection is minimal at only 0.35kN. The No8. LS2 connections were less stiff and weaker than the previous No.8 connections. This is due to the different rail timber which was of a smaller cross section and a lower quality of timber. This different timber was used for reasons of availability and cost. The joints still failed by head pull through.

The coefficient of variation for the stiffness for the screw type connectors is around 30%. This is compared to 17.5% for the nail connectors. The higher variation for the screw connectors could result from the failure mode. The screwed connections all failed by head pull through of the screw whereas the nailed connections failed by nail withdrawal. The nails were withdrawing from the C16 graded studwork timber whereas the screw heads were pulling through the ungraded rail timber. The ungraded timber is more variable and less consistent than the C16 graded timber and therefore it produces more varied results. The opposite is true for the maximum load achieved. One of the nailed joints reached a significantly lower maximum load, 50% of the highest

maximum, and as a result the coefficient of variation for the nail connectors is 25.2%. The load sustained following the peak was much less varied.

The characteristic values for stiffness and maximum load of the No.8 LS2 screwed connections will be used in the theoretical analysis of the composite hemp-lime and timber walling. The 5% characteristic strength and stiffness of these connections are 1.20kN and 647N/mm respectively.

3.9 Conclusions

This chapter has detailed the materials that will be used during this study. The relevant properties have either been established from laboratory testing or taken from manufacturer's published values. During this study the properties presented in this chapter will be used in all theoretical analysis.

The characterisation of the materials and connections has shown that the properties of the hemp-lime, timber and connections are variable. This is a result of using natural materials that have received a low level of processing. For this reason 5% characteristic values should be used during design and detailing in practice and consideration to the variability must be taken into account. Average values will be used during the theoretical analysis in this study.

4 Theoretical analysis of full scale wall panels

4.1 Introduction

In this chapter of the thesis theoretical predictions of the structural performance of hemp-lime and timber studwork composite walling will be made. Vertical compression, in-plane racking and out-of-plane bending loading conditions will be analysed and predictions in advance of experimental work made for each load case. The material properties presented in Chapter 3 will be used for predicting the performance. The predicted performance will be compared with the experimental test results in Chapters 6, 7 and 8.

4.2 Wall types

Several different configurations on studwork framing, hemp-lime, render and sheathing board will be analysed theoretically. The different types are detailed below in Figure 4.1 to Figure 4.8. All the walls are 2400mm high with 300mm thick hemp-lime and 38mm by 89mm C16 sawn timber studs. In all calculations the hemp-lime and timber studs will be assumed to have a stable moisture content of 12%.

Wall type 1 shown in Figure 4.1 consisted of timber studs cast into the centre of the hemp-lime wall. This type of wall was used initially as it is the simplest form of composite construction with only two different elements.

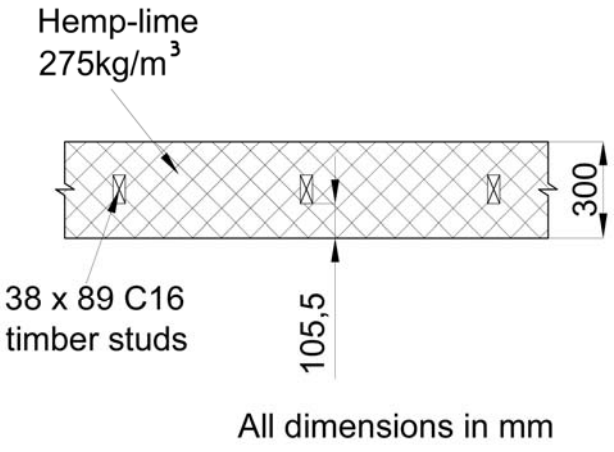

Figure 4.1 Wall type 1plan view

Wall type 2 shown in Figure 4.2 is similar to wall type 1 however the studs are located on the edge of the hemp-lime wall. In this situation there is a requirement for horizontal rails to prevent the hemp-lime and studwork elements from separating. The horizontal rails are at 600mm centres.

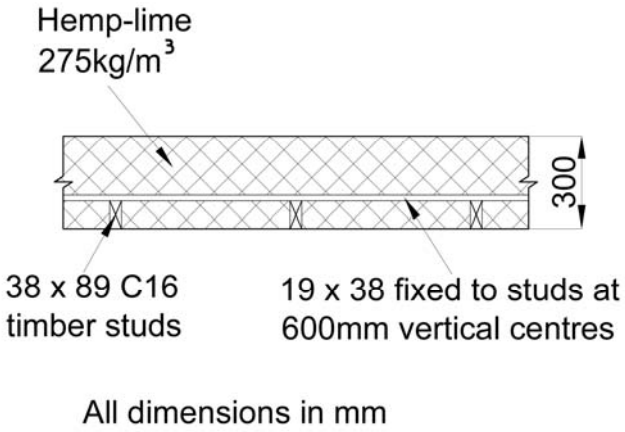

Figure 4.2 Wall type 2 plan view

Wall type 3 shown in Figure 4.3 is again similar to wall type 1 however the studs are set in from the hemp-lime surface by 50mm. In this case rails are not used. This type of wall will be specifically used to investigate the effects of the studs bursting through the face of the hemp-lime if buckling failure occurs about the major axis.

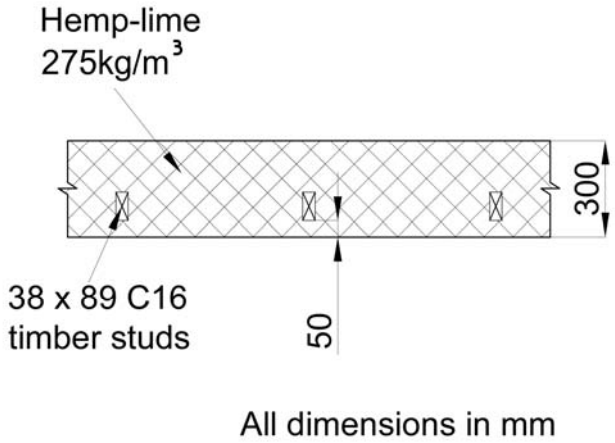

Figure 4.3 Wall type 3 plan view

Wall type 4 shown in Figure 4.4 is identical to wall type 3 apart from the addition of horizontal rails as used in wall type 2. Again wall type 4 will be used to investigate the bursting of the studs through the hemp-lime surface and the effects the rails have upon this.

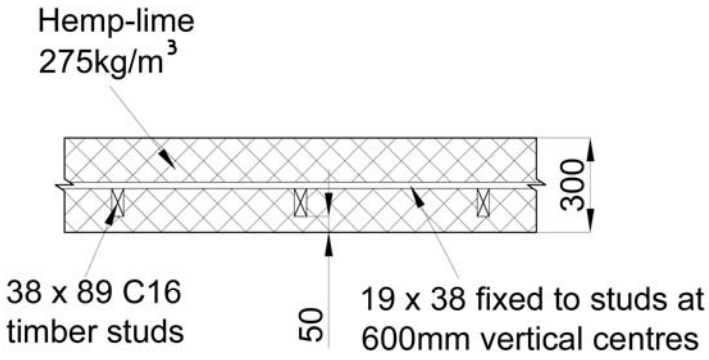

All dimensions in mm

Figure 4.4 Wall type 4 plan view

Wall type 5 shown in Figure 4.5 is identical to wall type 2 apart from the addition of sheathing board to one surface of the wall. The sheathing board is fixed to the exposed surface of the studs. This type of construction allows the sheathing to act as a permanent shutter increasing the speed of construction.

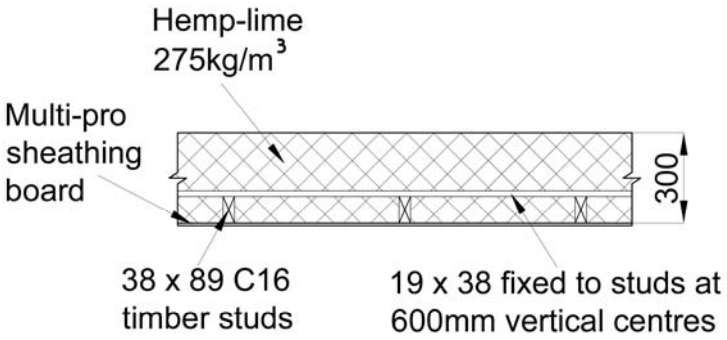

All dimensions in mm

Figure 4.5 Wall type 5 plan view

Wall type 6 shown in Figure 4.6 consists of hemp-lime with both wall surfaces rendered. This type of wall was specifically designed for testing the out of plane bending performance of hemp-lime.

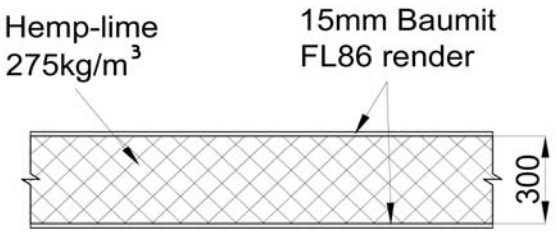

All dimensions in mm

Figure 4.6 Wall type 6 plan view

Wall type 7 shown in Figure 4.7 is identical to wall type 1 apart from the addition of render on both faces of the hemp-lime. This wall type was designed to allow comparison of the bending performance with wall type 6 when a studwork frame is included.

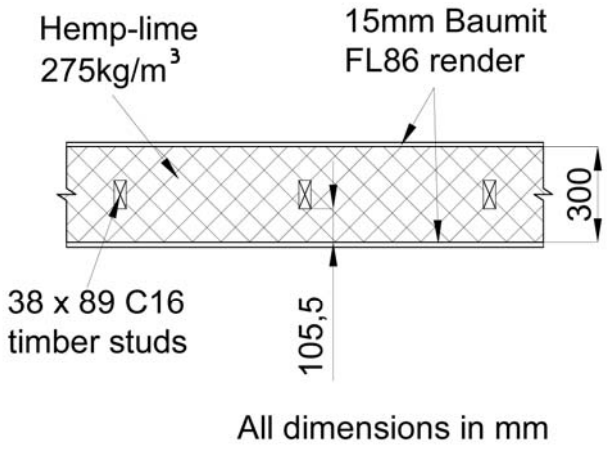

Figure 4.7 Wall type 7 plan view

Wall type 8 shown in Figure 4.8 is identical to wall type 5 apart from the addition of render on the exposed surface of the hemp-lime. This is the most complete build up of composite wall with all of the elements.

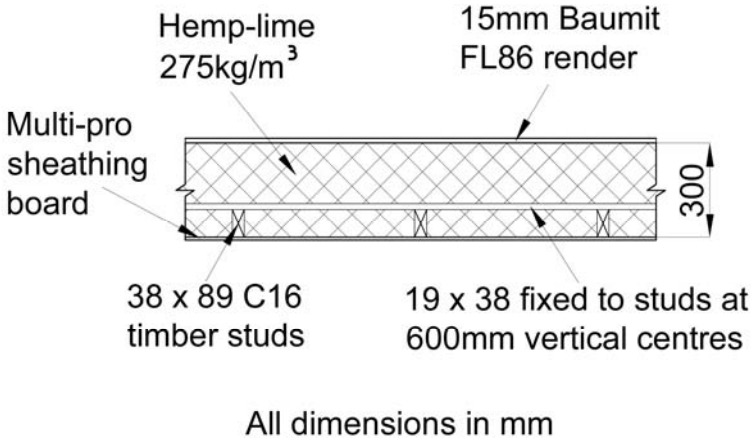

Figure 4.8 Wall type 8 plan view

4.3 Vertical compression loading

The buckling of compression members is covered in section 6 of BS EN 1995 (2004) with clauses for checking the stability of columns in clause 6.3.2. The design procedure in BS EN 1995 (2004) uses buckling curves to take into consideration the decrease in

strength of a real compression member when compared to an infinitely stiff theoretical member. The buckling curves were formed by using computer simulations of loaded columns that were randomly selected and representative of actual timber sections with defects and initial eccentricities (Eurofortech, 1995). Computer simulations were used as it is much more time and cost effective than testing actual timber columns. The buckling curves indicate the effect of slenderness on the characteristic load bearing capacity of actual pin ended timber columns.

This approach allows for the calculation of load bearing capacity for columns that are either unrestrained along their length or have intermediate restraints that shorten the effective length. It does not allow for the use of a continuous medium, such as hemp-lime, to restrain the columns. For this reason other theoretical approaches will be developed to predict the performance of the composite hemp-lime and timber studwork framing under compressive loading.

4.3.1 Concentric stud loading

Concentric vertical loading is the most simple load case. The theoretical buckling loads of unrestrained timber studs can be predicted using Euler buckling with Equation 4.1. The Euler buckling theory assumes that the column is initially straight and loaded with a single concentric compressive load. It also assumes that the column is pin ended at both ends. In the studwork frames that will be used throughout this study the studs are fixed at their top and bases to the header and footer rails by nailed connections. The nailed connections are not true pinned connections as they offer a small amount of rotational resistance. However the resistance they offer will be minimal compared with the overall compressive loads and therefore for the theoretical predictions can be assumed to be pinned.

$$P_E = \pi^2 \frac{EI}{l^2}$$

Equation 4.1

Where P_E = Euler buckling load, E = Elastic modulus, I = Second moment of area, and l = length of stud.

When applying this theory to timber studwork framing the following assumptions have been made:

- Studs have pinned ends
- There is no initial eccentricity
- Timber has a moisture content of 12%

The material properties and geometric data for the 38mm by 89mm C16 studs is shown in Table 4.1. All the material properties have been taken from the results shown in Section 3.5. The compressive strength parallel to the grain has been calculated from the curve for compressive strength and moisture content shown in Section 3.5.

Table 4.1 Timber properties

Area, A	3382 mm^2
Second moment of area, I_{minor}	$0.407x10^6$ mm^4
Second moment of area, I_{major}	$2.232x10^6$ mm^4
Elastic modulus (average), E	9837 N/mm^2
Compressive strength, $\sigma_{c\ parallel}$	46.1 N/mm^2
Compressive strength (average), $\sigma_{c\ perpendicular}$	9.3 N/mm^2
Bending strength (average), σ_b	71.7N/mm^2
All properties at 12% moisture content	

Using the properties in Table 4.1 and Equation 4.1, the theoretical Euler buckling load about the minor axis of a 2400mm long stud is 6.9kN. If the stud was restrained to prevent buckling about the minor axis, theoretical major axis Euler buckling occurs at 37.6kN. These calculations show that if the hemp-lime is able to provide enough restraint to prevent minor axis buckling then failure could occur by major axis buckling. In Wall type 1 where the hemp-lime completely surrounds the studs then restraint will also be provided to the major axis and buckling may be prevented.

With wall type 1, where the studwork frame is cast into the centre of the hemp-lime, the stud may fail in several different ways when loaded in compression. It could either buckle into the hemp-lime at a higher load than the Euler buckling load or it will be restrained by the hemp-lime and prevented from buckling in which case it will fail by

local crushing of the timber. The theory of a bar buckling on an elastic foundation can be used to calculate the buckling load of the stud when surrounded by hemp-lime. This theory is detailed by Timoshenko and Gere (2009) and a diagram is shown in Figure 4.9. When applying this theory to a stud with an applied compressive load the surrounding elastic medium is not a foundation as it would be under a beam and therefore it will be termed a restraint to ensure clarity.

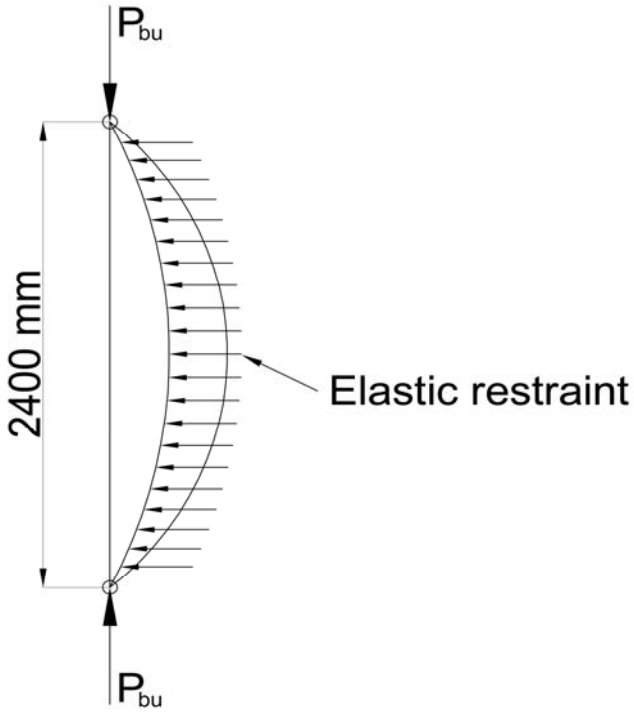

Figure 4.9 Column buckling on elastic restraint

The critical load can be calculated from:

$$P_{bu} = \frac{2m^2\pi^2 EI}{l^2}$$

Equation 4.2

Where *m* is the number of half sine waves in the buckled shape of the stud.

When a pin ended column buckles its deflected shape is a half sine wave. However when there is some intermediate support, such as an elastic restraint, the number of half sine waves the buckled shape takes will depend upon the stiffness and location of the support. Timoshenko and Gere (2009) provide a solution for finding *m* in Equation 4.2 and hence the buckled shape the studs will take.

$$m^4 = \frac{\omega l^4}{\pi^4 EI}$$

Equation 4.3

Where ω is the modulus of the elastic restraint.

For the case of a timber stud surrounded by hemp-lime the hemp-lime is assumed to be the elastic restraint. The modulus of the restraint has been calculated from the average material properties in Chapter 3 and is the load required to compress the hemp-lime by 1.0mm per square mm of contact area. Therefore per mm length along the stud the modulus of restraint for buckling is:

$$\omega_{minor} = 0.061 \times 89 = \underline{5.43N/mm^2}$$
$$\omega_{major} = 0.061 \times 38 = \underline{2.32N/mm^2}$$

Where ω_{minor} is for buckling about the minor axis and ω_{major} is for buckling about the major axis. The hemp-lime has been assumed to be elastic. When hemp-lime is loaded in compression it follows the stress deflection profile shown in Figure 4.10, which is not linear elastic. At small levels of strain the hemp-lime will behave in an elastic manner until the binder matrix begins to rupture. Therefore if the horizontal buckling deflection of the stud into the hemp-lime is low, and hence only causing low strains in the hemp-lime, the hemp-lime can be assumed to be acting in a linear elastic manner. The calculated horizontal deflections of the studs into the hemp-lime when loaded in compression are less than 0.5mm.

When applying this theory to composite timber studwork framing and hemp-lime walling the following assumptions have been made:

- Studs are pin ended
- There is no initial eccentricity
- The hemp-lime is elastic
- Hemp-lime does not burst due to deflections about major axis
- Timber has a moisture content of 12%

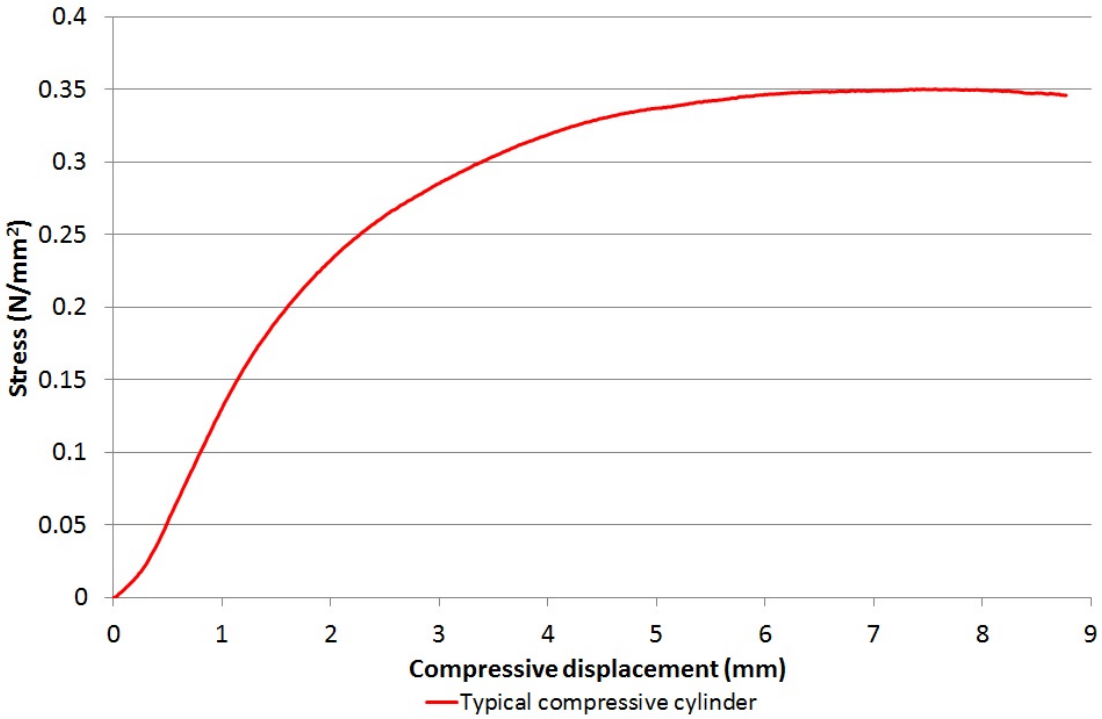

Figure 4.10 Hemp-lime typical compressive loading response

Using Equation 4.3 the buckled shapes, *m*, for the timber studs in wall type 1 can be calculated. The buckled shape, *m*, must be an integer and is the number that causes P_{bu} from Equation 4.2 to be a minimum. For the 2400mm long studs used in the walls with the material and geometric properties shown in Table 4.1 the buckled shape will be:

- Minor axis buckling, $m = 5$
- Major axis buckling, $m = 2$

The buckled shapes are shown in Figure 4.11 along with the buckled shape for a stud without any restraint.

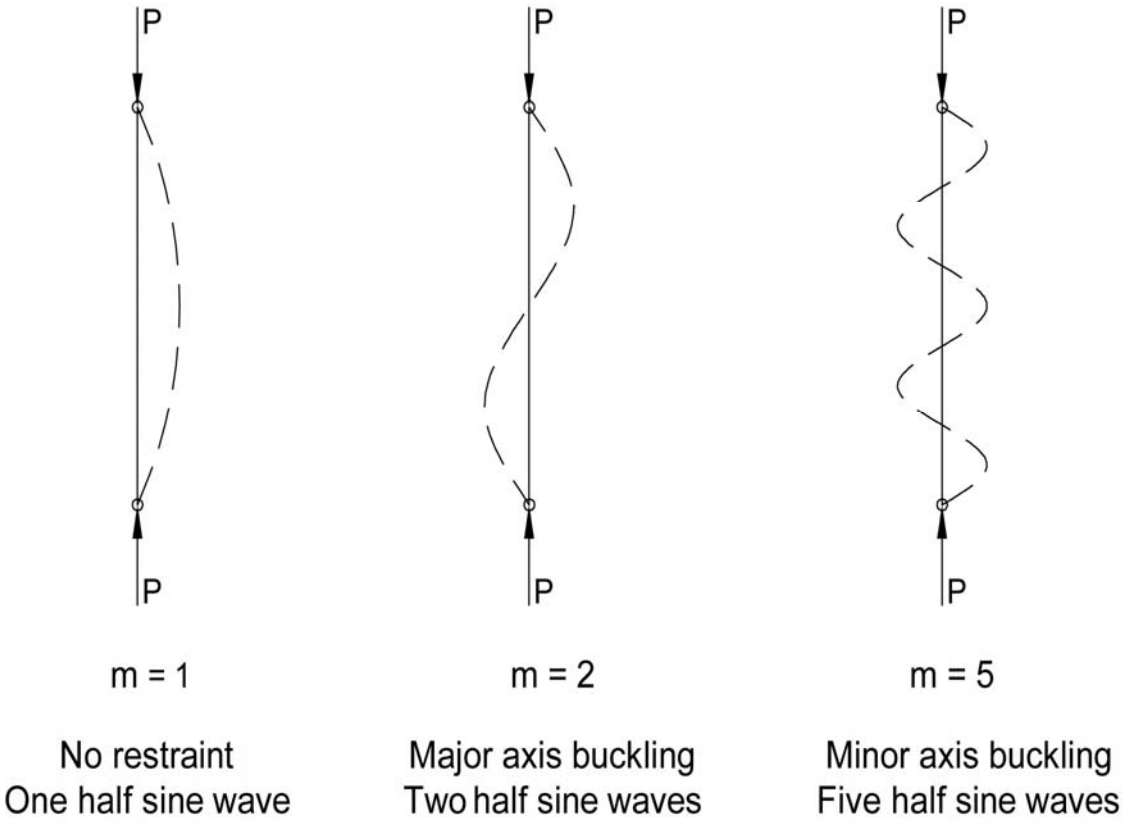

Figure 4.11 Elastic restraint buckled shapes

With Equation 4.2 and the buckled shapes, m, the buckling load, P_{bu}, for both axes can be calculated. The buckling load about the minor axis is:

$$P_{bu\ minor} = \frac{2 \times 5^2 \times \pi^2 \times 9837 \times 0.407 \times 10^6}{2400^2} = \underline{298.8kN}$$

The buckling load about the major axis is:

$$P_{bu\ minor} = \frac{2 \times 2^2 \times \pi^2 \times 9837 \times 2.232 \times 10^6}{2400^2} = \underline{489.1kN}$$

These two buckling loads are significantly higher than the Euler buckling loads calculated for un-restrained studs. This shows that the hemp-lime will increase the buckling load. However the local crushing loads of the studs or the header and footer rails may be lower than the enhanced buckling loads calculated above and therefore these need to be checked.

Using the compressive strength parallel to the grain and the area shown in Table 4.1 the crushing load of the stud is simply the compressive strength multiplied by the area. In this calculation the moisture content is assumed to be 12% and as the timber is crushing locally defects in the timber have been ignored and the average compressive strength is used. The crushing load for the studs is:

$$P_{crushing} = \sigma_{c\,parallel} \times Area$$
$$P_{crushing} = 46.1 \times 3382 \; = \; \underline{155.9kN}$$

Using the compressive strength perpendicular to the grain and the area shown in Table 4.1 the bearing capacity of the header and footer rails can be checked. Again this is simply calculated by multiplying the compressive strength by the area of the stud bearing into the header and footer. The crushing load for the header and footer rails is:

$$P_{bearing} = \sigma_{c\,perpendicular} \times Area$$
$$P_{bearing} = 9.3 \times 3382 \; = \; \underline{31.5kN}$$

Four possible failure loads have been calculated for wall type 1 under compression loading. The failure mode will be the one that has the lowest predicted load. This is local crushing failure of the header and footer rails at 31.5kN. This type of failure is unlikely to be catastrophic as the header and footer will slowly compress as the load increases above 31.5kN. Therefore higher loads may be achieved. The failure mode with the next lowest load is crushing of the stud parallel to the grain at 155.9kN. This may occur, however the vertical deflections are likely to be high due to crushing of the header and footer rails. Therefore design loads should be kept below the bearing failure load perpendicular to the grain, $P_{bearing}$. It is unlikely that the buckling loads will be reached as they are significantly higher than either crushing load.

As the hemp-lime is providing the restraint against buckling the buckling loads may be sensitive to the modulus of the restraint. By using the minimum and maximum elastic modulus of the hemp-lime from Chapter 3 the minimum and maximum modulus of restraint can be calculated:

$$\omega_{minor\,min} = 2.38N/mm^2$$

$$\omega_{major\ min} = 1.02N/mm^2$$

The maximum modulus of restraint is:

$$\omega_{minor\ max} = 11.58N/mm^2$$
$$\omega_{major\ max} = 4.95N/mm^2$$

Considering the minimum modulus of restraint the buckled shapes from Equation 4.3 will be:

- Minor axis buckling, *m* = 4
- Major axis buckling, *m* = 2

Now considering the maximum modulus of restraint the buckled from Equation 4.3 shapes will be:

- Minor axis buckling, *m* = 6
- Major axis buckling, *m* = 3

Comparing the buckled shapes with those previously calculated for the average results when the minimum modulus is used the minor axis buckled shape changes and when the maximum modulus is used both buckled shapes change. In all cases these changes to the buckled shapes are by a maximum of one half sine wave. This does affect the buckling load, but in all cases the buckling loads are still significantly higher than the stud and header and footer crushing loads. With the minimum modulus the buckling loads are:

$$P_{bu\ minor} = \frac{2 \times 4^2 \times \pi^2 \times 9837 \times 0.407 \times 10^6}{2400^2} = \underline{197.0kN}$$

$$P_{bu\ minor} = \frac{2 \times 2^2 \times \pi^2 \times 9837 \times 2.232 \times 10^6}{2400^2} = \underline{489.1kN}$$

Therefore while the buckled shapes are sensitive to changes in the modulus of restraint it does not affect the failure load of the stud as the buckling loads are still significantly greater than the crushing loads.

When calculating the failure mode and load for wall type 2 a similar approach can be taken as with wall type 1. Again failure will occur by either buckling about one of the axes, crushing of the stud or crushing of the header and footer rails. The stud crushing load, header and footer crushing loads and buckling load about the minor axis will remain the same as with wall type 1.

Major axis buckling will be dependent upon the stiffness of the horizontal rail to stud connections. Timoshenko and Gere (2009) present a theory for finding a solution to the buckling load of a column supported by elastic intermediate supports as shown in Figure 4.12.

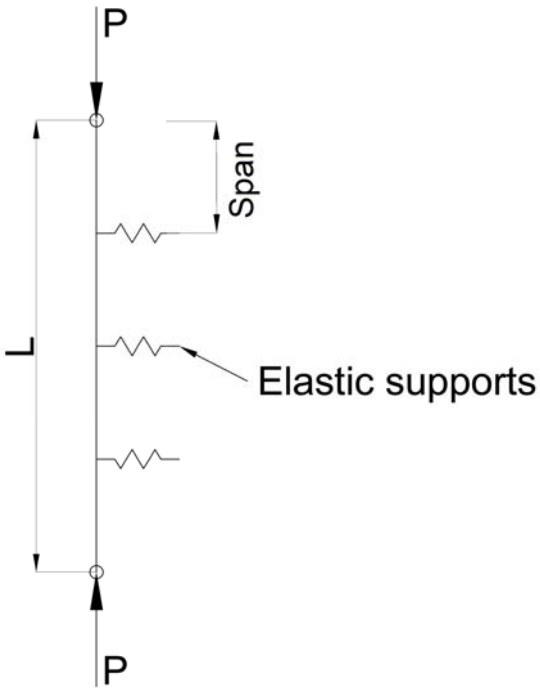

Figure 4.12 Column with elastic restraints

First, the minimum value of stiffness of the elastic supports at which they act as though they are rigid, μ_{rigid}, is calculated using the geometric and material properties of the column from Table 4.1 and:

$$\mu_{rigid} = \frac{nP_{crit}}{rl}$$

Equation 4.4

Where: $n =$ number of spans, $r =$ constant dependent upon the number of spans, and,

$$P_{crit} = \frac{n^2\pi^2 EI}{l^2}$$

Equation 4.5

Values of r are shown in Table 4.2 for various numbers of spans (n).

Table 4.2 Values of γ for different spans (Timoshenko and Gere, 2009)

n	2	3	4	5	6	7
r	0.500	0.333	0.293	0.276	0.268	0.263

If the stiffness, μ, of the actual connections is less than μ_{rigid} then they must be considered when calculating the buckling load for the column. If $\mu_{rigid} > \mu$ then the column can be treated as though it has rigid supports. The buckling load can then be calculated using Euler buckling in Equation 4.1 assuming the effective column length of l/n with pinned ends. The minimum condition occurs when the intermediate supports have no stiffness and therefore $\mu = 0$. In the case the column buckles at the Euler buckling load with a length of l.

When $0 < \mu < \mu_{rigid}$ the buckled shape of the column will be dependent upon the stiffness of the elastic supports. Figure 4.13 shows the four possible buckled shapes for a column with four equal spans as used in the wall type 2. In case 1 the intermediate supports have no stiffness. In cases 2 and 3 the intermediate supports have a stiffness that is less than μ_{rigid} and therefore they affect the buckled shape of the column. In case 4 the stiffness of the supports in higher than μ_{rigid} and act as though they are rigid.

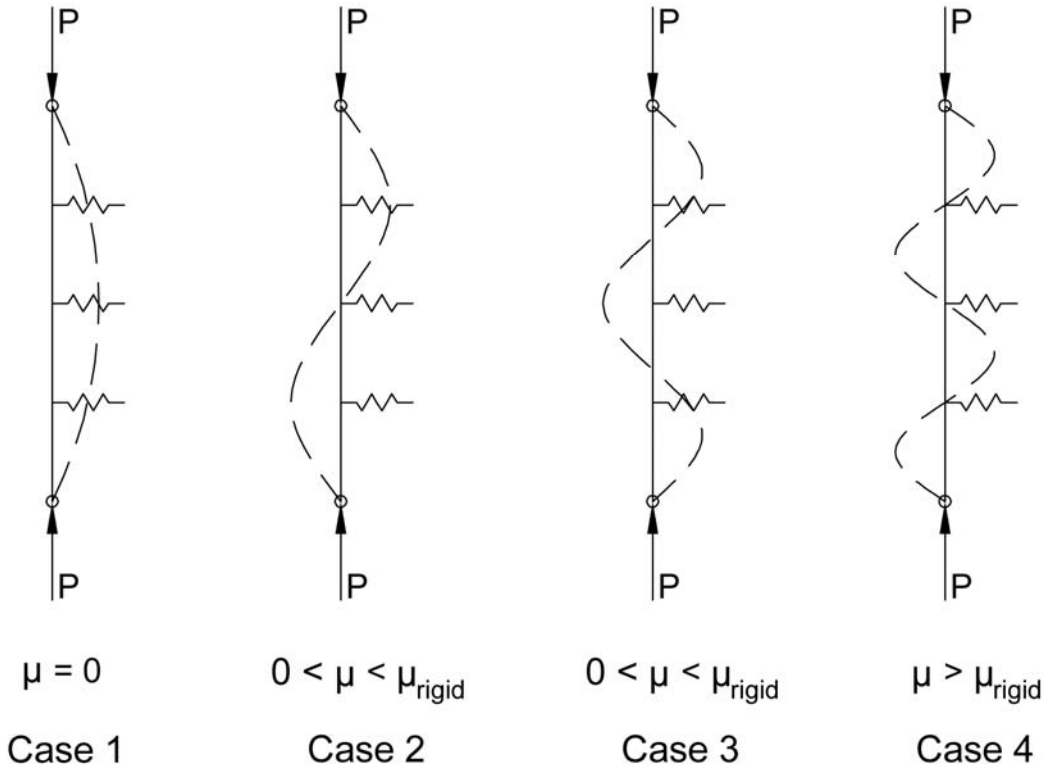

Figure 4.13 Possible buckled shapes

For wall type 2 μ_{rigid} is calculated below using Equation 4.4 and Equation 4.5:

$$P_{crit} = \frac{4^2 \times \pi^2 \times 9873 \times 2.232 \times 10^6}{2400^2} = \underline{604.1kN}$$

$$\alpha_{rigid} = \frac{4 \times 604100}{0.293 \times 2400} = \underline{3421N/mm}$$

Therefore if the stiffness of the connections between the horizontal rails and the studs is less than 3421N/mm they need to be considered when calculating the buckling loads of the studs.

By considering the each of the cases shown in Figure 4.13 and calculating P_{crit} and the Euler bucking load, P_E, for the case when $\alpha = 0$, Timoshenko and Gere (2009) show that the variation in critical load due to changing stiffness of the supports can be plotted. This is shown in Figure 4.14 with the ratio $\mu l\ /P_E$ on the x axis and P_{crit}/P_E on the y axis. Line A to B represents case 1, B to C case 2, C to D case 3 and once the stiffness of the supports reaches μ_{rigid} at point D the column will behave as shown in Case 4.

The curve shown is specific for the 2400mm long 38mm by 89mm C16 stud used for wall type 2 and therefore P_E and l are constant.

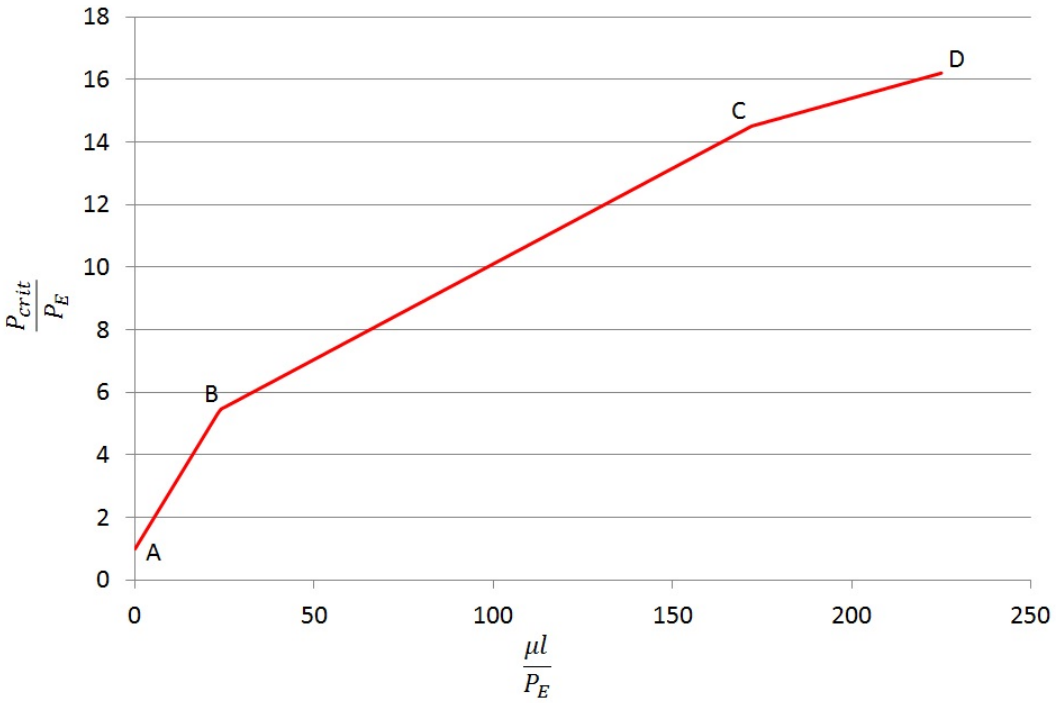

Figure 4.14 Relationship between critical load and support stiffness

From the curve plotted in Figure 4.14 the ratio P_{crit}/P_E for any value of μ can be found and hence P_{crit} can be calculated. To enable more accurate calculations the equations of the three lines plotted are shown below:

- AB: $y = 0.1875x + 1$ for $0 < x < 23.7$
- BC: $y = 0.0611x + 4$ for $23.7 < x < 172.0$
- CD: $y = 0.0320x + 9$ for $172.0 < x < 218.4$

When this theory has been applied to wall type 2 the following assumptions have been made:

- Studs are pin ended
- There is no initial eccentricity
- The connections between the rails and studs are elastic
- The rails do not pull through the hemp-lime
- Timber has a moisture content of 12%

Chapter 3 details the stiffness of the rail to stud connections. Two types of connections are to be used in the experimental wall type 2 specimens. Nailed connections will be used in some as will No. 8 LS2 screwed connections. The measured stiffness of the nailed connections is 1578N/mm and the stiffness of the screwed connections is 647N/mm. Therefore in both of these cases the stiffness of the intermediate supports needs to be considered. As explained in Chapter 3 the screwed connections have a lower stiffness as they used a different type of timber rail. The peak loads for the screwed connections are much higher at 1.66kN compared with 0.80kN for the nailed connections.

Using the curve shown in Figure 4.14 P_{crit} can be found for both connection types. In all cases P_E is the same and is calculated as:

$$P_{\mathrm{E}} = \frac{\pi^2 EI}{l^2}$$

$$P_E = \frac{\pi^2 \times 9873 \times 2.232 \times 10^6}{2400^2} = \underline{37.6kN}$$

Using P_E and $l = 2400$ the critical load for each type connection is as follows:

- $P_{crit\ nailed} = \underline{381.8kN}$
- $P_{crit\ screwed} = \underline{245.2kN}$

As previously mentioned wall type 2 will fail either by buckling, crushing of the studs or crushing of the header and footer rails. The crushing loads are the same as those calculated for wall type 1 and are 155.9kN for the studs and 31.5kN for the header and footer rails. Therefore as with wall type 1 failure will initially occur in the header and footer rails, but the load is likely to continue to rise as they crush and compress. Ultimate failure is likely to occur at 155.9kN when the stud crushes locally. This will be at a large vertical displacement due to the crushing of the header and footer. The stud could crush at any location along its length. It is most likely to crush where there is a significant defect, such as a concentration of knots.

The sensitivity of the studs to changes in the stiffness of the elastic supports can easily be investigated by finding the critical load from Figure 4.14 while varying the stiffness

μ. If $\mu = 323.5N/mm$, which is half the stiffness of the screwed connections, then from Figure 4.14 the critical load is 183.2kN. From this result it can be seen that when the connection stiffness has been reduced by 50%, the critical load is reduced by 25.3%. While changing the stiffness of the elastic supports does affect the buckling load, it does not affect the failure mode as the crushing loads are still lower. These results confirm that a restraint only needs a capacity of 2% of the axial load in order to prevent buckling from occurring (IStructE and TRADA, 2007).

In conclusion, for both wall types 1 and 2 when loaded with a concentric vertical load the studs will not buckle, but will fail by crushing of the stud and header and/or footer rails.

4.3.2 Eccentric stud loading

Often studwork frames are subjected to eccentrically applied loads where floors connect to the top of walls. Due to the geometry of the studwork frames the load will be eccentric along the minor axis causing a bending moment about the major axis. Initially the failure of a stud without hemp-lime will be analysed. On an individual stud the failure load can be calculated by expressing the eccentric load as a concentric compressive load and an applied moment at the end of the stud as shown in Figure 4.15.

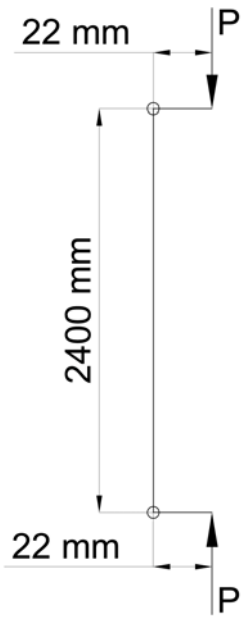

Figure 4.15 Stud with eccentric compressive load

From Timoshenko and Gere (2009) the deflection along the column is given by:

$$y = \frac{M_p l^2}{8EI} \frac{2}{u^2 \cos u} \left[\cos\left(u - \frac{2ux}{l}\right) - \cos u \right]$$

Equation 4.6

Where: $u = kl/2$, $k = \sqrt{P/EI}$ and M_p is the applied end moment.

By taking the second derivative of Equation 4.6 the bending moment along the column can be found. The maximum bending moment will occur at the centre of the column when $x = l/2$ and from Timoshenko and Gere (2009) the equation to find it is:

$$M_{max} = M_p \sec u$$

Equation 4.7

A stud will fail when the stresses within the section caused by the applied loads exceed the strength. For stud B shown in Figure 4.15 the maximum bending stress will occur at the centre of the column caused by the concentric compressive load P_{con} and the applied moment M_p. The bending moment that causes the bending stress to equal the bending strength can be found from:

$$\frac{M}{I} = \frac{\sigma}{y}$$

Equation 4.8

By setting $M_{max} = M$ in Equation 4.7 and rearranging, P can be found from u and M_p can be found as $M_p = Pe$ where e is the eccentricity of the applied load P.

In applying this theory to the studs used during this study the following assumptions have been made:

- Studs are pin ended
- There is no initial eccentricity within the stud
- The stud is restrained about its minor axis to prevent minor axis buckling

- The load is applied eccentrically about the minor axis to cause major axis bending
- The eccentricity of the applied load P is 22mm
- Timber has a moisture content of 12%

The eccentricity of 22mm has been chosen as it is equal to a quarter of the depth of the timber stud and is calculated to cause buckling failure of the studs about their major axis before crushing failure occurs. The theory presented here can be used for any eccentricity.

For the pin ended stud shown in Figure 4.15 the moment which causes bending failure can be found by rearranging Equation 4.8 and setting $\sigma = \sigma_b$ from Table 4.1:

$$M = \frac{64.6 \times 2.232 \times 10^6}{(89/2)} = \underline{3.2kNm}$$

Then using Equation 4.7 and setting $M_{max} = M$, and using the expanded expressions for u and M_o, P_{ecc}, the eccentric buckling load, can be found:

$$M_{max} = Pe \sec\left(\frac{\sqrt{P/EI}\, l}{2}\right)$$

$$3.2 \times 10^6 = P \times 22 \times \sec\left(\frac{\sqrt{P/(9873 \times 2.232 \times 10^6)} \times 2400}{2}\right)$$

$$P_{ecc} = \underline{28.9kN}$$

Therefore the stud will buckle about its major axis at a vertical load of 28.9kN with an eccentricity of 22mm. This is the load at which the bending stress in the timber exceeds the bending strength of 64.6N/mm^2.

When analysing wall types 1, 2, 3 and 4 it is slightly harder to predict the failure mode. The behaviour and resistance of the hemp-lime to bursting through of the stud as it buckles is not known. The following analysis and predictions assumes that the hemp-lime does not burst. However it is possible that the hemp-lime will burst potentially by hinging or a cone type failure as shown in Figure 4.16. The bursting of the hemp-lime is

discussed further in Chapter 6 once the experimental testing and analysis has taken place.

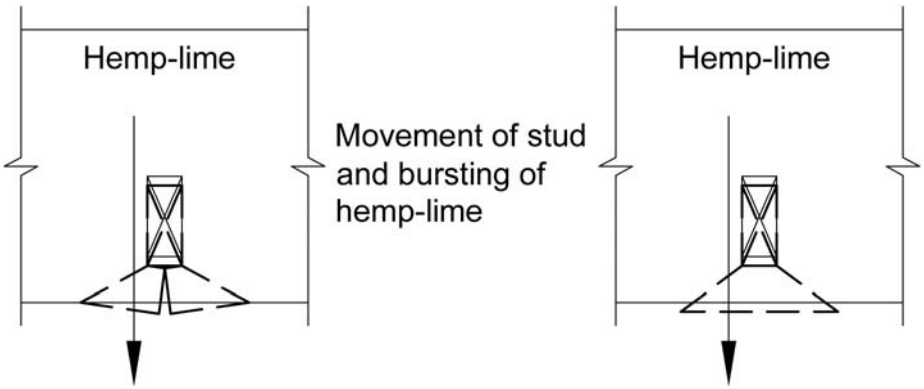

Figure 4.16 Predicted bursting of hemp-lime, hinging (left), cone type failure (right)

As with a concentric load, a composite studwork and hemp-lime wall with an eccentric load will fail in one of several ways. The stud will either buckle about its major or minor axis, crush locally or the header and footer rails will crush. The theory of a beam on an elastic foundation can be used to predict the behaviour of an axially loaded column. The eccentric load can be split into a concentric load and an applied end moment in the same manner as previously with the stud without hemp-lime. This is shown in Figure 4.17.

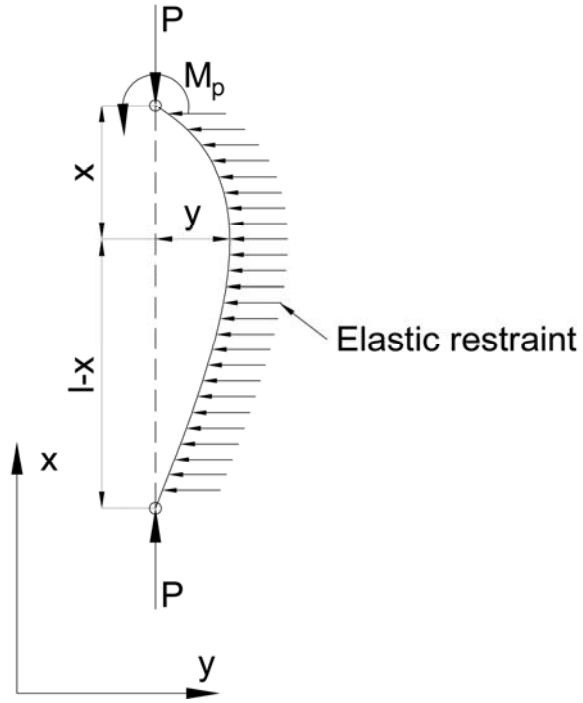

Figure 4.17 Eccentric load with elastic restraint

A moment has only been applied at one end as this is representative of the testing load application. The eccentric load will only be applied at the top of the stud and therefore there will be no eccentricity at the base as the support at the base of the stud is along its centroid.

The deflection at any point along the column shown in Figure 4.17 can be calculated using the following equation from Hetényi (1946):

$$y = \frac{M_p}{EI}\frac{1}{2\alpha\beta}\left[\frac{(\cosh\beta l \sinh\beta(l-x)\sin\alpha x) - (\cos\alpha l \sinh\beta x \sin\alpha(l-x))}{\cosh\ ^2\beta l - \cos\ ^2\alpha l}\right]$$

Equation 4.9

Where:

$$\alpha = \sqrt{\sqrt{\frac{k}{4EI}} + \frac{P}{4EI}}$$

$$\beta = \sqrt{\sqrt{\frac{k}{4EI}} - \frac{P}{4EI}}$$

Where: $k = bk_o$ with k_o as the modulus of the elastic restraint and b as the width of the column buckling into the elastic restraint.

By differentiating Equation 4.9 twice the bending moment at any point along the length of the column can be calculated. The equation for the bending moment is:

$$\frac{d^2y}{dx^2} = M = \frac{M_p}{2\alpha\beta}\frac{D_1 - D_2}{\cosh\ ^2\beta l - \cos\ ^2\alpha l}$$

Equation 4.10

Where:

$$D_1 = [\cosh\beta l\{\beta^2 \sin\alpha x \sinh\beta(l-x) - \alpha^2 \sin\alpha x \sinh\beta(l-x) - 2\alpha\beta\cos\alpha x \cosh\beta(l-x)\}]$$

$$D_2 = [\cos\alpha l\{\beta^2 \sinh\beta x \sin\alpha(l-x) - \alpha^2 \sinh\beta x \sin\alpha(l-x) - 2\alpha\beta\cosh\beta x \cos\alpha(l-x)\}]$$

With Equation 4.9 and Equation 4.10 the maximum deflection and maximum moment along the length of the column can be calculated.

In applying this theory to wall types 1, 3 and 4 the modulus of the hemp-lime acting as the elastic restraint is the same as used previously with concentric loads. The modulus of the elastic restraint for buckling about the minor axis, k_{minor}, is 5.43N/mm^2 and for buckling about the major axis, k_{major}, is 2.32N/mm^2. Using this and the timber stud material and geometric properties shown in Table 4.1 the maximum bending moments, deflections and their locations along the column can be found for bending about the major axis.

When analysing wall type 1, 3 and 4 with this theory the following assumptions have been made:

- Studs are pin ended
- There is no initial eccentricity within the stud
- The load is applied eccentrically about the minor axis to cause major axis bending
- The eccentricity of the applied load P is 22mm
- The hemp-lime does not burst
- Timber has a moisture content of 12%

Equation 4.9 and Equation 4.10 have been programmed into a spreadsheet to allow solutions for P and x to be found that cause the timber compressive stress to be equal to the compressive strength. Once P has been determined in this manner the maximum horizontal deflection and the distance, x, it occurs along the column can be solved for the calculated value of P.

For all of the wall types the maximum moment occurs at the top of the stud at the point where the moment is applied. By considering the bending stress and compressive stress in the section the stress profile can be plotted as shown in Figure 4.18.

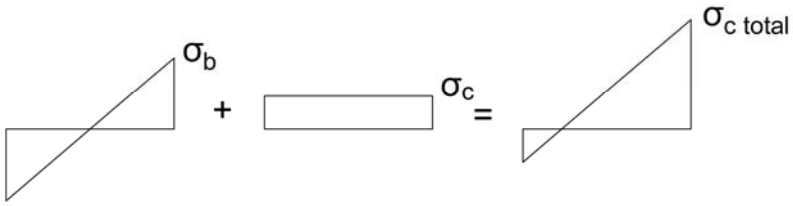

Figure 4.18 Stresses in stud

By using Equation 4.10 and Equation 4.11 and combing them for the bending and compressive stresses it is possible to find P when $x = 0$.

$$\sigma_{c\ total} = \sigma_c + \sigma_b = \frac{P}{A} + \frac{M_{max}\ I}{y}$$

Equation 4.11

Therefore the compressive load that causes the compressive stress to be equal to the compressive strength is 62.8kN. At this load the stud will crush locally. As previously noted the other failure modes are minor axis buckling and crushing of the header and footer rails. Minor axis buckling will occur at the same load as for a concentric load as there is not eccentricity about the major axis. From previous calculations this was 279.1kN. Crushing of the header and footer rails will also occur at the same load as for a concentrically loaded stud and this was 31.5kN. Therefore it can be concluded that taking into account the stated assumptions the header and footer rails will crush initially before the stud crushes locally at the point of maximum moment. This is similar to the results shown from the analysis of the concentrically loaded studs.

At a compressive load of 62.8kN the horizontal deflection can be calculated using Equation 4.9. By solving the equation using the spreadsheet to find y_{max}, x is shown to be equal to 343.6mm. Setting $P = 62.8kN$ and $x = 343.6mm$ and using Equation 4.9:

$$y_{max} = \underline{2.4mm}$$

A horizontal deflection of the magnitude may cause the stud to burst through the hemp-lime. The exact characteristics of the hemp-lime when subjected to this type of loading are not known from materials testing and therefore this will be discussed further in Chapter 6 following testing and analysis of the wall panel specimens.

With wall type 2 the same theoretical approach can be used as with wall types 1, 3 and 4, however in this case it is the stud to rail connections that are restraining the stud and not the hemp-lime. It will be assumed that the horizontal rails will remain securely fixed within the hemp-lime and not burst through the surface. The rails restrain the stud at three discrete points. Therefore if the stiffness of these connections is divided by the length of the stud the equivalent elastic foundation stiffness can be found.

From Chapter 3 the stiffness of the nailed connections is 1578N/mm and for the screwed connections the stiffness is 647N/mm. Therefore the equivalent elastic foundation stiffnesses are:

$$k_{nail} = \frac{2217 \times 3}{2400} = \underline{2.77N/mm^2}$$

$$k_{screw} = \frac{1410 \times 3}{2400} = \underline{1.76N/mm^2}$$

The minor axis buckling, stud crushing and header and footer rail crushing loads will remain the same as those calculated previously for wall type 1, 3 and 4. When applying the theory by Hetényi (1946) shown in Equation 4.9 and Equation 4.10 to wall type 2 the following assumptions have been made:

- Studs are pin ended
- There is no initial eccentricity within the stud
- The load is applied eccentrically about the minor axis to cause major axis bending
- The eccentricity of the applied load P is 22mm
- The horizontal rails do not burst through the hemp-lime
- Timber has a moisture content of 12%

Using the equivalent stiffness and the method of finding the load that causes the compressive stress to equal the compressive strength shown above for wall types 1, 3 and 4 the peak load is 62.8kN. This is the same as the maximum load for wall types 1, 3 and 4 as the maximum moment occurs at the top of the stud and therefore the elastic restraint has no effect on it. The peak horizontal deflection will be affected by the elastic

restraint stiffness. The peak displacements are shown below for wall type 2 when $P = 62.8kN$:

- $y_{\max nail} = \underline{2.6mm}$
- $y_{\max screw} = \underline{4.4mm}$

$y_{\max nail}$ occurs at 358mm from the top of the stud and $y_{\max screw}$ occurs at 453mm from the top of the stud.

The peak deflections do illustrate the differences in restraint stiffness. The horizontal rails are at 600mm vertical centres. Using Equation 4.9 the horizontal displacements at 600mm from the top of the studs are 2.1mm for the nailed connections and 4.2mm for the screwed connections. From Chapter 3 it can be seen that the nailed connections reach their peak load at an average displacement of 0.4mm and following this the stiffness dramatically reduces. Therefore by using Equation 4.9 and setting $y = 0.4mm$ and $x = 600mm$ the load that will cause this deflection is calculated to be 18.2kN. This is lower than the unrestrained stud failure load and therefore this stud will fail at the unrestrained failure load of 28.9kN.

With screwed connections the same process can be followed. From Chapter 3 the peak load is reached at an average displacement of 3.0mm. By using Equation 4.9 again and setting $y = 3.0mm$ and $x = 600mm$ the load to cause this deflection is 48.2kN. Therefore in wall type 2 with screwed rail connections the stud will fail by buckling about the major axis at a load of 82.4kN when the rail to stud connection fails.

Finally, eccentric loading of studs to cause buckling out of the wall surface in the manner described above is unlikely to occur in a building structure. The studs are likely to be positioned on the inner face of the wall to allow the use of permanent formwork, or nearer the inner face of the hemp-lime to allow easier connection to be made with floor and roof constructions. In these configurations the resulting moment from the eccentrically applied roof and floor loads would cause the studs to want to buckle towards the outer face of the wall and therefore into a thicker mass of hemp-lime. This will reduce the probability of bursting of the hemp-lime as there will be a thicker mass

of hemp-lime resisting the horizontal deflections. The thickness of hemp-lime cover to the studs to resist such forces will be discussed in Chapter 6.

4.4 In-plane racking loading

The design of timber studwork shear walls to resist in-plane forces is covered in both BS 5268 (1996) and BS EN 1995 (2004). In BS 5268 (1996) set racking resistances per metre of wall are given for defined constructions. Providing the wall being designed follows the construction build up outlined then it is assumed it will achieve the racking resistance shown in Table 2 of BS 5268 Part 6.1 (1996) as a minimum. It is also assumed that if the set out construction is followed then the wall will have sufficient stiffness to keep deflections within allowable limits.

BS EN 1995 (2004) approaches design in a slightly different way as it does not set out racking resistances for standard constructions, but allows for the calculation of racking resistance based on the sheathing board to stud connector shearing capacity. With composite hemp-lime and timber studwork framing the design method followed in BS 5268 (1996) is not applicable and the method set out in BS EN 1995 (2004) might only be applicable if there is a sheathing board present. In addition both design standards assume the walls have sufficient stiffness and do not allow for the calculation of deflections. Therefore other methods of performance will be used that are more suited to hemp-lime and studwork construction.

4.4.1 Hemp-lime and studwork only

As with compression loading the hemp-lime in wall types 1 and 2 can be thought of as an elastic foundation which resists forces that the studs exert upon it. Taking each stud individually, they can be assumed to be acting as a cantilever on an elastic hemp-lime restraint with an axial load, as shown in Figure 4.19, with the top of the stud as the free end. This theory is presented by Hetényi (1946) with both ends of the column free and unrestrained. As discussed previously the connections between the studs and the header and footer rails have been treated as pinned even though they do have some small rotational resistance. In the case presented below the ends are free and not fixed in

position by pinned connections. Hetényi (1946) also presents the case for a cantilever with a fixed end. The difference between the results for this case and a case when the column has a free end is less than 0.1% and therefore assuming the ends are free will not invalidate the results.

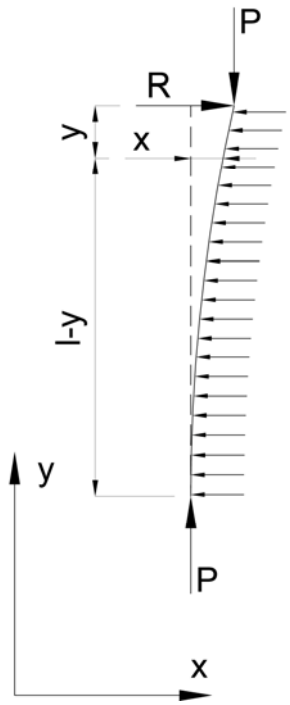

Figure 4.19 Cantilever on elastic foundation

Hetényi (1946) derives the formula for the deflection in the x direction as:

$$x = \frac{R}{2\lambda^2 EI}\,\frac{1}{H_1 H_2}\,F$$

Equation 4.12

Where:

$$H_1 = \alpha(3\beta^2 - \alpha^2)\sinh\beta l + \beta(3\alpha^2 - \beta^2)\sin\alpha l$$

$$H_2 = \alpha(3\beta^2 - \alpha^2)\sinh\beta l - \beta(3\alpha^2 - \beta^2)\sin\alpha l$$

$$\begin{aligned} F = \{&\alpha(3\beta^2 - \alpha^2)\sinh\beta l[2\alpha\beta\cos\alpha y\cosh\beta(l-y) \\ &+ (\beta^2 - \alpha^2)\sin\alpha y\sinh\beta(l-y)] \\ &- \beta(3\alpha^2 - \beta^2)\sin\alpha l\,[2\alpha\beta\cosh\beta y\cos\alpha(l-y) \\ &+ (\beta^2 - \alpha^2)\sinh\beta y\sin\alpha(l-y)]\} \end{aligned}$$

$$\lambda = \sqrt[4]{\frac{k}{4EI}}, \qquad \alpha = \sqrt{\sqrt{\frac{k}{4EI}} + \frac{P}{4EI}}, \qquad \beta = \sqrt{\sqrt{\frac{k}{4EI}} - \frac{P}{4EI}}$$

This theory assumes linear elastic behaviour of the restraint. When applying this theory to composite studwork and hemp-lime walling the hemp-lime is considered the elastic restraint. As shown in Chapter 3 and in Figure 4.10 the relationship between stress and displacement of the hemp-lime is not linear. Therefore in order to apply this theory to wall types 1 and 2 the stiffness of the elastic restraint needs to be varied as deflection increases. A polynomial curve can be calculated to fit all of the hemp-lime cylinder results shown in Chapter 3. This is shown for the compressive stress and displacement results in Figure 4.20.

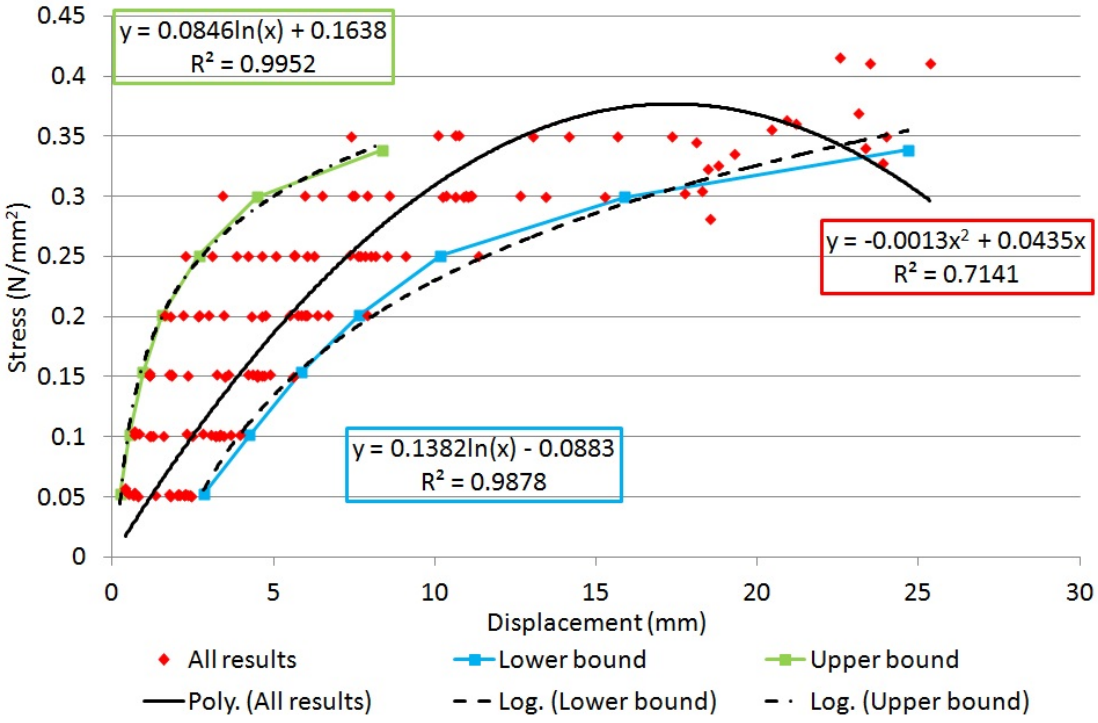

Figure 4.20 Hemp-lime showing elastic modulus variation

A second order polynomial shows the best fit for the results and the equation of the line is shown in Figure 4.20. The wide spread of results means that the R^2 value is quite low, however the trend line does fit well within the range of results. The upper (95^{th} percentile) and lower (5^{th} percentile) bounds for the elastic modulus of the hemp-lime are also shown with logarithmic trend lines showing the best fit. By taking the derivative of the line equation the slope of the line can be found at any point, and hence

the elastic modulus of the hemp-lime at any point. The elastic modulus of the hemp-lime restraint is:

$$\frac{dy}{dx} = \theta = -0.0026x + 0.0435$$

Equation 4.13

The deflection of the end of the beam with the applied horizontal load is of most interest in this situation as this will be the point at which the greatest deflection occurs. By using Equation 4.12 to find the deflection at the end of the studs and taking into consideration the changing elastic modulus of the hemp-lime the overall deflection at the top of the studwork frame can be calculated. As well as the hemp-lime resisting the racking force, the joints between the studs and the header and footer rails will resist global rotation of the studwork frame. As the footer rail is securely fixed to the foundation, the racking load will cause the rest of the studwork frame to rotate around point A in Figure 4.21 consequently loading the joints. The vertical load of 5kN per stud is used as it is a requirement of BS EN 594 (1996).

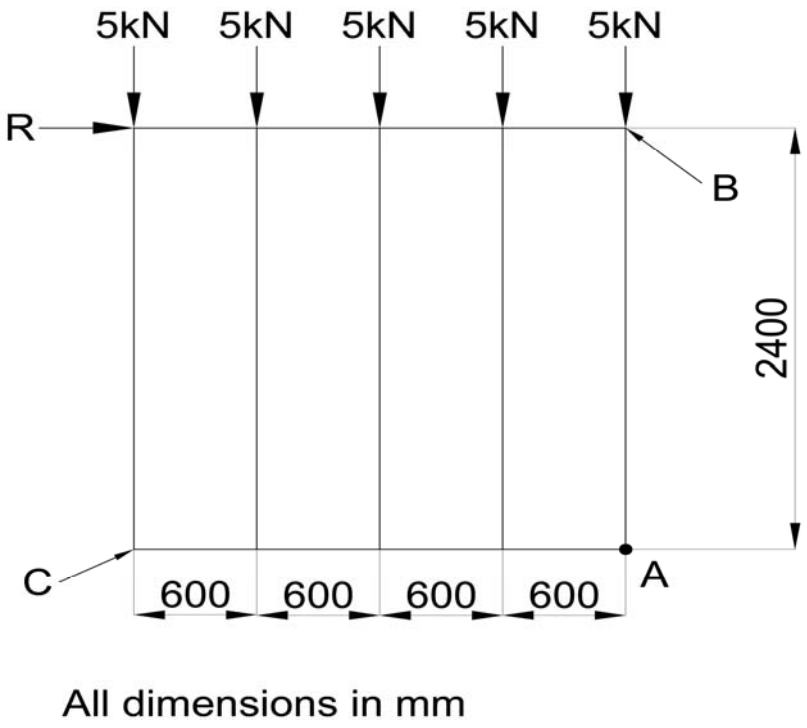

Figure 4.21 Racking wall loading

By taking moments about point A, with constant vertical loads of 5kN, the racking load at which the joint at C will begin to experience a tensile force rather than compressive force can be calculated. Taking moments about point A:

$$R \times 2.4m = 5 \times 0.6 + 5 \times 1.2 + 5 \times 1.8 + 5 \times 2.4$$

$$R = \frac{5 \times 0.6 + 5 \times 1.2 + 5 \times 1.8 + 5 \times 2.4}{2.4}$$

$$R = \underline{12.5kN}$$

Therefore when the racking load is greater than 12.5kN the leading stud joints will begin to be loaded in tension and the stiffness of the joint, at C, has to be considered. This deflection caused by the global rotation of the frame about point A can then be added to the deflection calculated from Equation 4.12 to find the total deflection of the frame.

When applying this theory to wall types 1 and 2 the following assumptions have been made:

- Studs are pin ended
- Timber has a moisture content of 12%
- The footer rail remains firmly fixed to the foundation
- The studwork frame moves within the hemp-lime and the hemp-lime remains on the foundation
- The vertical loads are constant

For the calculation of the racking load and deflection curve plot for wall types 1 and 2 the elastic modulus of the hemp-lime restraint has been calculated from Equation 4.13 at 2.5mm intervals of deflection as shown in Table 4.3. The elastic modulus could be calculated at as many points as necessary.

Table 4.3 Hemp-lime restraint elastic modulus

Displacement $x$mm in Figure 4.20	**Elastic modulus from Equation 4.13 (N/mm^2)**	**Upper bound elastic modulus (N/mm^2)**	**Lower bound elastic modulus (N/mm^2)**
< 2.5	0.037	0.072	0.027
5.0	0.031	0.023	0.024
7.5	0.024	0.000	0.021
10.0	0.018	0.000	0.018
12.5	0.011	0.000	0.015
15.0	0.005	0.000	0.012

With the elastic modulus of the hemp-lime restraint the deflections at the top of the studs can be calculated using Equation 4.12 when $R < 12.5kN$ and then using the following equation when $R > 12.5kN$:

$$x = \left(\frac{R}{2\lambda^2 EI}\frac{1}{H_1 H_2}F\right) + \left(\frac{R - 12.5kN}{k_{connector}}\right)$$

Equation 4.14

Where: $k_{connector}$ is the stud to header and footer rail connector stiffness.

The stiffness and strength of the stud to header and footer rail connections are shown in Chapter 3. Nailed connections and double thread screw connections will be used in the wall types 1 and 2 and therefore they will be analysed here. In wall types 1 and 2 four of the five studs are supported by the elastic foundation and therefore in the calculations below the racking load is divided by four to enable calculation of the deflection at the top of each stud. The calculations below are for nailed connections with $k_{connector} = 433N/mm$.

When $R < 12.5kN$ Equation 4.12 is used. Therefore with the following conditions $x < 2.5mm$, $y = 0mm$, $N = 5.0kN$ and $R = 3.5kN$:

$\alpha = 0.00395$, $\beta = 0.00386$, $\lambda = 0.0039$, $H_1 = 0.0006$, $H_2 = 0.0006$ and
$F = 9.48 \times 10^{-5}$

$$\therefore x = \frac{(R/4)}{2\lambda^2} EI \frac{1}{H_1 H_2} F$$

$$x = \frac{(3500 \div 4)}{2 \times 0.0039^2} \times 9873 \times 0.407 \times 10^6 \times \frac{1}{0.0006 \times 0.0006} \times 9.48 \times 10^{-5}$$

$$x = \underline{2.1mm}$$

When $R > 12.5kN$ Equation 4.14 is used. Therefore with the following conditions $x > 10.0mm$, $y = 0mm$, $N = 5.0kN$ and $R = 13.0kN$:

$\alpha = 0.00294,\ \beta = 0.00282,\ \lambda = 0.00288,\ H_1 = 1.9 \times 10^{-5},\ H_2 = 1.9 \times 10^{-5}$ and $F = 1.39 \times 10^{-7}$

$$x = \left(\frac{(R/4)}{2\lambda^2 EI} \frac{1}{H_1 H_2} F\right) + \left(\frac{(R/4) - (12.5kN/4)}{k_{connector}}\right)$$

$$x = \left(\frac{(13000 \div 4)}{2 \times 0.00288^2} \times 9873 \times 0.407 \times 10^6 \times \frac{1}{1.9 \times 10^{-5} \times 1.9 \times 10^{-5}} \times 1.39 \times 10^{-7}\right) + \left(\frac{(13000 \div 4) - (12500 \div 4)}{433}\right)$$

$$x = \underline{11.6mm}$$

The racking load and displacement curves shown in Figure 4.22 have been calculated in the way shown above for both connector types and the changing elastic modulus of hemp-lime shown in Table 4.3.

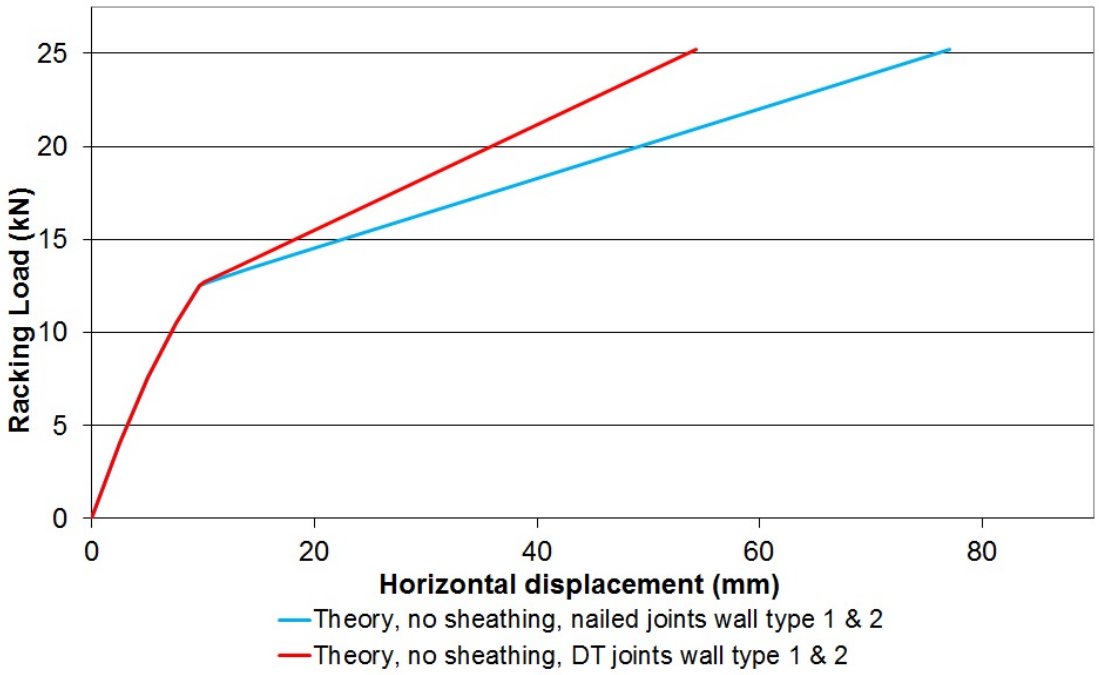

Figure 4.22 Racking loading predictions (wall types 1 and 2)

These calculations show that for wall types 1 and 2 the initial performance and stiffness will be the same before the stiffness of the studwork framing joints begins to influence the overall panel stiffness. Following this the walls with the double thread screw connectors will retain a higher stiffness. The wall panels are likely to fail when the leading stud joints fail, which will occur at large displacements. The vertical loads that were included throughout this analysis actually only have a minimal effect on the racking stiffness of the wall panel. If they are ignored the stiffness is only 3.6% lower. They do however have a large effect on the global rotation of the panel and help to prevent over turning and separation of the leading stud to header and footer joints.

With this theory the resistance to deflection of the top of the stud under racking loads is provided by the hemp-lime restraint. Therefore the results could be highly dependent upon the elastic modulus of the hemp-lime restraint. Figure 4.23 shows the calculated results if the upper and lower bounds of elastic modulus are used. Also included in Figure 4.23 are the original results for comparison.

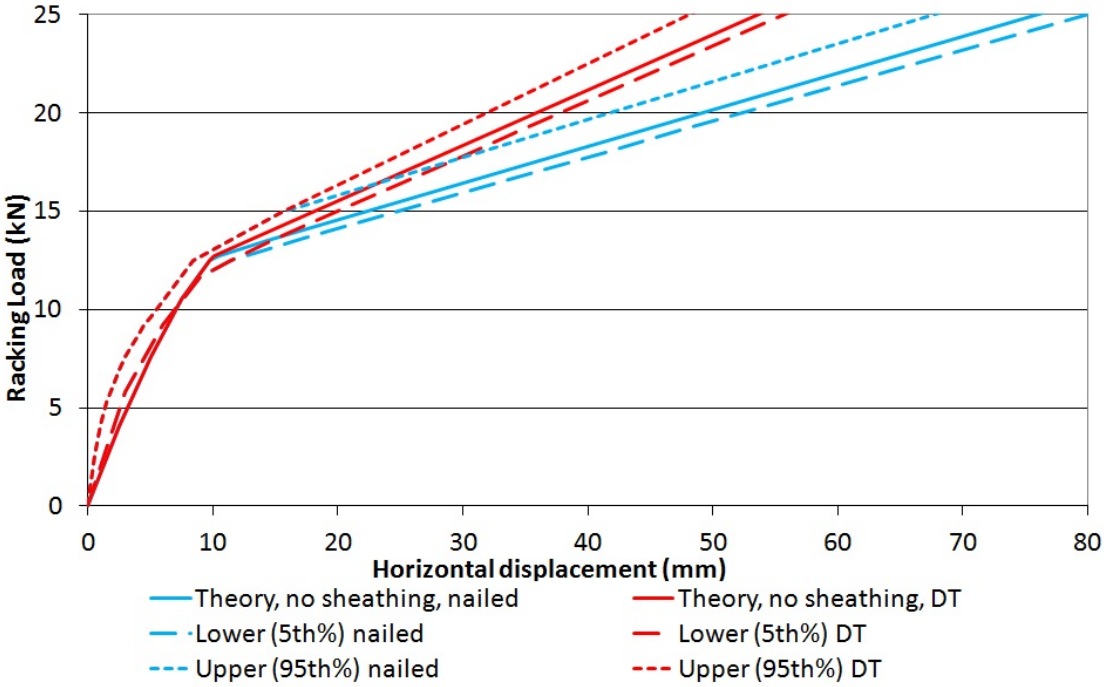

Figure 4.23 Racking sensitivity analysis

The calculated results shown in Figure 4.23 show that the elastic modulus of the hemp-lime restraint does have an effect on the performance of the wall under in-plane racking loads. With a racking load of 12.5kN applied the horizontal deflection could be increased by 14% or decreased by 18% depending upon the elastic modulus of the hemp-lime. With this type of wall construction the deflections at serviceability loads are likely to dominate design and the reduced stiffness of the wall could have a serious effect. Therefore the elastic modulus of the hemp-lime restraint should be carefully considered when using this design method.

4.4.2 Hemp-lime, studwork and sheathing board

Calculations of the stiffness and strength of wall type 5 with hemp-lime; timber studwork framing and sheathing board needs to be approached in a different way. The sheathing board is much stiffer than the hemp-lime and therefore the load transfer between the sheathing and studwork will dominate the performance.

When a racking load is applied to wall type 5 the group of connectors fixing the sheathing to the studs experiences a moment. This moment is resisted by the polar modulus of the connector group. The fixings in the corners of the sheathing board are

most heavily loaded and will therefore fail first and govern the strength of the panel. This method of determining the strength of shear wall panels is described in several publications including Baird and Ozelton (1984) and Eurofortech (1995).

The polar modulus of a group of connectors is found by summing the squared distance from each connector to the origin for both the x and y axes.

$$x\ axis\ polar\ modulus = \sum x_i^2$$

$$y\ axis\ polar\ modulus = \sum y_i^2$$

Equation 4.15

Once the polar modulus has been calculated the force in the x or y direction for any connector can be found:

$$F_{xi} = \frac{Rhy_i}{\sum y_i^2}$$

$$F_{yi} = \frac{Rhx_i}{\sum x_i^2}$$

Equation 4.16

Where: $h = height\ of\ panel$, $R = racking\ load$ and
$x_i\ and\ y_i\ is\ the\ distance\ to\ the\ connector\ being\ considered.$

Therefore the total force on a connector is:

$$F_i = \sqrt{F_{xi}^2 + F_{yi}^2}$$

Equation 4.17

Using these equations the racking load required to cause the force in the corner connectors to exceed their strength can be calculated and therefore the panel failure load can be predicted. The racking deflections can also be predicted as the stiffness of the sheathing to stud connections are also known from Chapter 3. Figure 4.24 shows the layout of connectors on wall type 5.

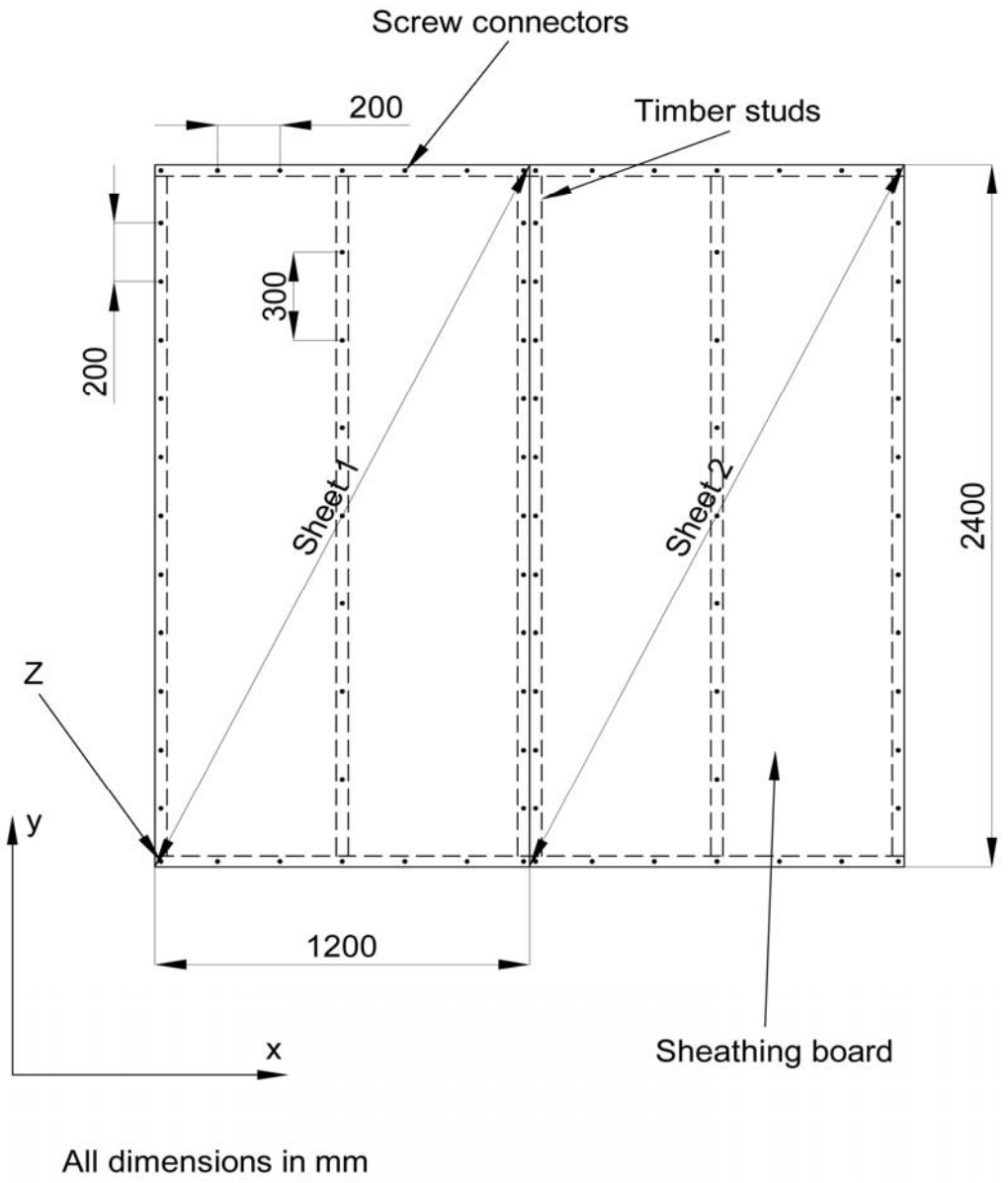

Figure 4.24 Sheathing connector spacing

When applying this theory to wall type 5 the following assumptions have been made:

- Studs are pin ended
- Timber has a moisture content of 12%
- The footer rail remains firmly fixed to the foundation
- The studwork frame moves within the hemp-lime and the hemp-lime remains on the foundation
- There is no deflection of the sheathing board in-plane or out-of-plane

- Vertical loads on the studs have been ignored as when following this design procedure in BS EN 1995(2004) the vertical load is considered separately to check if overturning will be an issue.

When applying this analysis method to wall type 5 each sheathing board is treated separately and then the failure loads are summed to get a wall panel failure load. For sheet 1 shown in Figure 4.24 the polar modulus of the connector group can be calculated using Equation 4.15:

$$\sum x_i^2 = 30 \times 600^2 + 4 \times 200^2 + 4 \times 400^2$$
$$\sum x_i^2 = \underline{11.6 \times 10^6 mm^2}$$

$$\sum y_i^2 = 18 \times 1200^2 + 4 \times 1000^2 + 2 \times 900^2 + 4 \times 800^2 + 6 \times 600^2 + 4 \times 400^2 + 2 \times 300^2 + 4 \times 200^2$$
$$\sum y_i^2 = \underline{37.2 \times 10^6 mm^2}$$

Using Equation 4.16 and the polar modulus the force in the corner connectors in both the x and y direction can be calculated:

$$F_{xi} = \frac{Rhy_i}{\sum y_i^2}$$
$$F_{xi} = \frac{R \times 2400 \times 1200}{37.2 \times 10^6} = \underline{0.077R}$$

$$F_{yi} = \frac{Rhx_i}{\sum x_i^2}$$
$$F_{yi} = \frac{R \times 2400 \times 600}{11.6 \times 10^6} = \underline{0.124R}$$

Therefore the total force is:

$$F_i = \sqrt{(0.077R)^2 + (0.124R)^2}$$
$$F_i = \underline{0.143R}$$

The sheathing to stud connector capacity from Chapter 3 is 1.75kN. Therefore the failure load of sheet 1 in Figure 4.24 is:

$$1.75 = 0.143R$$

$$R = \underline{12.24kN}$$

For the entire wall panel shown in Figure 4.24 the failure load will be:

$$2R = 2 \times 12.24 = \underline{24.48kN}$$

The stiffness of the wall panel can be calculated in a similar manner using the polar modulus of the fastener group. However, in this instance the stiffness of the fasteners is used rather than the strength. As the fasteners in the corners of the panel are most heavily loaded, they will also show the highest displacements. The horizontal displacement of the entire wall panel needs to be found and therefore only the horizontal component of the fastener displacement will be used. As shown in Chapter 3 the shear stiffness of the sheathing to stud connections varies. The sheathing to stud connection stiffness curve is shown in Figure 4.25.

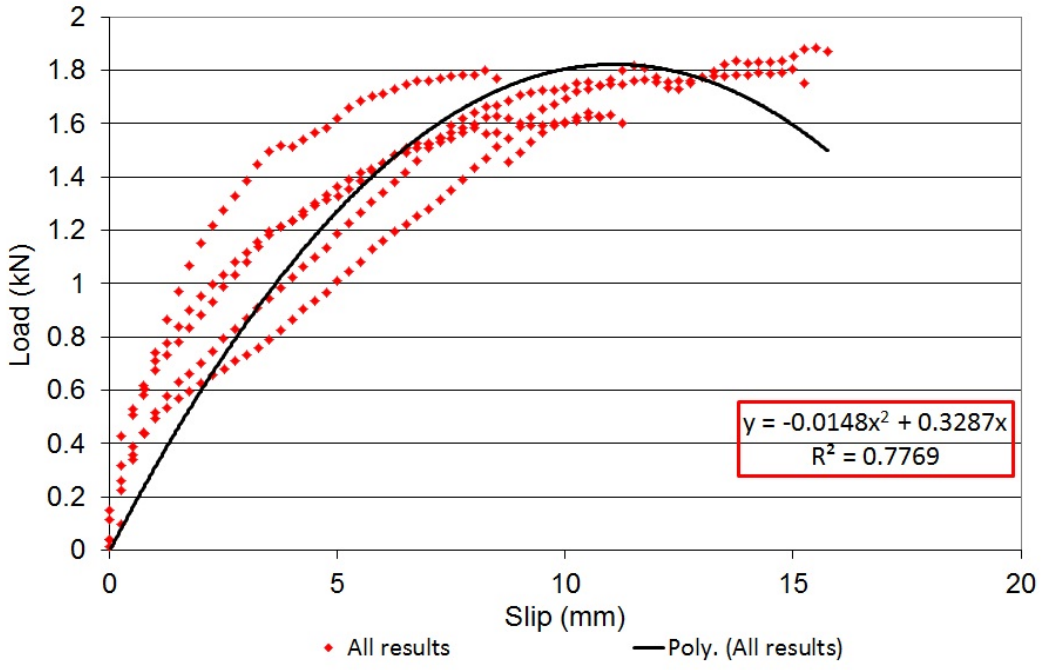

Figure 4.25 Sheathing to studs theoretical stiffness

A polynomial line can be found to fit the results and this can be used to find the stiffness at any amount of slip. As with the hemp-lime stiffness, the spread of the results means that the R^2 value is quite low, however the trend line does fit the within the spread of the results well. The stiffness of the sheathing to stud connections can be found at any point along the curve by differentiating the equation for the line for all of the results to find its gradient.

$$\frac{dy}{dx} = \phi = -0.0296x + 0.3287$$

Equation 4.18

As with the in-plane load analysis on wall types 1 and 2 the stiffness of the connection between the sheathing and studs has been calculated at discrete points to allow ease of calculation. These are shown in Table 4.4.

Table 4.4 Sheathing to stud theoretical stiffness

Displacement $x$mm in Figure 4.25	**Stiffness from Equation 4.18 (N/mm)**	**Upper bound stiffness (N/mm)**	**Lower bound stiffness (N/mm)**
< 2.5	254.7	840.3	238.8
5.0	180.7	361.3	198.8
7.5	106.7	0.0	158.8
10.0	32.7	0.0	118.8

Using Equation 4.16 the force in the corner connectors can be calculated for any racking load. Once the force is known the displacement can be calculated as the stiffness of the connections is known.

When $x < 2.5mm$, $R = 4kN$:

$$\delta = \frac{F_{xi}}{connector\ stiffness} = \frac{496}{254.7} = \underline{1.95mm}$$

This calculation has been carried out for the range of loads up to the predicted failure load of 24.48kN and the load displacement curve for wall type 5 is shown in Figure

4.26 along with the predictions for wall types 1 and 2 for comparison. From the calculations and the predicted results shown in Figure 4.26 it can be seen that wall type 5 is much stiffer than wall types 1 and 2. This is entirely due to the high stiffness sheathing board resisting the racking forces rather than the low stiffness hemp-lime. For the wall type 5 the displacement of the leading stud joints has not been considered in the calculations of strength or stiffness. These joints will be much stronger in a wall panel with sheathing as the sheathing board is screwed to the header and footer rails. As a result they are unlikely to fail in the same way as the joints on wall types 1 and 2 which rely solely on the connections between the studs and the header or footer rail.

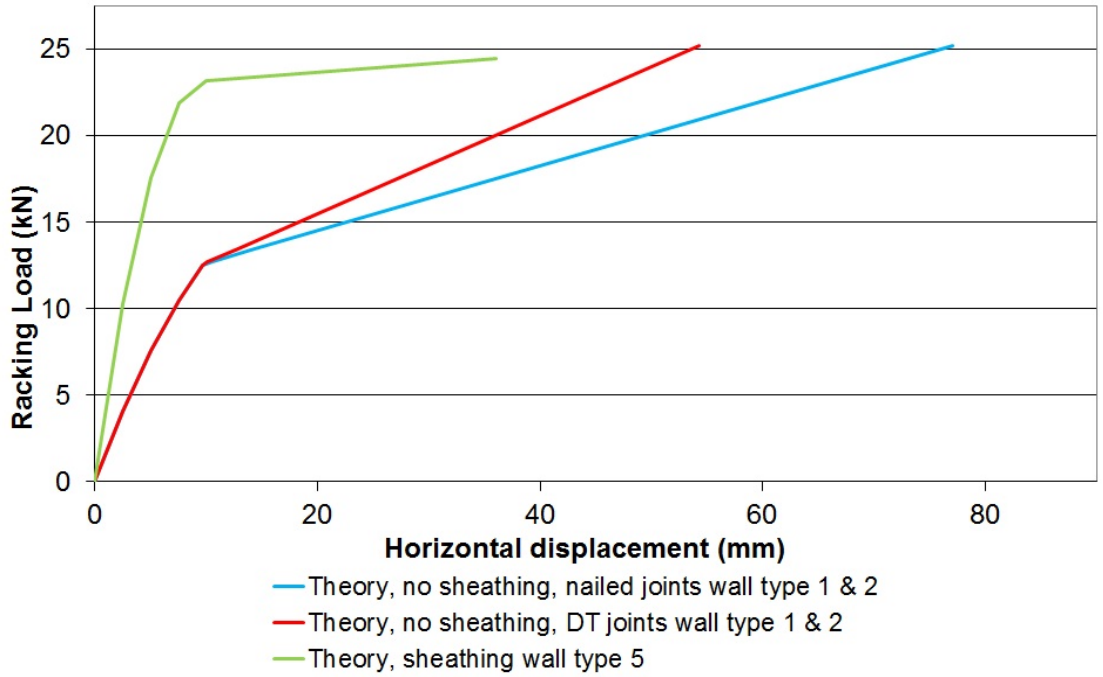

Figure 4.26 Wall type 5 predicted performance

The sensitivity of the racking performance to changes in the sheathing connector stiffness needs to be considered. With wall type 5 any variation in the stiffness and strength of the sheathing to stud connections will affect the performance in a linear manner as the theory assumes linear behaviour of the connectors. Therefore if the connector shear strength is reduced by 50% then the racking strength of the panel will also be reduced by 50%.

The stiffness of the wall panels is likely to govern their design as the peak load is not reached until high displacements which would be undesirable. Therefore wall type 5 provides the greatest resistance to in-plane racking when serviceability deflection limits

are applied. IStructE and TRADA (2007) state that for timber frame dwellings with masonry if the racking design guidance in BS EN 1995 (2004) is followed the deflections will be limited to h/333 (where h = panel height) and if stricter limits of h/500 are needed then the racking strength should be increased proportionally. As the finish on hemp-lime construction is likely to be render which is brittle, and potentially less able to accommodate movements that masonry, these limits should also be applied. Applying the strictest limit of h/500 the allowable deflections would be $2400/500 = 4.8mm$. At this deflection limit wall type 5 shows the greatest racking resistance of 17.0kN and wall types 1 and 2 have a resistance of 7.3kN.

The effect of render on the racking resistance has not been considered. In straw bale construction the render is often relied upon to provide load resistance and the same could be suggested here as both materials have a low stiffness and strength. However with this type of hemp-lime construction with a studwork frame encapsulated by the hemp-lime the load is transferred from the studwork frame into the hemp-lime. As the hemp-lime has minimal strength and stiffness it is unlikely that much of this load will then be transferred into a render skin and therefore it has been ignored.

4.5 Out-of-plane bending

Under out-of-plane bending loads the extent of interaction between the different materials in the wall build up needs to be considered. In the simplest case of wall type 6 (only hemp-lime and render) the wall can be treated as a sandwich panel with the hemp-lime spacing the render skins apart. The hemp-lime is assumed to carry the shear forces within the wall and prevent the render from buckling. A similar approach could also be taken with wall type 8 constructed from hemp-lime, studwork frame and render. However a more accurate prediction of performance might be found if an equivalent section is used, where all of the materials are adjusted for size based on their relative stiffness while still maintaining the initial EI value (elastic modulus multiplied by second moment of area). This approach will be used with all of the different wall constructions and the interaction between the different materials (hemp-lime, timber studs, render, Multi-pro sheathing) will be taken into consideration.

All of the predictions ignore any applied vertical load that may be present when this type of construction is used in a building. This is because initially the load cases will be kept separate from each other to allow understanding of how the composite construction performs with each load case as this type of construction has not been studied previously.

4.5.1 Wall type 6 - Hemp-lime and render only

For wall type 6 where there is only hemp-lime and render an equivalent section can be used to predict the performance. Considering a 1.0m wide section of wall, with 300mm thick hemp-lime, 15mm thick render on each face and using the material properties shown in Table 4.5 this results in the section shown in Figure 4.27. With the section transformed the materials properties of the render can be applied to the whole section and it can be considered to act as one.

Table 4.5 Material properties

Property	Render	Hemp-lime
Elastic modulus, E (N/mm^2)	1573	39.7
Compressive strength, σ_c (N/mm^2)	2.2	0.4
Bending strength, σ_b (N/mm^2)	0.9	0.035

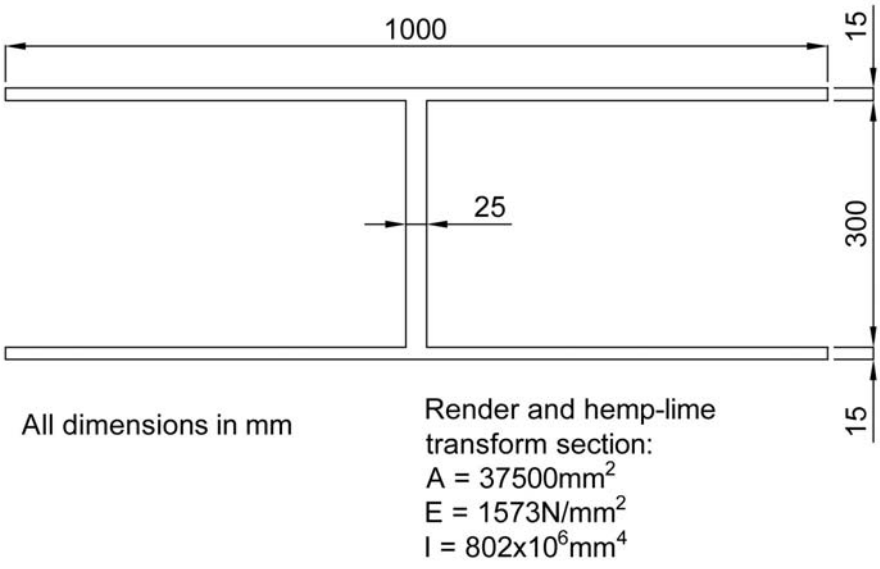

Figure 4.27 Transformed section

The values in Table 4.5 are all average values. With the equivalent section the bending deflection at the centre of the span can be found using the deflection formula for a simply supported beam with an applied uniformly distributed load (udl):

$$\delta_b = \frac{5wl^4}{384EI}$$

Equation 4.19

The shear deflection at the centre of the beam can found from:

$$\delta_v = \int_0^x \frac{qS}{GA} dx$$

Equation 4.20

Where $q = factor\ dependant\ upon\ the\ shape\ of\ the\ cross\ section$,
$S = shear\ force$, $G = shear\ modulus$ and $A = cross\ sectional\ area$.

Equation 4.19 and Equation 4.20 allow for the deflection of the wall to be predicted but not the maximum load. With the equivalent section it is possible to predict the applied load that will cause the most highly stressed area to reach its bending strength and therefore fail. Under a uniformly distributed load the surface of the render will be the area with the highest stress. Using Equation 4.21 the bending moment at which the stress in the surface of the render is equal to its strength can be calculated.

$$\frac{M}{I} = \frac{\sigma}{y}$$

Equation 4.21

Where $M = bending\ moment$, $I = second\ moment\ of\ area$, $\sigma = stress$ and
$y = distance\ from\ neutral\ axis$.

The load at which the bending moment occurs can then be found from:

$$M = \frac{wl^2}{8}$$

Equation 4.22

Where $M = bending\ moment$, $w = uniformly\ distributed\ load$ and

$l = length\ of\ beam.$

When applying this theory to wall type 6 the following assumptions have been made:

- There is full interaction between the hemp-lime and the render so that no slip occurs between them.
- The shear forces are carried by the hemp-lime

For a wall type 6 when analysed as a simply supported beam Equation 4.20 becomes for the deflection at the centre of the span:

$$\delta_v = \int_0^x \frac{q(wx - 1200w)}{GA}\,dx$$

$$\therefore\ \delta_v = \frac{q(wx^2 - 1200w)}{2GA}$$

Equation 4.23

For a rectangular cross section $q = 1.5$. For wall type 6 the deflection due to bending will be calculated using the equivalent section and the render material properties and the shear deflections will be calculated using the original dimensions of the hemp-lime and the hemp-lime material properties as the shear forces are being assumed to be carried entirely by the hemp-lime. Using Equation 4.19 and Equation 4.23 and the material properties in Table 4.5 the total deflection when a load of 2.0kN/m is applied is:

$$\delta_{total} = \delta_b + \delta_v$$

$$\delta_{total} = \left[\frac{5 \times 2 \times 2400^2}{384 \times 1573 \times 802 \times 10^6}\right] + \left[2 \times \left(\frac{1.5 \times (2 \times 1200^2 - 1200 \times 2)}{18.9 \times 300000} - \frac{1.5 \times (2 \times 0^2 - 0 \times 2)}{18.9 \times 300000}\right)\right]$$

$$\delta_{total} = 1.2mm$$

The same calculations can be carried out for any load and as the relationship is linear the deflections can be easily found for any load. The failure of wall type 6 will occur when the extreme fibre stress in the render exceeds the render strength. The

compressive strength of the render is higher than the bending strength and therefore the render will rupture on the tensile face rather than the compressive face. Using Equation 4.21 and Equation 4.22 the load that causes the render to rupture can be found. From Equation 4.21:

$$M = \frac{\sigma_b I}{y}$$

$$M = \frac{0.9 \times 802 \times 10^6}{(330/2)}$$

$$M = \underline{4.37kNm}$$

Therefore the load that causes rupture of the render is:

$$w = \frac{8M}{l^2}$$

$$w = \frac{8 \times 4.37 \times 10^6}{2400^2}$$

$$w = \underline{6.1kN}$$

Once the render has ruptured and cracked the hemp-lime will crack as the bending strength of the hemp-lime is much lower than that of the render and therefore it will not be able to sustain the applied load. The predicted strength and stiffness calculated above are displayed graphically in Figure 4.28.

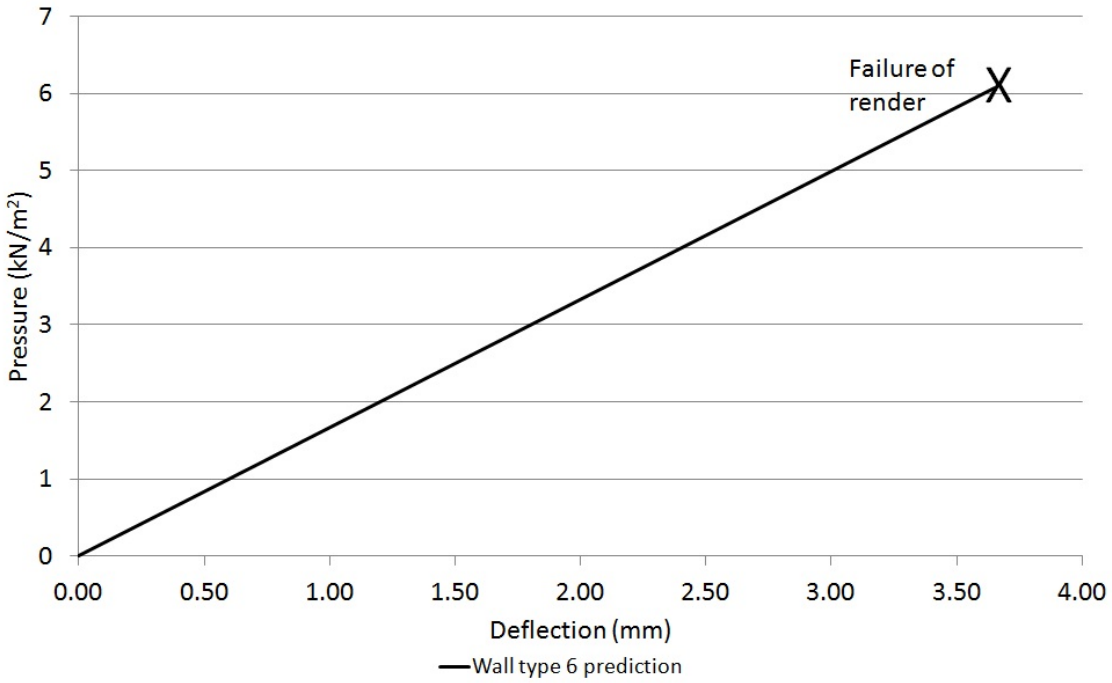

Figure 4.28 Wall type 6 out-of-plane bending predictions

These predictions show that this type of wall is expected to perform with a linear load displacement relationship and fail in a brittle manner once the peak load has been reached.

4.5.2 Wall type 7 - Hemp-lime, render and studwork frame

The performance of wall type 7 can be calculated in a similar manner to wall type 6. The timber studwork frame in the centre of the wall will be ignored when calculating the initial stiffness of the wall. This assumption is being made as the timber frame is on the centre line of the section and therefore during initial loading it will experience minimal bending. The equations used for wall type 6 can also be used for calculating the initial stiffness and render rupture load for wall type 7. When analysing the performance of wall type 7 the following assumptions have been made:

- Before cracking of the render the hemp-lime and render provide the resistance to bending
- Post render cracking, only the timber studwork frame provides resistance

- Shear defections have been ignored in the studwork framed as the studs are slender sections and the shear deflection will be a very low percentage of the total deflection.
- There is full interaction between the hemp-lime and the render so that no slip occurs between them.
- Initially the shear forces are carried by the hemp-lime.

With these assumptions the initial stiffness and load at which the render cracks will remain the same as for wall type 6. The post crack stiffness and strength can be calculated for the timber studwork frame using Equation 4.19, Equation 4.21 and Equation 4.22 in the same manner as above for the hemp and render section of wall type 6. The results of these calculations are shown in Figure 4.29 along with the predicted results for wall type 6 for comparison.

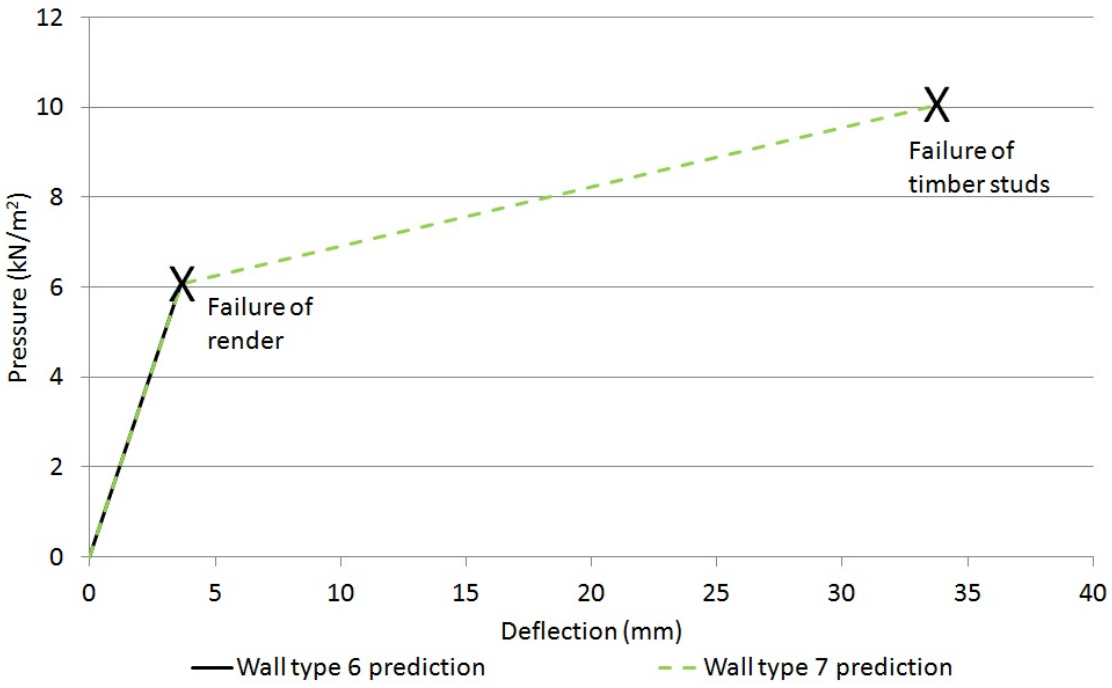

Figure 4.29 Wall type 7 out-of-plane bending predictions

These predictions show that this type of wall is expected to perform with a linear load displacement relationship until the render and hemp-lime crack. Following this a linear load displacement relationship will continue with a lower stiffness until the timber studs fail in bending. This type of failure is preferred as the wall has some post cracking ductility and ability to continue to resist out-of-plane loading.

4.5.3 Wall type 8 - hemp-lime, render, timber studs and sheathing board

Wall type 8 requires more careful consideration in respect to how the materials interact with each other. The Multi-pro sheathing board is screwed to the timber studs and the shear resistance and slip modulus of these connections need to be included in any predictions as they are not assumed to have full interaction. In this type of wall construction there are horizontal timber rails fixed to the studs to prevent separation of the hemp-lime and studwork frame. The rails allow for some interaction between the studwork frame and the hemp-lime as they will resist slip along the interface between the two materials.

The interaction between different parts of the construction can be analysed using the theory of partial interaction. This is often used for the design and analysis of composite steel and concrete floor constructions. Annex B of BS EN 1995 (2004) details a method for calculating the effective EI (elastic modulus multiplied by second moment of area) of the combined section taking into consideration the partial interaction between timber and one or two other wood based materials. The effective EI can then be used in calculating the deflection of the combined section. This method will be followed for this type of wall.

Figure 4.30 shows the theoretical section as detailed in BS EN 1995 (2004) with the material interfaces. Figure 4.31 shows the assumed section for the wall type 8. A 600mm wide section of wall has been taken as this is the spacing of the studs and therefore allows the calculations to be carried out per stud for simplicity. As with the previous two wall constructions (wall types 6 and 7) the hemp-lime and render are assumed to act compositely and therefore have been transformed into one T shaped render section. This then partially interacts with the timber studs, which in turn partially interact with the sheathing board.

As shown in Figure 4.31 the transformed render and hemp-lime section overlaps with the timber section, as it does in the actual wall build up. When calculating the effective EI, the interaction plane has been taken as shown in Figure 4.31 at the top of the timber section, but the area and second moment of area of the transformed section are

calculated over the whole section height. The does not strictly follow Annex B in BS EN 1995 (2004), however these assumptions have been made as the hemp-lime and timber do overlap in the real wall constructions.

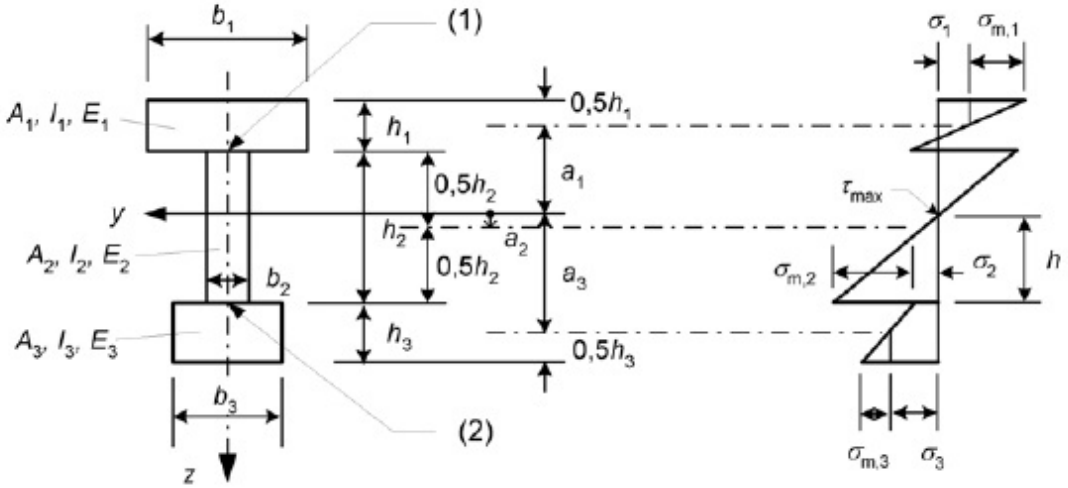

Figure 4.30 BS EN 1995 (2004) partial interaction section

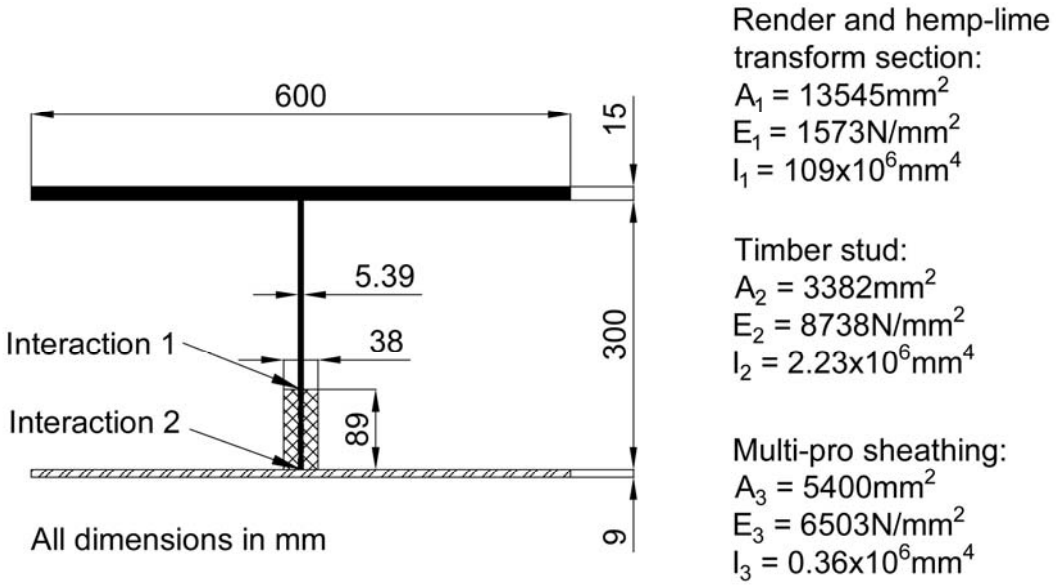

Figure 4.31 Composite render, hemp-lime, timber and sheathing board section for wall type 8

The effective EI is calculated in BS EN 1995 (2004) using the section shown in Figure 4.30 as follows:

$$(EI)_{ef} = \sum_{i=1}^{3} (E_i I_i + \gamma_i E_i A_i a_i^2)$$

Equation 4.24

Where:

$$\gamma_2 = 1$$

$$\gamma_i = \left[1 + \frac{\pi^2 E_i A_i s_i}{J_i l^2}\right]^{-1}$$

$$a_2 = \frac{\gamma_1 E_1 A_1 (h_1 + h_2) - \gamma_3 E_3 A_3 (h_2 + h_3)}{2\sum_{i=1}^{3} \gamma_i E_i A_i}$$

Where: $s_i = connector\ spacing, J_i = slip\ modulus\ for\ the\ interaction\ plane.$

Once EI_{ef} has been found the deflection in the centre of the span can be calculated using Equation 4.19 and Equation 4.20. BS EN 1995 (2004) also provides a formula for calculating the stresses within the section. The equation for finding the extreme fibre stress in section 1 of the composite cross section is:

$$\sigma_i + \sigma_{m,i} = \sigma = \frac{\gamma_i E_i a_i M}{(EI)_{ef}} + \frac{0.5 E_i h_i M}{(EI)_{ef}}$$

Equation 4.25

Where: $M = bending\ moment$

When applying this theory to wall type 8 the following assumptions have been made:

- Shear forces are carried by the hemp-lime and the connections between the different materials.
- Shear deflections within the hemp-lime will be calculated separately and added to the deflections calculated with the effective EI.
- Once the render and hemp-lime crack, shear defections have been ignored in the studwork framed as the studs are slender sections and the shear deflection will be a very low percentage of the total deflection.
- There is full interaction between the hemp-lime and the render so that no slip occurs between them.

The spacing of the connections at interaction plane 1 in Figure 4.31 is $s_1 = 600mm$. This is the distance between the horizontal rails. The slip modulus $J_1 = 1652N/mm$. This is the slip modulus of the rail to stud connections from Chapter 3. The spacing of

the connections in interaction plane 2 is $s_2 = 147mm$. This figure is an average of the spacing of the screw connectors over one sheet of sheathing. On studs that are at the edge of boards the screws are spaced at 200mm centres and on studs that are in the centre of the boards they are spaced at 300mm. The spacing s_2 also considers the screws connecting the sheathing board to the header and footer rails as these are contributing to the connection between the studwork frame and sheathing.

For the cross section of wall type 8 shown in Figure 4.31:

$$\gamma_1 = \left[1 + \frac{\pi^2 \times 1573 \times 13545 \times 600}{1652 \times 2400^2}\right]^{-1} = \underline{0.070}$$

$$\gamma_3 = \left[1 + \frac{\pi^2 \times 6503 \times 5400 \times 147}{764 \times 2400^2}\right]^{-1} = \underline{0.079}$$

$$a_2 = \frac{[0.070 \times 1573 \times 13545 \times (315 + 89)] - [0.079 \times 6503 \times 5400 \times (89 + 9)]}{2 \times [(0.070 \times 1573 \times 13545) + (1 \times 9873 \times 3382) + (0.079 \times 6503 \times 5400)]}$$

$$a_2 = \underline{4.38mm}$$

$$\therefore a_1 = NA_1 + NA_2 - a_2 = 254.6 + 44.5 - 4.38 = \underline{294.7mm}$$

$$a_3 = NA_2 + NA_3 + a_2 = 44.5 + 4.5 + 4.38 = \underline{53.4mm}$$

Using Equation 4.24 the effective EI can be calculated:

$$(EI)_{ef} = \sum_{i=1}^{3} (E_i I_i + \gamma_i E_i A_i a_i^2)$$

$$(EI)_{ef} = (1573 \times 109 \times 10^6 + 0.070 \times 1573 \times 13545 \times 294.7^2) + (9873 \times 2.23 \times 10^6 + 1.0 \times 9873 \times 3382 \times 4.38^2) + (6503 \times 36450 + 0.079 \times 6503 \times 5400 \times 53.4^2)$$

$$(EI)_{ef} = 3.32 \times 10^{11} Nmm^2 \; per \; 600mm \; width \; of \; wall$$

$$\therefore (EI)_{ef} = \underline{5.54 \times 10^{11} Nmm^2} per \; 1000mm \; width \; of \; wall$$

Comparing the calculated effective EI over 1000mm width of wall with the summation of EI of the individual parts (hemp-lime and render, timber, sheathing) the effective EI

is 73% higher. This shows that interaction between the various elements will significantly add to the bending stiffness of the wall panels. As this type of wall construction is asymmetric it will behave in a different way when loaded from opposite directions. Therefore the performance will be predicted from each direction separately. Initially the performance with the rendered face in tension will be analysed. Using the effective EI and Equation 4.19 and Equation 4.20 the deflection can be calculated at any load. When the load $w = 1.0kN/m$:

$$\delta_{total} = \delta_b + \delta_v = \left[\frac{5wl^4}{384EI}\right] + 2\left[\frac{k(wx^2 - 1200w)}{2GA}\right]_0^{1200}$$

$$\delta_{total} = \left[\frac{5 \times 1 \times 2400^4}{384 \times 5.54 \times 10^{11}}\right] + \left[2 \times \left(\frac{1.5 \times (1 \times 1200^2 - 1200 \times 1)}{2 \times 18.9 \times 300000} - \frac{1.5 \times (1 \times 0^2 - 0 \times 1)}{2 \times 18.9 \times 300000}\right)\right]$$

$$\delta_{total} = \underline{0.92mm}$$

This method of calculating the deflection is valid until one of the components of the composite wall section fails. As with wall types 6 and 7 this will be the extreme fibre as the stress will be greatest here. Therefore the tensile failure stress of the render can be found from Equation 4.25 by setting $\sigma = 0.9N/mm^2$ which is the render bending strength:

$$\sigma = \frac{\gamma_1 E_1 a_1 M}{(EI)_{ef}} + \frac{0.5 E_1 h_1 M}{(EI)_{ef}}$$

$$0.9 = \frac{0.070 \times 1573 \times 294.7 \times M}{5.54 \times 10^{11}} + \frac{0.5 \times 1573 \times 315 \times M}{5.54 \times 10^{11}}$$

$$\therefore M = \underline{1.78kNm}$$

From the bending moment the load can be calculated using Equation 4.22:

$$w = \frac{1.78 \times 8}{2.4^2}$$

$$w = \underline{2.4kN/m^2}$$

Once the render has cracked the hemp-lime is also likely to crack as it is much weaker and it has been assumed that the hemp-lime and render no longer contribute to the strength and stiffness of the wall. Therefore following cracking of the render and hemp-lime the load will continue to be carried by the studwork framing and sheathing board. The stiffness of the wall at this point can be calculated using the same method from BS EN 1995 (2004), but now with only one interface between the timber and the sheathing. The theoretical section for this situation is shown in Figure 4.32 from BS EN 1995 (2004).

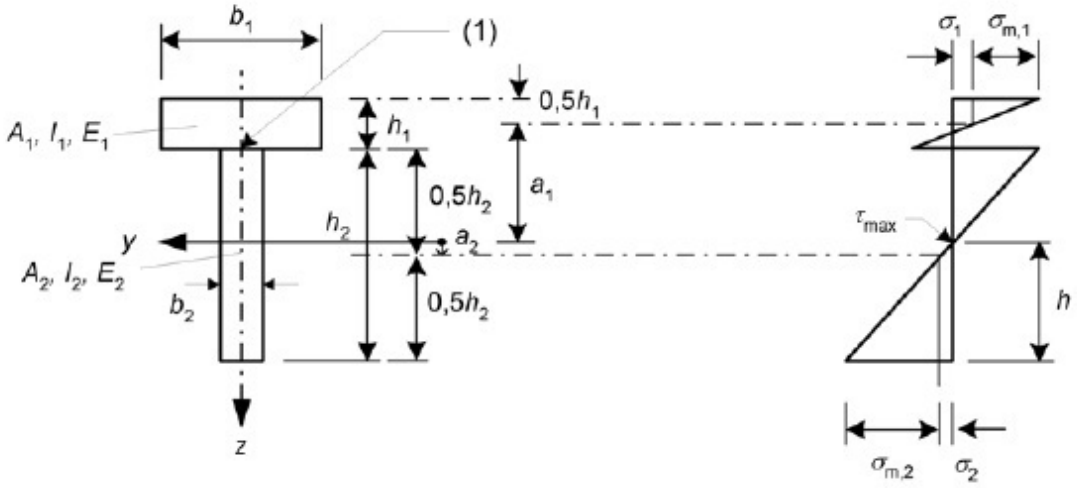

Figure 4.32 Stud and sheathing theoretical section (BS EN 1995-1.1, 2004)

Using the same method as shown previously the effective EI of the studwork and sheathing section is 4.50×10^{10}N/mm^2 per metre length of wall. The stiffness and maximum load have been calculated in the same way as for the entire wall section with failure occurring when the extreme fibre stress in the timber exceeds its strength. This will happen when the load reaches 11.28kN/m^2. The calculated predictions of strength and stiffness are plotted on the graph in Figure 4.34 which shows load against displacement at mid height of the wall.

When wall type 8 is being loaded in the opposite direction with a positive load applied to the rendered face so that the sheathing board is in tension its performance can be treated in a similar manner. The deflection of the entire wall section can be calculated as previously when the rendered face is in tension and therefore the initial stiffness will be the same. Again the initial failure will occur in the most highly stressed fibre. With loading in this direction this may either be in the surface of the sheathing board, in the

hemp-lime surface below the sheathing board or in the timber stud. The stresses in each location and the corresponding bending moments and loads can be calculated using Equation 4.25.

For the sheathing the bending strength from Chapter 3 is $\sigma_b = 12.4N/mm^2$ and the bending moment that causes the bending stress to equal the bending strength is:

$$\sigma_3 = \frac{\gamma_3 E_3 a_3 M}{(EI)_{ef}} + \frac{0.5 E_3 h_3 M}{(EI)_{ef}}$$

$$12.4 = \frac{0.079 \times 6503 \times 53.38 \times M}{5.54 \times 10^{11}} + \frac{0.5 \times 6503 \times 9 \times M}{5.54 \times 10^{11}}$$

$$\therefore M = \underline{120.8kNm}$$

Following the same calculation for the timber where in the equivalent section $\sigma_b = 71.7N/mm^2$:

$$\sigma_2 = \frac{\gamma_2 E_2 a_2 M}{(EI)_{ef}} + \frac{0.5 E_2 h_2 M}{(EI)_{ef}}$$

$$71.7 = \frac{1 \times 9873 \times 4.38 \times M}{5.54 \times 10^{11}} + \frac{0.5 \times 9873 \times 89 \times M}{5.54 \times 10^{11}}$$

$$\therefore M = \underline{82.3kNm}$$

With the hemp-lime, which is represented as an equivalent render section, the tensile stresses at the interface with the sheathing board and timber can be calculated from the stress profile shown in Figure 4.30 as σ_1 and σ_{1m} are known as is h_1 and the neutral axis of section 1. A detailed profile of the stresses in section 1 is shown in Figure 4.33.

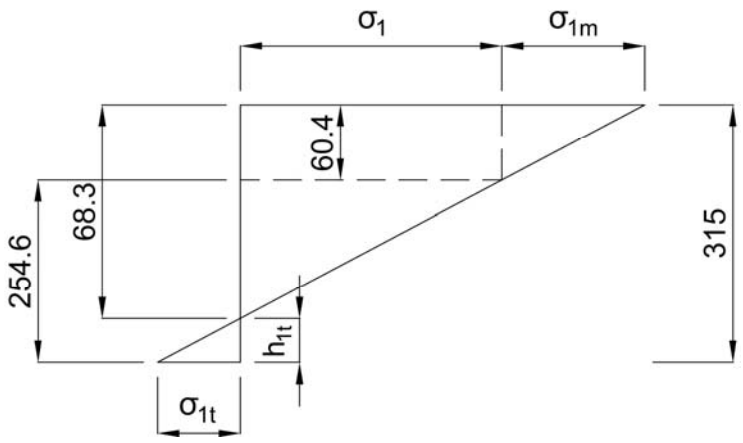

Figure 4.33 Section 1 stresses

From the geometry in Figure 4.33 and when $\sigma_{1t} = 0.9N/mm^2$:

$$\sigma_{1t} = \frac{\sigma_1 + \sigma_{1m}}{68.3} h_{1t}$$

$$0.9 = \frac{5.88 \times 10^{-8} M + 4.47 \times 10^{-7} M}{68.3} \times (315 - 68.3)$$

$$\therefore M = \underline{0.49kNm}$$

From these three calculations it is clear that the hemp-lime will fail in tension first. The load at which this will happen is:

$$w = \frac{8M}{l^2} = \frac{8 \times 0.49}{2.4^2} = \underline{0.68kN/m^2}$$

Once failure of the hemp-lime has occurred the following assumptions have been made:

- The hemp-lime and render do not contribute to the stiffness of the wall section
- Shear defections have been ignored in the studwork framed and sheathing as the studs are slender sections and the shear deflection will be a very low percentage of the total deflection.

The stiffness of the wall type 8 with the sheathing in tension following failure of the hemp-lime will be the same as when the render was in tension and as previously the effective EI will be 4.50x10^{10}N/mm^2 per metre length of wall. When loaded in this direction wall type 8 could fail in one of two ways. Either the studwork frame or sheathing board will fail in bending or the connections between the two will fail. BS EN 1995 (2004) shows that the load on individual fasteners can be calculated from:

$$F_i = \frac{\gamma_i E_i A_i a_i s_i}{(EI)_{ef}} V$$

Equation 4.26

The average fastener shear capacity from Chapter 3 is $F = 1.75kN$ and therefore the shear force that causes the connectors to fail is:

$$1.75 \times 10^3 = \frac{0.093 \times 9873 \times 3382 \times 45.4 \times 147}{2.58 \times 10^{10}} V$$

$$V = 2.46kN\ per\ 600mm\ length\ of\ wall$$

$$\therefore V = \underline{4.10kN}\ per\ 1000mm\ length\ of\ wall$$

The load to cause this shear force is:

$$w = \frac{4.10 \times 2}{2.4} = \underline{3.4kN/m^2}$$

Alternatively the sheathing board of timber could fail in bending. The extreme fibre stress in the sheathing from Figure 4.32 is calculated using Equation 4.25:

$$\sigma_1 + \sigma_{m1} = \sigma_1 = \frac{\gamma_1 E_1 a_1 M}{(EI)_{ef}} + \frac{0.5 E_1 h_1 M}{(EI)_{ef}}$$

$$12.4 = \frac{1 \times 6503 \times 3.56 \times M}{2.58 \times 10^{10}} + \frac{0.5 \times 6503 \times 9 \times M}{2.58 \times 10^{10}}$$

$$\therefore M = \underline{6.1kNm}$$

The timber tensile stresses can be calculated in the same way as the hemp-lime stresses previously by considering the geometric properties of the stress profile within the material. By doing this the moment to cause the stresses in the timber to equal the strength can be seen to be:

$$M = \underline{4.6kNm}$$

Therefore the stud will fail by bending before the sheathing and the load at which this bending moment will occur is:

$$w = \frac{8 \times 4.6}{2.4^2} = 6.38kN/m^2$$

Based on these calculations the sheathing to stud connections will fail first at a load of 3.4kN/m^2. These results are shown in Figure 4.34 along with the predictions for wall types 6 and 7 for comparison.

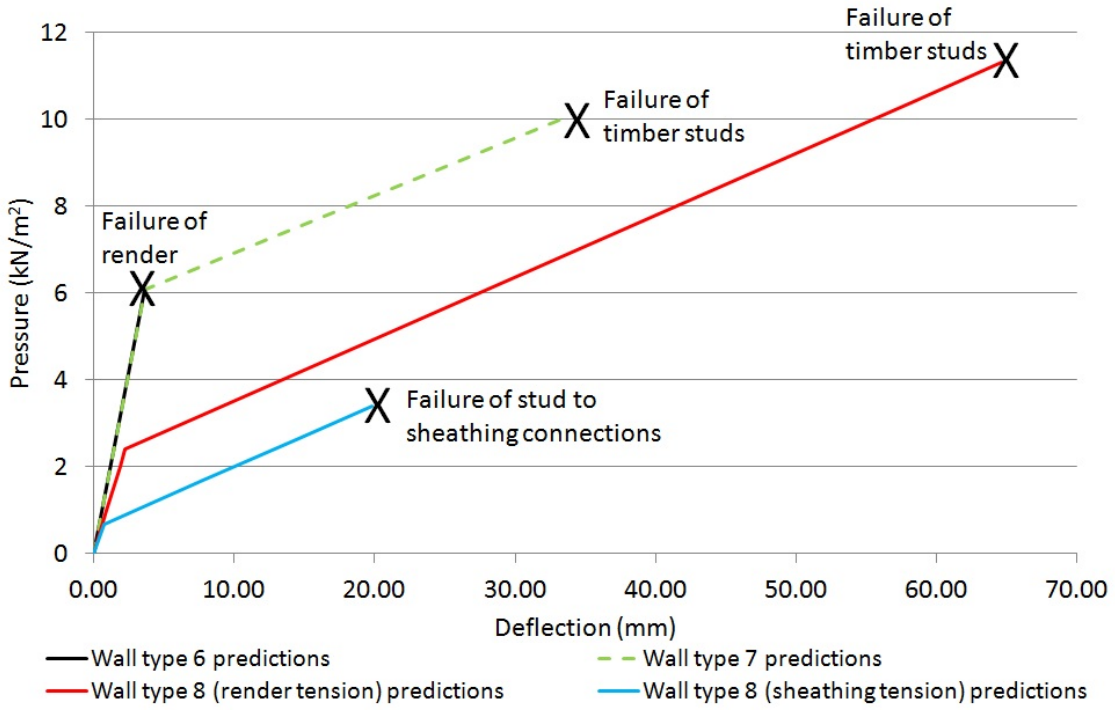

Figure 4.34 All bending wall predictions

Comparing all of the predictions shown in Figure 4.34, it can be seen that the initial stiffness of the wall panels is similar for all of the wall types with wall types 6 and 7 being slightly stiffer. The main difference is that on wall type 8 the render cracking load is lower when the render is in tension. It is also clear that the lack of studwork framing in wall type 6 causes a brittle failure and a lack of load carrying capacity following the cracking of the render and hemp-lime.

With all of the wall types the thickness of the render has the potential to significantly affect the results. Figure 4.35 shows the effect render thickness has on the deflection of wall type 6 when subjected to three different loads. These results show that the thickness of the render affects the out-of-plane deflection of the walls. With no render and an applied load of 2kN/m^2 the horizontal deflection of the hemp-lime at the centre of the wall is 6.7mm. With 15mm of render on both faces this is reduced by 92% to 0.4mm which clearly shows the decrease in deflection when render is applied. Figure 4.35 also shows that there is a decreasing gain in stiffness as the thickness of the render increases above 15mm to 20mm. The large increases in deflection should be carefully considered if the render is applied at thicknesses less than 10mm.

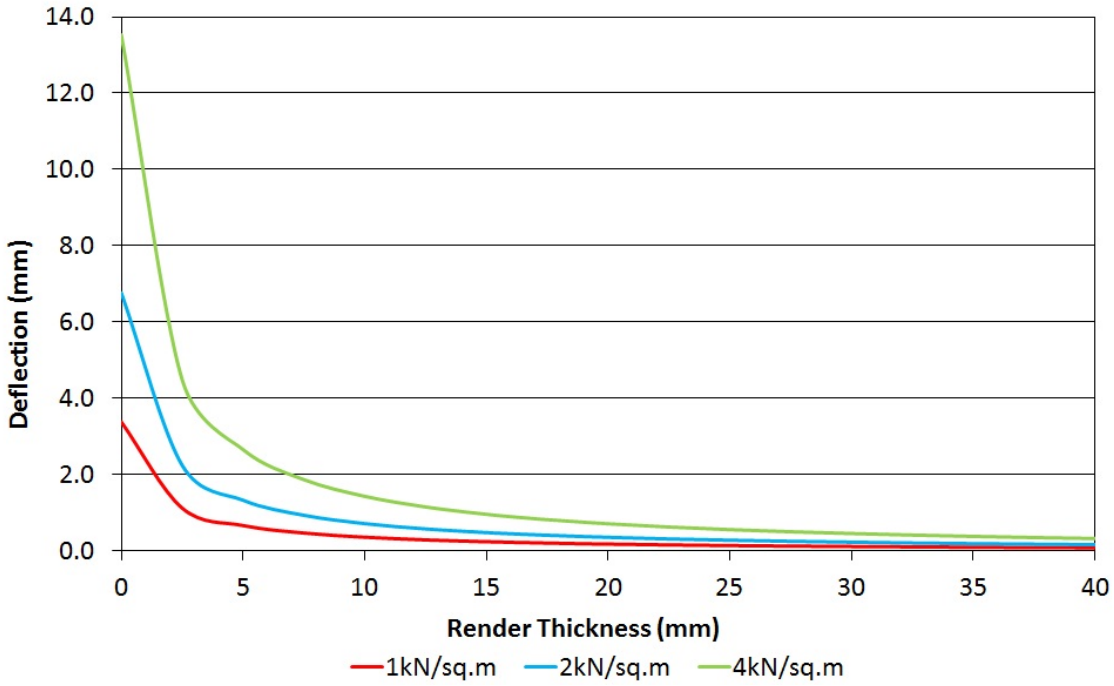

Figure 4.35 Effect of render thickness

4.6 Conclusions

The predictions made during this chapter will be compared with the experimental results in the following chapters. Under compressive loading prediction of peak loads or buckling loads have been made. With both concentric and eccentric loads the predicted peak loads of the composite hemp-lime and timber studwork walls are higher than those for the unrestrained studs. From a theoretical approach this shows that the hemp-lime does enhance the load capacity of the studwork framing. The precise failure mode of the stud with eccentric loading and hemp-lime cover cannot be predicted at this stage and this will be discussed further in Chapter 6.

Under in-plane racking loading the stiffness and maximum load for wall type 5 was predicted. For wall types 1 and 2 only the stiffness has been predicted. This is because large deflections have been predicted and therefore the maximum load is less critical than the stiffness. The performance of a studwork frame without hemp-lime has not been predicted. The stiffness and strength of this frame are expected to be very low as the joints between the studs and header and footer rails have very low rotational resistance. Therefore the composite hemp-lime and studwork frames will have a much higher stiffness and strength.

Under out-of–plane bending both the stiffness and strength has been predicted. This has shown the importance of the render in the both the stiffness and strength. It has also shown that the timber frame might introduce some continued load capacity and ductility once the render and hemp-lime have failed.

Throughout the theoretical analysis combined load effects have generally been ignored. Only combined in-plane racking and compressive loads have been analysed. The same will be true during the experimental study. There is currently very limited understanding of the behaviour of composite hemp-lime and timber studwork framing. Therefore by initially treating the load cases individually a more complete picture can be built of the construction's behaviour and combined loads are outside the scope of this study. Combined load effects could be an area for further research.

The effect of openings within walls has not been considered. Initially while the understanding of the composite behaviour of this type of wall construction is limited openings could be treated in a simple manner. The complete sections of wall either side of an opening could be designed to resist the loads applied to the section of wall panel with the opening. This is a quick and simple approach that only requires the loads on the wall panel with the opening in to be calculated and then added to the adjacent wall panels.

Finally the predicted performance for each wall type is summarised in Table 4.6. Due to the difficulties in predicting the performance with eccentric compressive loads these predictions have not been included.

Table 4.6 Summary of predicted performance

Wall type	**Compression (concentric loading)**	**Racking**	**Bending**
1	Header/footer bearing failure at 31.5kN Stud crushing at 155.9kN	Initial stiffness 1.3kN/mm. Initial separation of leading stud joint at 12.5kN	-

2	Header/footer bearing failure at 31.5kN Stud crushing at 155.9kN	Initial stiffness 1.3kN/mm. Initial separation of leading stud joint at 12.5kN	-
3	Header/footer bearing failure at 31.5kN Stud crushing at 155.9kN	-	-
4	Header/footer bearing failure at 31.5kN Stud crushing at 155.9kN	-	-
5	-	Initial stiffness 3.5kN/mm. Failure of sheathing connections at 24.5kN.	-
6	-	-	Bending stiffness of 1.7kN/mm. Failure at 6.1kN/m^2.
7	-	-	Initial bending stiffness of 1.7kN/mm. Failure of render at 6.1kN/m^2. Failure of timber studs at 10kN/m^2.
8	-	-	Render in tension: Render failure at 2.4kN/m^2, stud failure at 11.3kN/m^2. Sheathing in tension: Failure of render at 0.68kN/m^2, sheathing connector failure at 3.4kN/m^2.

5 Experimental Wall Panel Specimens

5.1 Introduction

This chapter details the large scale wall panel test specimens used throughout this study. Details of the design, manufacture and storage prior to testing are presented.

5.2 Large scale wall panels

The details, method of construction and storage of the large scale wall panels will be divided into three sections as the wall panels were built on three separate occasions with slightly differing construction processes each time. For this reason their details and construction methods will be separated accordingly into the initial large scale wall panel (called Initial), the first series of large scale testing (called LS1) and the second series of large scale testing (called LS2). The large scale walls have been separated as shown in Table 5.1 which also shows the name given to each specimen.

When using composite hemp-lime and studwork construction there are two locations the studwork framing is generally positioned in, either in the centre of the hemp-lime (Figure 5.1) or on the edge of the hemp-lime (Figure 5.2). Both of these techniques are currently used in the construction of composite hemp-lime and studwork framing. When the studwork frame is in the centre of the hemp-lime it is fully encapsulated and as a result the studwork framing and hemp-lime cannot separate. Additionally full encapsulation may be structurally beneficial. When the studwork frame is on the edge of the hemp-lime permanent shuttering can be used against one face of the wall which allows for faster construction and easier finishing of the walls internally as the permanent shuttering can simply be skim plastered. However as the studwork frame could separate from the hemp-lime additional horizontal rails have to be used. The different positioning of the studwork frames are detailed in Table 5.1.

Figure 5.1 Studwork frame in centre of hemp-lime (Wall C1)

Figure 5.2 Studwork frame on edge of hemp-lime (Wall R5)

Table 5.1 Large scale wall panel specimen names

Load case	Specimen name	Test series	Wall type	Studwork frame placement	Construction date	Test date
C = Compression, S = Stud	Wall C1	Initial	-	Centre	4/11/2009	4/12/2009
	Wall C2	LS1	1	Centre	Apr/May 2010	Oct/Nov 2010
	Wall C3	LS1	2	Edge	Apr/May 2010	Oct/Nov 2010
	Wall C4	LS2	1	Centre	Aug 2011	Nov 2011
	Wall C5	LS2	3	50mm cover	Aug 2011	Nov 2011
	Wall C6	LS2	4	50mm cover	Aug 2011	Nov 2011
	Wall C7	LS2	2	Edge	Aug 2011	Nov 2011
	Stud S1	Initial	-	-	4/11/2009	4/12/2009
	Stud S2	LS1	-	-	Oct 2010	Oct 2010
	Stud S3	LS1	-	-	Oct 2010	Oct 2010
	Stud S4	LS1	-	-	Oct 2010	Oct 2010
	Stud S5	LS2	-	-	Nov 2011	Nov 2011
	Stud S6	LS2	-	-	Nov 2011	Nov 2011
	Stud S7	LS2	-	-	Nov 2011	Nov 2011
	Stud S8	LS2	-	-	Nov 2011	Nov 2011
	Stud S9	LS2	-	-	Nov 2011	Nov 2011
	Stud S10	LS2	-	-	Nov 2011	Nov 2011
R = Racking	Wall R1	LS1	1	Centre	Apr/May 2010	Oct/Nov 2010
	Wall R2	LS1	2	Edge	Apr/May 2010	Oct/Nov 2010
	Frame R3	LS1	-	-	Nov 2010	Nov 2010
	Wall R4	LS2	2	Edge	Aug 2011	Nov 2011
	Wall R5	LS2	5	Edge	Aug 2011	Nov 2011
B = Bending	Wall B1	LS1	6	-	Apr/May 2010	Oct/Nov 2010
	Wall B2	LS1	7	Centre	Apr/May 2010	Oct/Nov 2010
	Wall B3	LS2	8	Edge	Aug 2011	Nov 2011
	Wall B4	LS2	8	Edge	Aug 2011	Nov 2011
Wall type as shown in Chapter 4						

5.2.1 Initial large scale wall panel

Wall C1 used the same wall and frame dimensions and materials as Helmich (2008), but the density of the hemp-lime was much lower and in line with the current practice (Lime Technology, 2010b). Helmich (2008) showed that hemp-lime enhanced the compressive capacity of the frame when using hemp-lime at 466kg/m^3, this test aimed to investigate whether an enhancement to compressive strength was also achieved when the density was reduced to 275kg/m^3.

Both Wall C1 and Stud S1 were constructed using identical Metsec lightweight steel framing. Despite the fact that lightweight steel was unlikely to be used in composite hemp-lime and studwork construction it was chosen here as the properties are consistent and it is also the material used by Helmich (2008). A cross section through one of the studs is shown in Figure 5.3. The frames were constructed from three 2.5m long lipped channel studs at 600mm centres with channel section header and footer rails. The studs were bolted to the header and footer using M12 nuts and bolts. Detailed drawings of the wall panels are shown in Figure 5.4 and Figure 5.5.

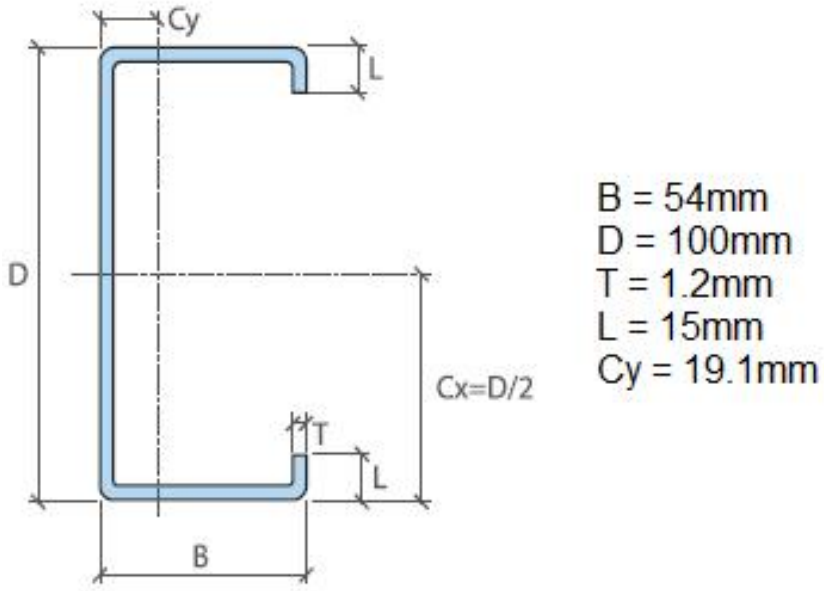

Figure 5.3 Metsec stud dimensions

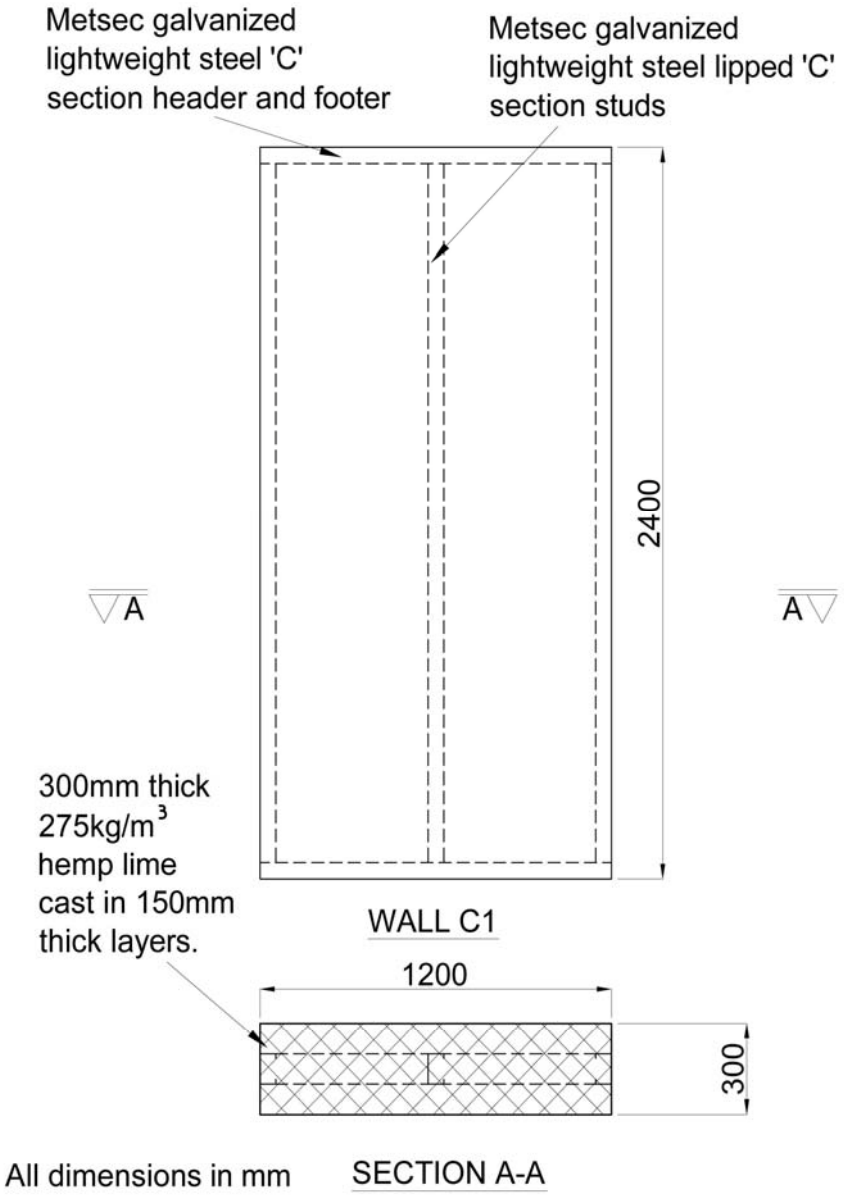

Figure 5.4 Wall C1 drawing

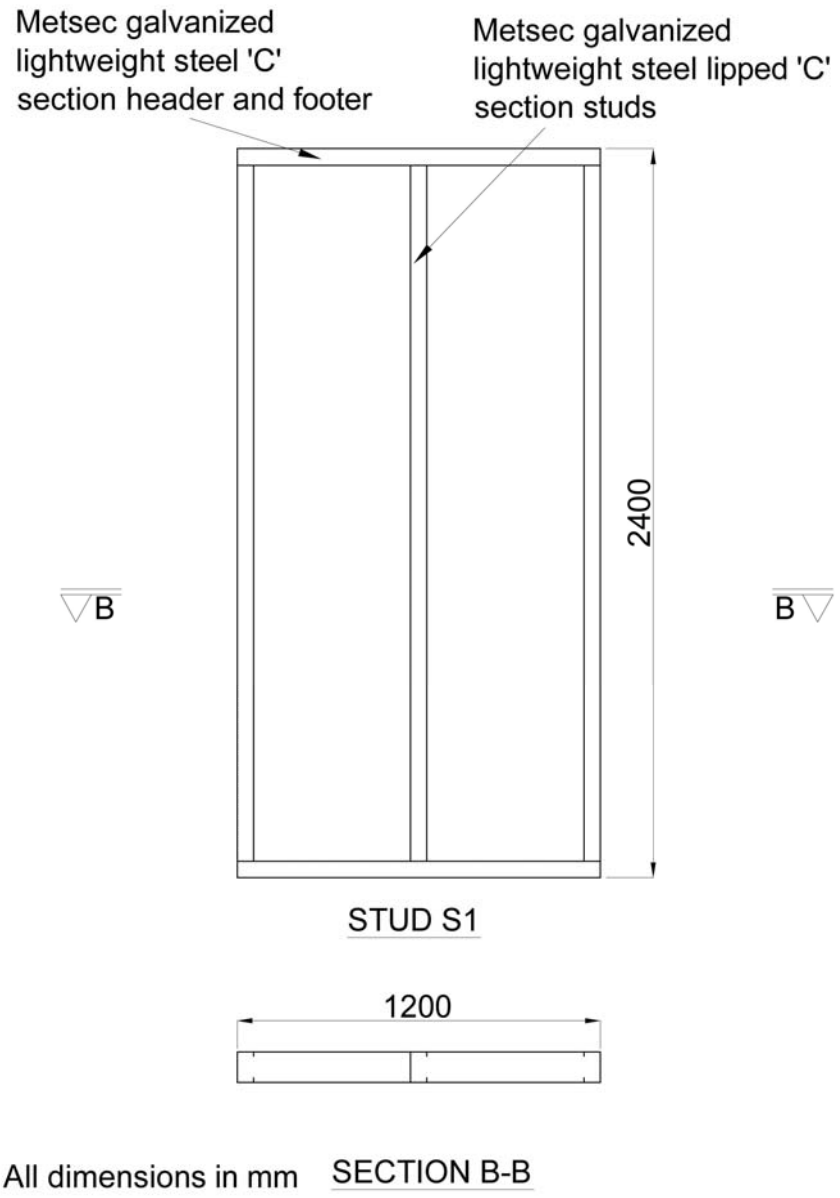

Figure 5.5 Stud S1 drawing

Hemp-lime was cast around one of the frames. The frame was positioned in the centre of the shuttering and a wall 1.25m wide by 0.3m thick by 2.45m high was cast. The hemp-lime was mixed in a small pan mixer at the University of Bath. The water and binder were initially added and mixed into a slurry. The hemp shiv was then added and mixed with the slurry for two to three minutes until both were fully mixed. Each mix was carefully weighed and corresponded to a 150mm layer in the wall at the target dry density of 275kg/m^3. The wall was cast in three lifts of equal height over three days in order to minimise any potential settlement due to the self-weight of the wet hemp-lime mix (Figure 5.6).

Figure 5.6 Wall casting – First lift

The shuttering was removed 24 hours after the final lift had been cast. Prior to removing the shutting the hemp-lime had settled by 10mm. Upon removal of the shuttering the hemp-lime settled by a further 10mm and over the following week settled by a further 15mm to result in a total settlement of 35mm (Figure 5.7). The hemp-lime was left to cure for 28 days prior to testing.

Figure 5.7 Hemp-lime settlement

5.2.2 Large Scale series one (LS1)

This series of wall panel specimens consisted of six composite hemp-lime and timber studwork walls (Walls C2, C3, R1, R2, B1 and B2) and four timber only frames (Studs S2, S3, S4 and Frame R3). Details of all of the specimens are shown in Table 5.2 to Table 5.4. Detailed drawings of the wall panel specimens are shown in Figure 5.8 to Figure 5.15. These panels were chosen as they are representative of what is used in buildings as well as being suitable for each type of load test being undertaken. All of the panels are 2.4m high as this is the standard studwork framing storey height. The panels for compression testing are 1.8m wide. This allows there to be three studs within the wall panel with half a stud centre either side of the outer studs. This configuration has been chosen to allow compression testing of the centre stud with minimal edge effects while still allowing some interaction between adjacent studs. The wall panels for in plane racking are 2.4m wide. This conforms to the standard studwork wall panel racking test specimen size set out in BS EN 594 (1996) and this test standard will be followed as closely as possible. The wall panels for out of plane testing are 1.8m wide, the same as the compression panels. This width was again a compromise between reducing edge effects with a large enough width while also creating a wall panel that could physically be tested and moved for testing.

Table 5.2 Compression test wall details

Compression Testing	
Description	**Details**
Studs S2, S3 and S4: Timber stud with header and footer rails only. 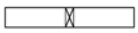 Plan	– C16 timber stud with C16 header and footer. – 38 x 89mm stud, header and footer. – 2.4 m high by 0.6m wide. – Header and footer connections with 2No. 3mm x 75mm nails per connection.
Wall C2: Timber stud with header and footer rails cast into the centre of the hemp lime. Wall type 1  Plan	– Three C16 timber studs with C16 header and footer. – 38 x 89mm stud, header and footer. – 2.4 m high by 1.8m wide. – Header and footer connections with 2No. 3mm x 75mm nails per connection. – 275 kg/m^3 hemp lime (oven dry density). – Hemp lime cast 300mm thick, tamped in 150mm high layers with maximum lift of 900mm per day.
Wall C3: Timber stud with header and footer rails cast into the edge of the hemp lime. Wall type 2  Plan	– Three C16 timber studs with C16 header and footer. – 38 x 89mm stud, header and footer. – 2.4 m high by 1.8m wide. – Header and footer connections with 2No. 3mm x 75mm nails per connection. – 25 x 50mm rail fixed to stud at 600mm vertical centres to fix hemp lime to the stud. – 275 kg/m^3 hemp lime (oven dry density). – Hemp lime cast 300mm thick, tamped in 150mm high layers with maximum lift of 900mm per day.

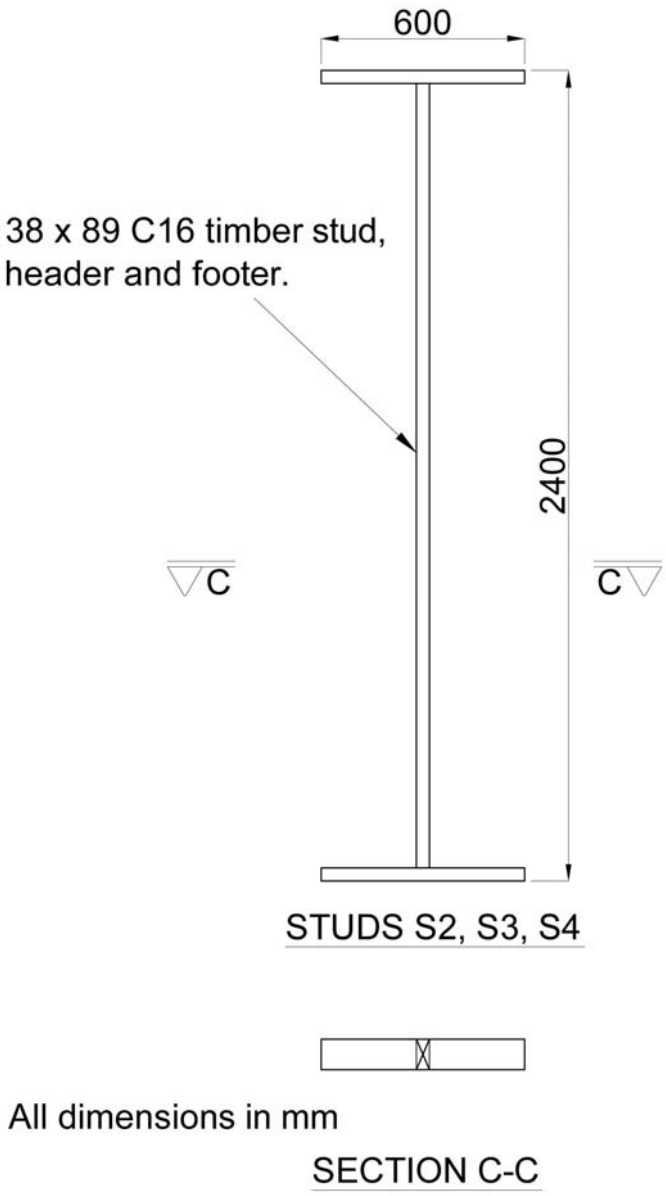

Figure 5.8 Studs S2, S3, S4 drawing

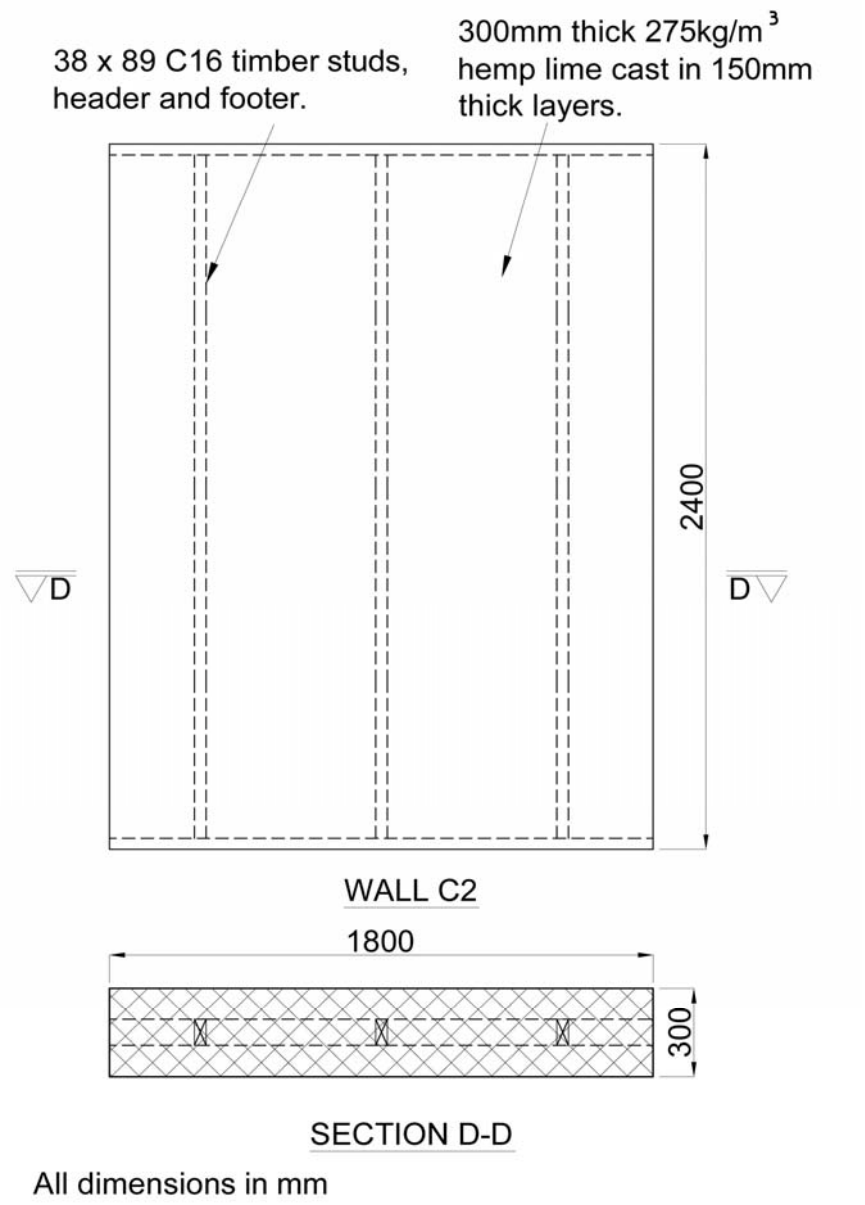

Figure 5.9 Wall C2 drawing

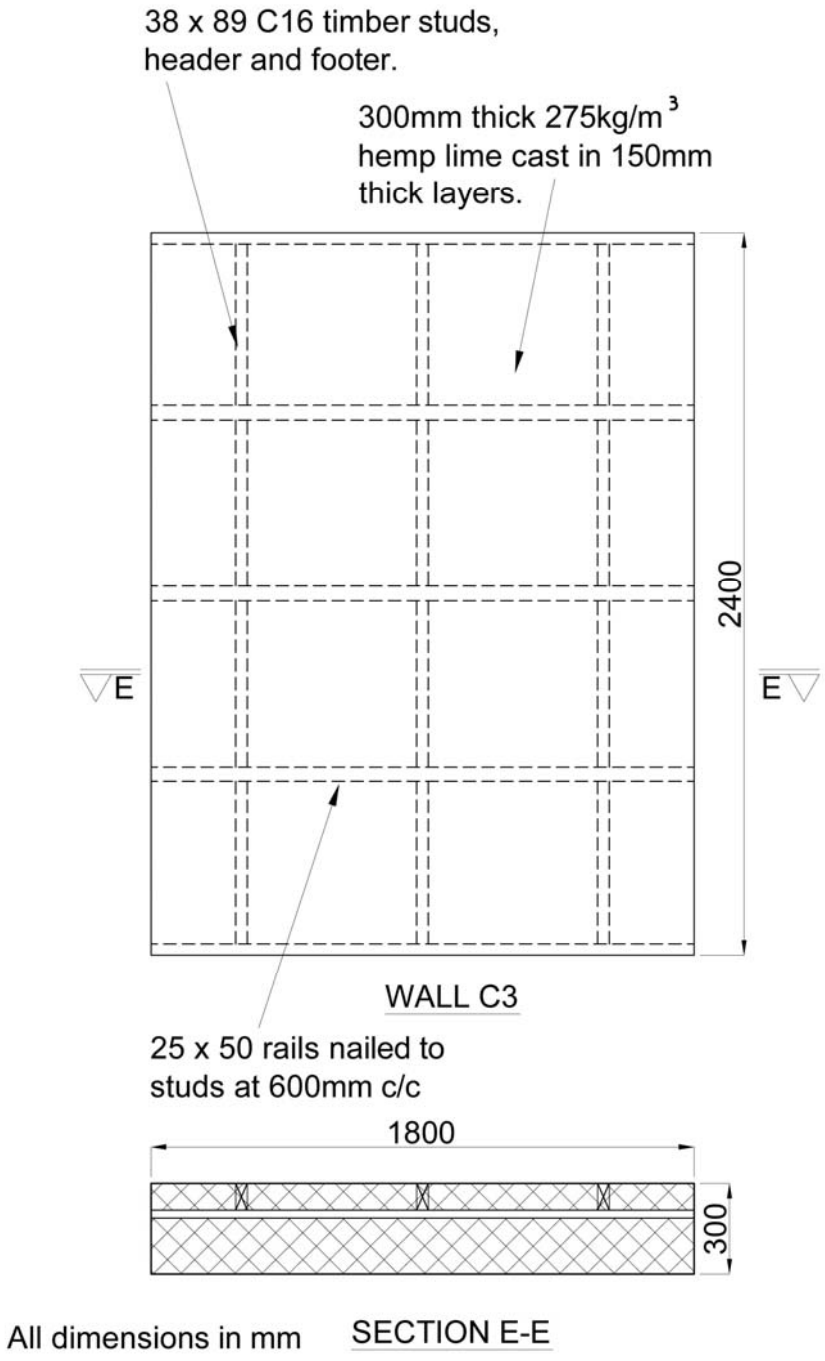

Figure 5.10 Wall C3 drawing

Table 5.3 Racking test wall details

Racking Testing	
Description	**Details**
Frame R3: Wall panel with timber studs with header and footer rails only. 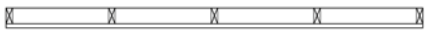 Plan	– Wall panel made from C16 timber studs with C16 header and footer. – 38 x 89mm studs, header and footer. – 2.4 m high by 2.4m wide. – Studs at 600mm c/c. – Header and footer connections with 2No. 3mm x 75mm nails per connection. – 25 x 50mm rail fixed to stud at 600mm vertical centres to fix hemp lime to the stud. – Vertical load of 5kN per stud.
Wall R1: Wall panel with timber studs with header and footer rails cast into the centre of the hemp lime. Wall type 1  Plan	– Wall panel made from C16 timber studs with C16 header and footer. – 38 x 89mm stud, header and footer. – 2.4 m high by 2.4m wide. – Studs at 600mm c/c. – Header and footer connections with 2No. 3mm x 75mm nails per connection. – 275 kg/m^3 hemp lime (oven dry density). – Hemp lime cast 300mm thick, tamped in 150mm high layers with maximum lift of 900mm per day.
Wall R2: Wall panel with timber stud with header and footer rails cast into the edge of the hemp lime. Wall type 2  Plan	– Wall panel made from C16 timber studs with C16 header and footer. – 38 x 89mm stud, header and footer. – 2.4 m high by 2.4m wide. – Studs at 600mm c/c – Header and footer connections with 2No. 3mm x 75mm nails per connection. – 25 x 50mm rail fixed to stud at 600mm vertical centres to fix hemp lime to the stud.

	– 275 kg/m^3 hemp lime (oven dry density). – Hemp lime cast 300mm thick, tamped in 150mm high layers with maximum lift of 900mm per day.

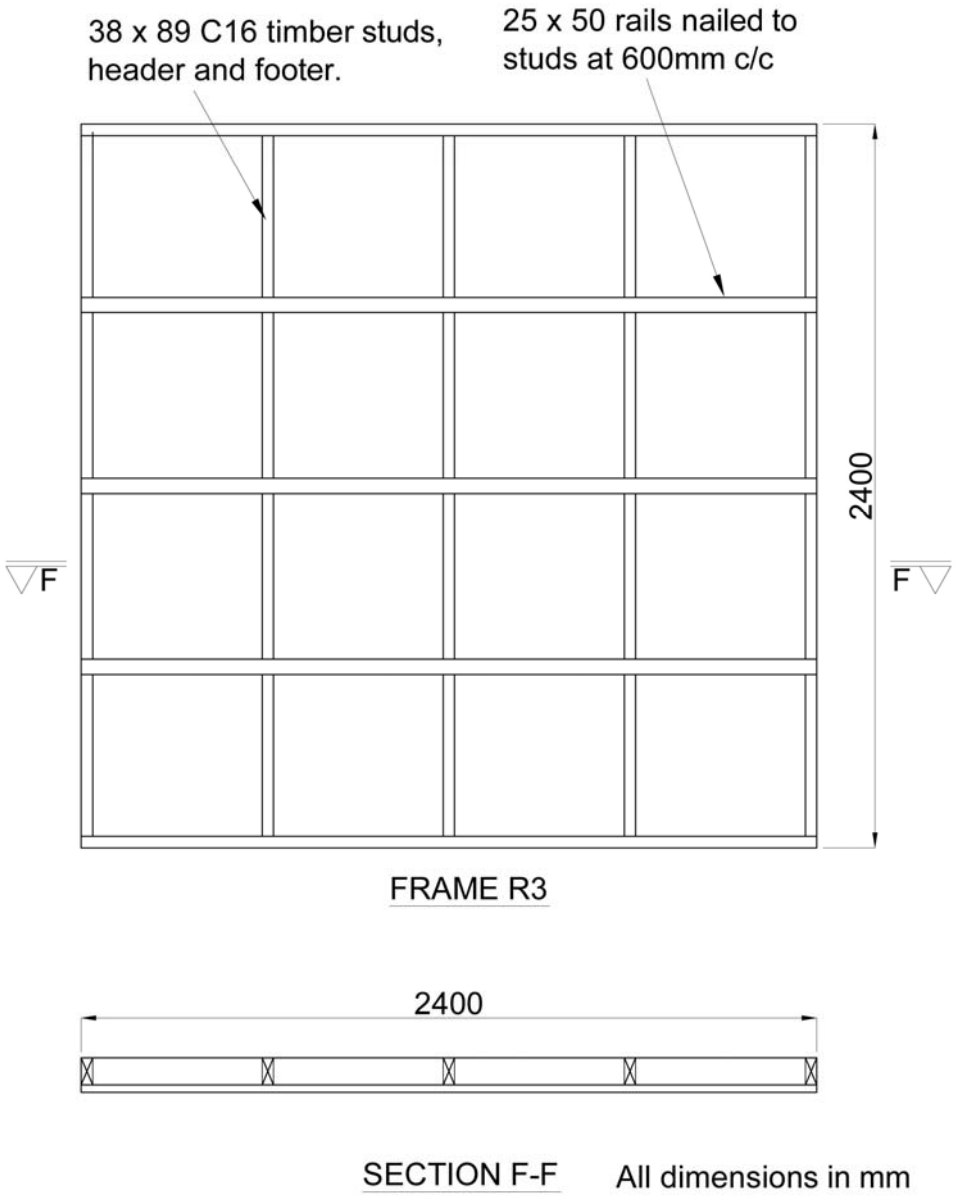

Figure 5.11 Frame R3 drawing

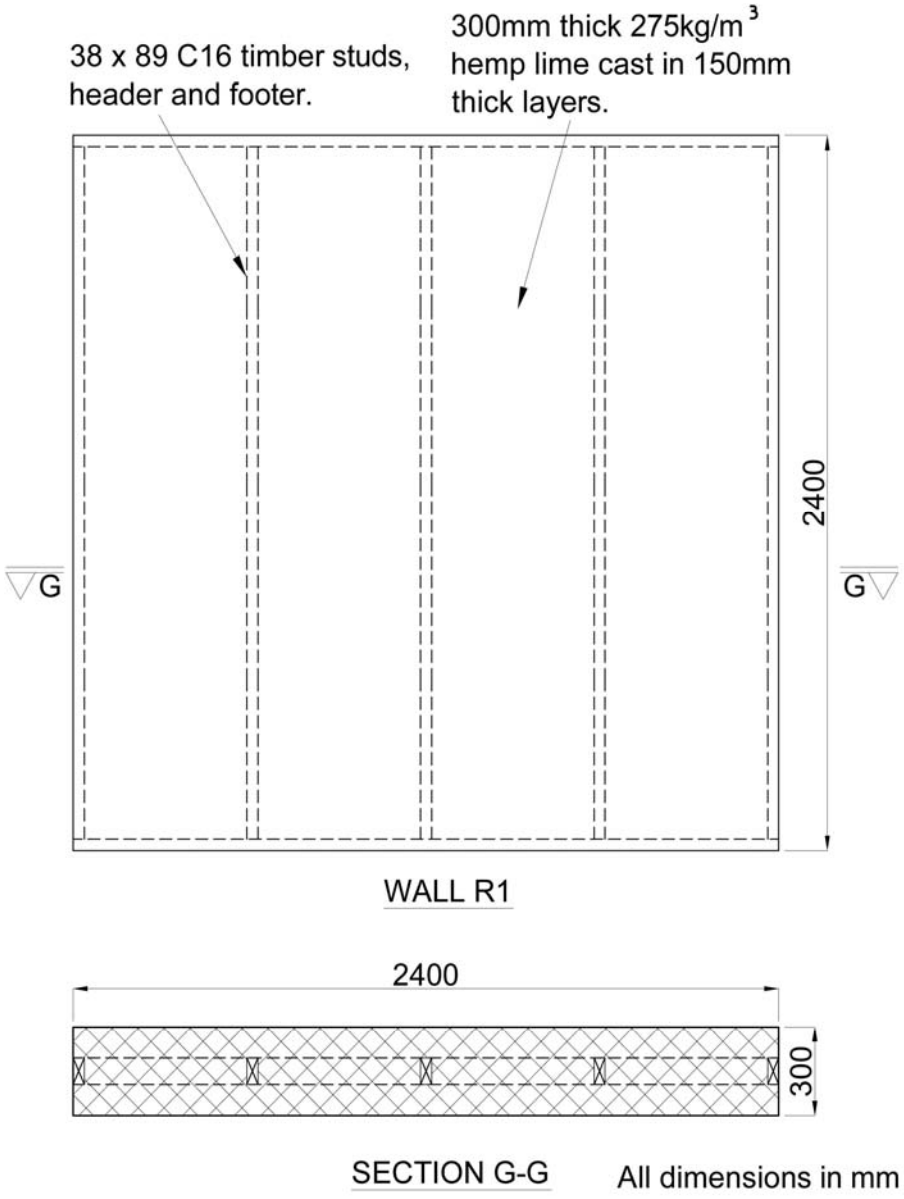

Figure 5.12 Wall R1 drawing

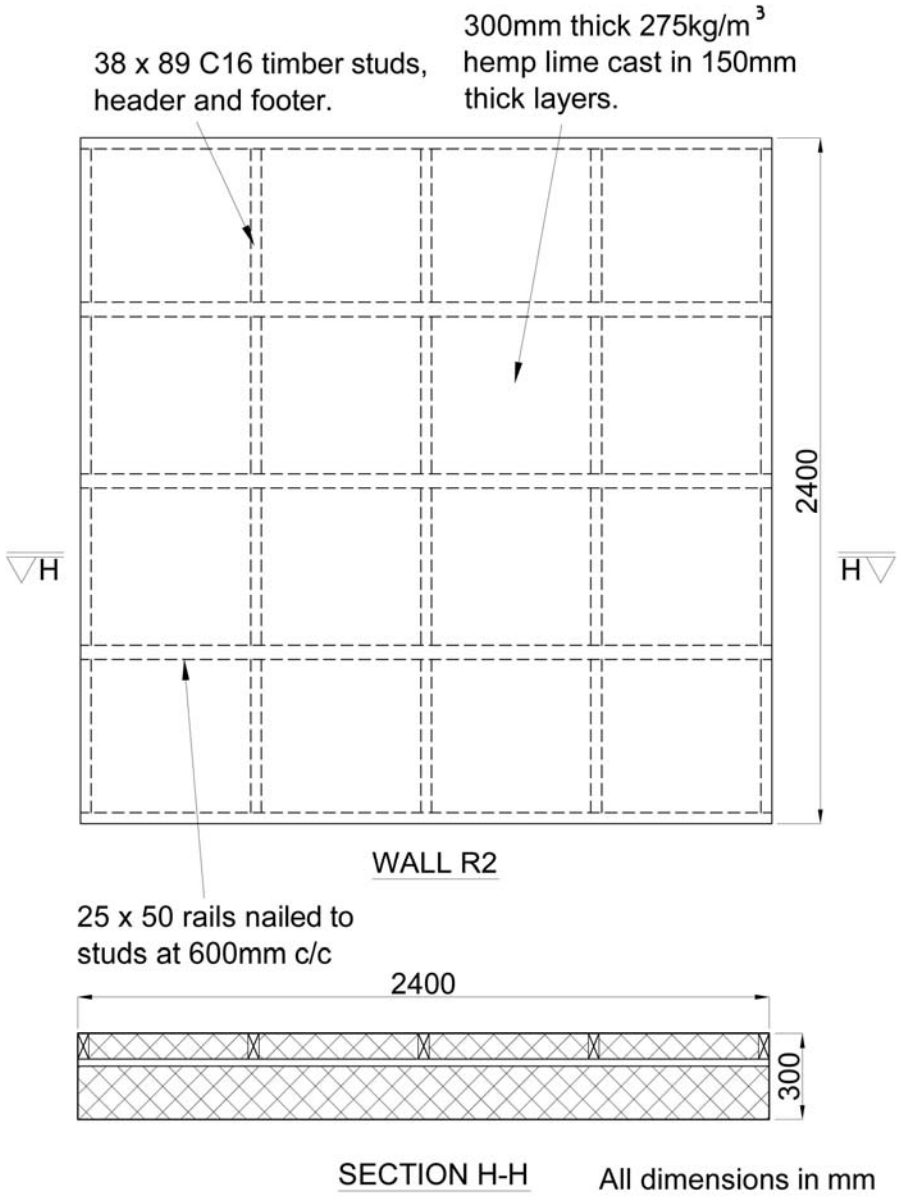

Figure 5.13 Wall R2 drawing

Table 5.4 Bending test wall details

Bending Testing	
Description	**Details**
Wall B1: Hemp-lime and render only wall panel Wall type 6  Plan	– 275 kg/m^3 hemp lime wall (oven dry density). – 2.4 m high by 1.8m wide. – Hemp lime cast 300mm thick, tamped in 150mm high layers with maximum lift of 900mm per day. – 15mm render both faces
Wall B2: Wall panel with timber studs with header and footer rails cast into the centre of the hemp lime. Wall type 7  Plan	– Wall panel made from C16 timber studs with C16 header and footer. – 38 x 89mm stud, header and footer. – 2.4 m high by 1.8m wide. – Studs at 600mm c/c. – Header and footer connections with 2No. 3mm x 75mm nails per connection. – Hemp lime cast 300mm thick, tamped in 150mm high layers with maximum lift of 900mm per day. – 275 kg/m^3 hemp lime (oven dry density). – 15mm render both faces.

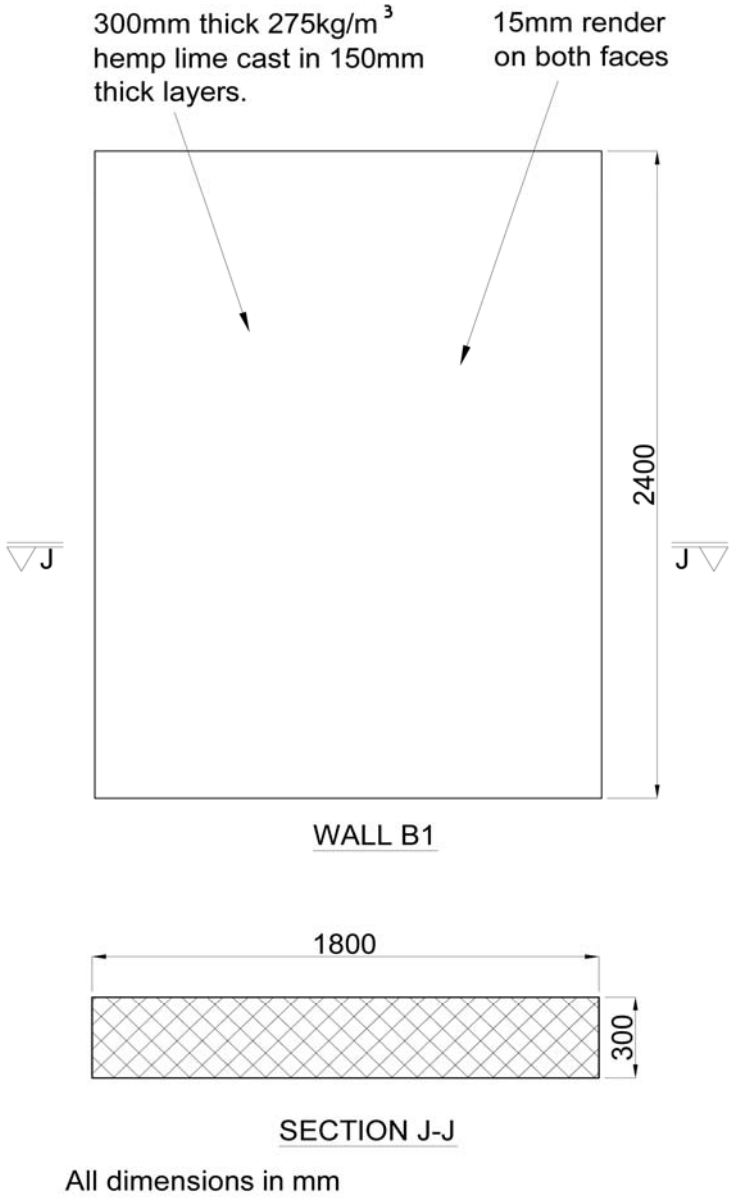

Figure 5.14 Wall B1 drawing

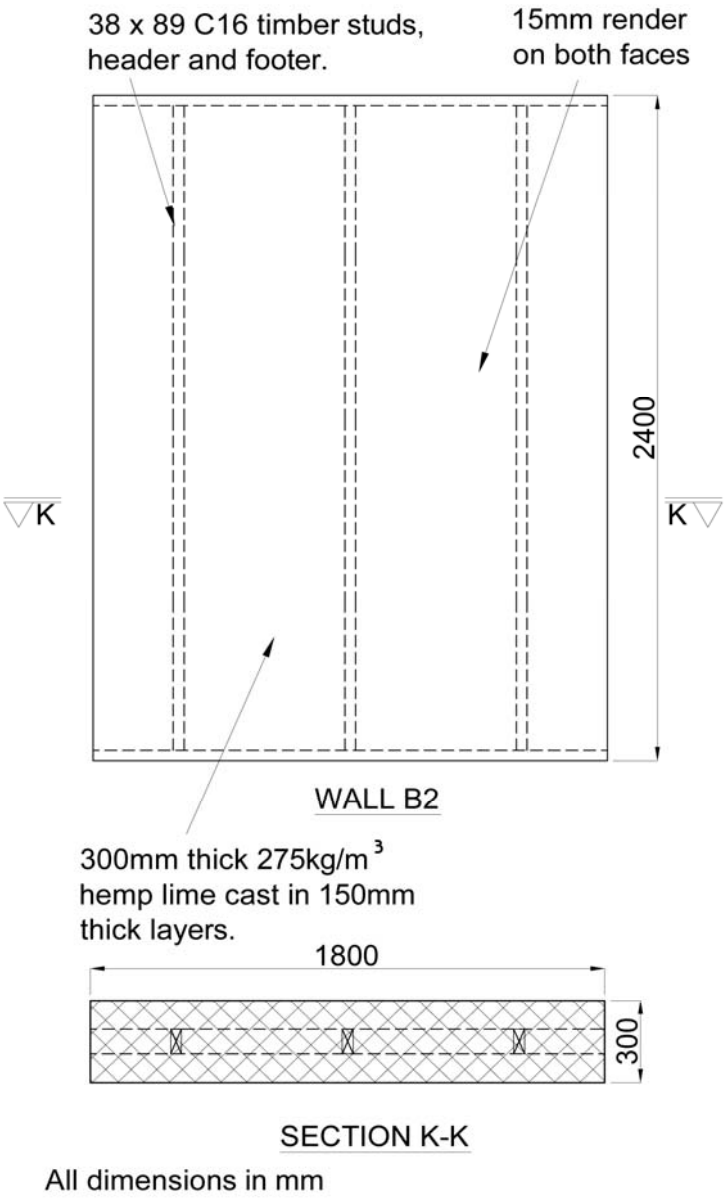

Figure 5.15 Wall B2 drawing

The six hemp-lime composite wall panels were constructed at an industrial warehouse unit in Wootton Bassett during April and May 2010 (Figure 5.16). The specimens were cast one at a time. Hemp-lime was cast around each frame over a period of 3 days with a maximum lift of 900mm per day in order to minimise settlement of the wet material due the self-weight of the fresh material above it.

Figure 5.16 Casting of wall panels at Wootton Bassett

The hemp lime was mixed in a small pan mixer (Figure 5.17). The hemp shiv and binder were initially added and mixed before the water was slowly added until hemp, binder and water were fully mixed. The hemp and the binder were mixed first rather than the binder and water as the mixer used had a trap door in its base to empty the pan and as a result the slurry would leak if it was mixed first. Each mix was carefully weighed and corresponded to a 150mm layer in the wall at the target dry density of 275kg/m^3. All wall panels were cast in three lifts.

Figure 5.17 Hemp shiv in pan mixer

The shuttering was removed 24 hours after the final lift had been cast (Figure 5.18). Between the time of removal of the shuttering and testing (roughly 5 months) the hemp-lime had settled by an average of 35mm, with the majority of this happening within the first week after shuttering was removed. The wall panels specimens were left in the industrial unit until they were transported to the structures laboratory at the University of Bath for testing. The wall panels were between 175 and 200 days old.

Figure 5.18 Wall panels drying at Wootton Bassett

The timber only panels and test studs (Frame R3 and Studs S2, S3, S4) were constructed in the Structures Laboratory at the University of Bath immediately before testing.

5.2.3 Large Scale series two (LS2)

This series of wall panel specimens consisted of eight composite hemp-lime and timber studwork walls (Walls C4, C5, C6, C7 R4, R5, B3 and B4) and six timber only frames (Studs S5 to S10). Details of the wall panels are shown in Table 5.5 to Table 5.7. Detailed drawings of the panels are shown in Figure 5.19 to Figure 5.26. These panels were chosen as they follow the same general design as those used during the first series of large scale tests, but incorporated design changes that resulted from analysis of the results from the first series of large scale tests. All of the panels are 2.4m high as this is the standard studwork framing storey height. The panels for compression testing are

1.2m wide with three studs. As with the LS1 walls this allows for the testing of the central stud while taking into account the effects of adjacent studs and further testing on the outer studs if they are undamaged. The wall panels for in plane racking are 2.4m wide. This conforms to the standard studwork wall panel racking test specimen size set out in BS EN 594 (1996) and this test standard will be followed as closely as possible. The wall panels for out of plane testing are 1.8m wide. This width was a compromise between reducing edge effects with a large enough width while also creating a wall panel that could physically be tested and moved for testing.

The compression test panels (Walls C4, C5, C6 and C7) have been designed to investigate the effect of thickness of hemp-lime cover to the studwork framing. The compression tests in LS1 on Walls C2 and C3 investigated minor axis buckling and also showed major axis buckling not to be a failure mode when the stud was concentrically loaded. Therefore these compression test panels in LS2 have been designed to be loaded eccentrically to force failure about the major axis and at the same time investigate the effects of hemp-lime cover. The effect of hemp-lime cover on minor axis buckling will not be investigated as this scenario is not representative of hemp-lime and timber studwork framing construction. During testing of Wall C3 it became apparent that the connections between the horizontal rails and the studs could be improved. For this reason screwed connections rather than nailed connection were used on Walls C6 and C7. The full results of the LS1 tests will be discussed in following chapters.

Table 5.5 Compression test wall details

Compression Testing	
Description	**Details**
Wall C4: Timber stud with header and footer rails cast into the centre of the hemp-lime. Wall type 1  Plan	– Three C16 timber studs with C16 header and footer. – 38 x 89mm stud, header and footer. – 2.4 m high by 1.2m wide. – Header and footer connections with 2No. 3mm x 75mm nails per connection. – 275 kg/m^3 hemp-lime (oven dry density). – Hemp-lime cast 300mm thick, tamped in 150mm high layers.

Wall C5: Timber stud with header and footer rails cast into the hemp-lime with 50mm cover to the studs. No horizontal rails. Wall type 3  Plan	– Three C16 timber studs with C16 header and footer. – 38 x 89mm stud, header and footer. – 2.4 m high by 1.2m wide. – Header and footer connections with 2No. 3mm x 75mm nails per connection. – 275 kg/m^3 hemp-lime (oven dry density). – Hemp-lime cast 300mm thick, tamped in 150mm high layers.
Wall C6: Timber stud with header and footer rails cast into the hemp-lime with 50mm cover to the studs. Wall type 4  Plan	– Three C16 timber studs with C16 header and footer. – 38 x 89mm stud, header and footer. – 2.4 m high by 1.2m wide. – Header and footer connections with 2No. 3mm x 75mm nails per connection. – 25 x 50mm rail fixed to stud with No.8 x 50mm long screws at 600mm vertical centres to fix hemp-lime to the stud. – 275 kg/m^3 hemp-lime (oven dry density). – Hemp-lime cast 300mm thick, tamped in 150mm high layers.
Wall C7: Timber stud with header and footer rails cast into the edge of the hemp-lime. Wall type 2 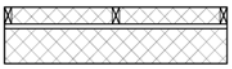 Plan	– Three C16 timber studs with C16 header and footer. – 38 x 89mm stud, header and footer. – 2.4 m high by 1.2m wide. – Header and footer connections with 2No. 3mm x 75mm nails per connection. – 25 x 50mm rail fixed to stud with No.8 x 50mm long screws at 600mm vertical centres to fix hemp-lime to the stud. – 275 kg/m^3 hemp-lime (oven dry density). – Hemp-lime cast 300mm thick, tamped in 150mm high layers.

Studs S5, S6, S7, S8, S9, S10: Timber stud ⊠ Plan	– C16 timber stud with C16 – 38 x 89mm stud. – 2.4 m high.

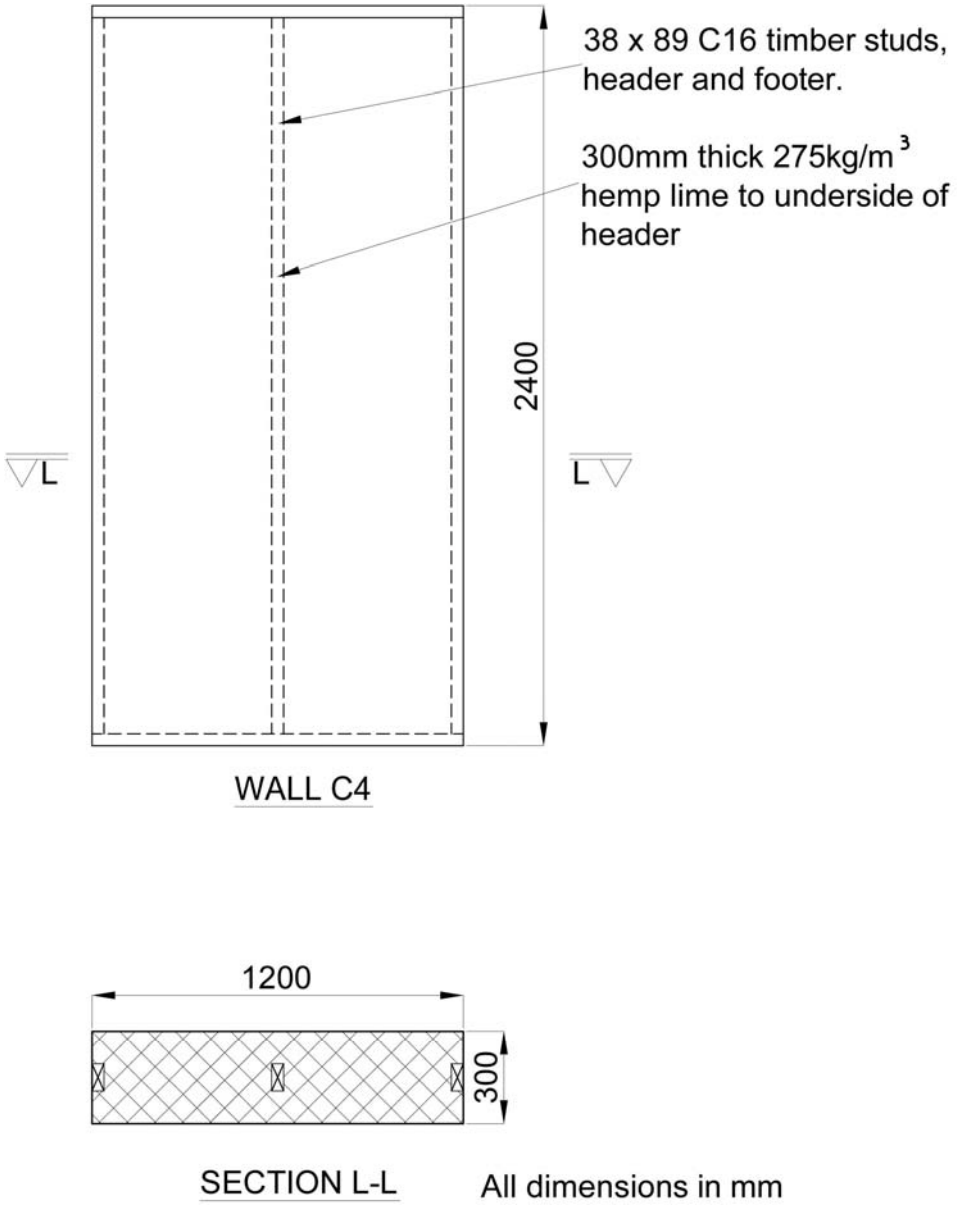

Figure 5.19 Wall C4 drawing

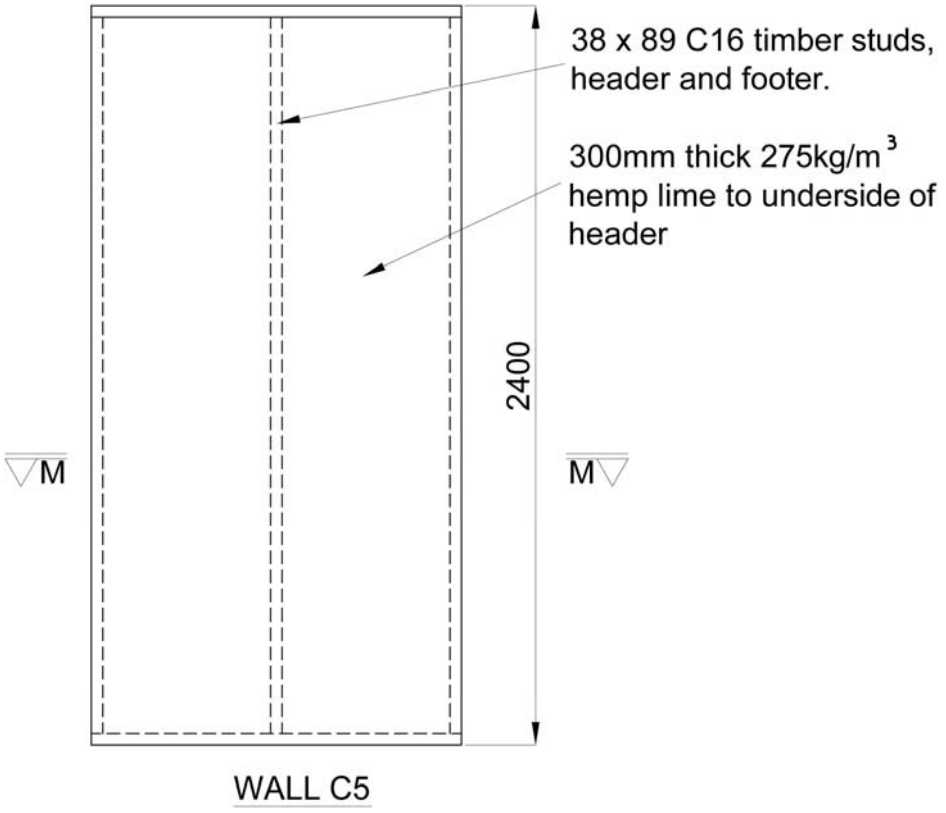

Figure 5.20 Wall C5 drawing

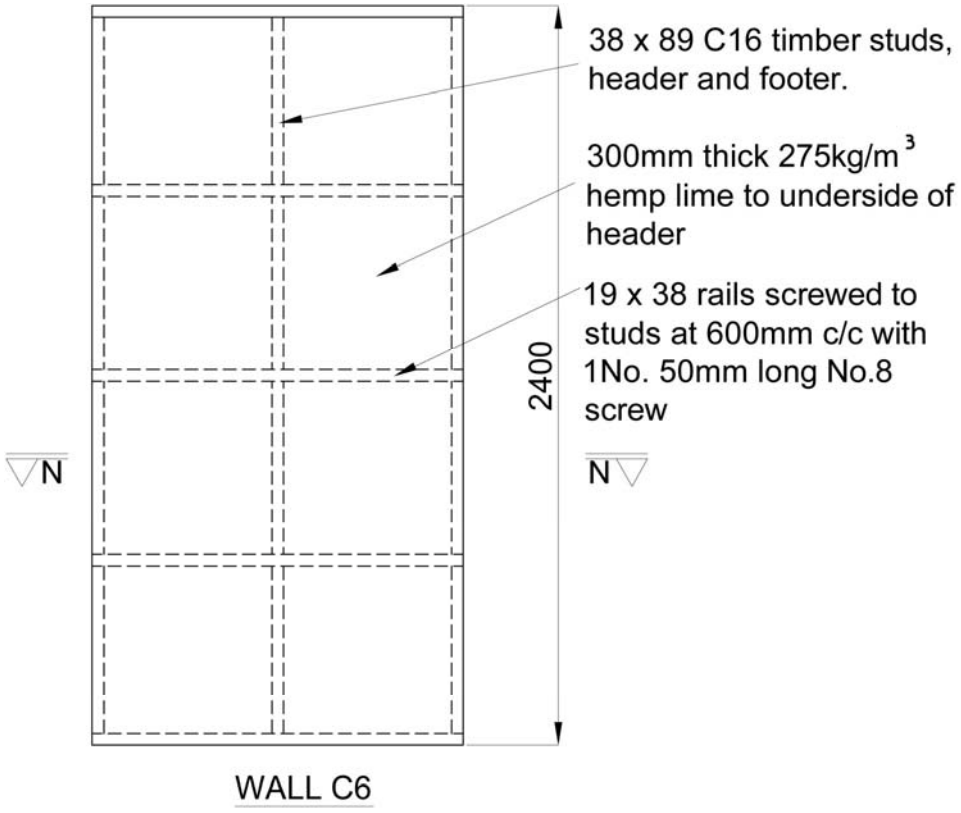

Figure 5.21 Wall C6 drawing

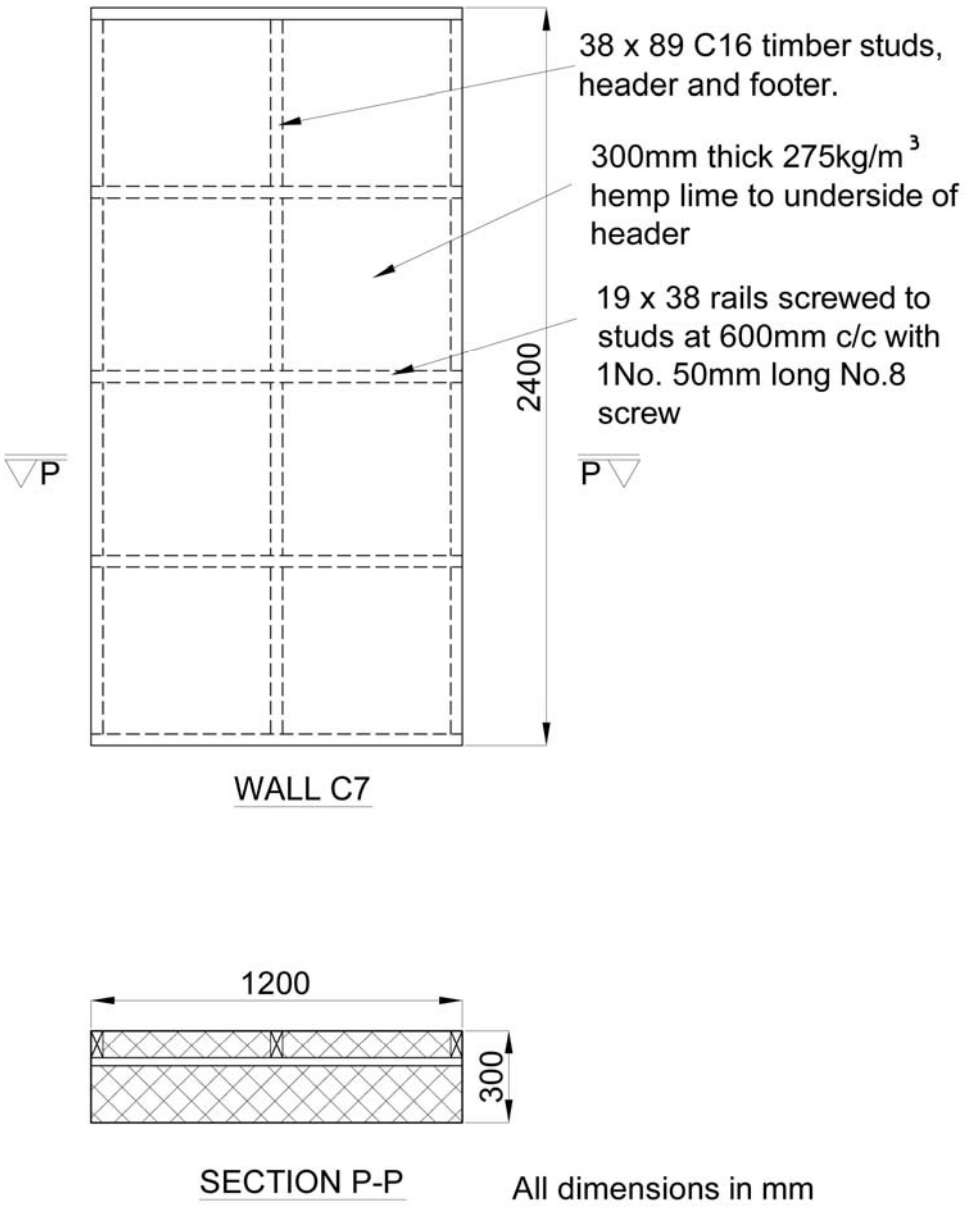

Figure 5.22 Wall C7 drawing

The design of Walls R4 and R5 was influenced by the findings from testing undertaken on Walls R1 and R2. The racking tests on Walls R1 and R2 showed that the connections between the leading stud (stud closest to racking load) and the header and footer rails were a weak point. As a result the design of Walls R4 and R5 was changed to incorporated connections with increased stiffness and strength. Walls R1 and R2 were plain hemp-lime and studwork walls. Walls R4 and R5 have been designed to allow investigation of the effects on racking stiffness and strength of using sheathing boards as permanent formwork.

Table 5.6 Racking test wall details

Racking Testing	
Description	**Details**
Wall R4: Wall panel with timber stud with header and footer rails cast into the edge of the hemp-lime. Wall type 2 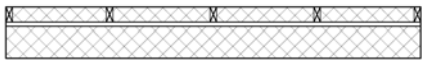 Plan	– Wall panel made from C16 timber studs with C16 header and footer. – 38 x 89mm stud, header and footer. – 2.4 m high by 2.4m wide. – Studs at 600mm c/c – Header and footer connections with 2No. 3mm x 75mm nails per connection. – Leading stud to header/footer connected using 2No. 6.5mm dia. x 150mm long Heco Topix CC screws – 25 x 50mm rail fixed to stud with No.8 x 50mm long screws at 600mm vertical centres to fix hemp-lime to the stud. – 275 kg/m^3 hemp-lime (oven dry density). – Hemp-lime cast 300mm thick, tamped in 150mm high layers
Wall R5: Wall panel with timber studs with header and footer rails cast into the edge of the hemp-lime with Multi-pro XS permanent shuttering board on one face. Wall type 5 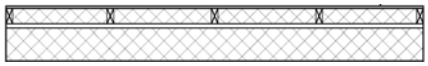 Plan	– Wall panel made from C16 timber studs with C16 header and footer. – 38 x 89mm stud, header and footer. – 2.4 m high by 2.4m wide. – Studs at 600mm c/c – Header and footer connections with 2No. 3mm x 75mm nails per connection. – Leading stud to header/footer connected using 2No. 6.5mm dia. x 150mm long Heco Topix CC screws – 25 x 50mm rail fixed to stud with No.8 x 50mm long screws at 600mm vertical centres to fix hemp-lime to the stud. – 9mm Multi-pro XS fixed using 40mm long

	drywall screws at 200mm c/c on perimeter and 300mm c/c in centre. – 275 kg/m^3 hemp-lime (oven dry density). – Hemp-lime cast 300mm thick, tamped in 150mm high layers

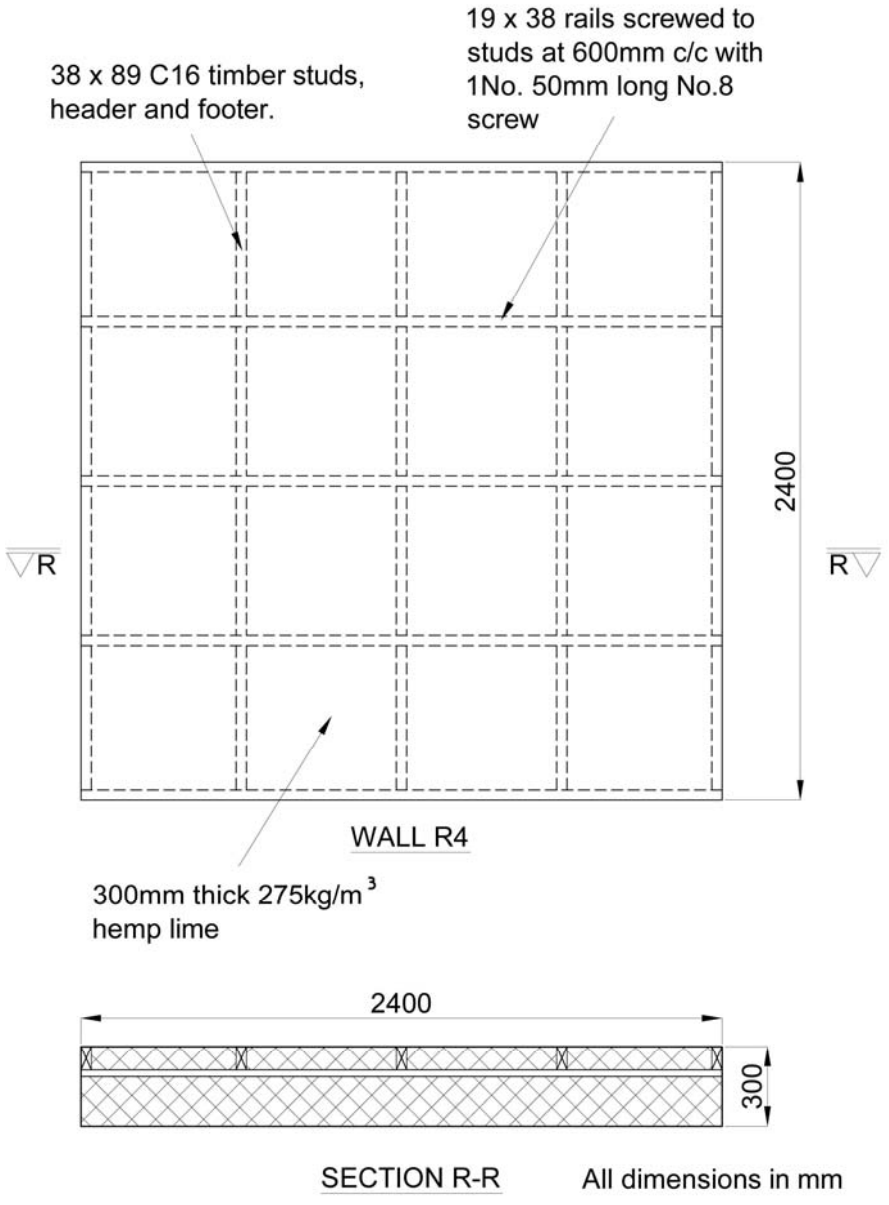

Figure 5.23 Wall R4 drawing

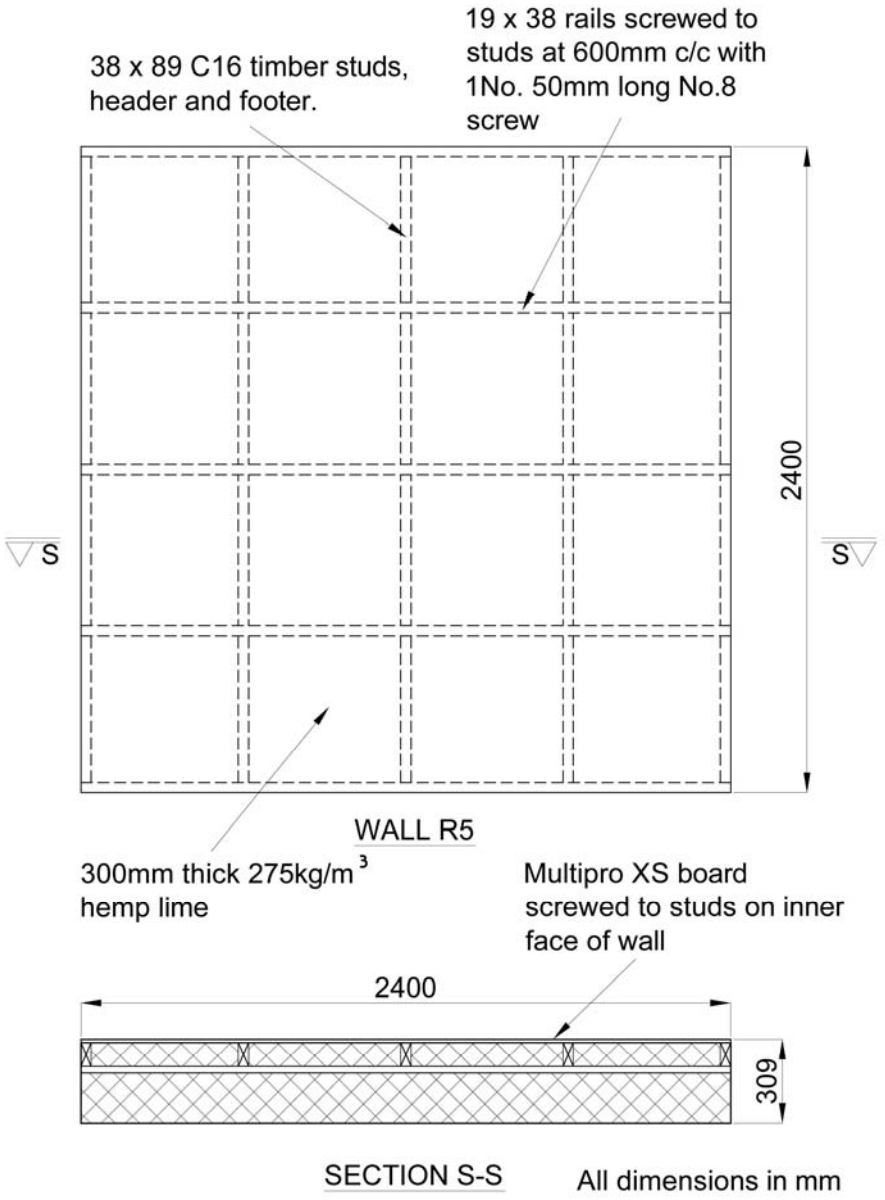

Figure 5.24 Wall R5 drawing

Walls B3 and B4 have been designed considering the results from Walls B1 and B2. Walls B1 and B2 showed the effects of render thickness and the presence of timber studwork frame under out of plane bending loads. It is unlikely that both faces of the hemp-lime would have render applied to them and therefore Walls B3 and B4 were designed to investigate the effects of having a sheathing board fixed to one face of the walls as a permanent shutter. This will allow investigation of the performance of Walls B3 and B4 as they are loaded in out of plane bending in different directions (sheathing in tension or compression).

Table 5.7 Bending test wall details

Bending Testing	
Description	**Details**
Wall B3: Wall panel with timber studs with header and footer rails cast into the edge of the hemp-lime with Multi-pro XS permanent shuttering board on one face. Wall type 8 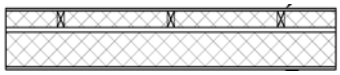 Plan	– Wall panel made from C16 timber studs with C16 header and footer. – 38 x 89mm stud, header and footer. – 2.4 m high by 1.8m wide. – Studs at 600mm c/c. – Header and footer connections with 2No. 3mm x 75mm nails per connection. – 25 x 50mm rail fixed to stud with No.8 x 50mm long screws at 600mm vertical centres to fix hemp-lime to the stud. – 9mm Multi-pro XS fixed using 40mm long drywall screws at 200mm c/c on perimeter and 300mm c/c in centre. – Hemp-lime cast 300mm thick, tamped in 150mm high layers – 275 kg/m^3 hemp-lime (oven dry density). – 15mm render on one face
Wall B4: Wall panel with timber studs with header and footer rails cast into the edge of the hemp-lime with Multi-pro XS permanent shuttering board on one face. Wall type 8 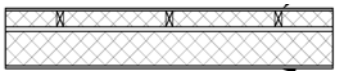 Plan	– Wall panel made from C16 timber studs with C16 header and footer. – 38 x 89mm stud, header and footer. – 2.4 m high by 1.8m wide. – Studs at 600mm c/c. – Header and footer connections with 2No. 3mm x 75mm nails per connection. – 25 x 50mm rail fixed to stud with No.8 x 50mm long screws at 600mm vertical centres to fix hemp-lime to the stud. – 9mm Multi-pro XS fixed using 40mm long drywall screws at 200mm c/c on perimeter and 300mm c/c in centre.

	– Hemp-lime cast 300mm thick, tamped in 150mm high layers – 275 kg/m^3 hemp-lime (oven dry density). – 15mm render on one face

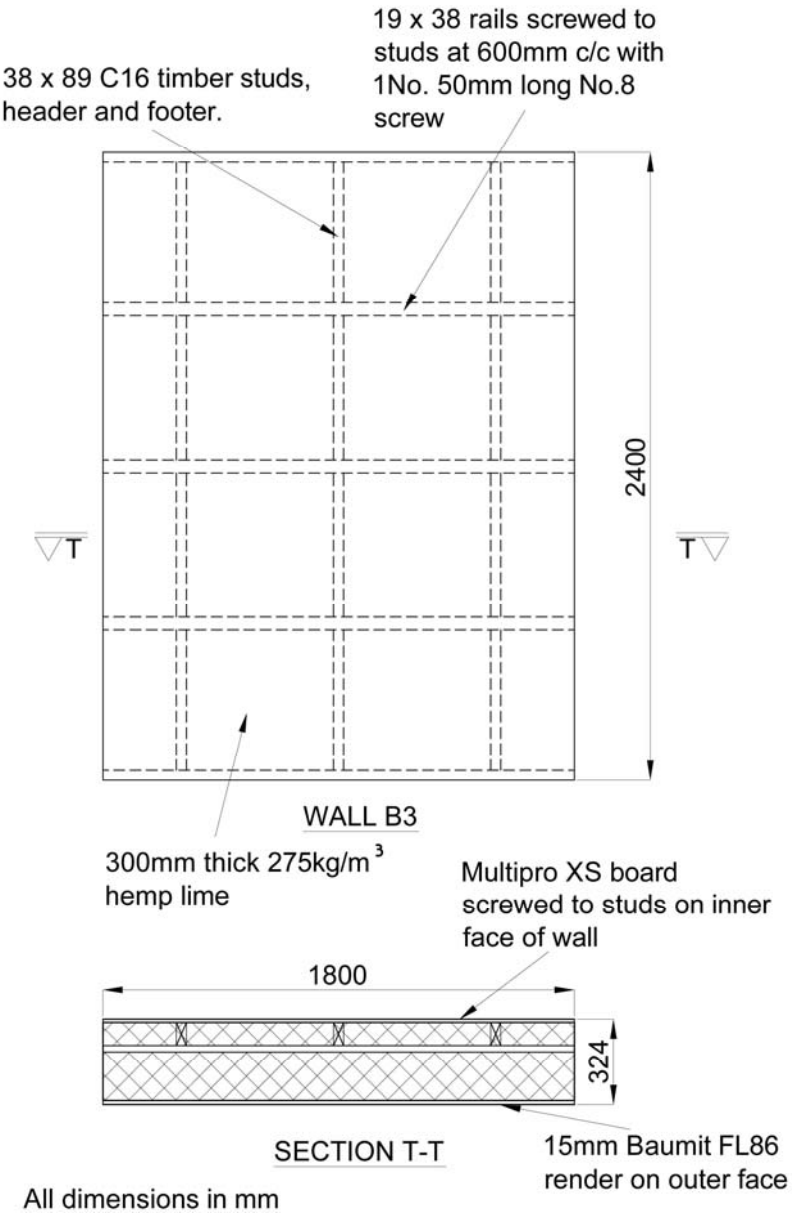

Figure 5.25 Wall B3 drawing

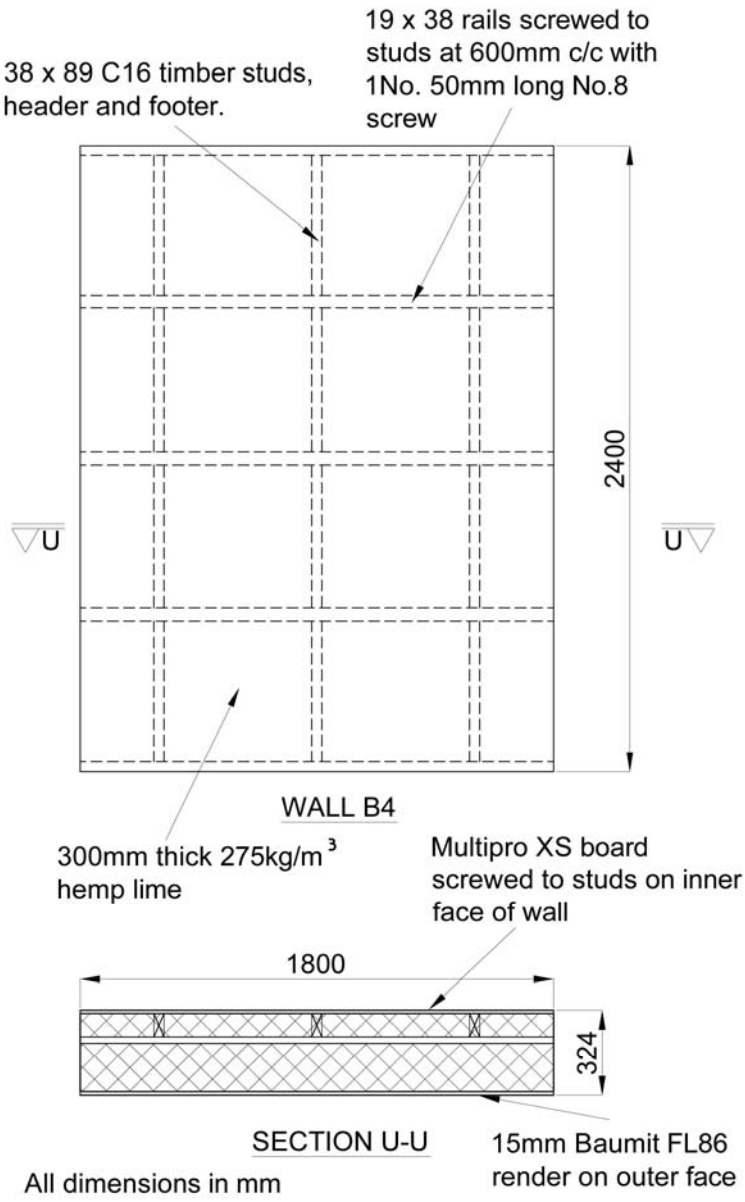

Figure 5.26 Wall B4 drawing

The eight hemp-lime and timber studwork composite wall panels were constructed at Lime Technology's Steventon Storage Facility in August 2011 (Figure 5.27). Hemp-lime was cast around each frame in a single lift due to time constraints. The hemp-lime was mixed in both a large animal feed mixer powered by a tractor (Figure 5.28) and a pan mixer depending upon availability. The hemp shiv and binder were initially added and mixed before the water was slowly added until hemp, binder and water were fully mixed. The mixed hemp-lime was then removed from the mixer and placed into the shuttering. It was spread within the shuttering by hand and lightly tamped around the edges to ensure a good surface finish.

Figure 5.27 Wall panels at Steventon soon after casting

Figure 5.28 Animal feed mixer

The shuttering was removed 72 hours after casting. Some settlement of the hemp-lime was observed in all of the walls. The majority of this settlement occurred prior to the

shuttering being removed and was largely due to the weight of wet hemp-lime in the upper parts of the wall panels compressing the freshly cast material further down the wall. The total settlement in the walls was roughly 50mm and occurred throughout the height of the walls. Figure 5.29 shows the settlement around horizontal rails and Figure 5.30 show the settlement under the header.

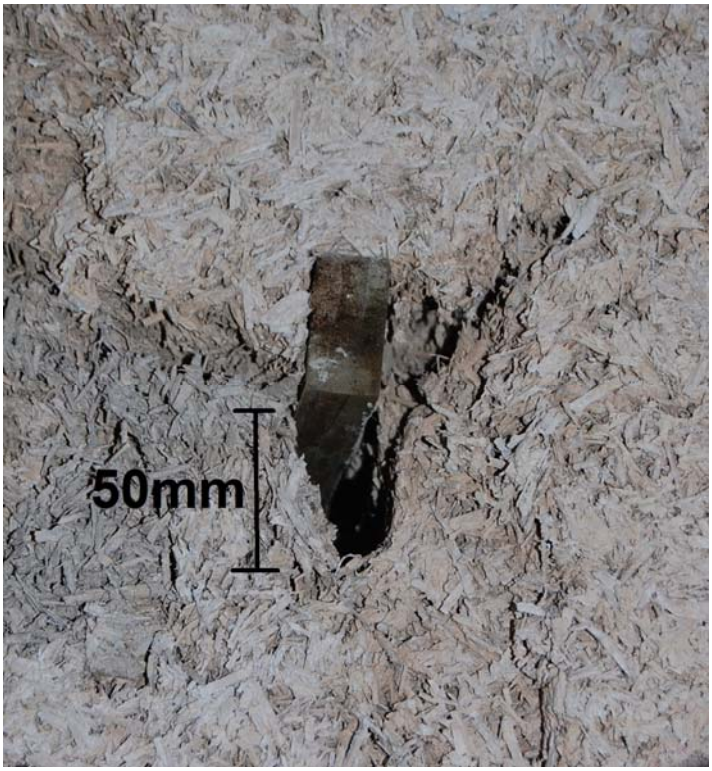

Figure 5.29 Settlement at horizontal rail

Figure 5.30 Settlement of hemp-lime at top of wall

In order to increase the rate of drying the hemp-lime wall panels were placed in an accelerated drying chamber. This is a sealed space that is heated to 45^{o}C and the air is

regularly exchanged to remove moisture from the atmosphere within the chamber. This method of drying has been developed by Lime Technology Ltd and allowed the drying period of the wall panel specimens to be reduced. The effects of elevated temperature and increased drying speeds have been investigated as there were concerns that this may adversely affect the properties of the hemp-lime. As shown in Chapter 3 there are no adverse effects as long as hemp-lime is not artificially dried for the first 14 days after casting and the temperature is kept below 50^{o}C.

Prior to being placed in the drying chamber the panels were stored outside under shelter for 10 weeks. The panels were in the chamber with the heaters and fans running for five days. The panels then remained in the drying chamber for a further week until they were transported to the structures laboratory at the University of Bath for testing. The wall panels were tested between 84 and 105 days old.

5.3 Conclusions

This chapter has detailed the design considerations, specifications and construction method for each of the full scale wall panel specimens tested during this investigation. The difference in construction process between the first series of walls (LS1) and the second series of walls (LS2) is due to lessons learnt during construction of the LS1 walls as well as the availability of equipment.

The testing methods, results, analysis and discussion for the wall panels will be presented in the following chapters by loading type (compression, in plane racking, bending) in the same way that the specimen details have been in this chapter. This allows for quick comparison and discussion between the results from the LS1 tests and the LS2 tests.

6 Experimental Study: Compression performance of wall panels

6.1 Introduction

Composite hemp-lime and studwork frame wall panels were tested under compressive loading, and compared with unconfined studwork frames, in order to investigate the level of confinement and enhancement provided by the hemp-lime. One hemp-lime wall panel with light-weight cold formed steel studwork framing (Wall C1) was initially tested. Thereafter, one wall panel with a timber studwork frame cast into the centre of the hemp-lime (Wall C2) and one with the frame cast on the edge of the hemp-lime (Wall C3) were tested. Walls C4 to C7 had timber studwork frames cast into the hemp-lime with different amounts of hemp-lime cover to the studwork framing. Finally a lightweight steel studwork only frame (Stud S1) and nine timber only studwork frames (Stud S2 to S10) were tested with differing loading conditions and end restraint conditions.

6.2 Methodology and test set up

All of the compression tests followed the same general test procedure and test set up, although there were some differences in stud end restraint and loading scheme which will be detailed in the following sections. All of the test specimens were subjected to a compressive point load applied with a hydraulic jack and manual pump. The load was measured with a load cell and the displacements at various points on the test specimens were measured using LVDTs. Both the load and displacement were recorded with a System 6000 acquisition module.

6.2.1 Test set up and testing procedure for Wall C1 and Stud S1

The test set ups for both Wall C1 and Stud S1 are shown in Figure 6.1. Both Wall C1 and Stud S1 were restrained at their top corners using metal plates fixed back into the laboratory strong wall to prevent toppling of the specimens during testing. The load was applied through a pin to allow free rotation of the central loaded studs about their minor axis. To achieve this a 100mm square, 25mm thick steel plate was placed onto the

header of the studwork frames centred about the studs neutral axis. A 20mm diameter steel pin was placed onto the steel plate before another 100mm square steel plate was placed on top of the pin. The load was then applied to the top steel plate. The load was measured with a load cell and LVDTs measured the displacement of the walls at the locations shown in Figure 6.2 and Figure 6.3. In Wall C1 the LVDTs measured the vertical displacement of the top of the loaded stud and the surface of the hemp-lime along the line of the loaded stud. In Stud S1 the LVDTs were positioned to measure the vertical displacement at the top of the stud and horizontal displacement about the minor and major axis. Any twist of the walls on plan or tilting forwards or backwards was monitored using a load cell fixed to the steel restraint plates at each of the top corners of the walls.

Figure 6.1 Stud S1 (left) and Wall C1 (right) test set ups

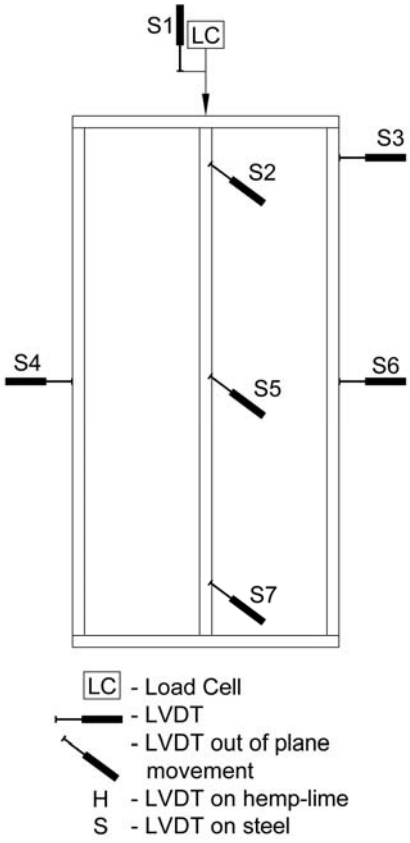

Figure 6.2 Stud S1 LVDT and load cell locations

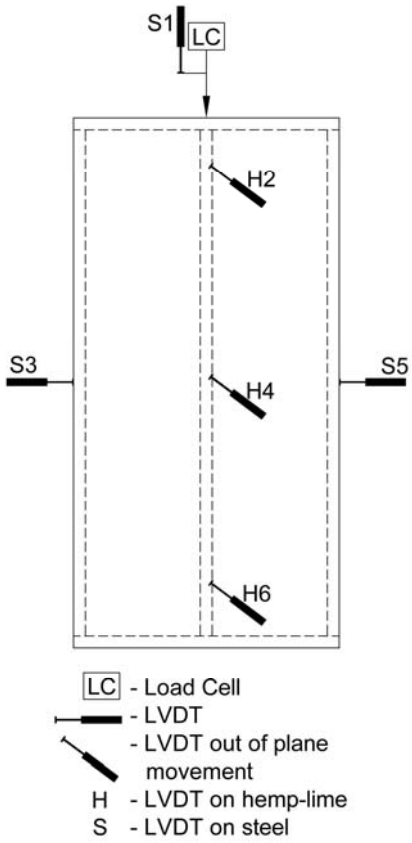

Figure 6.3 Wall C1 LVDT and load cell locations

Wall C1 and Stud S1 were tested using the same loading regime. The load was applied and increased to 10kN. It was then removed and the residual deflection recorded. The load was the reapplied and increased to 20kN, then removed. This process of loading, unloading and increasing the load in increments of 10kN continued until failure occurred. Load increases of 10kN were used as this is roughly 30% of the predicted buckling load of 35.51kN for the lightweight steel section that was being used. By increasing the load in this manner the elastic response of the stud could be studied before failure occurred in both the studs with and without hemp-lime restraint.

6.2.2 Test set up and testing procedure for Walls C2, C3 and Studs S2 to S4

The test set up for the hemp-lime composite and timber studwork frame wall panels Walls C2 and C3 is shown in Figure 6.4 and the test set up for Studs S2, S3 and S4 is shown in Figure 6.5. All of the specimens were restrained at the top in the same way as Wall C1 and Stud S1 with steel plates to prevent toppling. The compressive load was also applied in the same way through the neutral axis of the timber studs with a pin to allow rotation about the minor axis. The applied load was measured by a load cell and in all tests LVDTs measured the displacement at the locations shown in Figure 6.6 and Figure 6.7. On Walls C2 and C3 the LVDTs recorded the movement of the hemp-lime surface and on Studs S2 to S4 the movement of the stud about both its major and minor axis were measured. Any out of plane twisting of the walls on plan was monitored using a load cell at each of the top corners of the walls. The loaded studs were also fitted with two uniaxial strain gauges (60mm long), one on each of the larger faces at mid height to record any bending deflection of the studs about their minor axis.

Figure 6.4 Hemp-lime composite compression test

Figure 6.5 Studs S2, S3 and S4 compression test set up

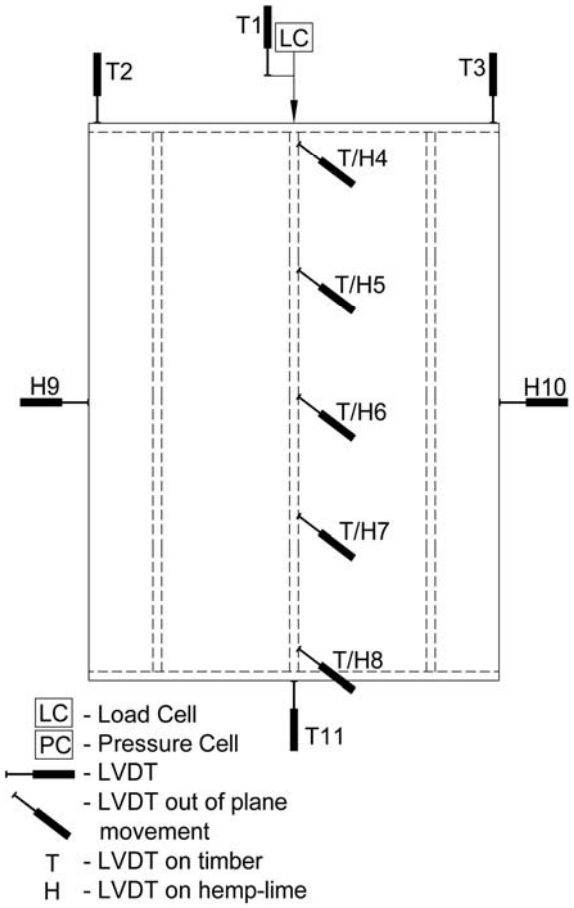

Figure 6.6 Walls C2 and C3 LVDT and load cell locations

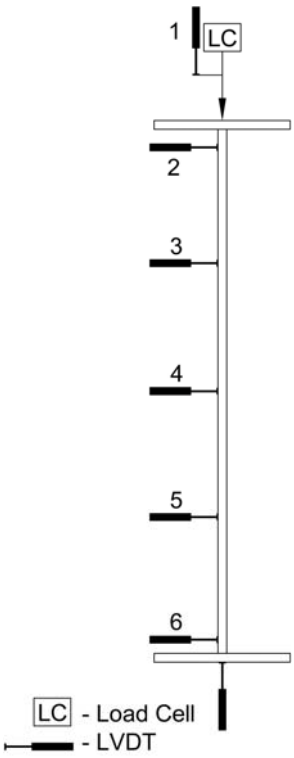

Figure 6.7 Studs S2 to S4 LVDT and load cell locations

Walls C2 and C3 were tested using the following loading regime: the load was applied and increased to 5kN; it was then removed and the residual deflection recorded; the load was the reapplied and increased to 10kN, then removed. This process of loading, unloading and increasing the load in increments of 5kN continued until failure occurred. This loading process was chosen for the same reasons as with Wall C1. The predicted buckling load for the timber studs being used in 6.1kN. Therefore by only loading to 5kN initially allows the elastic pre-buckling behaviour to be studied in detail. Studs S2 to S4 were initially loaded with 1kN and the reading from the two strain gauges on the timber were recorded. If the strains recorded from the two strain gauges were significantly different then the stud was unloaded, the loading point adjusted and then reloaded again to 1kN. This process was repeated until the strains were within 10% of each other at which point loading continued until failure. This process was carried out to ensure that the studs were being loaded concentrically and therefore buckling was not influenced by the position of loading.

6.2.3 Methodology and test set up for Walls C4 to C7 and Studs S5 to S10

The test set up for the hemp-lime composite and timber studwork frame wall panels Walls C4 to C7 is shown in Figure 6.8 and the test set up for Studs S5 to S10 is shown in Figure 6.9.

Walls C4 to C7 were restrained at their top corners with steel plates to prevent overturning during testing. The compressive load was applied in the same manner as previous compression test specimens through a pin, however in Wall tests C4 to C7 the pin was orientated to allow free rotation of the stud about its major axis as buckling of the studs about their major axis was being investigated. In addition, as the studs were loaded directly, rather than through a timber header plate, a steel shoe was fabricated to fit over the top of the test stud (Figure 6.10) to prevent localised crushing or premature splitting damage.

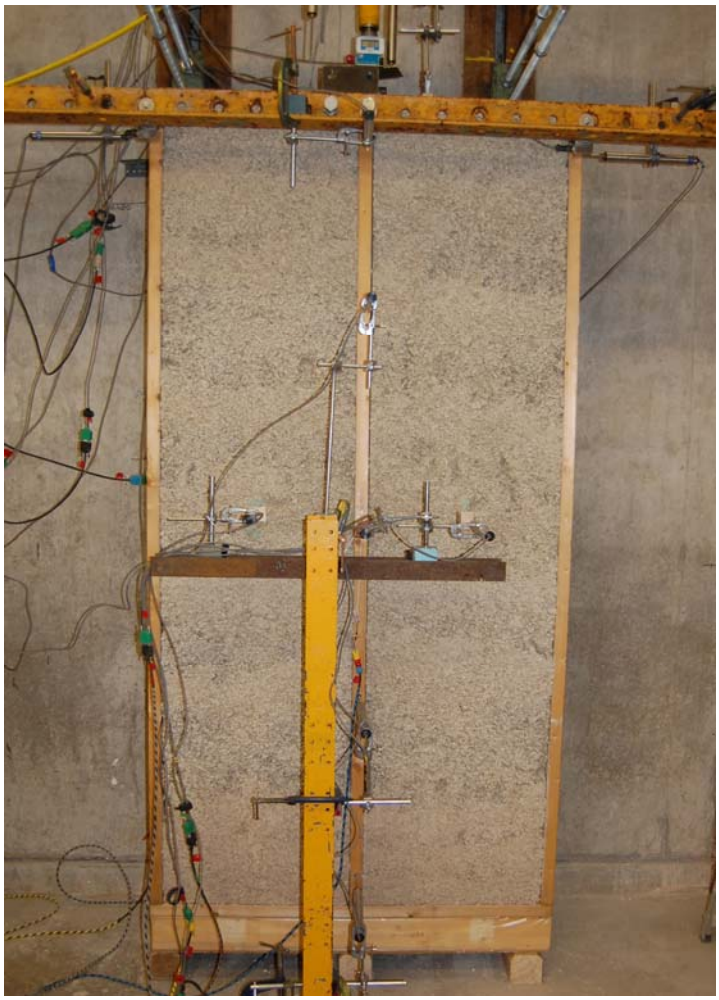

Figure 6.8 Hemp-lime composite compression test

A load cell measured the compressive load and LVDTs measured the displacement at the locations shown in Figure 6.11. The LVDTs either measured surface movement of the hemp-lime or, in the case of Wall C7, direct movement of the stud as it was exposed. Out of plane twisting of the walls on plan was detected through a load cell at each of the top corners of the walls. Two uniaxial strain gauges were fixed to the loaded studs, one on each of the larger faces at mid height to detect bending of the studs about their major axis.

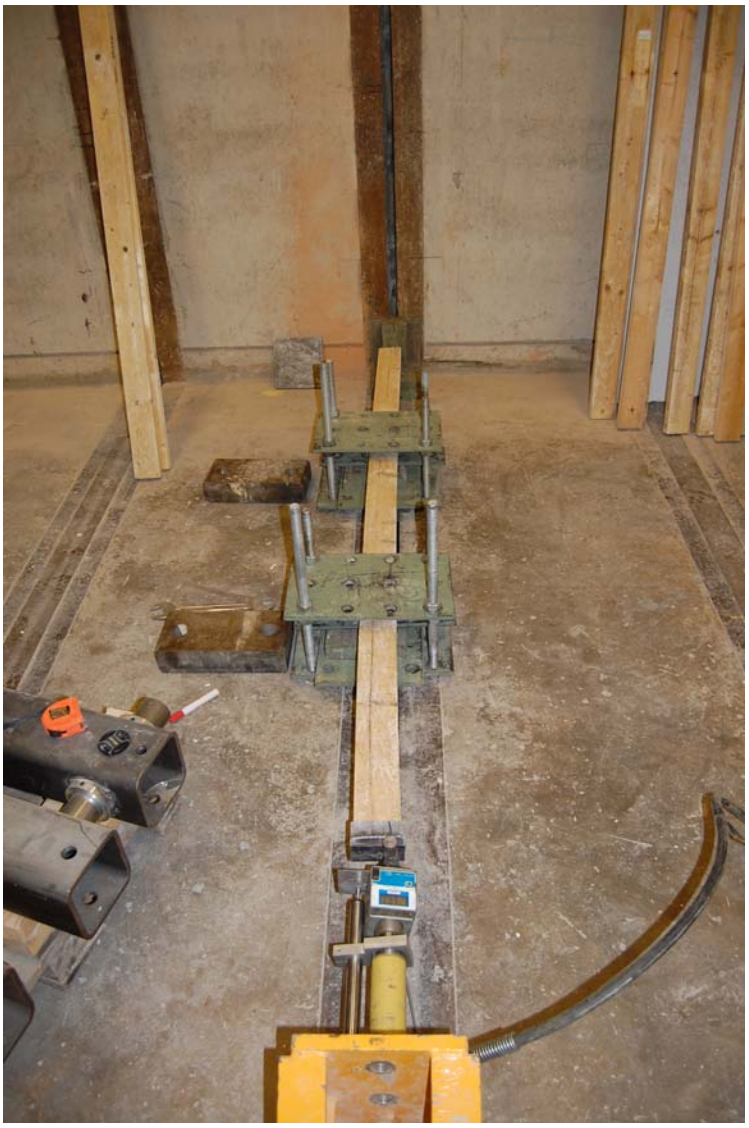

Figure 6.9 Timber stud compression test

Figure 6.10 Steel loading shoe on top of timber stud

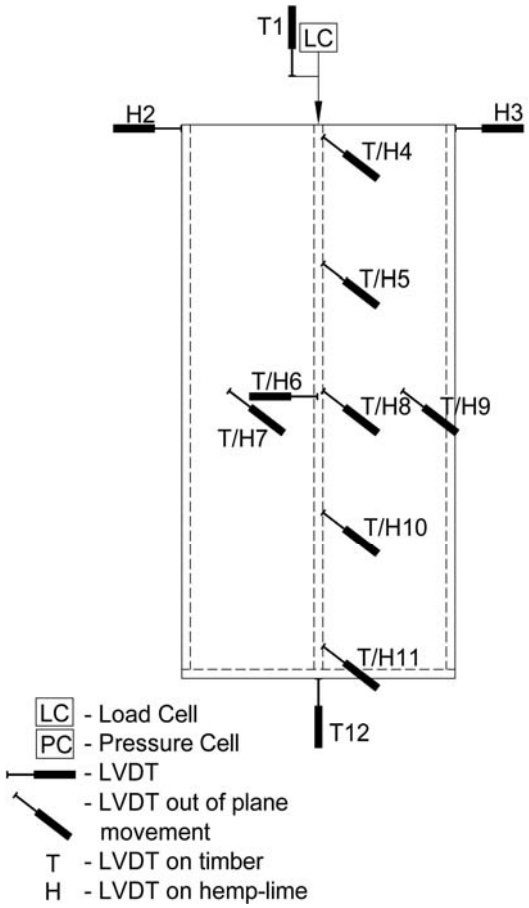

Figure 6.11 Walls C4 to C7 LVDT and load cell locations

Walls C4 to C7 were tested under eccentric loading, in order to force the studs to buckle out of the face of the walls about their major axis. Four eccentricities were used: 0mm, 11mm, 22mm and 27mm from the major axis of the stud. Walls C4 to C7 were tested with the following loading regime: the load was increased to 15kN with an eccentricity of 0mm to bed the stud and shoe in, then the load was removed and the loads and displacements zeroed; the load was then increased to 15kN with an eccentricity of 0mm, then removed and the residual displacements recorded. The loading and unloading cycle was repeated three times. This process was then repeated for eccentricities of 11mm, 22mm and 27mm in order to observe the elastic response. Following this the stud was loaded to failure with an eccentricity of 22mm. This eccentricity of 22mm was chosen as a load of 25.0kN was calculated to cause buckling failure about the major axis and therefore buckling was likely to occur unless the hemp-lime or horizontal rails restrains the stud.

Studs S5 to S10 were tested lying flat on the floor. They were restrained at their third points to prevented minor axis movement while allowing major axis movement. This was achieved by placing the studs between steel plates and rollers aligned parallel with their length, the arrangement for which is shown in Figure 6.12. The load was measured using a load cell and the vertical displacement of the top of the studs was measured using an LVDT as shown in Figure 6.13.

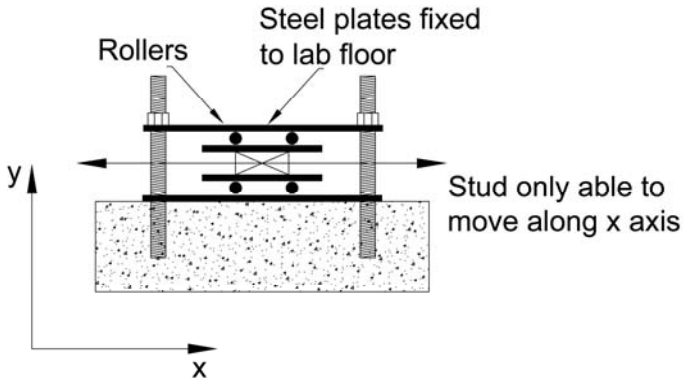

Figure 6.12 Stud hold down arrangement

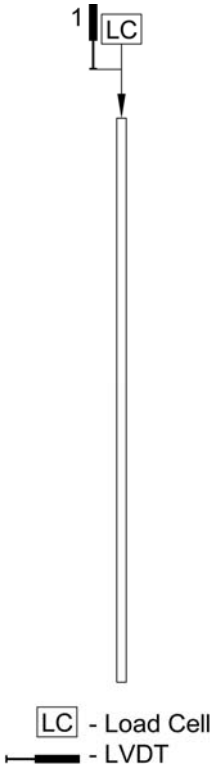

Figure 6.13 Studs S5 to S10 LVDT and load cell locations

The load was applied through a pin that allowed free rotation about the major axis. The studs were tested with an eccentricity of 22mm and were loaded steadily to failure without any load cycling. Studs S5, S6 and S7 had a pinned base that allowed free

rotation about the major axis while Studs S8, S9 and S10 had a fixed base, as this is a closer representation of the fixing conditions of the studwork frames in Walls C4 to C7.

6.3 Results

6.3.1 Initial test - Wall C1 and Stud S1

Figure 6.14 presents the results from the tests on Wall C1 and Stud S1. Applied compressive load is plotted against vertical displacement of the top of the central stud.

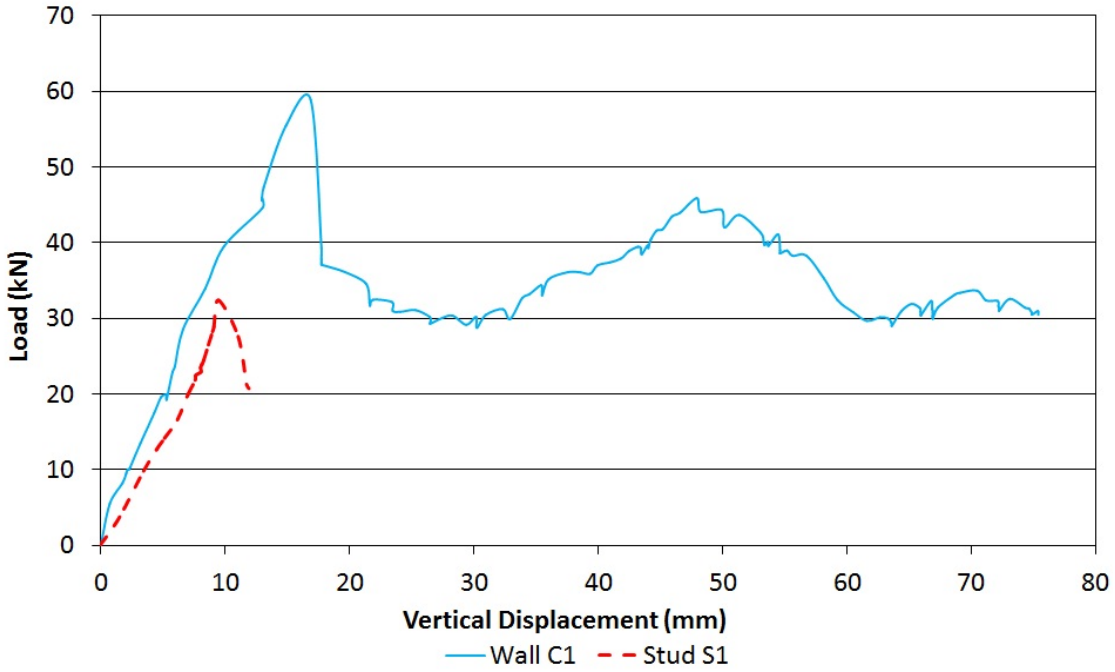

Figure 6.14 Vertical compression results

The maximum load sustained by Stud S1 was 33.3kN at a vertical displacement of 9.7mm. During loading the stud deflected horizontally and twisted in addition to vertical axial shortening prior to buckling (Figure 6.15). The out-of-plane horizontal deflection at the centre of the stud was 27.7mm immediately prior to the stud buckling. Failure occurred by torsional buckling of the central stud at its mid-height (Figure 6.16). Following buckling failure the central stud sustained a load of just over 20kN, however this was at increasingly large deflections of over 11.0mm. The stiffness of the stud, calculated between loads of 10kN and 20kN, prior to buckling was 2847N/mm.

Figure 6.15 Horizontal deflection and twisting of stud

Figure 6.16 Torsional buckling failure of steel stud (Stud S1)

The maximum load sustained by Wall C1 (hemp-lime restrained frame) was 60.3kN at a vertical deflection of 16.4mm. Failure occurred by local crushing of the central steel stud at its base (Figure 6.17). The stiffness of the stud, calculated between loads of 10kN and 20kN was 3559N/mm. Despite the significant crushing of the stud the wall was still able to sustain loads of 30 – 35kN until the test was stopped at a total displacement of 75mm. The rise in load at a displacement of 30mm is a result of the header rail of the frame bearing directly onto the hemp-lime. This rise continued until the hemp-lime spalled on both the front and back surfaces. Figure 6.18 shows this as well as the significant vertical displacement of the frame header. There was no horizontal bulging of the hemp-lime surface detected by the LVDTs on the surface of the hemp-lime during the test.

Figure 6.17 Crushing of central steel stud in hemp-lime restrained wall

Comparing these results with those from Helmich (2008) both the unrestrained stud and the hemp-lime restrained stud failed at slightly lower loads, however the modes of failure were the same. For the unrestrained stud Helmich (2008) recorded a maximum load of 38.5kN compared with 33.3kN for Stud S1. The stud cross section and length were the same for both tests. As lightweight cold formed steel sections have consistent properties the only reason for the difference in failure load is the alignment of the applied load. With the hemp-lime restrained stud Helmich (2008) recorded a maximum load of 75kN compared with 60.3kN for Wall C1. The hemp-lime used by Helmich (2008) was of a much higher density (466kg/m^3) than in Wall C1 (267kg/m^3). This may have had some influence, but both studs failed by local crushing and therefore should have failed at around the same load. Again the alignment of the applied compressive load may have contributed.

Figure 6.18 Hemp-lime bursting and deflection of header

Following testing, specimens of the hemp lime from Wall C1 were taken for compression, moisture content and carbonation testing. Three hemp-lime prisms were loaded in compression using the Dartec 100kN loading frame (Figure 6.19). The hemp-lime prisms were capped with dental plaster in the same way that the hemp-lime cylinders in Chapter 3 were in order to provide a flat level loading surface. The properties of the prisms are shown in Table 6.1 and the results from the tests are shown in Figure 6.20. The individual moisture contents of the hemp-lime prisms taken from Wall C1 were not taken, however the moisture content and dry density of the hemp-lime were taken from other specimens and were 40% and 267kg/m^3 respectively.

Table 6.1 Wall C1 hemp-lime prism specimens

Specimen	**b (mm)**	**d (mm)**	**h (mm)**	**Bulk Density (kg/m^3)**
A	355	305	370	427
B	340	305	365	423
C	330	305	360	422

Figure 6.19 Compression testing of specimen No. 4 from wall

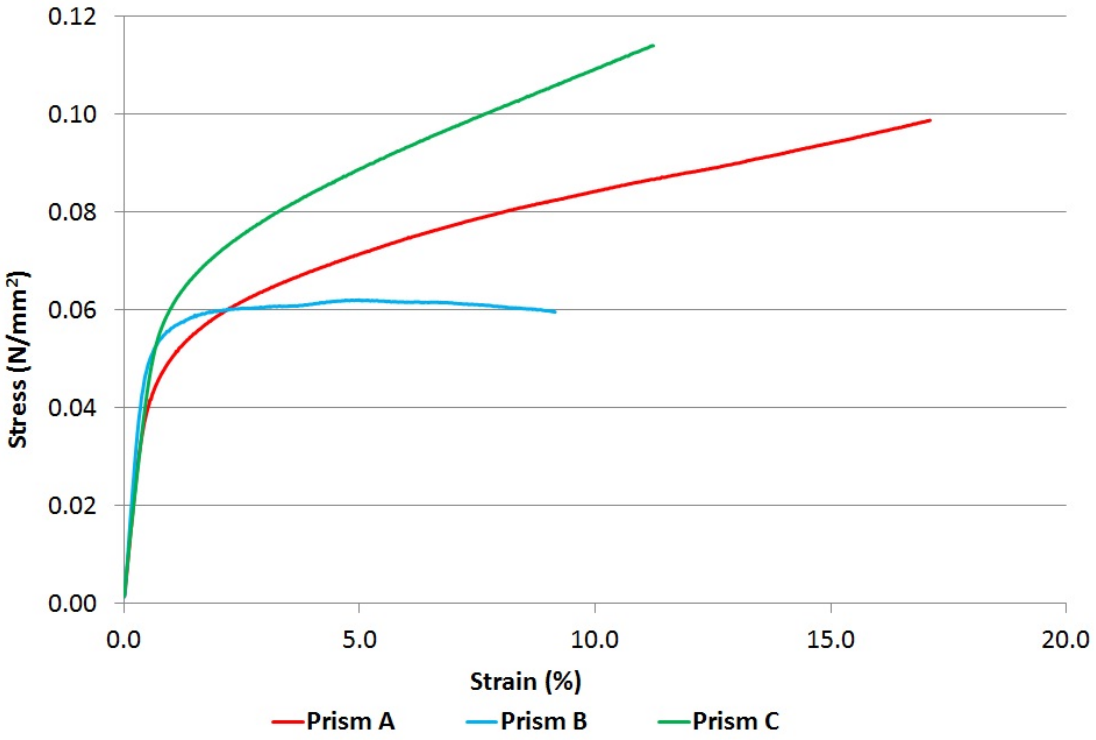

Figure 6.20 Hemp lime wall samples compressive strength

When using prismatic samples it is more difficult to determine a peak compressive strength as the applied stress can continue to increase with strain, as shown in prisms A and C. From Figure 6.20 the compressive strength has been taken at 8% strain as this is the strain at which peak compressive strength occurred in hemp-lime cylinder

specimens cast using the same mix as used in the wall and tested at the same time. The average compressive strength at 8% strain is 0.08N/mm^2. The average initial tangent modulus is 10.5N/mm^2. The specimens were tested 'wet' as per the accompanying wall, which partially explains their very low strength and stiffness. Compared with the material properties of the hemp-lime derived from cylinder testing in Chapter 3 the average compressive strength is the same as the Initial cylinders. The initial modulus is lower than the cylinders. The lower modulus of the prisms is due to the effect of the exposed surface of the hemp-lime drying and forming a stiffer dry layer. This layer accounts for a larger proportion of the total area on the cylinders (150mm diameter) than the prisms (300mm square). The average dry density of the hemp-lime in Wall C1 was 267kg/m^3.

Three specimens of hemp-lime were sprayed with phenolphthalein solution to determine the level of carbonation. As can be seen from Figure 6.21 there had been very little carbonation during the 28 days between casting and testing. The outer 5mm of hemp lime has carbonated. The lack of carbonation beyond the outer edges is not surprising as the average wall material moisture content was measured, by oven drying, at 40.0%. Carbonation cannot occur at elevated moisture levels. The lack of carbonation will be another contributing factor in the low stiffness and strength of the hemp-lime.

Figure 6.21 Hemp lime showing level of carbonation

6.3.2 First Large Scale tests (LS1)

Figure 6.22 presents the results of applied load against vertical displacement of the top of the studs from Walls C2 and C3 and unrestrained timber Studs S2, S3 and S4. There was some difficulty during testing of Wall C3 (studwork frame on edge of hemp-lime). The central stud was the first to be tested and as it was being loaded in compression at 55kN the studwork frame rotated about its base away from the hemp-lime (Figure 6.23). The rotation caused the connection between the horizontal rails and studs to fail and as a result secure connection between the framing and hemp-lime mass was lost. Once the load had been removed the frame was pushed back into the hemp-lime and the lateral restraints at the top corners of the wall panel were applied to the studwork frame rather than the hemp-lime as previously. The stud was re-loaded until failure occurred. The two outer studs (RH and LH) were tested with lateral restraints on the studwork frame to prevent rotation occurring again.

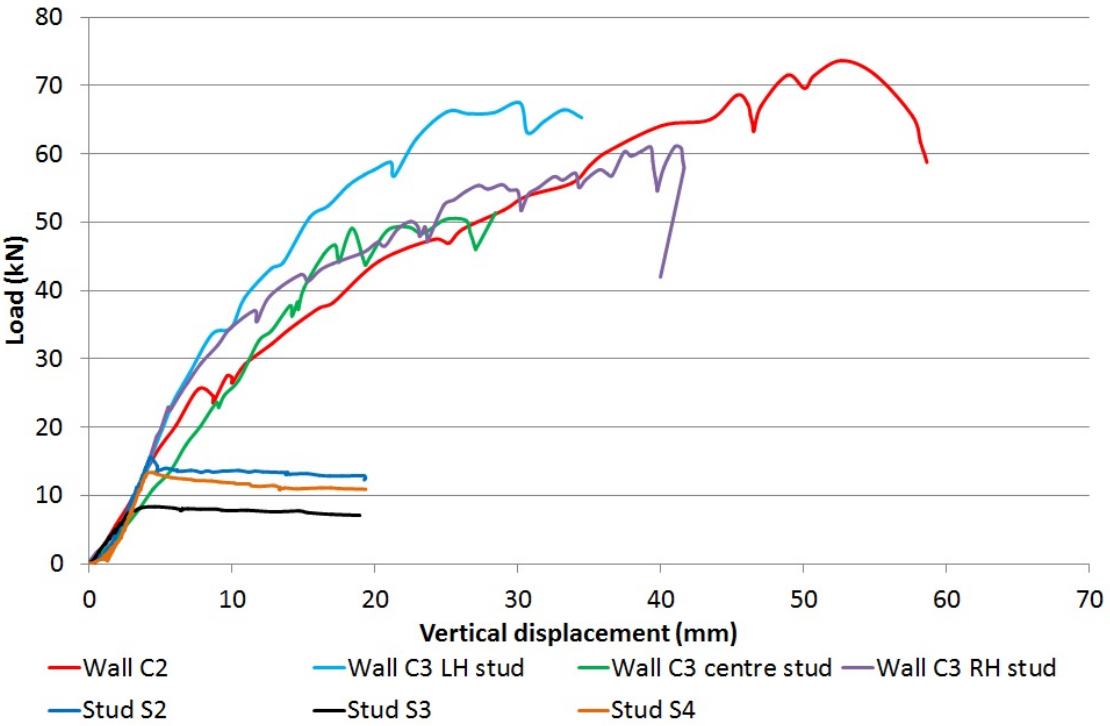

Figure 6.22 Walls C2, C3 and Studs S2, S3, S4 compressive test results

Figure 6.23 Wall C3 studwork frame rotation during loading of central stud

From Figure 6.22 the three unrestrained timber studs (Studs S2, S3, S4) achieved maximum compressive loads of 15.9kN, 8.4kN and 13.7kN. At these maximum loads each stud buckled about its minor axis as expected (Figure 6.24) and following this continued to sustain a reduced load until the timber failed by bending at around the mid height of the stud (Figure 6.25). This is the expected behaviour of an unrestrained timber stud and the variation in maximum load is due to the variations in the timber (knots, splits) and the initial curvature of the studs.

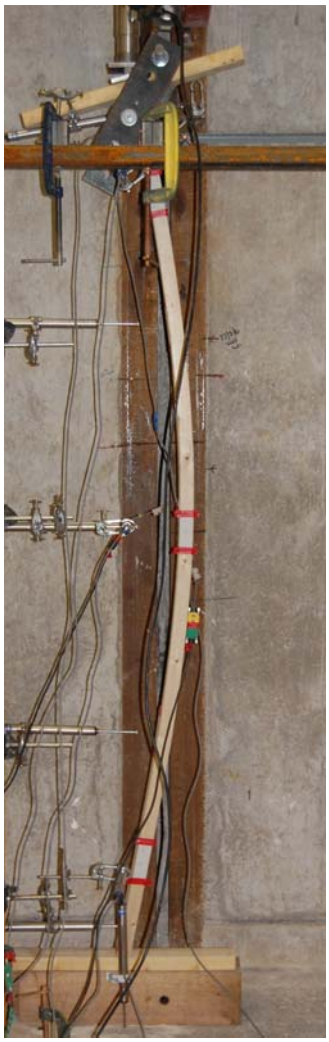

Figure 6.24 Buckled stud

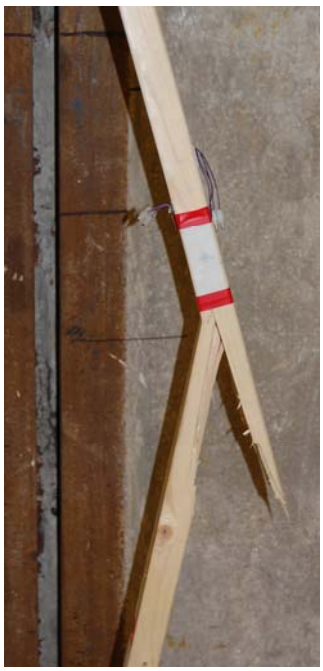

Figure 6.25 Post buckling failure

From Figure 6.22 Wall C2 (studwork frame in centre of hemp-lime) achieved a maximum load of 75.0kN at a vertical displacement at the top of the loaded stud of 53.5mm. During testing there was no indication either visually or from the LVDT readings that minor or major axis bucking was occurring. Following the test the hemp-lime was slowly and carefully dismantled in order to establish how the stud had behaved and failed. Again there were no signs that the stud had buckled as the hemp-lime was still tightly packed around the stud and showed no signs of crushing. The stud had failed by crushing together with compression failure perpendicular to the grain of the sole plate. The stud crushed and rolled forward at the location of two knots 1.9m from its base (Figure 6.26). The sole plate had failed in bearing under the stud and a similar bearing failure was also apparent in the header plate at the top of the stud (Figure 6.27).

Figure 6.26 Wall C2 central stud failure

Figure 6.27 Sole plate bearing failure

The initial stiffness of all of the unrestrained timber studs and the hemp-lime restrained stud in Wall 1 are similar at roughly 3500N/mm. It is clear from Figure 6.22 that after the unrestrained studs have buckled the stiffness of the stud in Wall 1 remains constant until a load of 25.5kN is reached at which point the stiffness reduces to roughly 1100N/mm. These results show that buckling of the stud has not occurred as the stud retains its initial stiffness to a much higher load than the unrestrained studs. Additionally once the stiffness reduces the stud continues to carry a significant load and completely fails at a load over five times greater than the unrestrained studs. Once the unrestrained studs had buckled they lost all of their stiffness.

Wall C3 (studwork frame on edge of hemp-lime) showed similar results to Wall C2, despite the problems with the test set up as mentioned previously. Figure 6.22 shows that all of the studs in Wall C3 had very similar stiffnesses to the stud in Wall C2. All three studs in Wall C3 behaved in a similar manner as the stud in Wall C2 with no buckling detected about either the minor or major axis.

Both the centre stud and the right hand stud showed bearing failures of the sole plate. The left hand stud showed bearing failure of the sole plate combined with crushing/rotation of the stud base (Figure 6.28). From Figure 6.22 the maximum load carried by the centre stud (restrained at top) was 53.3kN, the right hand stud was 63.0kN and the left hand stud was 67.5kN.

Figure 6.28 Wall C3 – Crushing and rotation of left hand stud

Figure 6.29 presents the results of applied load against vertical displacement of the top of the central stud from Wall C2, Studs S2, S3, S4 and two studs that were tested in Wall R1 after the racking testing had taken place. Compression testing was carried out on Wall R1 as the racking test had not significantly damaged the wall.

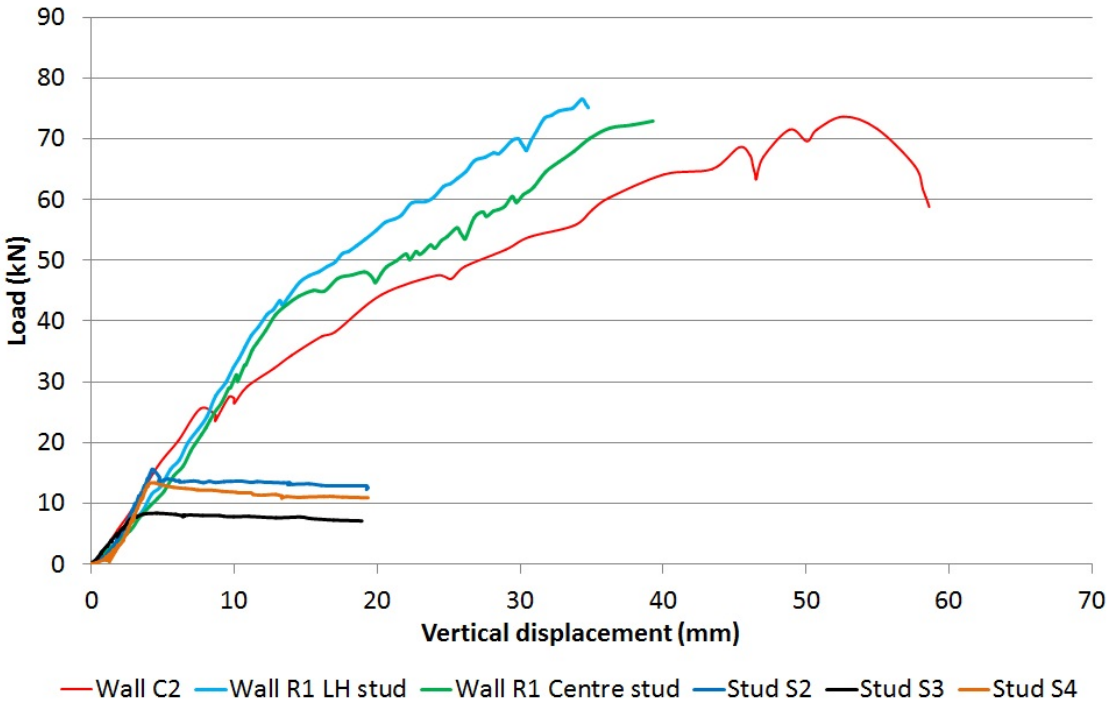

Figure 6.29 Walls C2, R1 and Studs S2, S3, S4 compressive test results

Due to the racking testing on Wall R1 when it was loaded in compression there was an initial horizontal displacement at the top of the studwork frame of 17.3mm. This deflection and the fact the wall had already been subjected to severe loading conditions will have affected the performance under compressive loading.

Both the left hand stud and the central stud in Wall R1 failed by crushing of the sole and header plates perpendicular to the grain (Figure 6.30). Neither stud showed any other signs of failure and the testing had to be stopped at 75kN due to the limits of the testing equipment being reached. The initial stiffness of the studs taken between 10kN and 20kN was 3377N/mm for the left hand stud and 3407N/mm for the centre stud.

Figure 6.30 Wall R1 – Bearing failure on sole plate

Following testing of the walls and studs specimens of the timber were taken and the moisture content was measured. The moisture content was measured by cutting a section of timber from the studs and weighing before and after it had been dried in an oven. The specimens of timber were only removed from the oven once their weight had stabilised and reached equilibrium. Table 6.2 shows the average moisture content in each stud.

Table 6.2 Moisture content of studs

Wall	Stud	Average Moisture content %	Position within hemp-lime
C2	Centre	18.3	Centre
C3	Left	18.7	On edge
C3	Centre	19.6	On edge
C3	Right	17.9	On edge
R1	Left	21.7	Centre
R1	Centre	21.3	Centre
R1	Right	21.6	Centre
S2	NA	12.8	NA
S3	NA	12.8	NA
S4	NA	12.9	NA

Following testing specimens of the hemp-lime were also taken and the moisture content, compressive strength and carbonation depth were recorded. The moisture content was measured using the same method followed for the timber moisture contents of weighing before and after drying in an oven. Table 6.3 shows the moisture content for Walls C2, C3 and R1 and

Table 6.3 Hemp-lime moisture content

Wall	Moisture Content (%)			Dry density (kg/m^3)
	Inner	Outer	Average	
C2 – Base	28.1	20.9	24.5	338
C2 – Middle	25.4	11.4	18.4	260
C2 – Top	21.9	13.1	17.5	296
C2 - Average	**25.1**	**15.1**	**20.1**	**298**
C3 – Base	27.5	16.3	21.9	293
C3 – Middle	25.7	15.4	20.5	263
C3 – Top	21.8	12.8	17.3	274
C3 - Average	**25.0**	**14.8**	**19.9**	**277**
R1 – Base	25.7	19.9	22.8	282
R1 – Middle	25.0	17.4	21.2	249
R1 – Top	18.3	10.4	14.3	276
R1 - Average	**23.0**	**15.9**	**19.5**	**269**

Table 6.4 shows the compressive strength of the hemp-lime prisms. The moisture content was measured at the base, middle and top of the walls on both the outer and inner areas. The outer area moisture contents were taken from the outer 30mm of hemp-lime surface and the inner areas were taken from the centre of the hemp-lime.

Table 6.4 Walls C2, C3, and R1 hemp-lime compressive strength

Wall	Specimen location	b (mm)	d (mm)	h (mm)	Compressive strength σ_c (N/mm^2)
C2	Base	285	300	210	0.52
C2	Middle	260	300	230	0.24
C2	Top	300	290	300	0.38
C3	Base	300	305	420	0.38
C3	Middle	300	300	285	0.26
C3	Top	255	300	315	0.37
R1	Base	300	300	410	0.31
R1	Middle	300	300	330	0.28
R1	Top	300	300	400	0.39
Average					**0.35**

The average moisture content of the inner areas of hemp-lime was 24.4%. This is slightly higher than the average moisture content of the timber studs. The average moisture content of both the inner and outer areas of hemp-lime is 19.8% which is almost the same as the average for the studs. The studs are lower than the inner areas of hemp-lime as some of them were exposed on one face and therefore were able to dry more easily. All of the inner areas of the walls had a higher moisture content than the outer areas, which is to be expected. Additionally the moisture content of the hemp-lime increased from the top of the wall to the bottom which again is to be expected as water will slowly move down the walls under the influence of gravity.

The average compressive strength of the hemp-lime prisms was 0.35N/mm^2 which is higher than those the prisms taken from Wall C1. This will be as a result of the walls being left for longer between casting and testing. As a result the hemp-lime was much drier and additional carbonation will have taken place. The compressive strength of prisms compares well with the compressive strength of the material properties cylinders

in Chapter 3. The average compressive strength of LS1 cylinders was 0.45N/mm^2 and the average for both LS1 and LS2 was 0.39N/mm^2. The slightly higher average compressive strength of the cylinders is likely to be due to them having lower moisture content, as they dry more quickly than full thickness walls.

All of the prism specimens were sprayed with phenolphthalein solution in order to determine the level of carbonation. Figure 6.31 shows one of the prisms after spraying and is typical of the levels of carbonation. The hemp-lime had on average carbonated by 30mm from each of the exposed wall faces.

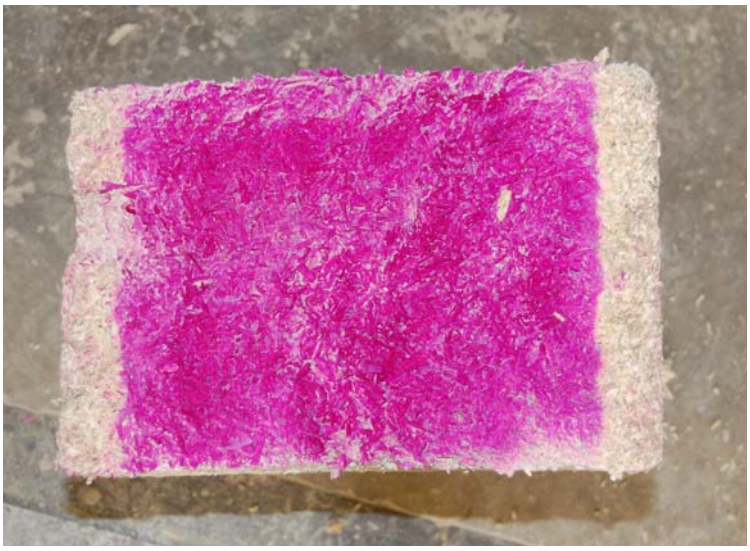

Figure 6.31 Hemp lime showing level of carbonation

6.3.3 Second large scale tests (LS2)

Figure 6.32 present the results of the compression tests on Studs S5 to S10 showing applied load against vertical displacement at the top of the studs. Figure 6.33 presents the results of applied load against vertical displacement of the top of the central stud from Walls C4 to C7 and typical results for the individual unrestrained timber studs. All of the results plotted are with 22mm eccentricity.

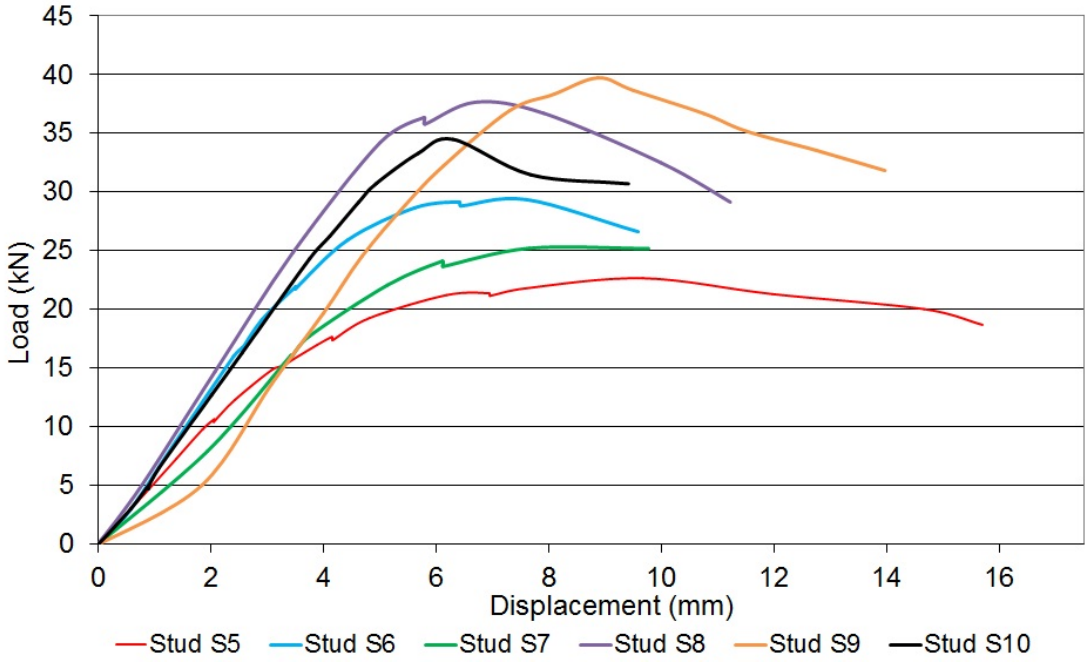

Figure 6.32 Studs S5 to S10 compression test results

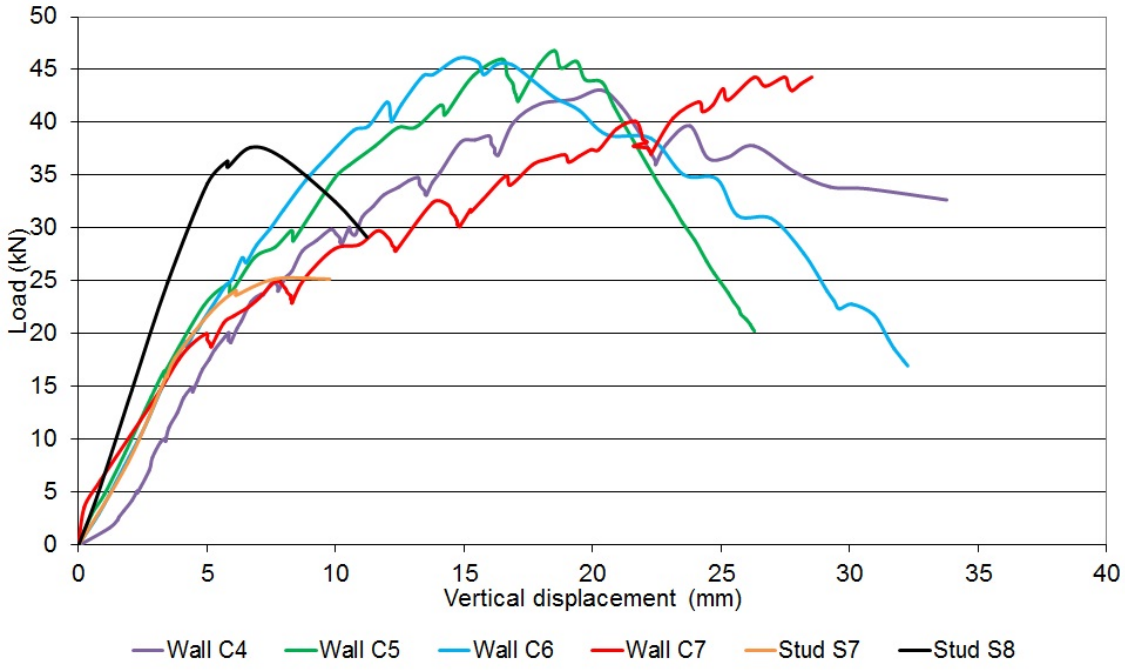

Figure 6.33 Walls C4 to C7 and timber studs compressive test results

From Figure 6.32 Studs S5, S6 and S7 (studs with pinned bases) all failed at loads between 20kN and 30kN while Studs S8, S9 and S10 (studs with fixed bases) all failed between 30kN and 40kN. Additionally Studs S8, S9 and S10 had a higher initial stiffness. The maximum average load of the unrestrained timber studs with pinned bases was 26.1kN and the average initial stiffness (taken between 5kN and 15kN) was

5954N/mm. The three studs with pinned bases all failed by bucking before snapping of the stud at mid height (Figure 6.34).

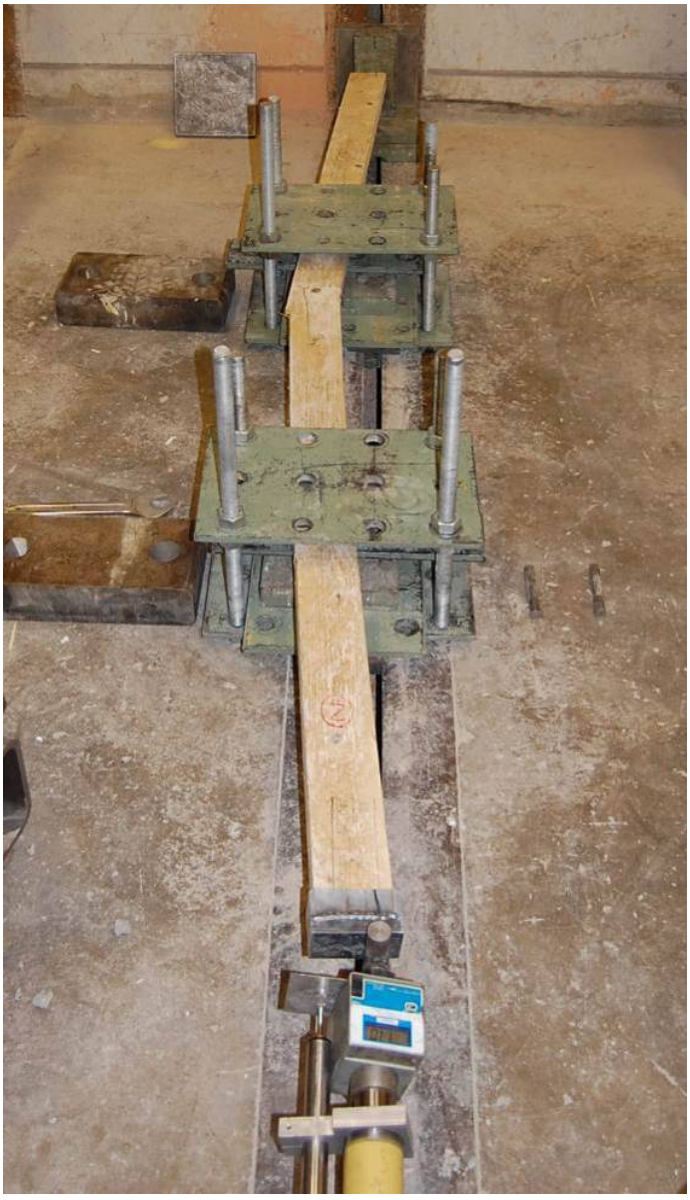

Figure 6.34 Failed stud with pinned base

The studs with the fixed bases were tested as they are a closer representation of the arrangement within the hemp-lime composite wall panels where the studs are fixed to the footer rail. By testing with a fixed base it enables better comparisons between the results for the studs and the wall panels. The maximum average load achieved by the studs with fixed bases was 38.1kN and the average initial stiffness was 6924N/mm^2. These studs also failed by buckling and then by snapping of the stud at around 800mm from the top of the stud (Figure 6.35).

Figure 6.35 Failed stud with fixed base

There was some difficulty during testing of Wall C4 (studwork frame in centre of hemp-lime), the first wall to be tested. The stud was loaded by the pin through a steel plate. Unfortunately the steel plate allowed too much rotation which resulted in the load being applied to one edge of the stud. This resulted in the stud splitting (Figure 6.36). Following this, the shoe shown in Figure 6.10 was manufactured and used to prevent these problems occurring again.

Figure 6.36 Wall C4 splitting of stud

From Figure 6.33 Wall C7 (studwork frame on edge of hemp-lime) achieved a maximum load of 45.2kN at a vertical displacement of 28.4mm. During testing there was no indication either visually or from the LVDT readings that minor axis buckling was occurring. The stud failed by buckling about its major axis at mid height (Figure 6.37). Upon failure of the stud there was a sudden reduction in load and the stud was unable to resist further load. There was no damage to the hemp-lime surrounding the stud and as shown in Figure 6.38 and Figure 6.39 the horizontal rail stayed in place with the screw pulling through the rail. This occurred on all three rails.

Figure 6.37 Wall C7 central stud failure

Figure 6.38 Horizontal rail within hemp-lime

Figure 6.39 Screw in failed stud

Wall C5 and Wall C6 were very similar in design and as a result showed similar results. Both walls had 50mm cover of hemp-lime to the timber studs. Wall C6 had horizontal rails whereas Wall C5 did not. Wall C6 achieved a maximum load of 47.6kN at a vertical displacement of 15.0mm and Wall C5 achieved a maximum load of 47.4kN at a vertical displacement of 18.4mm. Both walls failed with combination of buckling and crushing of the stud around 600mm from the top of the wall. In addition to this the hemp-lime burst at the top of the walls along the line of the failed stud where the stud buckled out of the wall. The extent of this bursting of the hemp-lime is shown in Figure 6.40 for Wall C5 and Figure 6.41 shows the crack the formed along the line of the stud to the base of the wall. Wall C6 displayed very similar characteristics.

Figure 6.40 Wall C5 – hemp-lime bursting

Figure 6.41 Wall 5 - cracking along line of stud

From Figure 6.33 it can be seen that the post failure behaviour of Wall C5 and Wall C6 is slightly different. Once the stud has failed in Wall C5 the load reduces very quickly to around 20kN. In Wall C6 once the stud has failed and the hemp-lime burst the load does not reduce at such a fast rate, however it does reduce to a similar level of around 20kN. Wall C5 did not have any horizontal rails and therefore once the stud had failed and the hemp-lime had burst there was no other element to resist the load. In Wall C6 the rails were present to resist some of the load. In Wall C6 one the stud had started to fail and the hemp-lime started to burst increasing amounts of load will have been transferred on the rail which in turn resulted in the screws pulling through the rail. This transferring of load between different elements of the wall has made the failure of the wall very slightly less brittle.

When Wall C5 and Wall C6 are compared with Wall C7 it can be seen that the hemp-lime in Walls C5 and C6 is helping to resist buckling of the stud. In Wall C7 the stud was only prevented from buckling about is major axis by the horizontal rails. Failure occurred at a vertical deflection of the stud was 28.4mm. While Walls C5 and C6 failed at similar loads to Wall C7 their vertical displacements were much lower at 15.0mm and 18.4mm. The 50mm of hemp-lime cover is reducing the outward buckling displacement of the studs and hence reducing the vertical displacement. Once this resistance was lost with the bursting of the hemp-lime the studs failed and in the case of Wall C6 increased the load on the rail. As the load was already at the same level as the failure load for Wall C7 the screws fixing the rails and stud will have failed almost immediately.

Wall C4 had the studwork frame in the centre of the hemp-lime. Figure 6.33 shows that the maximum load was 43.1kN at a displacement of 20.3mm. It was at this load that the top of the stud split as shown in Figure 6.36. There were no signs that the stud had buckled about either axis and once the wall was deconstructed this was confirmed. Below the split in the stud the timber had locally crushed and failed in compression (Figure 6.42). Therefore the hemp-lime prevented buckling about either axis.

Figure 6.42 Crushing of stud in Wall C4

Upon deconstruction of the walls, all of the footer plates showed crushing under the bases of the studs (Figure 6.43). This is to be expected as the compression resistance perpendicular to the grain is lower than the resistance parallel to the grain. Materials testing (see Chapter 3) has shown that for this type and grade of timber the average compression resistance perpendicular to the grain is 9.3N/mm^2 when loaded with a 38mm by 89mm section whereas compression resistance parallel to the grain is 42.9N/mm^2.

Figure 6.43 Crushing of footer plate on Wall C7

All of the hemp-lime restrained studs (Walls C4 to C7) achieved higher maximum loads than the unrestrained timber studs. This shows that the hemp-lime and horizontal rails are restraining the studs from buckling and therefore increasing their resistance to buckling. All of the wall panels and the timber studs had a similar initial stiffness apart from the individual studs with fixed bases (S5, S6, S7). These have a slightly higher initial stiffness, an average of just under 7000N/mm compared with about 6000N/mm for the studs with pinned bases (S8, S9, S10) and Walls C4 to C7. The difference between the pin ended and fixed end studs is due to the ability of the pin ended studs to rotate freely therefore allowing more horizontal deflection and as a result more vertical deflection. The reason Walls C4 to C7 are less stiff than the fix ended studs is likely to be due to the footer rail crushing prior to failure of the stud and therefore increasing the vertical displacement and reducing the recorded stiffness.

Following testing of the walls and studs specimens of the timber were taken and the moisture content was measured. Table 6.5 shows the average moisture content in each stud.

Table 6.5 Moisture content of studs (LS2)

Wall	**Stud**	**Average Moisture content %**	**Position within hemp-lime**
C4	Base of centre stud	22.0	Centre
C4	Middle of centre stud	21.7	Centre
C5	Base of centre stud	22.2	50mm Cover
C5	Middle of centre stud	21.3	50mm Cover
C6	Base of centre stud	17.7	50mm Cover
C6	Middle of centre stud	20.7	50mm Cover
C7	Base of centre stud	15.0	Edge
C7	Middle of centre stud	11.9	Edge
S5 – S10	Average	11.2	-

As with Walls C2, C3 and R1 the moisture content of the studs at the time of testing was quite high. The studs in Walls C4, C5 and C6 that were completely surrounded by hemp-lime show the highest moisture content ranging from 22.0% to 17.7% with an average of 20.9%. The studs in Wall C7 that had one face exposed had lower moisture contents with the mid height of the stud having a moisture content only 0.7% higher

than Studs S5 to S10 which had not been cast into hemp-lime. This shows the faster drying times when elements are exposed to continually circulating air near their surface.

As with Walls C2, C3 and R1 specimens of hemp-lime were taken from Walls C4 to C7 in order to establish the moisture content and compressive strength. The moisture content and dry density are shown in Table 6.6 and the compressive strengths are shown in Table 6.7. The same method of oven drying to find moisture content was used.

Table 6.6 Hemp-lime prism moisture content (LS2)

Wall	Moisture Content (%)			Dry density (kg/m^3)
	Inner	Outer	Average	
C4 – Base	21.1	10.2	15.7	314
C4 – Middle	21.0	7.5	14.3	-
C4 – Top	12.0	6.8	9.4	366
C4 - Average	**18.0**	**8.2**	**13.1**	**340**
C5 – Base	19.9	8.6	14.3	365
C5 – Middle	21.1	8.6	14.9	319
C5 – Top	8.1	7.5	7.8	356
C5 - Average	**16.4**	**8.3**	**12.3**	**347**
C6 – Base	15.0	10.6	12.8	323
C6 – Middle	23.6	8.5	16.1	268
C6 – Top	19.7	9.8	14.8	316
C6 - Average	**19.4**	**9.6**	**14.6**	**302**
C7 – Base	17.2	9.4	13.3	327
C7 – Middle	9.0	7.5	8.3	301
C7 – Top	6.9	7.3	10.6	381
C7 - Average	**11.0**	**8.1**	**10.7**	**337**

Table 6.7 Walls C4, C5, C6 and C7 hemp-lime compressive strength

Wall	Specimen location	b (mm)	d (mm)	h (mm)	Compressive strength σ_c (N/mm^2)
C4	Base	152	161	299	0.56
C4	Middle	174	168	323	0.44
C4	Top	168	150	312	0.26
C5	Base	165	152	308	0.46
C5	Middle	154	146	302	0.41
C5	Top	141	139	310	0.25
C6	Base	173	133	316	0.25
C6	Middle	141	156	310	0.07
C6	Top	152	173	310	0.39
C7	Base	152	153	300	0.14
C7	Middle	163	181	312	0.18
C7	Top	164	179	316	0.31
Average					**0.31**

The average moisture content of the inner areas of hemp-lime was 16.2%. In all of the walls apart from C6 the moisture content was lower at the top of the walls and in Walls C5 and C7 it was half the moisture content of the base. The mid height and base areas had similar moisture content on all of the walls. The top will generally be drier as there is a greater surface area for the water to evaporate from as the tops of the walls were not covered during drying and the water will slowly move down the walls under the influence of gravity. Wall C6 had higher moisture content at the top than the base. There are no definitive reasons for this, however the top of Wall C6 may have got wet during storage or transportation.

The average density of the hemp-lime was 331.4kg/m^3. This is higher than the target density of 275kg/m^3. The increase in density is due to the wall panels being constructed away from the laboratory using a construction process that was less easy to control and monitor. The increase in density by this amount should not have affected the results of the tests as changes by this amount do not significantly change the cylinder properties.

The average compressive strength of the hemp-lime prisms was 0.31N/mm^2 which is higher than those the prisms taken from Wall C1 but slightly lower than the average from Walls C2 and C3. The higher compressive strength than Wall C1 will again be due to lower moisture content and longer drying period. The average prism strength is slightly lower than the average LS2 cylinder compressive strength of 0.35N/mm^2 shown in Chapter 3. As with the prisms of hemp-lime from Walls C2 and C3 this is likely to be due to the difference in moisture content of the hemp-lime between the prisms and cylinders.

As with Wall C2 and C3 the prism specimens were sprayed with phenolphthalein solution in order to determine the level of carbonation. The hemp-lime had on average carbonated by 20mm to 30mm from each of the exposed wall faces.

6.4 Discussion

The results from Wall C1 and Stud S1 confirm the findings from Helmich (2008) that cast hemp-lime can prevent buckling in lightweight steel studs. The results also showed that lower density hemp-lime confines a stud located centrally within the hemp-lime matrix and as a result global buckling is prevented. The hemp-lime increased the failure load of the frame by over 80%. However the theoretical section capacity of the stud calculated using BS 5950-5 (1998) of 72.5kN was not reached. This could be because the hemp-lime did not provide full confinement to the stud or possibly due to local buckling failure at the base of the stud. Additionally there may have been some initial eccentricity in the stud which will have reduced its capacity.

The results from the tests on Wall C2 showed that hemp-lime does prevent buckling, as with lightweight steel studs, of timber studs when loaded in compression. Wall C3 showed that with the timber studs on the edge of the wall buckling about the minor axis is again prevented. In this situation it is prevented by both the hemp-lime and horizontal rails. Buckling of the stud out of the wall face about its major axis is a possibility with the studs on the edge of the hemp-lime. This is likely to have been prevented by the horizontal rails as they were fixed to the stud and into the hemp-lime and the buckling load for the studs about their major axis is 33.4kN. Their connections were by 2.65mm diameter by 50mm long nails that only offer modest pull out resistance; however a

single central horizontal restraint of only 2% of the vertical load is all that is required to prevent buckling (IStructE and TRADA, 2007). The nailed connections on average provide a maximum of 0.8kN of restraint per connection. The maximum failure load of any of the studs in Wall C3 was 67.5kN (left hand stud) and 2% of this load is 1.35kN. This is greater than the single connection resistance, but there were three rails equally spaced along the height of the stud which will have all contributed to the buckling resistance. For this reason the connections were improved in Walls C4 to C7.

Walls C4, C5, C6 and C7 have shown the effects of eccentric loading and bursting of the stud through the hemp-lime which were areas of investigation raised following the testing of Wall C3. Walls C4 to C7 were designed to test the major axis buckling response of the hemp-lime and timber studs with different amounts of hemp-lime cover. Full confinement was still achieved, even with an eccentric load, with the stud in the centre of the hemp-lime mass in Wall C4. The studs in Walls C5 to C7 all buckled about their major axis when loaded with an eccentric load. Wall C3 and Wall C7 were of the same construction apart from the fixings connecting the horizontal rails to the studs. When comparing their performance Wall C7 failed at a much lower load of 45.2kN whereas the studs in Wall C3 failed between 53.5kN and 67.5kN. The lower failure load is due to the eccentrically applied load which at 45kN vertical load applies a moment to the end of the stud of 0.99kNm. However, if the horizontal rail to timber stud connections Wall C7 had been nails, as used in Wall C3, rather than the 4mm diameter 50mm long screws that were used then the failure load would have been much lower. The initial stiffness of the rail to stud connection with the nailed connections is 2216N/mm and the 4mm diameter screwed connections is 2194N/mm. However, the maximum load for the nail is 0.8kN whereas the screw is 2.2kN. This shows the large improvement in fixing strength that has been gained by using screwed connections.

It is not possible to compare the results from the Initial compression tests, Large Scale 1 tests or Large Scale 2 tests as each series was designed to investigate different aspects of behaviour. The Initial compression tests on Wall C1 and Stud S1 can be compared with the work by Helmich (2008), Large Scale 1 and Large Scale 2 with the work by Dutton (2009) and Mukherjee (2012).

Comparing the results from Helmich (2008) with Wall C1 and Stud S1 Helmich (2008) achieved higher loads with both the hemp-lime restrained stud and unrestrained stud. The higher load on the hemp-lime restrained stud (75.0kN compared with 60.3kN) is likely to be due to the higher density of the hemp-lime used by Helmich (2008) of 466kg/m^3 compared with 267kg/m^3 used in Wall C1 as the hemp-lime mix proportions and type of studwork framing were the same. The unrestrained stud tested by Helmich (2008) achieved a maximum load of 38.5kN whereas Stud S1 reached a maximum of 33.3kN. As both of the studs were the same dimensions and manufactured to the same specification the difference must be due to initial eccentricities in the test set up causing a lower failure load in Stud S1.

Dutton (2009) and Mukherjee (2012) both found that timber studs were prevented from buckling about their minor axis when hemp-lime was cast on both sides of them. Dutton (2009) found that failure loads were increased by between 15% and 26% and Mukherjee (2012) found that when minor axis buckling was prevented by hemp-lime major axis buckling was a possible failure mode. The tests on Walls C2 and C3 also found that hemp-lime prevented minor axis buckling and increased the load capacity of the studs by up to 500%. However, major axis bucking was not found to be a failure mode as the hemp-lime surrounded the studs in Wall C3 and the horizontal rail resisted major axis buckling in Wall C2. Additionally the major axis buckling load was around the same as the crushing failure load so it may not have been reached. The tests on Walls C4 to C7 showed that the major axis buckling failures experienced by Mukherjee (2012) could be reduced and the major axis buckling load increased if hemp-lime is cast around the studs rather than just between the studs. This also provides a thicker wall build up and as a result increased insulation.

Studs S2, S3 and S4 had an average buckling load of 12.52kN. Comparing this with the predicted load of 6.9kN shown in Chapter 4 it is over two times higher. The predicted load used the Euler buckling equation and the materials properties obtained in Chapter 3. The reasons for the higher actual buckling loads are not obvious, but it is likely to be a result of the differences in the actual properties of the timber and the measured properties used in the theoretical analysis. The material properties used in the theoretical analysis were the average values and therefore there is a chance that the strength and stiffness of the studs used was higher.

Both Walls C2 and C3 were predicted to have bearing failure of the header and footer rails at 31.5kN followed by crushing failure of the stud at a load of 155.9kN. This calculation assumed the moisture content in the timber of 12.0%. The actual moisture content of the studs was 18.3% for Wall C2 and 19.6% for Wall C3. The moisture content of the stud in Wall C2 was only tested 24 hours after the hemp-lime had been removed and therefore at the time of testing it is likely it was similar to the moisture content of the studs in Wall R4 at 21.3%. With these moisture contents the compressive strength of the timber reduces from 46.6N/mm^2 at 12.0% to 21.9N/mm^2 at 21.3% and 23.7N/mm^2 at 19.6%. As a result the crushing load for Wall C2 is 74.1kN and for Wall C3 is 80.2kN. The stud in Wall C2 failed at a load of 75.0kN and therefore the prediction is accurate. The left hand stud in Wall C3 failed at load of 67.5kN. In this case the bearing failure of the footer rail caused the stud base to rotate forward inducing bending into the stud and resulting failure. This confirms that the capacity of the header and footer rail must be considered and may be a limiting factor in the design load capacity of this type of composite wall construction.

The eccentrically loaded studs, S5, S6 and S7, failed at an average load of 26.1kN by buckling about their major axis. The failure load predicted in Chapter 4 for these studs was 28.9kN. The actual and predicted loads vary by 7.3% and therefore the predictions are accurate when considering the variability in the material properties of timber.

In Chapter 4 the type of failures that might occur on Walls C4 to C7 were discussed and it was concluded that insufficient information was available to be able to predict the failures accurately. The hemp-lime on Walls C5 and C6 burst with similar geometry which is shown in Figure 6.44. Using this geometry the horizontal load required to burst the hemp-lime can be assessed. Assuming a cone type failure the hemp-lime will either fail in tension or shear. The tensile strength and the shear strength of the hemp-lime have not been measured. A lower bound value of shear strength can be calculated from the hemp-lime bending strength results shown in Chapter 3. All of the bending specimens failed in bending and therefore it can be assumed that the shear strength is higher than the bending strength for these sections. In this way the lower bound shear strength can be calculated as 0.014N/mm^2. The tensile strength can be assumed to be two thirds of the bending strength. The bending strength from Chapter 3 is 0.072N/mm^2 and therefore the tensile strength will be assumed to be 0.048N/mm^2. Using the shear

strength as a conservative approach the force required to push out the cone of hemp-lime can be simplified to the failure surface area multiplied by the shear strength.

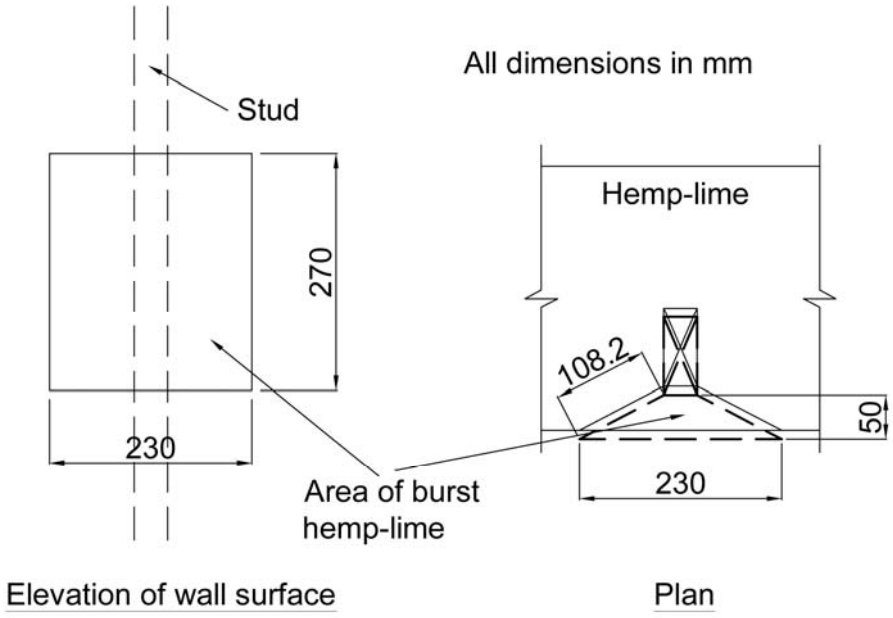

Figure 6.44 50mm hemp-lime cover bursting geometry

The failure surface area is:

$$A_{burst} = 2 \times (108.2 \times 270) = \underline{58428mm^2}$$

Therefore the force required to burst the cone out of the wall is:

$$F_{burst} = 58428 \times 0.014 = \underline{818N}$$

This can be seen as the restraining force. The force required to restrain a stud from buckling is 2% of the axial load (IStructE and TRADA, 2007). The failure load of the concentrically loaded stud in Wall C2 was 75.0kN. Therefore the load required to restrain this stud is 1.5kN. If the resistance offered by 50mm of hemp-lime is only 0.82kN, as calculated above, then hemp-lime will burst and the stud will buckle. The concentric failure load has been used for simplicity as the effects of bending of the studs induced by eccentric loads into the hemp-lime are not fully understood and further research is required here.

Considering Wall C4 where there was 105mm of hemp-lime cover the same approach can be taken. Using the same geometry as observed during the failure of Walls C5 and C6 the cone shown in Figure 6.45 is used.

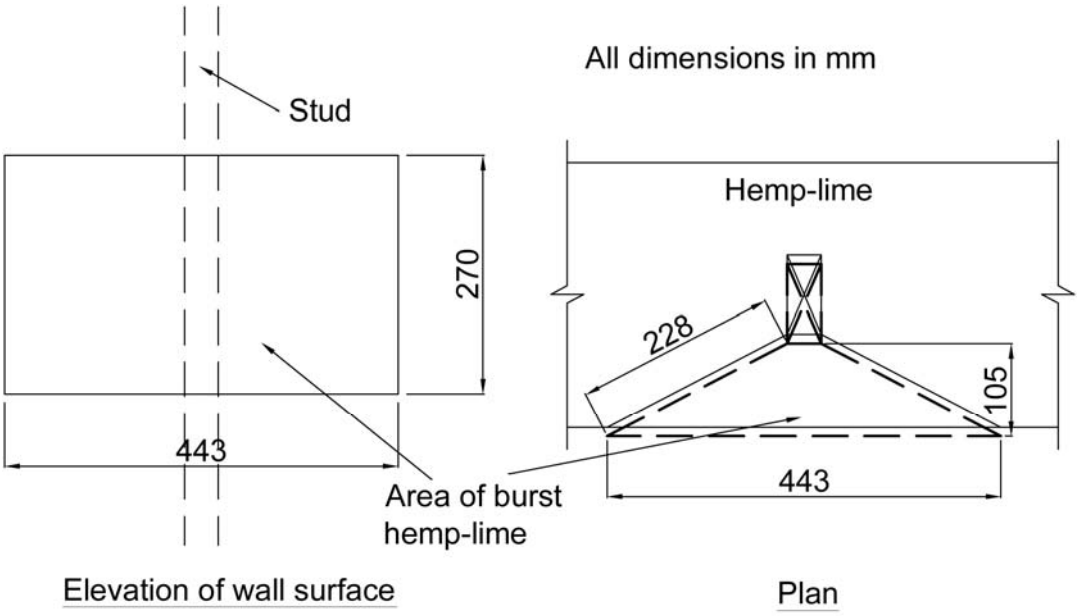

Figure 6.45 105mm hemp-lime cover bursting geometry

With the geometry shown in Figure 6.45 the failure surface area is:

$$A_{burst} = 2 \times (228 \times 270) = \underline{123120mm^2}$$

Therefore the force required to burst the cone out of the wall is:

$$F_{burst} = 123120 \times 0.014 = \underline{1724N}$$

Again, comparing this to the concentric failure load of 75.0kN this is 2.3% and therefore the stud will be restrained and the hemp-lime will not burst. This was the case on Wall C4. With this simple analysis two rules can be set out:

- If $F_{burst} < 2\%\ axial\ load$ the hemp-lime will not burst.
- If $F_{burst} > 2\%\ axial\ load$ the hemp-lime will burst.

Wall C7 failed at a load of 45.2kN and the predicted failure load was 82.4kN. Wall C7 failed by buckling out of the wall with the timber failing at 990mm from the base of the

wall. This indicates that the loading and support conditions on the stud were similar to a column with an applied moment at each end rather than just at the top. This could have been due to crushing of the footer rail causing the base of the stud to rotate. The theoretical analysis used the average material properties and connection stiffness. If the 5% characteristic values are used the calculated failure load is 48.2kN. This is closer to the actual failure load, but still higher.

The stud failed at the location of several knots and therefore a weak point. If the knots had not been present it may have failed at a different location or higher load. The elastic modulus of the timber was found by testing small clear specimens which are free from any defects and therefore the actual elastic modulus for the tested stud may have been lower than even the 5% characteristic values.

In all of the wall panels the bearing failure of the footer rail will have had an effect on the failure of the stud and crushing of the footer rail should be considered during design as the timber is weaker when crushed perpendicular to the grain.

6.5 Conclusions

The tests on Stud S1 and Wall C1 have confirmed that hemp lime at a dry density of 267kg/m^3 (average wet density = 423.9 kg/m^3) allows an increase in the vertical load capacity of light weight steel framing. The hemp lime used in this test was still very wet at time of testing and had not really carbonated at all, however previous studies using Tradical HB binder have shown very little change in strength between 28 days and 90 days (Hirst *et al.*, 2012).

The tests on Walls C2 and C3 and Studs S2 to S4 have shown that hemp-lime at a dry density of 275kg/m^3 prevents minor and major axis buckling of 38mm by 89mm by 2.4m long C16 timber studs with concentric loading when cast into the centre or on the edge of a 300mm thick wall. Several crushing failure modes were observed due to variability in the timber studs being tested. The test on Wall C3 also showed that the method of fixing the timber rails to the studwork framing was insufficient to prevent rotation of the frame about its base.

The compressive tests on Walls C4 to C7 and Studs S5 to S10 have shown that hemp-lime prevents buckling of the timber studs about their major axis even when subjected to an eccentric load. On Wall C4 where the studwork frame was in the centre of the hemp-lime the timber studs did not buckle about either axis. On Walls C5 and C6 where the studwork frame was set 50mm in from the surface of the hemp-lime, both the hemp-lime and the horizontal rails restrain the studs and increase the buckling load about their major axis. Finally on Wall C7 where the studs were on the edge of the hemp-lime the horizontal rails restrained the studs about their major axis and increased the buckling load. The improved rail to studwork frame fixings also prevented premature failure of these joints.

The theoretical predictions have shown mixed results. With concentric loading the actual results and the predicted results correlate well. With eccentric loading there is a greater difference. With the eccentrically loaded stud the failure mode, by crushing or buckling, was correctly predicted for all of the walls apart from Wall C7. The failures occurred at the points of maximum horizontal deflection rather than at the theoretical point of maximum moment. This could be a result of the way that the test set up applied the load. The most critical aspect of load prediction in respect to designing with this type of construction is that bearing failure of the footer and header rails are likely to dominate design rather than the failure load of the studs as long as the studs do not buckle at their unrestrained buckling loads.

There is further work required to understand studs bursting through the surface of the hemp-lime both experimentally and theoretically. Only two specimens have shown this phenomenon and therefore the data available for analysis is very small. A more advanced theoretical model needs to be developed to allow accurate prediction of the horizontal forces being applied to the hemp-lime and when and how it might burst. This may require more detailed material properties for the hemp-lime including tension and shear. Finally design recommendations for the design of composite hemp-lime and studwork walling are given in Chapter 9.

7 Experimental Study: Racking performance of wall panels

7.1 Introduction

Composite hemp-lime and timber studwork framing walls (Wall R1, R2, R4 and R5) were tested under in-plane racking loading to establish their combined composite performance and potential enhancement provided by the hemp-lime. For comparison a simple timber only studwork frame (Frame R3) was tested. Wall R1 had the studwork timber frame cast into the centre of the hemp-lime while Walls R2, R4 and R5 had the timber studwork frames cast onto the edge of the hemp-lime. Full details of the wall panels are shown in Chapter 5.

7.2 Methodology and test set up

The racking test set up was the same for all of the wall panels (Walls R1, R2, R4 and R5). The test set up is shown in Figure 7.1. Frame R3 was tested lying flat on the floor, for reasons of stability during the test; the setup is shown in Figure 7.2. All of the racking tests followed the set up outlined in BS EN 594 (1996) *Timber structures — Test methods — Racking strength and stiffness of timber frame wall panels* shown in Figure 7.3. A horizontal racking load was applied to the header plate via a hydraulic jack. Vertical point loads were applied to the top of each stud through the header plate. All of the loads were measured using load cells. In plane deflections around the perimeter of the panels were recorded using LVDTs measuring both the movement of the hemp-lime and the timber studwork frames (Figure 7.4). Both the loads and displacements were recorded using a System 6000 data acquisition module.

Figure 7.1 Racking test set up

Figure 7.2 Frame R3 test set up

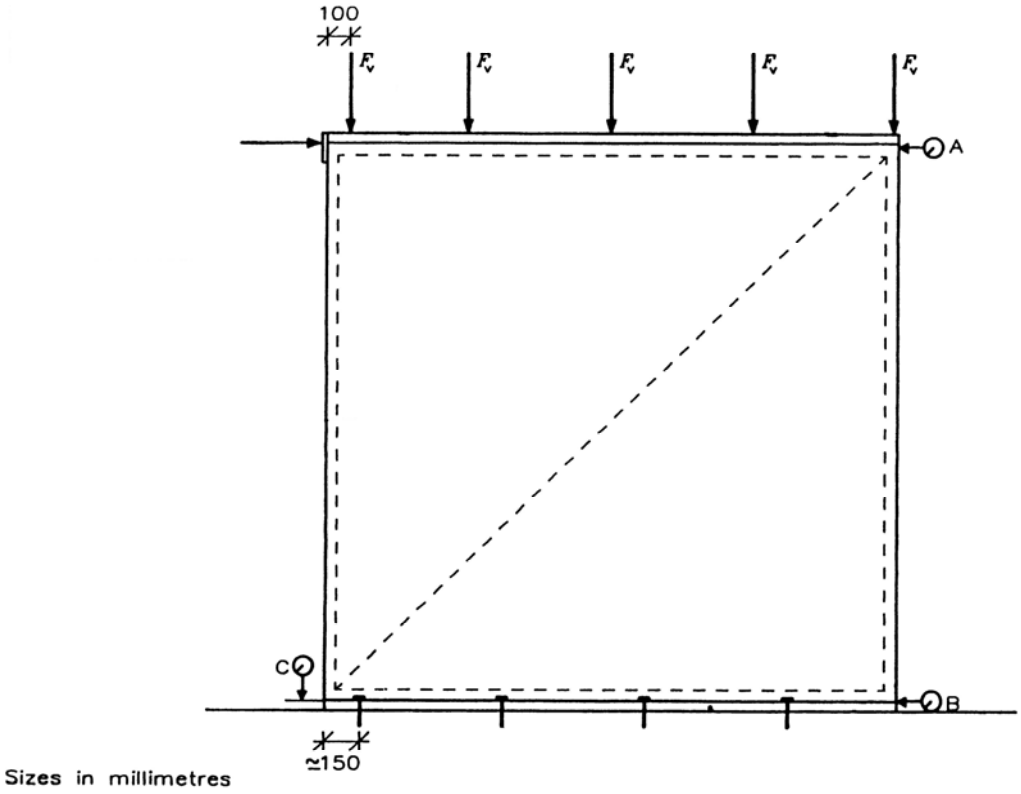

Figure 7.3 Racking test set up (BS EN 594, 1996)

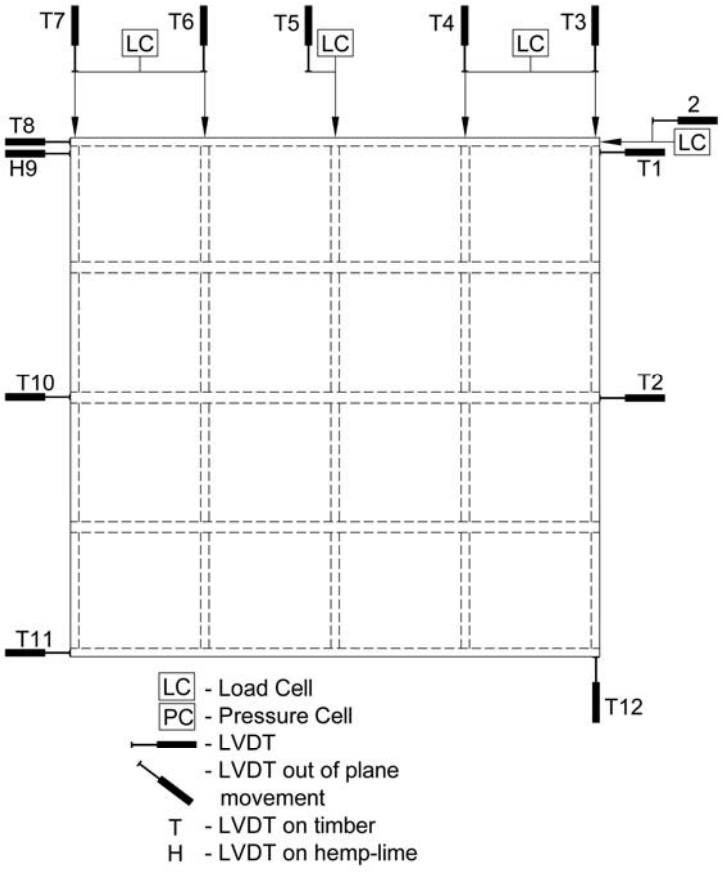

Figure 7.4 Racking test LVDT and load cell locations

All of the test panels were securely fixed to the laboratory floor to prevent sliding and uplift of their bases as set out in BS EN 594 (1996). The loading regime for all of the in-plane racking tests was based on the process set out in BS EN 594 (1996) and was as follows:

Stabilising cycle:

- Apply 5kN vertical loads to studs (F_v)
- Apply horizontal load of $0.1F_{max, est}$ and hold for two minutes
- Unload horizontal load and hold for five minutes

Stiffness cycle:

- Apply horizontal load of $0.4F_{max, est}$ and hold for five minutes
- Unload horizontal load and hold for five minutes

Strength cycle:

- Apply horizontal load of $0.4F_{max, est}$ and hold for five minutes
- Continue increasing horizontal load until failure occurs.

Failure was considered to have occurred when there was either a significant structural failure of the panel or the horizontal deflection at the top corner reached 100mm.

The test procedure is designed to test the resistance to racking of panels that are able to deform in plane both vertically and horizontally. The stabilising cycle allows settlements to occur within the wall panel. This would normally happen during construction as the upper storeys or roof is constructed and vertical load was slowly applied to the wall. The stiffness cycle allows the initial stiffness that is likely to dominate serviceability deflections to be established. Finally the strength cycle allows the ultimate strength of the wall panel to be found.

7.3 Results

7.3.1 Walls R1, R2 and Frame R3 (LS1)

Figure 7.5 shows in-plane racking test results for Wall R1, Wall R2 and for Frame R3. Racking load is plotted against horizontal deflection at the top of the walls.

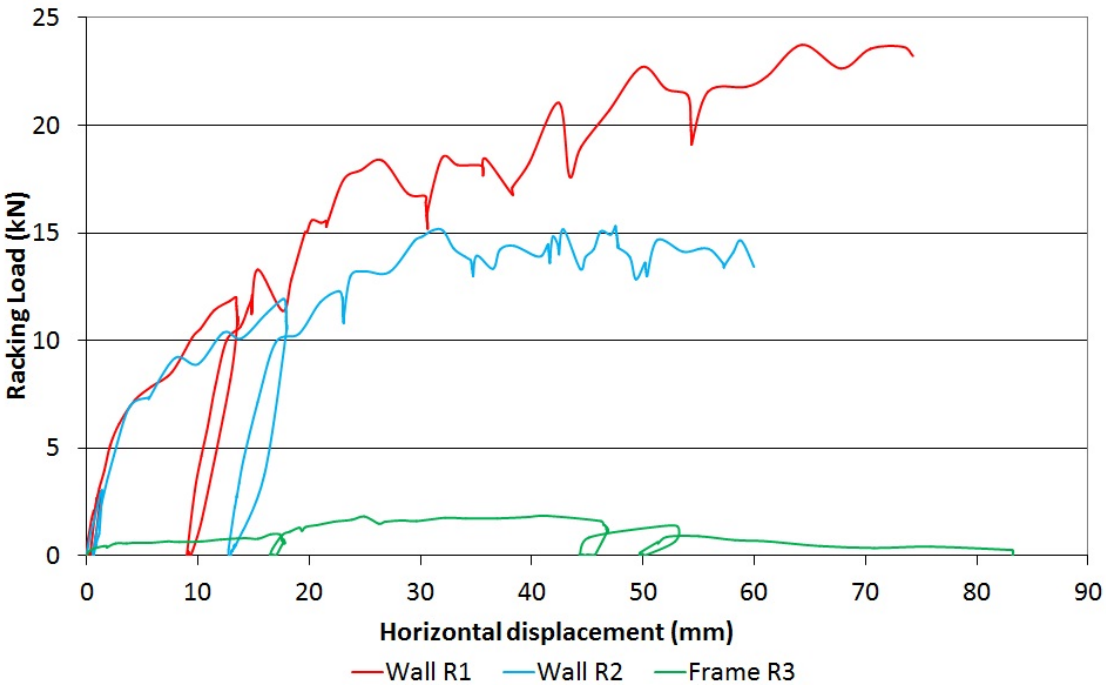

Figure 7.5 Racking results for Walls R1, R2 and Frame R3

From Figure 7.5 it is clear that the stiffness and strength of the timber only Frame R3 was very low with a maximum racking load of 1.5kN (0.6kN/m) at over 30mm horizontal displacement. This shows that the nailed connections in the studwork framing offer very minimal resistance to in plane racking loading.

Figure 7.5 shows that Walls R1 and R2 were considerably stronger and stiffer than Frame R3. Initially the testing regime from BS EN 594 (1996) was not followed and a racking load was applied to both Walls R1 and R2 without vertical loads applied to the studs. A racking load of 3kN was applied to Wall R1. The stiffness was 0.71kN/mm and once the load had been removed the residual deflection was 0.5mm. A racking load of 2.32kN was applied to Wall R2 which resulted in a horizontal deflection of 4.8mm which is equivalent to the height of the wall panel divided by 500. The loading was

stopped at this deflection as the wall panel needed to remain undamaged so that it could be tested with vertical loads applied. The stiffness of Wall R2 was 0.56kN/mm.

With the vertical loads applied (5kN per stud) Wall R1 was loaded to 3kN, which was assumed to be $0.1F_{max,\ est}$, the deflection was 1.1mm and the stiffness was 2.64kN/mm which is over three times stiffer than without the vertical pre-compression. Once the load was removed the residual horizontal displacement was 0.3mm. When reloaded the panel performed with a similar stiffness until a horizontal load of 7.5kN when the stiffness reduced. The reduction in stiffness corresponded with increased lift of the hemp-lime at the bottom corner of the panel below the horizontal load and the joint between the stud and the sole plate beginning to separate. With a racking load of 12kN ($0.4F_{max,\ est}$) applied the deflection was 13.3mm. The separation of the studwork joint and lifting of the hemp-lime is shown in Figure 7.6. After unloading from the 12kN load Wall 4 had a residual deflection of 9.0mm (h/267) which is outside the serviceability limits of h/500. The wall was reloaded and testing was continued.

Figure 7.6 Wall R1 showing hemp-lime lifting from base

Testing was stopped when the limits of the test equipment were reached at a horizontal deflection of 80mm. By this point the panel was considered to have failed as the leading stud (stud closest to horizontal load application) had separated from the sole plate.

As with Wall R1, once the vertical loads were applied to Wall R2 the stiffness increased significantly and with a 3kN horizontal load applied the deflection was 1.4mm and the

stiffness was 2.22kN/mm, both slightly lower than on Wall R1. When the panel was unloaded the residual horizontal deflection was 0.6mm which equates to h/4000. When reloaded the panel performed with a similar stiffness until a horizontal load of 6.5kN when the stiffness reduced to 0.37kN/mm. As with Wall R1 the reduction in stiffness corresponded with increased lift of the hemp-lime at the bottom corner of the panel and the joint between the stud and the sole plate beginning to separate. At a load of 9kN a diagonal shear crack appeared in the hemp-lime (Figure 7.7). It is likely that the tendency of the hemp-lime to crack is increased in Wall R2, due to the horizontal rails within the hemp-lime, as the rails exert a vertical lifting force on the hemp-lime as the studwork frame lifts. The cracking of the hemp-lime it is likely to account for the lower stiffness of Wall R2.

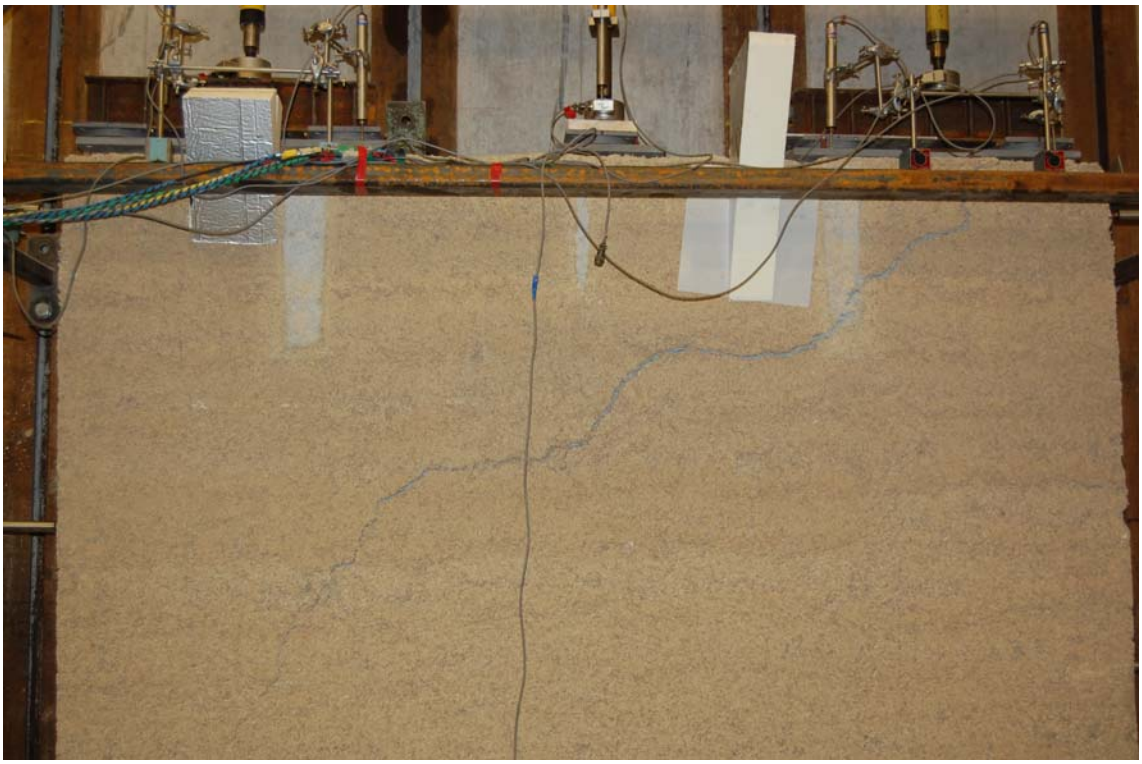

Figure 7.7 Wall R2 showing diagonal cracking

The pattern of cracking on Wall R2 is typical in racking tests with diagonal tension cracks. Once the 12kN horizontal load had been reached and the load removed the residual horizontal deflection was significant at 12.7mm. As the panel was reloaded the width of the diagonal crack increased as the horizontal rails between the studs lifted the hemp-lime. The horizontal load stayed roughly constant at 15kN once a deflection of 30mm was reached and more cracks formed in the hemp-lime (Figure 7.8). The test was

stopped before a deflection of 100mm was reached as the panel was considered to have failed.

Figure 7.8 Wall R2 showing cracking following testing

Table 7.1 shows the racking stiffness and racking strength of both walls calculated following the methods set out in BS EN 594 (1996)

Table 7.1 Racking stiffness and strength of Walls R1 and R2

	Racking stiffness (kN/mm deflection)	**Racking strength (kN/m length of wall)**
Wall R1	1.27	10.62
Wall R2	0.79	6.74

The racking strength is the highest load achieved by the panel during the test. Therefore these racking strength values were achieved at very high displacements of over 70mm for Wall R1 and over 40mm for Wall R2. The racking load sustained at serviceability deflections is maybe a more meaningful value for establishing if this type of wall panel is sufficient to resist the potential loads. At a horizontal deflection of h/500 (4.8mm) Wall R1 sustained a load of 3.02kN/m and Wall R2 sustained a load of 2.89kN/m.

The design racking resistance for both walls has been calculated using the methods set out in BS 5268-6.1 (1996) Section 5. The design racking resistance, R_b, of Wall R1 is 1.43kN/m and of Wall R2 is 0.89kN/m. These values include factors of safety as set out in BS 5268-6.1 (1996). Comparing these values with those given in Table 2 of BS 5268 (1996) for the design racking resistance of common sheathing materials Wall R1 has a greater racking resistance than Category 2 materials (0.9kN/m) and Wall R2 has a greater racking resistance than Category 3 materials (0.6kN/m) and a very similar racking resistance to Category 2.

There are two main reasons why Wall R2 did not perform as well as Wall R1. As already noted the horizontal rails give a better connection between the hemp-lime and the studs when subjected to lifting forces and therefore the hemp-lime was lifted along with the studwork frame under the horizontal racking load causing the hemp-lime to crack. In addition the hemp-lime in Wall R2 had not set properly and appeared 'floury' (Figure 7.9).

Figure 7.9 'Floury' hemp-lime

Only the outer 25mm to 30mm had set and the inner parts of the wall had very little cohesion and as a result shear cracks would have developed at lower loads than if the normal setting had occurred. However the initial stiffness of the wall appears to have

been unaffected by this as it is the same as Wall R1 which had well set hemp-lime. This is discussed in more detail in Chapter 5. The performance of Walls R1 and R2 could be enhanced if the joints on the leading stud were strengthened with screws to prevent pull out of the stud from the sole or header plates. Additionally improving the day joints in the hemp-lime may also enhance the performance of the walls. In Wall R2 cracking developed along these joints and in Wall R1 while there was no noticeable cracking during testing, upon de-construction these joints appeared as weak planes and it was significantly easier to break apart the hemp-lime at these locations.

As with the compression test wall panels specimens of timber studs and hemp-lime were taken from Walls R1 and R2. The moisture content of the timber is shown in Table 7.2.

Table 7.2 Moisture content of studs in Walls R1 and R2

Wall	**Stud**	**Average Moisture content %**	**Position within hemp-lime**
R1	Left	15.9	Centre
R1	Centre Left	21.7	Centre
R1	Centre	21.3	Centre
R1	Centre Right	21.6	Centre
R1	Right	14.7	Centre
R2	Left	15.5	Edge
R2	Centre Left	19.2	Edge
R2	Centre	18.8	Edge
R2	Centre Right	19.0	Edge
R2	Right	15.0	Edge

There is a 7% difference between the maximum and minimum moisture contents of the timber studs. This is due to their position with the walls. On Wall R2 the studs were all on the edge of the hemp-lime. Therefore the centre studs had one face exposed and the left and right studs had two faces exposed and the difference in moisture content as a result of this is clear with the edge studs roughly 4% drier than the centre ones. The difference on Wall R1 is even greater as the centre studs were completely surrounded and the left and right studs had one face exposed resulting in roughly a 6% difference in moisture content. On the centre studs from Wall R2 there was a difference of 4% to 5%

in moisture content between the exposed face and the inner face that was against the hemp-lime. Despite the high moisture content there was no evidence of decay on the studs. This is likely to be due to the alkaline environment created by the binder.

Table 7.3 shows the hemp-lime moisture content for Walls R1 and R2. The moisture content was measured at the base, middle and top of the walls on both the outer and inner areas by weighing the specimens of hemp-lime before and after oven drying.

Table 7.3 Hemp-lime moisture content Walls R1 and R2

Wall	Moisture Content (%)			Dry density (kg/m^3)
	Inner	Outer	Average	
R1 – Base	25.7	19.9	22.8	282.4
R1 – Middle	25.0	17.4	21.2	249.4
R1 – Top	18.3	10.4	14.3	275.6
R1 - Average	**23.0**	**15.9**	**19.5**	**269.1**
R2 – Base	26.4	16.0	21.2	298.7
R2 – Middle 1	26.0	17.0	21.5	295.7
R2 – Middle 2	21.9	11.3	16.6	-
R2 - Average	**24.8**	**14.8**	**19.8**	**297.2**

As with the compression test wall panels all of the inner areas of the walls had a higher moisture content than the outer areas and the moisture content of the hemp-lime increased from the top of the wall to the bottom. The average moisture content of both the walls is just below 20%, which is similar to the average moisture content of the timber studs. Specimens of hemp-lime from each wall were tested in compression in order to establish the compressive strength. The results from this are shown in Table 7.4.

Table 7.4 Walls R1 and R2 hemp-lime compressive strength

Wall	Specimen location	b (mm)	d (mm)	h (mm)	Compressive strength σ_c (N/mm^2)
R1	Base	300	300	410	0.31
R1	Middle	300	300	330	0.28
R1	Top	300	300	400	0.39
R2	Base	300	300	390	0.16
R2	Middle 1	300	305	360	0.23
R2	Middle 2	290	300	450	0.31
Average					**0.28**

The average compressive strength of the hemp-lime in Walls R1 and R2 is similar to the compressive strength of the hemp-lime in Walls C2 and C3. They were constructed at the same time using the same mixing procedure and therefore they should be similar. The base and one of the middle prisms from Wall R2 are of a lower compressive strength than the others taken from Walls R1 and R2. This is due to the 'flouring' that was present in that wall. Also it was not possible to take a prism specimen from the top of Walls R2 due to the 'flouring' resulting in the hemp-lime being very fragile. The prisms compressive strengths compare with the material properties cylinder strengths in the same way as Walls C2 and C3. The average prism compressive strength is slightly lower than the average cylinder strength. As Walls R1 and R2 were constructed at the same time as Walls C2 and C3 this is to be expected.

7.3.2 Walls R4 and R5 (LS2)

Wall R4 was constructed without Multi-pro XS sheathing boards. During transportation from the construction and drying facility to the testing laboratories Wall R4 was accidentally knocked over. Once at the structures laboratory it was returned to its upright position, however considerable damage had occurred to the hemp-lime. Figure 7.10 details the damage to the wall showing the crack locations and areas where hemp-lime had fallen away from the wall.

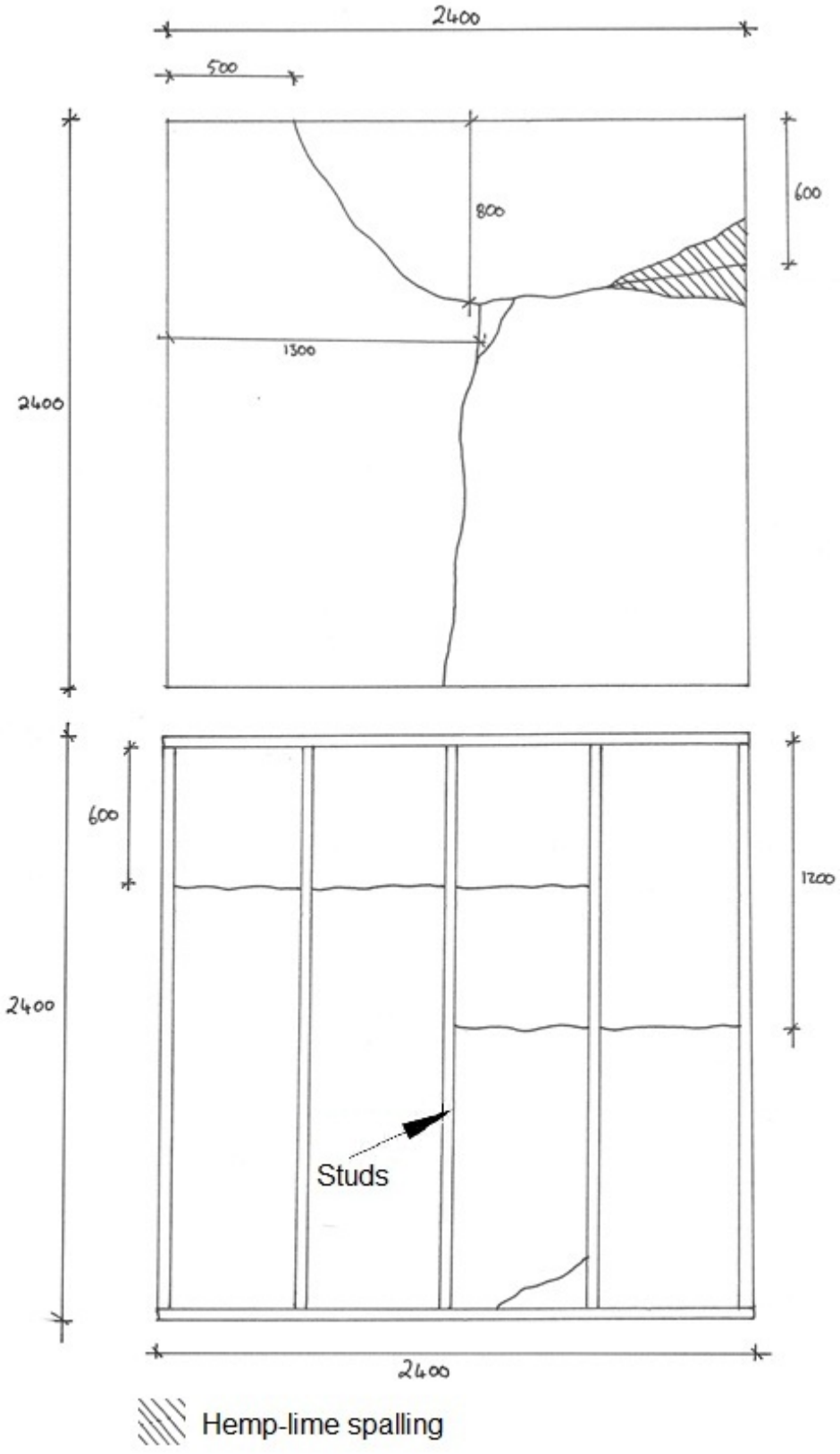

Figure 7.10 Damage to Wall R4 before testing (all dimensions in mm)

Wall R4 was constructed without Multi-pro sheathing board. In order to gain as much information as possible from each test panel Wall R4 had Multi-pro XS sheathing board fixed to one face and was initially loaded with the stabilising cycle (up to $0.1F_{max,\ est}$ =

3kN) and then up to 5kN. From the results of the racking tests on Walls R1 and R2 (LS1) a racking load of 5kN can be considered to be within the elastic range of the wall panels and would not cause permanent damage. Following this the Multi-pro XS board was removed from Wall R4 and the panel was tested following the procedure set out in BS EN 594 (1996) with $F_{max, est}$ = 30kN.

Wall R5 was constructed with Multi-pro XS sheathing board fixed to the studwork. This wall panel was tested in a similar manner to Wall R4, but in this case the Multi-pro XS board was removed while the wall was initially loaded with the stabilising cycle (up to $0.1F_{max, est}$ = 3kN) and then up to 5kN. Following this the Multi-pro XS board was re-fixed onto the studwork frame and the wall was tested again following the procedure set out above. Figure 7.11 shows the results for both walls.

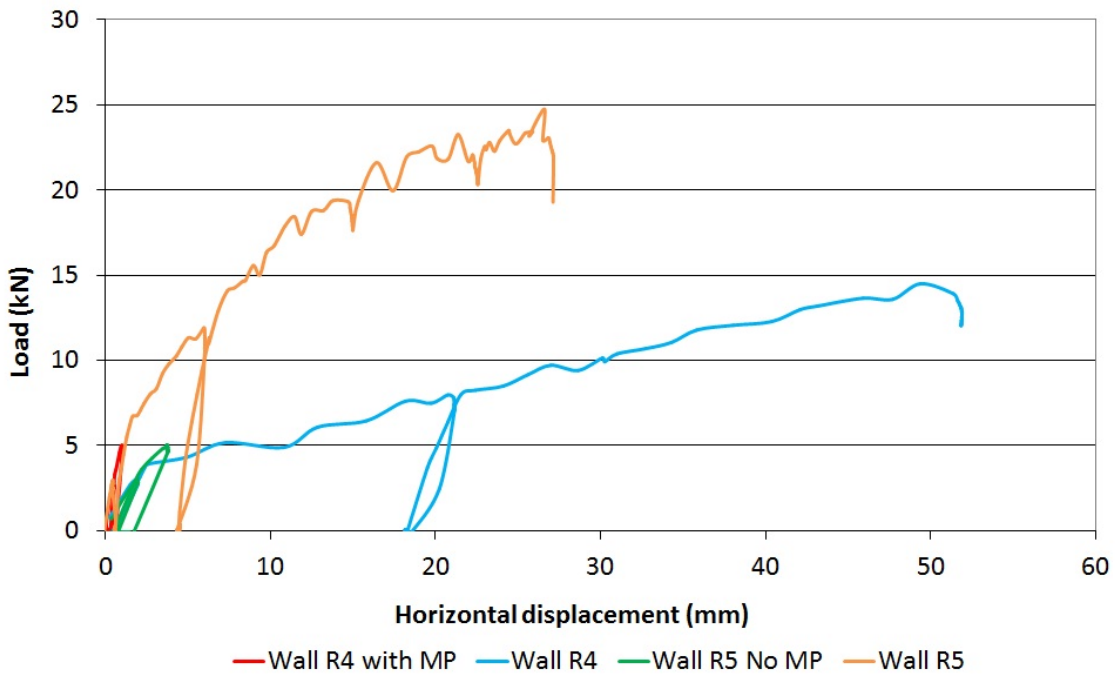

Figure 7.11 Racking results for Walls R4 and R5

With the Multi-pro XS attached Wall R4 had a horizontal deflection of 1.0mm with a raking load of 5kN. This corresponds to a stiffness of 5.18kN/mm. With the Multi-pro removed the deflection at 5kN racking load was 6.8mm which gives a stiffness of 0.78kN/mm. Wall R5 displayed similar results with a deflection at 5kN with Multi-pro board of 1.2mm and stiffness of 4.16kN/mm. Without Multi-pro the deflection at 5kN was 3.4mm with a stiffness of 1.48kN/m. While this is stiffer than Wall R4 without Multi-pro at 5kN, both Walls had the same stiffness up to a racking load of 4kN when

the stiffness of Wall R4 reduces significantly. This reduction is due to the damage sustained during transport.

Wall R4 was tested to failure without Multi-pro and Wall R5 was tested to failure with Multi-pro.

Figure 7.12 Wall R4 showing cracking following testing

Figure 7.12 shows the cracking pattern following testing to failure of Wall R4. These cracks are a combination of diagonal cracks that are usually associated with racking loads and cracks that have occurred at weakened points caused by the dropping of the panel. The cracks started to form and open up at a load of around 4kN where the stiffness of the panel significantly reduced. As the load increased from this point a significant permanent deformation was introduced to the panel. After the panel had been stressed with a racking load of 8kN the residual horizontal displacement at the top corner of the panel opposite the load application was 18.2mm. The testing was stopped when the panel was deemed to have failed due to the formation of the cracks. The leading stud joints, which had been strengthened, compared to those in Walls R1 and R2, had not failed however.

As shown in Figure 7.11 Wall R5 with no Multi-pro had the same initial stiffness as Wall R4 and displayed a less significant change in stiffness at around 4kN racking load. Wall R4 had numerous cracks in the hemp-lime as a result of it being accidentally knocked over which account for the change in stiffness at 4kN as the cracks began to open up further. These cracks were not present in Wall R5 and therefore the stiffness is constant. Wall R5 was only loaded to 5kN and therefore the stiffness beyond this point is unknown.

When tested to failure Wall R5 showed no cracking. Wall R5 was significantly stiffer than Wall R4 through all stages of testing. During testing the base of the hemp-lime and footer railed began to lift from the base as shown in Figure 7.13. This corresponds to the change in stiffness at a racking load of 7.5kN. While there was some uplift of the hemp-lime and footer rail, the joints between the leading stud and header and footer rails did not separate. This is due to the improved connection. Once the racking load had reached 12kN it was removed and the residual displacement was recorded as 4.5mm (h/533). This is within the serviceability limit for deflection of 4.8mm (h/500).

Figure 7.13 Wall R5 showing hemp-lime and timber lifting from base

When Wall R4 was loaded with Multi-pro board its initial stiffness was very slightly higher than that of Wall R5. This result shows that the Multi-pro board significantly

contributed to their stiffness as the hemp-lime in Wall R4 had been damaged prior to testing. The higher stiffness when compared to Wall R5 is likely to be due to the fact that Wall R4 was tested immediately after the Multi-pro board was attached, whereas Wall R5 was constructed and transported with the board attached which may have caused the screws to become slightly loose in their holes. As the displacements increased during testing the heads of screws through the Multi-pro into the studs in Wall R5 pulled through (Figure 7.14) and the boards sheared against the studs. Upon deconstruction of the wall some of the screws showed large deformations (Figure 7.15). Testing was stopped when the limits of the test equipment were reached.

Figure 7.14 Screws pulling through Multi-pro

Figure 7.15 Deformed screw after testing

Table 7.5 shows the racking stiffness and racking strength of both Walls calculated following the methods set out in BS EN 594 (1996).

Table 7.5 Racking stiffness and strength of Walls R4 and R5

	Racking stiffness (N/mm)	**Racking strength (kN/m)**
Wall R4	259	6.08
Wall R5	747	9.69

The racking strength is the highest load achieved by the panel during the test. Therefore, these racking strength values were achieved at very high displacements of over 50mm for Wall R4 and over 30mm for Wall R5. A serviceability deflection limit might be more appropriate for determining the maximum allowable racking load for this type of wall panel. An in-plane horizontal deflection limit of the height of the panel divided by 500 (h/500) could be applied. This deflection limit prevents damage to brittle materials such as renders and plaster that may be applied to the walls in the finished state. At a horizontal deflection of h/500 (4.8mm) Wall R4 sustained a load of 1.79kN/m and Wall R5 sustained a load of 4.04kN/m. Both of these racking loads are significantly lower than the maximum racking load achieved during the tests and therefore the deflection of the wall panels must be considered during the defining of design criteria.

The design racking resistance for both walls has been calculated using the methods set out in BS 5268-6.1 (1996) Section 5. The design racking resistance, R_b, of Wall R4 is 1.14kN/m and of Wall R5 is 1.94kN/m. These values include factors of safety as set out in BS 5268-6.1 (1996). Comparing these values with those given in Table 2 of BS 5268 (1996) for the design racking resistance of common sheathing materials Wall R5 has a greater racking resistance than Category 1 materials (1.68kN/m) and Wall R4 has a greater racking resistance than Category 2 materials (0.90kN/m).

Specimens of timber studs and hemp-lime were taken from Walls R1 and R2. The moisture content of the timber is shown in Table 7.6. The specimens of timber were weighed before and after being dried in an oven.

Table 7.6 Moisture content of studs in Walls R4 and R5

Wall	Stud	Average Moisture content %	Position within hemp-lime
R4	Footer	14.5	Edge
R4	Base of centre stud	15.0	Edge
R4	Middle of centre stud	13.8	Edge
R5	Footer	21.1	Edge with Multi-pro
R5	Base of centre stud	21.7	Edge with Multi-pro
R5	Middle of centre stud	20.6	Edge with Multi-pro

The average moisture content of the studs in Wall R4 was 14.4% and the average moisture content of the studs in Wall R5 was 21.3%. The moisture content of the studs in the two walls varies by 6.9%. Both walls were cast using the same mix proportions, at the same time and were dried together in the same conditions. The difference in average moisture content of the studs is due to the presence of Multi-pro sheathing board on Wall R5. The sheathing board is breathable (Resistant, 2012), however the moisture content of the studs clearly show that it does not allow as much moisture to leave the hemp-lime and timber as when there is no sheathing board present.

Table 7.7 shows the hemp-lime moisture content for Walls R4 and R5. The moisture content was measured at the base, middle and top of the walls on both the outer and inner areas by weighing the specimens of hemp-lime before and after oven drying.

Table 7.7 Hemp-lime moisture content Walls R4 and R5

Wall	Moisture Content (%)			Dry density (kg/m^3)
	Inner	Outer	Average	
R4 – Base	10.3	7.6	9.0	346.6
R4 – Middle	23.6	8.8	16.2	304.6
R4 – Top	7.6	7.7	7.7	292.4
R4 - Average	**13.8**	**8.1**	**11.0**	**314.5**
R5 – Base	24.9	9.5	17.2	268.8
R5 – Middle	22.1	12.2	17.2	270.3
R5 – Top	18.3	9.3	13.8	306.8
R5 - Average	**21.8**	**10.3**	**16.1**	**281.9**

There is a similar trend in the moisture content of the hemp-lime with Wall R4 having a lower average of 13.8% compared to the average in Wall R5 of 21.8%. This again is due to the sheathing board as the hemp-lime in Wall R5 is effectively drying from one face rather than from both. There is no definitive reason why the moisture content of the middle specimen of hemp-lime from Wall R4 was much higher moisture content than the other specimens from the wall.

Specimens of hemp-lime from each wall were tested in compression in order to establish the compressive strength. The results from this are shown in Table 7.8.

Table 7.8 Walls R4 and R5 hemp-lime compressive strength

Wall	Specimen location	b (mm)	d (mm)	h (mm)	Compressive strength σ_c (N/mm^2)
R4	Base	155	152	316	0.30
R4	Middle	164	151	297	0.23
R4	Top	171	166	309	0.16
R5	Base	174	167	304	0.21
R5	Middle	153	158	300	0.29
R5	Top	153	173	311	0.27
Average					**0.24**

As with the other walls from the Large Scale 2 series of testing the compressive strength is similar. The top of Wall R4 has a slightly lower compressive strength, however, this is due to the variations in the material as the hemp-lime in Wall R4 was of good quality. The prism compressive strengths compare well with the material properties cylinder strengths, in the same way as Walls C4 and C5; the average prism compressive strength was slightly lower than the average cylinder strength. As Walls R4 and R5 were constructed at the same time as Walls C4 and C5 this is to be expected.

The prisms of hemp-lime were sprayed with phenolphthalein solution in order to assess the progress of carbonation. The hemp-lime had carbonated 25mm to 30mm from the exposed faces of the walls. However on Wall R5 the hemp-lime had not carbonated behind the Multi-pro sheathing board. This result, as with the moisture content results,

also indicates that the sheathing board is preventing movement of air into the hemp-lime to allow drying and carbonation.

7.4 Discussion

The results from Walls R1, R2, R4 and R5 can be compared with the results from previous testing undertaken by CERAM on behalf of Lime Technology Ltd (CERAM, 2009b, a). There has been some discussion that the calculated design racking resistance, R_b, from these tests is incorrect. R_b has been recalculated from CERAM's results and these are the resistances presented here. Both walls tested by CERAM (2009b, a) were constructed with 200mm by 38mm C16 timber studs fixed together with nails. One wall was filled with hemp-lime (CERAM, 2009a), while the other wall had Multi-pro sheathing board fixed to the frame (CERAM, 2009b). The design racking resistance R_b for the wall with hemp-lime was 1.30kN/m and for the wall with Multi-pro was 1.64kN/m.

The design racking resistance of Wall R1 (1.43kN/m) was slightly higher than the design racking resistance than the studwork frame tested with 200mm hemp-lime infill (1.30kN/m), whereas Wall R2 (0.89kN/m) was lower. The wall tested by CERAM (2009a) was of a slightly different design to Wall R1, yet they have similar design racking resistances. Wall R1 had narrower studs, 89mm compared with 200mm, but had thicker hemp-lime, 300mm compared with 200mm. The much lower design racking resistance of Wall R2 could be due to two causes. Firstly the hemp-lime was of poor quality due to 'flouring'. While hemp-lime has low strength there is some cohesion between the shiv particles when it is correctly set. This was not the case with the hemp-lime that was displaying 'flouring'. Secondly Wall R2 had horizontal rails which, as previously noted, may have caused increased cracking within the hemp-lime at extreme displacements.

Wall R4 had a design racking resistance of 1.14kN/m, and Wall R5 had a design racking resistance of 1.94kN/m. The strength and stiffness of Wall R4 was affected by the damage to the panel. However Wall R4 still has a higher design racking resistance than Wall R2 which was of a similar design. The only design difference was the improved connection between the leading stud and the header and footer rails. This

prevented the joints opening and may have contributed to the improved performance. Unfortunately due to the 'flouring' in Wall R2 and the damage to Wall R4 it is not possible to draw any finite conclusions. This shows that the presence of hemp-lime and an improved leading stud connection has improved the performance of the wall system. Wall R5 had the greatest strength of the walls tested in this study and also had a higher design racking resistance than the two walls tested by CERAM (2009a, b). Wall R5 had improved leading stud connections, Multi-pro sheathing board and hemp-lime and as a result should have the highest racking resistance. The wall tested by CERAM (2009b) with Multi-pro sheathing board has a lower deign racking resistance because the connection to the leading stud failed. This was prevented in Wall R5 by the improved screwed connections. Additionally the hemp-lime will have improved the performance of Wall R5. The exact construction process, wall build up and hemp-lime properties of the CERAM (2009a, b) test panels are not known and therefore it is difficult to make any further comparisons.

The design racking resistance of Walls R1, R2, R4 and R5 can be compared to the basic racking resistances given in Table 2 of BS 5268-6.1 (1996) for standard constructions. Category 2 materials (12.5mm bitumen impregnated insulation board) have a basic racking resistance of 0.90kN/m while Category 1 materials (9.5 mm plywood, 12.0 mm particleboard, 6.0 mm tempered hardboard, 9.0 mm) have a basic racking resistance of 1.68kN/m. From this Walls R1 and R4 fall into Category 2 with Wall R2 only 0.01kN/m lower than Category 2 and Wall R5 has a design racking resistance higher than Category 1. A domestic scale building, with a 6m by 6m plan and 5.5m high elevations, in a typical location in the UK would be subjected to less than 1.0kN/m^2 wind load. Assuming the load is shared between the two parallel external walls and one internal shear wall the in plane racking load per wall would be less than 1.9kN/m. Therefore with improved leading stud connections, Multi-pro boarding and hemp-lime, as in Wall R5, the racking resistance of composite timber studwork framing with hemp-lime is sufficient for domestic scale buildings.

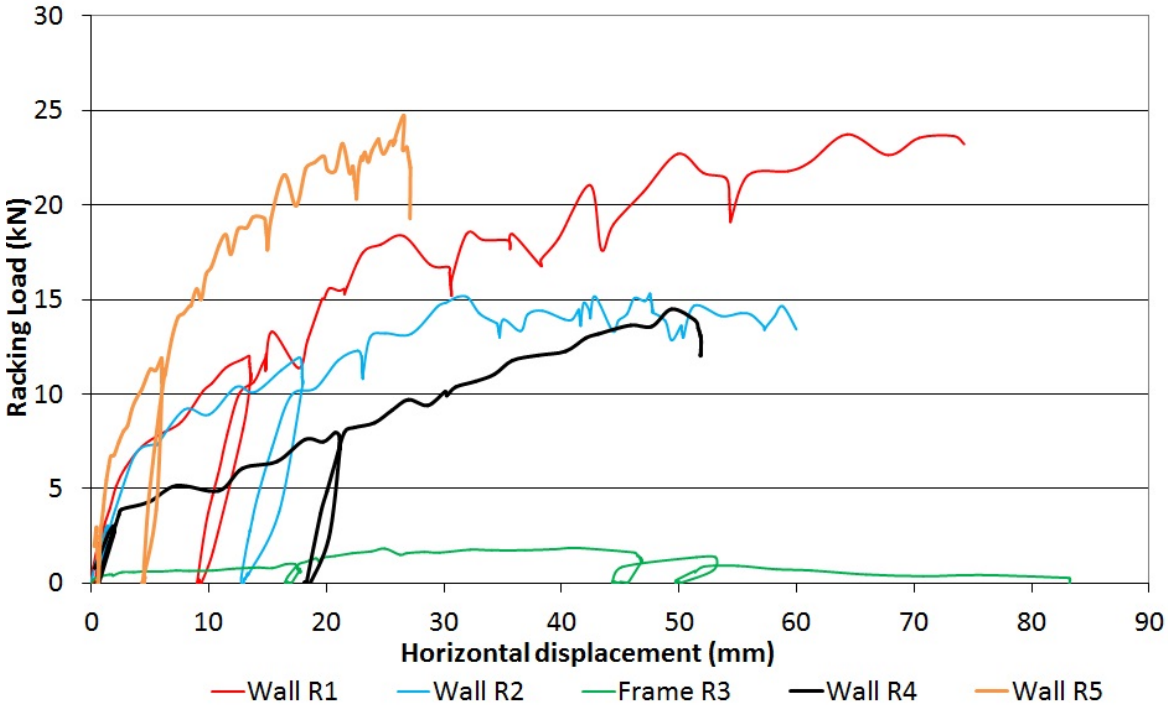

Figure 7.16 Racking test results for Walls R1, R2, R4, R5 and Frame R3

Figure 7.16 shows the results from all of the racking tests undertaken in this study. It can be seen that Wall R5 performed the best with the highest stiffness throughout the test as well as the highest racking load achieved. Wall R5 should be the strongest and stiffest due to the improved leading stud connection and Multi-pro sheathing board. Walls R1 and R4 both have similar stiffness during the second phase of testing when the stiffness had reduced. These walls were of similar construction with the only differences being that Wall R1 had the frame in the centre whereas Wall R4 had the frame on the edge and R4 had improved leading stud connections. Wall R4 should have performed better than Wall R1 due to the improved connection, however the lack of performance increase is likely to be due to the damage sustained by the panel when it was dropped during transport. There were large cracks present in the hemp-lime and as a result the stiffness reduced at a lower load than the other three walls. Despite the 'flouring' in Wall R2 and the dropping of Wall R4 all of the walls with hemp-lime were significantly stronger and stiffer than Frame R3.

In all of the tests the racking load did not suddenly drop after the peak load was reached and all of the walls with hemp-lime displayed some ductility. The hemp-lime helps to provide this ductility along with the multi-pro sheathing board on Wall R5. Hemp-lime is a ductile material under compressive loads when tested alone as seen in the materials

properties tests in Chapter 3. When it is being loaded by the studs during racking loading it also behaves in this way providing post peak load ductility to the wall panels. The sheathing board fulfils a similar function as the screws continue to pull through the board and deform as the overall wall deflections increase. At extreme deflections where the screws are caused to pull through the edges of the boards this ductility may decrease.

When hemp-lime and studwork composite walling is used for construction the outer surface needs protecting from the weather. This can either be provided by rain screen cladding or render. When render is used an enhancement to the racking performance may occur. Renders are commonly used within straw bale construction to increase the strength of load bearing straw bale walls and the same could be considered when using hemp-lime. There may be a small increase in racking performance when a render is used, but the studs transfer the racking loads to the centre of the hemp-lime mass or to the other face. Deflection in the hemp-lime across the depth of the wall is unlikely to allow transfer of the entire racking load into the render skin and therefore the enhancement in performance may be limited. Additionally when a render is used the serviceability deflection of the wall will have to be carefully considered to avoid cracking of the render as previously mentioned.

Figure 7.17 shows the predicted results for Walls R1 to R5 and the actual results from the experimental testing. The predicted and actual results for Wall R1 generally correlate well throughout the entire range of displacements and changing stiffness. The main difference is the stiffness between loads of 7.5kN and 12.5kN. From analysis of the experimental and theoretical performance the stiffness at this load is derived from the stiffness of the hemp-lime. Therefore the method used to predict the stiffness of the hemp-lime at different levels of displacement may need to be adjusted. Overall the results show that treating the studs as cantilevers on elastic foundations and considering the changing stiffness of the hemp-lime and the leading stud joint failure predicts the performance well. The strength of the panel was not predicted, however this is not considered to be as critical as the stiffness because the peak load occurs at very large displacements. The peak load may not have been reached during the testing of Wall R1 because the test was stopped as the displacement reached the limits of the testing equipment.

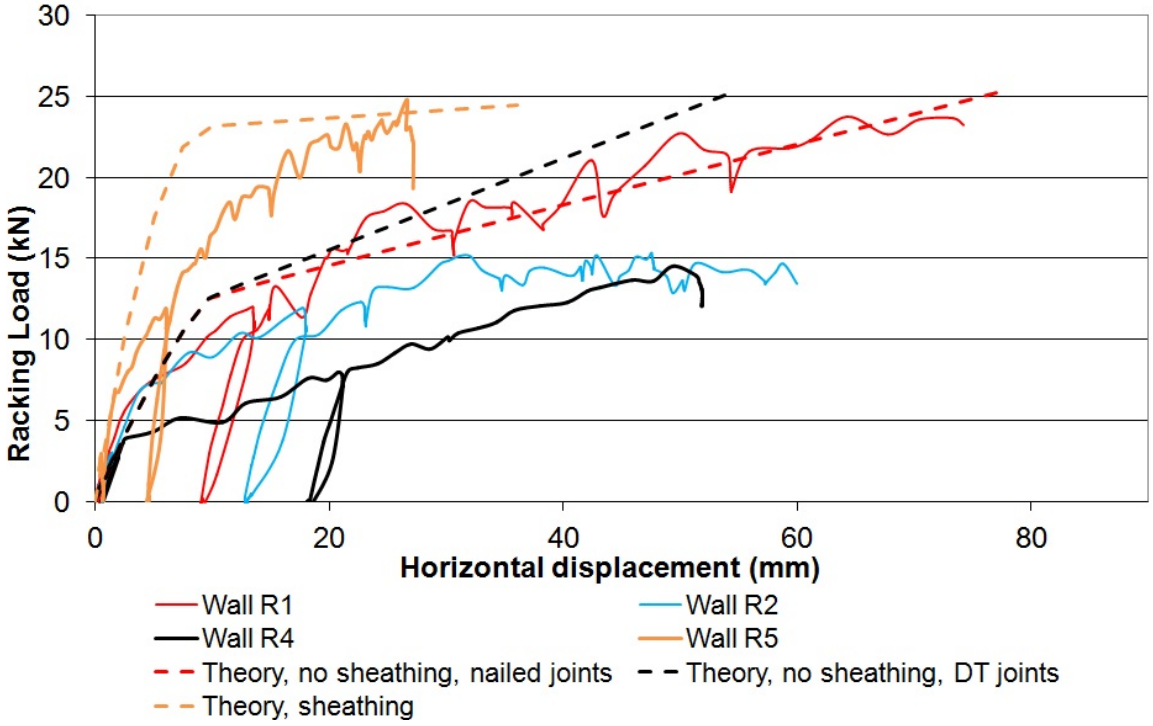

Figure 7.17 In-plane racking actual and predicted results

Wall R2 also shows good correlation to the predicted results until a load of 7.5kN is reached. At this point the stiffness of Wall R2 reduces. The drop in stiffness is associated with cracking of the hemp-lime which was largely caused by the flouring phenomenon which caused the weakness. If this had not been present then the results would most likely have been similar to Wall R1. The compressive strength of the hemp-lime in Wall R2 was only 70% of the hemp-lime in Wall R1 which was 85% of the compressive strength used in the theoretical analysis. The analysis in Chapter 4 showed how crucial the stiffness of the hemp-lime is to the performance of the composite wall construction under racking loads. Assuming the stiffness was also reduced by the same amount as the compressive strength the predicted results are actually as shown in Figure 7.18. The predicted results for Walls R1 and R2 have been calculated using the average vertical load applied during the duration of the test. For Wall R1 this was 4.35kN and for Wall R2 it was 3.78kN.

As shown in Figure 7.18 the correlation in results is much closer when the actual stiffness of the hemp-lime in the walls is used to predict the results rather than the average material properties shown in Chapter 3. Also shown in Figure 7.18 is the theoretical prediction when the 5% characteristic stiffness of the hemp-lime is used rather than the average. When the characteristic properties are used the stiffness is

similar to the actual experimental results of Wall R1. The only point where it is higher is at around 12.5kN before the leading stud joint stiffness is considered in the theoretical calculations. During design this load may need to be reduced by a suitable factor to account for the potential variation in vertical load or reduced to zero for the worst case. It is also slightly higher following this which is largely due to the trend line fitted to the 5% characteristic properties in Chapter 4. Further work may be required to find a better fit. These results confirm that the theory set out in Chapter 4 is suitable for this type of construction if the actual wall material properties or the characteristic properties are used.

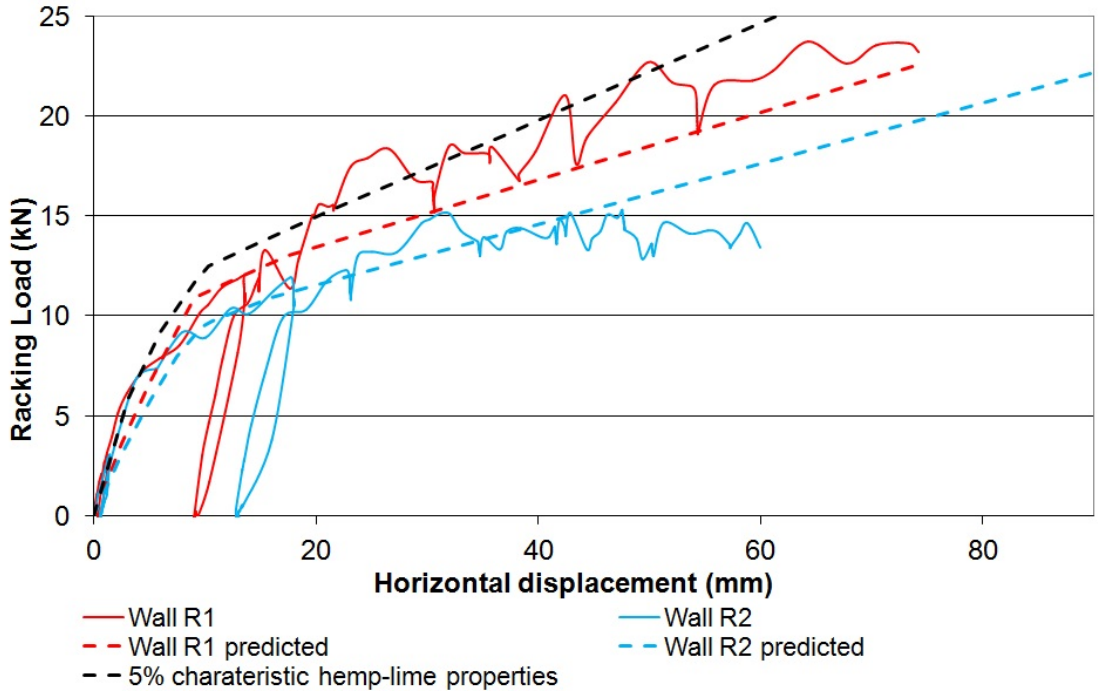

Figure 7.18 Adjusted theoretical predictions

The initial stiffness of Wall R4 and the theoretical prediction match well however the two results soon deviate as the stiffness of Wall R4 reduces. The reduction in stiffness is a result of the wall panel being accidentally dropped during transportation. If Wall R4 had not been dropped similar results to Wall R1 should have been seen but with a smaller reduction in stiffness at 12.5kN.

With Wall R5 the predicted stiffness is greater than the actual stiffness throughout the entire loading range; however the peak load is very similar at 24.5kN compared with 24.8kN for Wall R5. When Wall R5 was tested the sheathing board and the studwork frame moved differentially and the screws pulled through the sheathing. In the areas

where the screw movement was towards the edge of the sheathing boards the screws moved in such a way as to push through the edge of the sheathing as shown in Figure 7.14. This will have reduced the stiffness of the connection and may be one reason why the theoretical stiffness is higher. Additionally the panel had been transported prior to test and the sheathing had been removed and refitted. This could have caused the connections to be looser fitting causing reduced stiffness. Figure 7.19 shows the predicted results when the 5% characteristic sheathing connection stiffness is used.

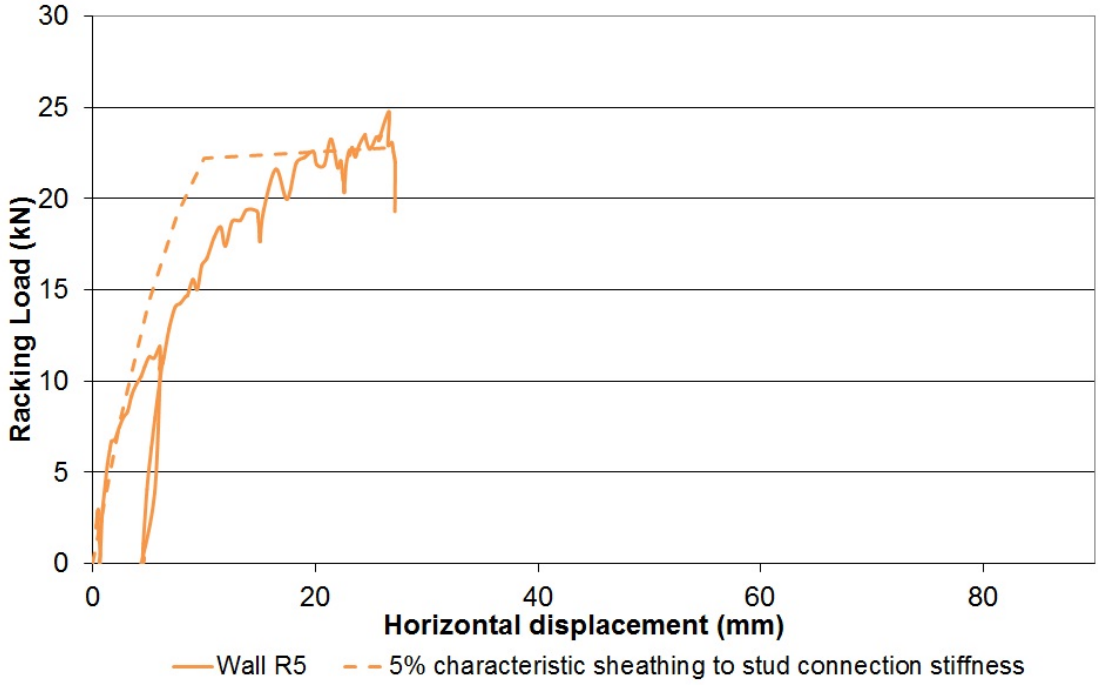

Figure 7.19 Wall R5 characteristic theoretical predictions

Using the characteristic stiffness of the connections improves the correlation; however the stiffness between 7.5kN and 22.5kN is still too high. This difference is still due to the screws pulling through the edges of the sheathing board. In order to improve the accuracy of the predictions in this load range further connection testing may be required.

7.5 Conclusions

The racking tests on Walls R1 and R2 and Frame R3 clearly showed that hemp-lime at a dry density of 275kg/m^2 increases the racking resistance of timber studwork frames. These tests also highlighted the failure modes for Walls R1 and R2 and the weakness of

their stud to header and footer connections when subjected to in-plane racking loads. This allowed the design of Walls R4 and R5 to target these areas for improved performance.

Walls R4 and R5 showed that the improved leading stud connections prevented failure by opening of the leading stud joints. This contributed to improving the overall performance of the panels by reducing rotation caused by the opening of the joints. The racking stiffness was improved significantly by the presence of Multi-pro boarding and as a result the racking stiffness of Wall R5 is higher than the wall constructions detailed in Category 1 in BS 5268 part 6.1.

The theoretical predictions correlate well with the actual test results when only hemp-lime and studwork framing are used as long as the hemp-lime and studwork frames are in a good condition. When there is a sheathing board present the correlation is not as good and further independent work is required to find a more accurate value for the stiffness of the sheathing to stud connections.

8 Experimental Study: Bending performance of wall panels

8.1 Introduction

Composite hemp-lime and timber studwork walling specimens and a hemp-lime only specimen were tested in out-of-plane bending in order to establish their capacity and the nature of composite action between the wall elements. Four specimens were tested over two laboratory test series.

8.2 Methodology and test set up

In the first series of testing one hemp-lime only wall panel (Wall B1) and one hemp-lime wall panel with a timber studwork frame cast into the centre of the hemp-lime (Wall B2) were studied. Both walls had both faces finished with lime based renders. In the second series of testing two identical wall panels were tested (Walls B3 and B4). Walls B3 and B4 were constructed with a timber studwork frame cast into the edge of the hemp-lime with Multi-pro XS sheathing board fixed to the studwork frame to form permanent formwork. The other exposed face of the walls was rendered. Walls B3 and B4 were loaded on differing faces so that in Wall B3 the rendered face was in tension and in Wall B4 the Multi-pro XS sheathed face was in tension. The details of the walls are shown in Chapter 5.

All the wall panels were tested using the same test set up and methodology. The wall panels were tested in out-of-plane bending spanning between supports at the top and bottom of the wall and a uniformly distributed load (UDL) was applied via an airbag. The wall panels were placed against the strong wall in the test laboratory with the face that was being loaded spaced 100mm away from the wall. The wall panels were placed on rollers at their base to allow them to move freely up to the horizontal supports when loaded (Figure 8.1).

Figure 8.1 Rollers at base of bending wall panels

The airbag was placed between the wall panels and the strong wall. When inflated the airbag reacts against the laboratory strong wall and the wall panel specimen, therefore loading the specimen. The airbag was inflated via a compressed air line with the rate of inflation being controlled using a regulator. The test set up is shown in Figure 8.2 and Figure 8.3.

Figure 8.2 Bending wall test set up

Figure 8.3 Bending wall test showing airbag behind wall

The applied load and the displacement across the surface of the wall panels were monitored and recorded. Figure 8.4 shows the positions of the LVDTs. For Walls B1 and B2 the applied load was measured by load cells at the support reactions and then converted into an applied UDL. For Walls B3 and B4 the applied load was measured via an air pressure cell in addition to the load cells measuring the support reactions. Displacements of the visible face of the wall panels were measured using LVDTs at the supports, at quarter and three quarter height and at mid-height. All of the pressure, load and displacement readings were recorded using a System 6000 data acquisition module

connected to a PC. In addition to measuring the loads and displacements, on Walls B3 and B4 the surface strains of the tension faces were measured using a 300mm long DeMec gauge with studs mounted directly onto the render and Multi-pro XS sheathing board.

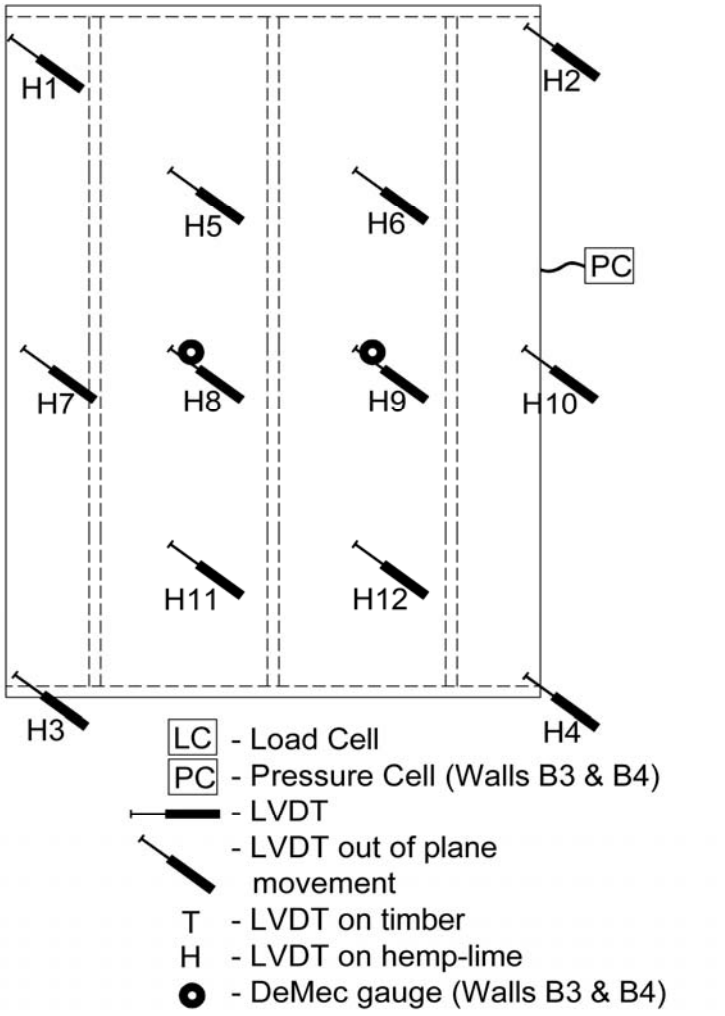

Figure 8.4 Bending test LVDT positions

During testing the Walls B1 and B2 were loaded until failure occurred with no cycling of the load. On Walls B3 and B4 the load was cycled. The load was applied initially to 0.5kN/m^2 and the surface strains were recorded using the DeMec gauge. The load was then removed and the surface strains and residual displacement were recorded. The load was then increased to 1.0kN/m^2 and the same process was repeated. The loading continued in increasing increments of 0.5kN/m^2 until failure occurred.

8.3 Results

8.3.1 Walls B1 and B2 (LS1)

Figure 8.5 shows the load plotted against displacement at the centre of the wall panel for both Walls B1 and B2.

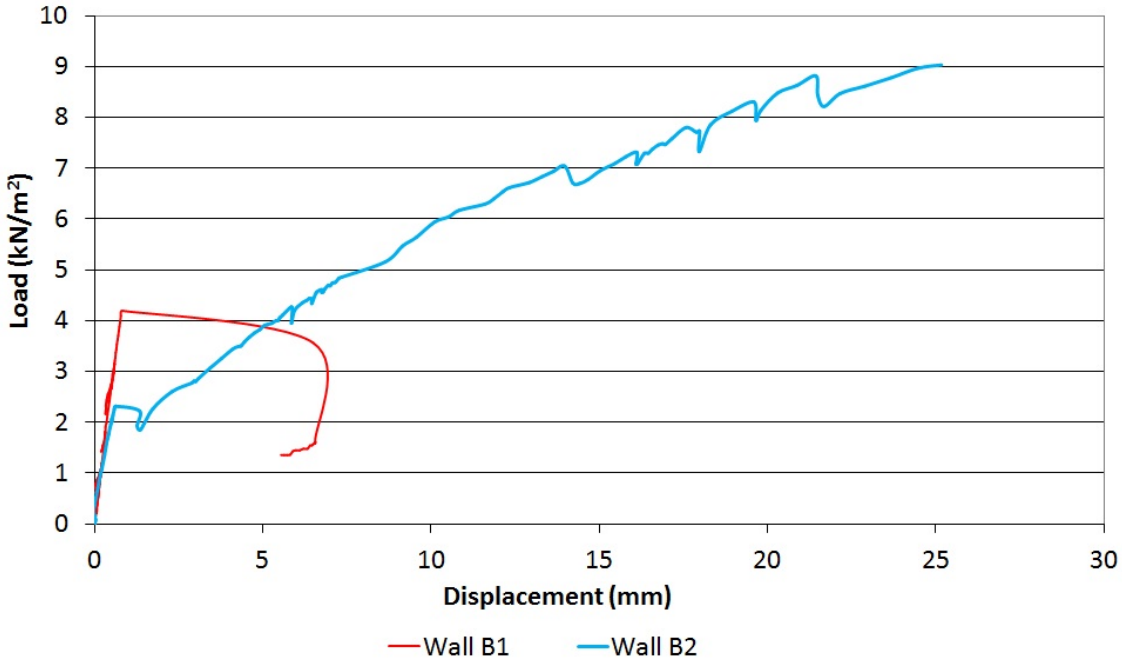

Figure 8.5 Bending test results for Walls B1 and B2

Both Wall B1 (hemp only) and Wall B2 (hemp and timber) performed in a similar way until the render on the wall face in tension and hemp-lime cracked (Figure 8.6). Wall B1 had an initial stiffness of 6.05kN/mm and Wall B2 had an initial stiffness of 3.28kN/mm. Following cracking of the render and hemp-lime the stiffness of Wall B2 reduced to 0.53kN/mm, but the load continued to be resisted by the timber studwork framing within the wall. On Wall B2 the render and hemp-lime cracked at a load of 2.3kN/m^2 and a displacement of 0.70mm. The stiffness of Wall B1 was constant until the render and hemp-lime cracked at a load of 4.2kN/m^2 and a displacement of 0.85mm. At this point as there was no studwork frame the wall was completely failed and had cracked through its entire depth.

Figure 8.6 Wall B2 – Cracked render and hemp-lime

The difference in cracking load and initial stiffness between Walls B1 and B2 is a result of variations in the thickness of the render and the quality of the hemp-lime. On Wall B1 the render on the tension face at the crack location was an average of 13.8mm thick whereas on Wall B2 it was 11.8mm thick, a difference of 17%. Additionally the hemp-lime in Wall B1 was generally fully set and had good cohesion. However on Wall B2 there were large patches of hemp-lime that had not set and had very little cohesion displaying the phenomenon of 'flouring'. 'Flouring' only occurred in two wall specimens in the LS1 series of tests. It is thought that it was caused by a small change in the formulation of the binder. Once the problem was identified by the suppliers of the binder the problems did not re-occur. This is discussed in more detail in Chapter 5.

While hemp-lime is considered to have very minimal tensile strength, this lack of cohesion will also have made a significant difference. Both walls failed at day joints which were 900 mm from the base of the walls. The cracking load of the render is likely to be the governing factor when using hemp-lime and timber studwork framing composite walling for structural load bearing applications. The render cracked at displacements of 0.70mm and 0.85mm. As the wall finishes are brittle, a deflection criteria of the wall height divided by 500 (h/500) can be assumed. Therefore the allowable deflection would be 4.8mm. The deflections at which the cracks occurred are less than 20% of this deflection and as a result deflection should not be used as a serviceability criterion in the design for out of plane bending.

Specimens of both the timber studs and hemp-lime were taken and the moisture content recorded. The results are shown in Table 8.1 and Table 8.2.

Table 8.1 Moisture content of studs

Wall	Stud	Moisture content %
B2	Left	21.7
B2	Centre	20.9
B2	Right	21.3

Table 8.2 Wall B1 and B2 Hemp-lime moisture content and density

	Moisture Content (%)			Dry density
Wall	**Inner**	**Outer**	**Average**	**(kg/m^3)**
B1 – Base	28.5	20.2	24.4	310.5
B1 – Middle	25.1	17.8	21.4	311.4
B1 – Top	22.8	13.1	17.9	317.6
B1 - Average	**25.5**	**17.0**	**21.2**	**313.2**
B2 – Base	24.3	22.2	23.2	311.7
B2 – Middle	21.5	21.2	21.4	-
B2 – Top	18.2	12.8	15.5	323.1
B2 - Average	**21.3**	**18.7**	**20.3**	**317.4**

Table 8.3 Walls B1 and B2 hemp-lime compressive strength

Wall	Specimen location	b (mm)	d (mm)	h (mm)	Compressive strength σ_c (N/mm^2)
B1	Base	305	325	440	0.28
B1	Middle	315	325	400	0.21
B1	Top	310	323	400	0.22
B2	Base	300	325	350	0.23
B2	Top	290	315	360	0.28
Average					**0.24**

The moisture contents of both the timber and hemp-lime show similar trends to those in the compression and racking walls. A prism specimen was not taken from the middle of Wall B2 as the hemp-lime was too fragile due to ‘flouring’. The compressive strengths

of the prisms that were taken are slightly lower than the average cylinder strengths. This is similar to the prisms from Walls C2, C3, R1 and R2. The average compressive strength for Wall B1 and B2 has also been influenced by the 'flouring' of the hemp-lime and therefore the difference is greater between the prism average strength and the cylinder average strength.

8.3.2 Walls B3 and B4 (LS2)

Figure 8.7 shows the load plotted against displacement at the centre of the wall panel for both Walls B3 (render in tension) and B4 (Multi-pro XS in tension).

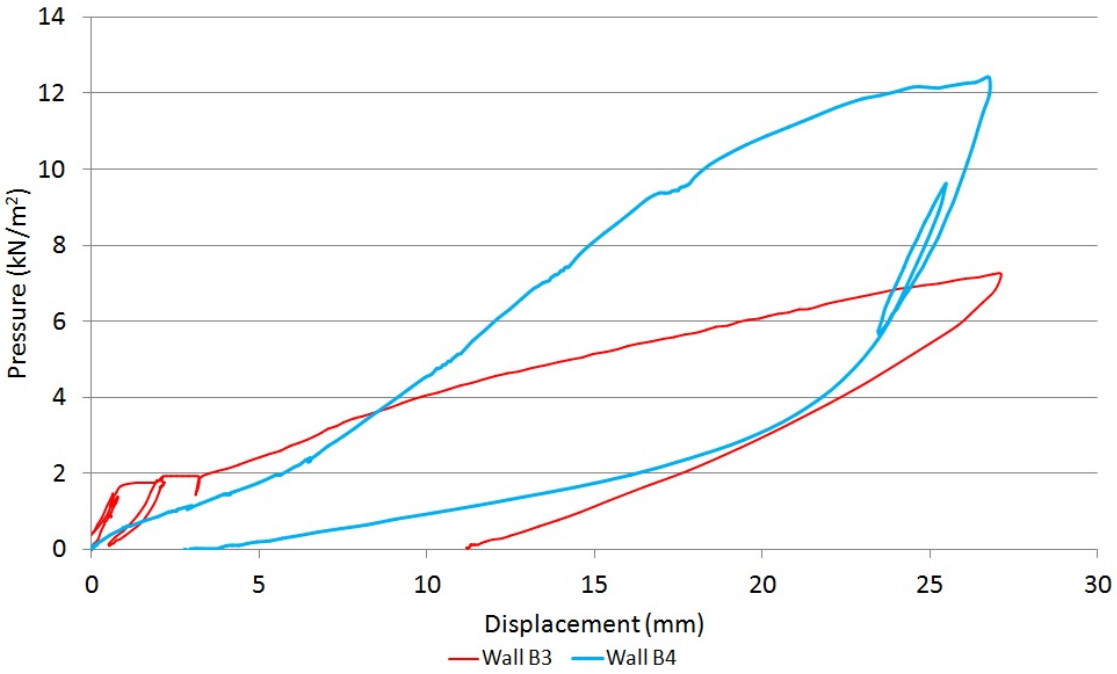

Figure 8.7 Bending test results for Walls B3 and B4

From Figure 8.7 it is clear that the two walls performed quite differently. Wall B3 had a much higher initial stiffness of 1.89kN/mm until the render cracked at a load of 1.69kN/m^2. Following this the stiffness reduced significantly to 0.32kN/mm. At this point the render and hemp-lime is fully cracked (Figure 8.8) and the bending stiffness of the section is largely from the timber frame and Multi-pro board.

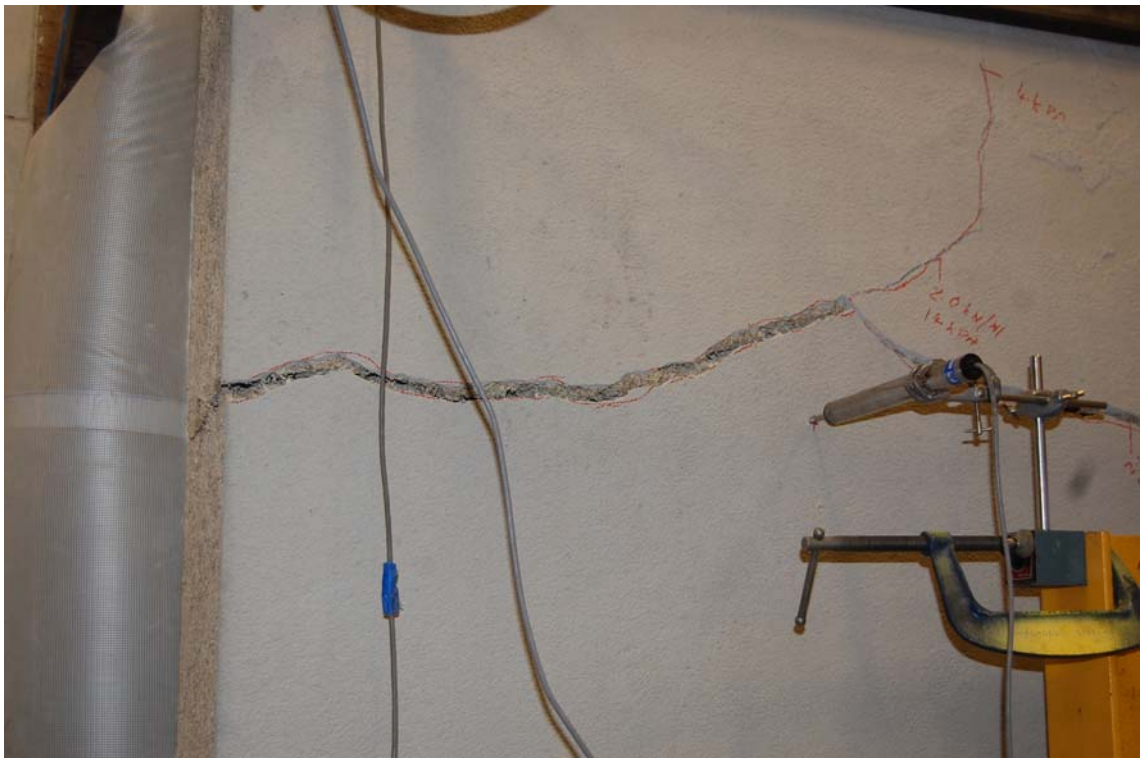

Figure 8.8 Wall B3 – Cracked render and hemp-lime

The render on Wall B3 cracked 600mm from the top of the wall. The crack occurred where the render was thinnest at an average thickness across the width of the wall of 13mm, compared to 18mm at mid height and 17mm at 600mm from the base. Additionally the crack formed at the location of one of the three horizontal rails in the wall. At these locations the hemp-lime had voids caused by settlement during construction (Figure 8.9) and therefore the cross section of hemp-lime is reduced causing a weak point.

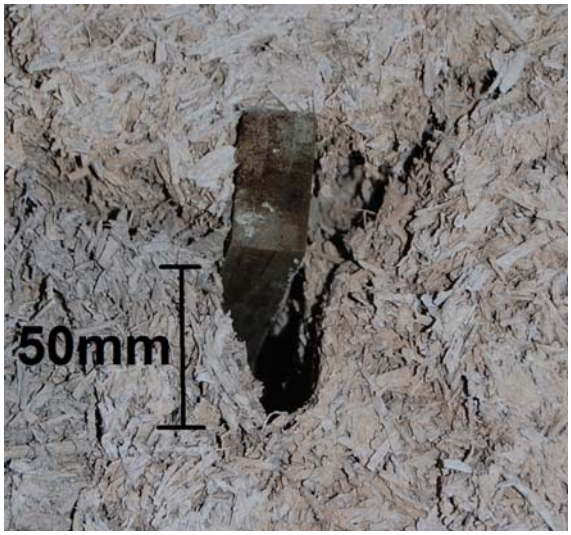

Figure 8.9 Void below horizontal rail

Wall B4 had a lower initial stiffness than Wall B3. This is due to the render being in compression rather than tension. As a result the stiffness of Wall B4 is more uniform than Wall B3 as there is no sudden cracking failure of the render and the associated reduction in stiffness. Wall B4 had an initial stiffness of 0.39kN/mm which then increased to 0.63kN/mm above a load of 2kN/m^2. The change in stiffness occurred as the hemp-lime started to crush against studs and put load onto Multi-pro board increasing stiffness of the panel. At a load of 5kN/m^2 the screw heads started to pull through the Multi-pro as shown in Figure 8.10. As a result there was a reduction in the composite action between the sheathing board and timber studs.

During testing a visible crack developed in the hemp-lime at mid height of the wall. Once the Multi-pro board was removed from the front of the wall the crack was clearly visible (Figure 8.11). After testing when Wall B4 had been removed from the test rig it was possible to see that the render on the compression face had a very fine crack at mid height of the wall in the same location as the hemp-lime crack (Figure 8.12). The render was a more uniform thickness than on Wall B3 with averages thicknesses of 17mm 600mm from the top, 16mm at mid height and 18mm 600mm from the base.

Figure 8.10 Screw head pulling through Multi-pro board

Figure 8.11 Cracking of hemp-lime in Wall B4

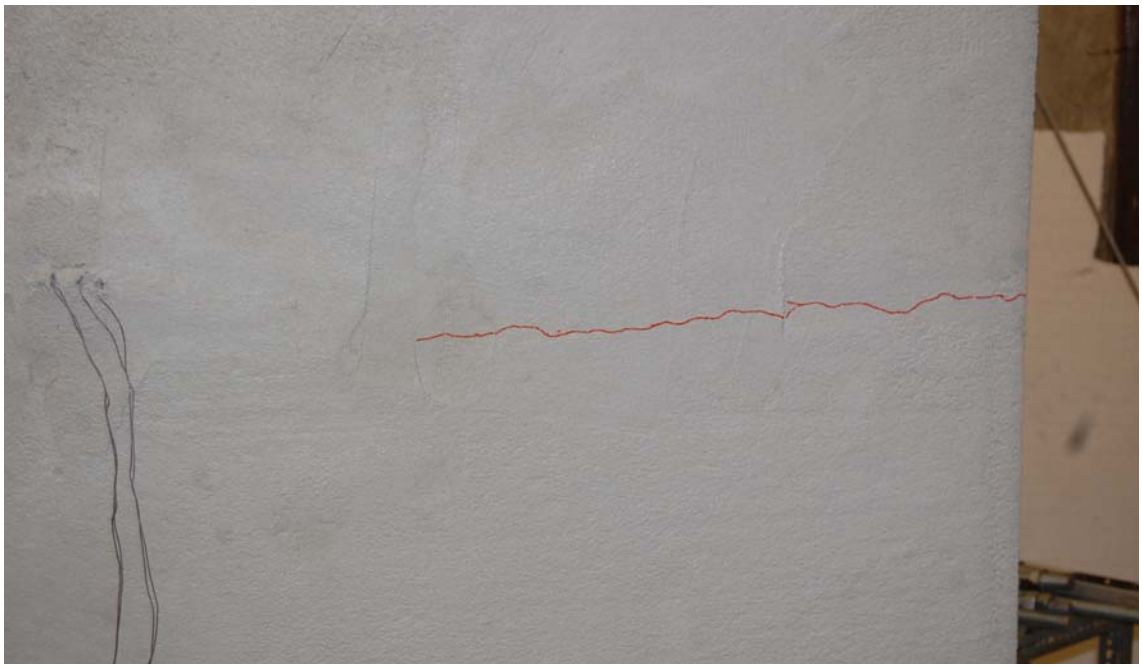

Figure 8.12 Crack on render face of Wall B4

Following testing specimens of the hemp-lime and timber were taken to measure the moisture content. Additionally the compressive strength of prisms of hemp-lime cut from the walls was tested. The moisture content of the timber studs are shown in Table 8.4, the moisture content of the hemp-lime is shown in Table 8.5 and the compressive strength of the hemp-lime is shown in Table 8.6.

Table 8.4 Wall B3 and B4 timber moisture content

Wall	Position	Moisture content %	Position within hemp-lime
3	Footer	20.0	Edge with Multi-pro
3	Base of centre stud	20.8	Edge with Multi-pro
3	Middle of centre stud	21.5	Edge with Multi-pro
4	Footer	19.8	Edge with Multi-pro
4	Base of centre stud	20.9	Edge with Multi-pro
4	Middle of centre stud	18.9	Edge with Multi-pro

Table 8.5 Wall B3 and B4 hemp-lime moisture content

Wall	Moisture Content (%)			Dry density (kg/m^3)
	Inner	Outer	Average	
B3 – Base	23.7	14.9	19.3	259.4
B3 – Middle	19.7	11.4	15.5	293.4
B3 – Top	13.1	7.8	10.4	259.4
B3 - Average	**18.8**	**11.3**	**15.1**	**276.4**
B4 – Base	20.1	8.5	14.3	272.5
B4 – Middle	20.7	9.4	15.0	281.0
B4 – Top	21.6	8.6	15.1	260.9
B4 - Average	**20.8**	**8.8**	**14.8**	**271.5**

Table 8.6 Wall B3 and B4 hemp-lime compressive strength

Wall	Specimen location	b (mm)	d (mm)	h (mm)	Compressive strength σ_c (N/mm^2)
B3	Base	148	160	307	0.32
B3	Middle 1	152	155	308	0.43
B3	Middle 2	161	163	301	0.25
B4	Base	173	164	305	0.34
B4	Middle	151	147	298	0.32
B4	Top	148	163	314	0.19
Average					**0.31**

The moisture content of both the inner areas of hemp-lime and the timber studs show similar trends to those from Wall R5 as Multi-pro sheathing was also used. The prisms compressive strengths compare with the material properties cylinders strengths in the same way as the other Large Scale 2 test wall panels. The average prism compressive strength is slightly lower than the average cylinder strength. As Walls B4 and B5 were constructed at the same time as the other Large Scale 2 walls this is to be expected.

8.4 Discussion

Figure 8.13 shows all of the results from all of the walls tested in bending to allow easy comparison. From Figure 8.13 Walls B1 and B2 had a higher initial stiffness than walls B3 and B4. This is a result of these walls being rendered on both faces. The render forms a very good bond with the hemp-lime and therefore when subjected to bending there is full interaction between the two materials. On Walls B3 and B4 there was only render on one face with Multi-pro sheathing board on the other. There is no bond between the Multi-pro sheathing board and the hemp-lime and therefore no interaction. As a result the stiffness of the section is lower.

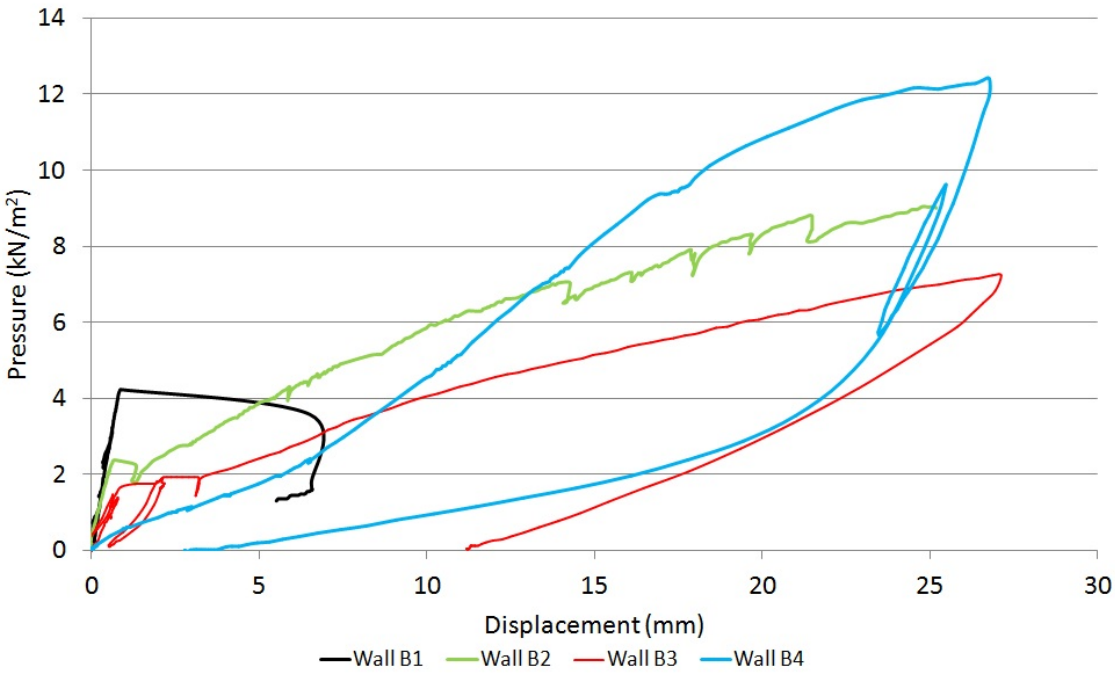

Figure 8.13 Bending test results for Walls B1, B2, B3 and B4

The post crack stiffness of Walls B2 and B3 is similar. Wall B3 was loaded with the rendered face in tension and the Multi-pro face in compression. Once the render on the tension face of both walls had failed and the hemp-lime section cracked the walls had similar constructions continuing to resist the applied load. On Wall B2 the load was being resisted by the timber studwork frame in the centre of the wall and the rendered face in compression and on Wall B3 by the timber studwork frame and Multi-pro sheathing on the compression face of the wall.

Figure 8.13 also shows the effect of render thickness on the cracking failure load of the render. Wall B1 which achieved the highest load before cracking of the render had the highest average thickness of render of 13.8mm at the crack location, whereas the render on Wall B2 was 11.8mm thick and on Wall B3 13.0mm thick. Additionally while the bending strength of the hemp-lime is minimal ($0.035N/mm^2$), it does contribute to the overall bending strength. The hemp-lime in Wall B2 displayed 'flouring' and therefore was of a lower quality and strength which will have also affected the cracking load of Wall B2. The thickness of the render needs to be strictly controlled during construction.

While the testing has been undertaken on specimens and with a test set up that is designed to be representative of the conditions found when this form of construction is used, the bending tests neglected any vertical dead load that would be present in a structure using this form of construction. For a two storey building this would be around 8kN/m at first floor level and 4kN/m at roof level. These permanent dead loads would affect the bending behaviour of the walls, however not significantly enough to make the results from these tests redundant.

The literature review undertaken in Chapter 2 showed that there has been limited investigation into the bending strength of hemp-lime, with the only published study by Elfordy et al. (2008) concentrating on small specimens of hemp-lime. Therefore it is not possible to compare the results from Walls B1, B2, B3 and B4 with any previous work.

Figure 8.14 shows the results for all of the bending walls and predictions for the actual test walls using the theory set out in Chapter 4.

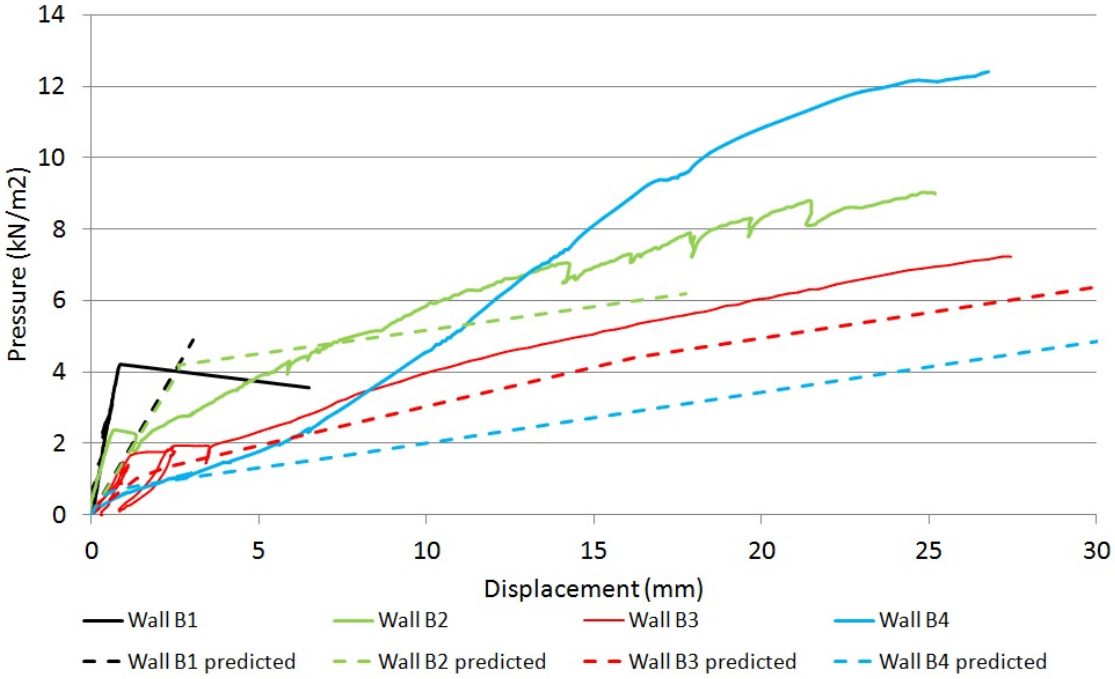

Figure 8.14 Out –of-plane bending predicted results and experimental results

With all of the wall panels the predicted initial bending stiffness is lower than the actual stiffness. If shear deflections are ignored when calculating the predicted bending stiffness the results are similar. Therefore either hemp-lime is transferring shear forces in a different way or the shear properties of the hemp-lime that were used in calculating the deflections differ from the actual properties. Further work is required to fully investigate the shear properties of hemp-lime; however this is outside the scope of this study.

The cracking loads of the render and hemp-lime are over predicted. This could be for several reasons. The material properties that were used to calculate the cracking load could be causing the error. The predictions were made using the average modulus of rupture of the render. A more accurate prediction will be found if the 5% characteristic strength is used as it will account for the variations in the render properties. Additionally on Wall B1 the render was only 13.8mm thick on average whereas the theoretical assumed 15mm of render. Considering the characteristic render properties and the thinner render the cracking load for Wall B1 can be calculated as 4.1kN and the actual load at which the render cracked was 4.2kN. On Wall B2 the render was only 11.8mm thick. Recalculating as with Wall B1 the render cracking load for Wall B2 would be 3.5kN and the actual cracking load was 2.2kN. Again this is over predicted,

however the hemp-lime in Wall B2 was weak due to ‘flouring’ and therefore this will have affected the performance so any further comparison is difficult to make.

On Wall B2 the predicted post crack stiffness is lower than the actual stiffness. The theoretical calculations assumed that once the render and hemp-lime had cracked they no longer contributed to the capacity of the wall. In reality they are likely to interact with the studwork frame and cause the increase in stiffness shown. The interaction between the materials is not fully understood and would require extensive further work to get a full understanding. Predicting the performance with only the studwork frame resisting the loads is not seen as a problem as using this theory will never over predict the performance.

The predicted and actual post crack stiffness of Wall B3 correlates well. This confirms that the method outlined in Chapter 4 using the partial interaction theory set out in BS EN 1995 (2004) is suitable for predicting the stiffness of the studwork frame and sheathing board.

Wall B4 shows the greatest post crack difference between the predicted performance and the actual results. The cause for actual results showing much greater stiffness and strength must be a result of how the different materials within the wall construction are interacting. As the load increases the interaction between the hemp-lime, studwork frame and sheathing board must increase. As pressure is increased on the rendered face the hemp-lime is pushed into the studwork frame and sheathing. This may lead to greater friction between the materials and therefore increase their slip modulus and hence increase the overall stiffness of the wall. Further research is needed in this area to find the actual cause.

8.5 Conclusions

These wall panel tests are significant as for the first time they have shown the performance of hemp-lime and composite studwork walling under out-of-plane bending loads.

Throughout much of the UK peak design wind loads are less than 1kN/m^2. The tests on Walls B1 and B2 show that under out-of-plane bending a 300mm thick hemp-lime wall with a dry density hemp-lime of 275kg/m^2 and 15mm of render on both faces is sufficient to resist design wind loads through much of the UK. The addition of the timber studwork frame increases the strength and integrity of the wall once the render and hemp-lime has cracked.

Walls B3 and B4 have shown that the bending performance of the wall panels varies depending upon the direction of the load. With the render in tension there is initially high stiffness before the render cracks. Post render failure the stiffness reduces; however due to the timber studwork frame the wall can still sustain a high and increasing load. With the render in compression the stiffness is initially lower, however it then increases as the load increases and the composite action of the timber frame, hemp-lime and Multi-pro board develops.

The predicted performance for Walls B1, B2 and B3 show good correlation to the actual results and the differences have been caused by difference in the material properties used in the predictions and those in the walls panels. The predictions for Wall B4 initially show good correlation, but then the results diverge. Further research is needed to find the exact cause.

9 Design recommendations

9.1 Introduction

In this chapter design recommendations are presented. These have been drawn from both the experimental and theoretical study. The recommended design process for designing a composite studwork and hemp-lime wall is also set out. Finally a design example is given to demonstrate the generality of the proposed approach.

9.2 Recommendations from theoretical and experimental studies

Design recommendations can be drawn from both the theoretical analysis and experimental study. These recommendations are variations to the current design process for composite studwork and hemp-lime walling that ignores the contribution of the hemp-lime. The recommendations allow the hemp-lime to be utilised in a load bearing capacity and improve the structural efficiency of the wall system.

When designing for concentric compressive loading the following recommendations should be considered:

- No need to rely on sheathing, as hemp-lime can prevent buckling of studs about both the minor and major axis.
- If sheathing is not used the studs can be spaced at centres to suit the design loads rather than sheathing sheet sizes.
- Stronger header and footer rail should be used if compression load capacity needs to be increased as the perpendicular bearing capacity of prepared timber is lower than the parallel to grain crushing capacity.

Both theoretical analysis and experimental testing have shown that under concentric compressive loading timber studs are prevented from buckling by hemp-lime at a density of 275kg/m^3. Therefore sheathing does not need to be relied upon to prevent buckling. However the use of sheathing may still be beneficial for use as a permanent shuttering or as a backing for applying internal finishes to. However if sheathing is not

used the studs can be spaced at centres to suit their applied loads rather than to suit the dimensions of sheathing sheets. Where high compressive loads are to be carried by the stud an engineered timber such as laminated veneer lumber (LVL) could be used for the header and footer rails. The compression strength perpendicular to the grain of LVL is between 4.0N/mm^2 and 9.0/mm^2 compared with 2.2N/mm^2 for C16 timber.

When designing for eccentric compressive loading in addition to the design recommendations made above for concentric loads the following should be considered:

- Direction of the eccentricity and the hemp-lime cover to the studs in the direction that the stud will deflect horizontally.
- Increased potential for the hemp-lime to burst.
- Fixings used in horizontal rails if present.

Experimental testing detailed in Chapter 6 has shown that the level of hemp-lime cover to the studs is particularly important when eccentric loads are applied. During testing when the studs had hemp-lime cover of 102.5mm bursting did not occur however when the cover was only 50mm the hemp-lime did burst causing failure of the studs. Therefore it is important to consider the direction of the eccentricity and the hemp-lime cover in the direction the stud will deflect. The force required to burst the hemp-lime should be checked in the process set out below in STEP 2 of compression design. If horizontal rails are used screwed fixings should be used as they have a higher pull out strength (average 2.19kN, No.8 screw 50mm long) than nails (average 0.8kN, 2.65mm diameter 50mm long).

When designing for in-plane racking loads the following recommendations should be considered:

- Improved leading stud (stud closest to racking load) to header and footer connections should be used to increase the stiffness and strength of the joints.
- No need to rely on sheathing as hemp-lime can resist applied in-plane racking loads providing improved leading stud connections are used.
- Sheathing board should be used if increased in-plane racking strength is required.

Improved leading stud connections should be used as this is a weak point in the overall construction. When an in-plane racking load is applied to a studwork frame there is a global rotational force applied to the entire frame causing it to rotate about the point diagonally opposite to the point where the racking load is applied. As the footer rail is fixed to the foundations this causes a vertical force to be applied to the leading stud joints. A simple nailed connection does not have a very high withdrawal capacity or stiffness (average capacity 0.55kN, average stiffness 433N/mm^2). Therefore improving the joint strength with screws such as 6.5mm dia. x 150mm long double thread screws (average capacity 9.89kN, average stiffness 2710N/mm^2) prevents the joints from failing and therefore increases the racking stiffness and strength. Using improved connectors on all of the studs will increase the capacity further.

There is no need to rely on sheathing boards to provide the resistance to in-plane racking loads. It has been shown both theoretically and by experimental testing in Chapters 4 and 7 that hemp-lime can provide the resistance to these applied loads providing improved connections are used. Without improved leading stud connections the racking stiffness is not sufficient. As with compressive loading a sheathing board may be beneficial for other reasons. However if a high in-plane racking stiffness is required a sheathing board can also be used in addition to improved connections and hemp-lime. The design racking resistance for both types of wall was calculated using the methods set out in BS 5268-6.1 (1996) Section 5. The design racking resistance, R_b, of a wall without sheathing is 1.14kN/m and one with sheathing is 1.94kN/m. These values include factors of safety as set out in BS 5268-6.1 (1996). Comparing these values with those given in Table 2 of BS 5268 (1996) for the design racking resistance of common sheathing materials the walls with sheathing have a greater racking resistance than Category 1 materials (1.68kN/m) and the walls without sheathing have a greater racking resistance than Category 2 materials (0.90kN/m).

When designing for out-of-plane bending loads the following recommendations should be considered:

- Careful attention should be taken to ensure that the applied render thickness is the same as the specified render thickness.

- When the render is contributing towards the section capacity it should be at least 10mm thick to avoid a steep drop in section capacity.
- When using sheathing on one face the direction of loading should be considered as the deflection characteristics of the wall panels vary.

The experimental testing (Chapter 8) showed that the thickness of the render can affect the bending performance of the wall panels. All of the test wall panels failed at the point where the render was thinnest. Therefore extra care should be taken to apply the render to the specified thickness and to take account of any undulations in the hemp-lime surface that may result in thin patches of render. Additionally theoretical analysis (Chapter 4) has shown that when the render thickness is reduced below 10mm there is a significant increase in the horizontal deflections of the wall panels when out-of-plane bending loads are applied.

Finally both theoretical analysis and the experimental study have shown that when a wall construction with render, hemp-lime, studwork frame and sheathing board is used the performance differs depending upon the direction of the applied load. Therefore this should be considered during the design process to allow for both positive and negative wind pressures.

9.3 Design process

This study has investigated several theoretical approaches to calculate the stiffness and strength of composite studwork frame and hemp-lime construction. These approaches have come from both BS EN 1995-1.1 (2004), which uses a limit state approach, and structural analysis theory. From the investigation the following design procedure has been developed. All material properties used should be characteristic values. In all cases suitable load and material properties safety factors should be applied by the designer. The following design checks are for 2.4m long studs in a 2.4m wide wall panel. For a full list of all of the symbols used please see the list of symbols at the beginning of this thesis.

Compression loading design checks:

Concentric loading:-

STEP 1: Determine buckling loads (both minor and major) using the appropriate theoretical approach.

For Wall type 1 (Studwork frame in centre of hemp-lime) use the theory of a column buckling on an elastic foundation as shown in Figure 9.1.

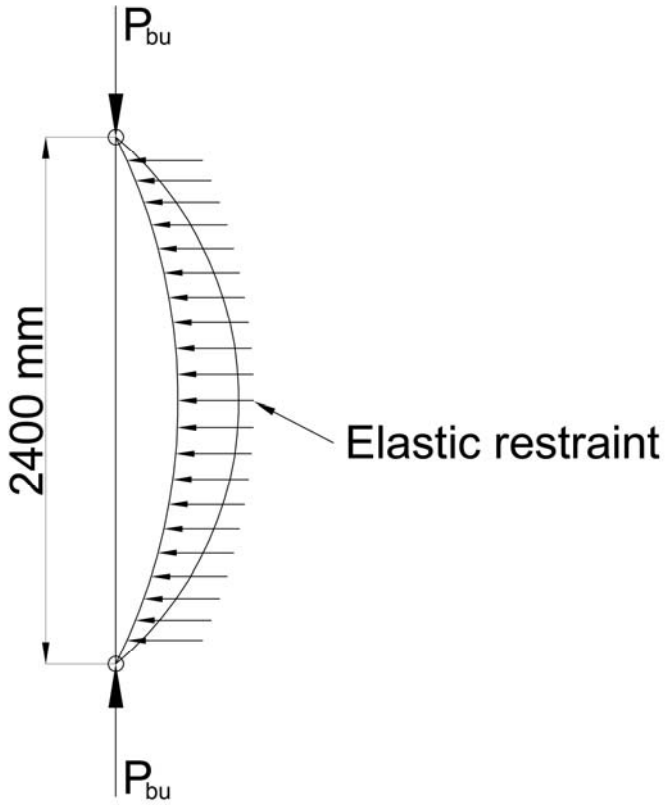

Figure 9.1 Column buckling on elastic foundation

The critical load (load at which the stud will buckle into the hemp-lime) can be calculated for each axis from:

$$P_{bu} = \frac{2m^2\pi^2 EI}{l^2}$$

Where *m* is the number of half sine waves in the buckled shape of the stud and is found from:

$$m^4 = \frac{\omega l^4}{\pi^4 EI}$$

Where ω is the modulus of the elastic restraint.

For Wall type 2 (Studwork frame on edge of hemp-lime with horizontal rails) the minor and major axis buckling loads need to be calculated in different ways. For minor axis buckling the approach detail above for Wall type 1 should be followed. For major axis buckling the theory presented by Timoshenko and Gere (2009) for finding the buckling load of a column supported by intermediate elastic restraints (Figure 9.2) should be used.

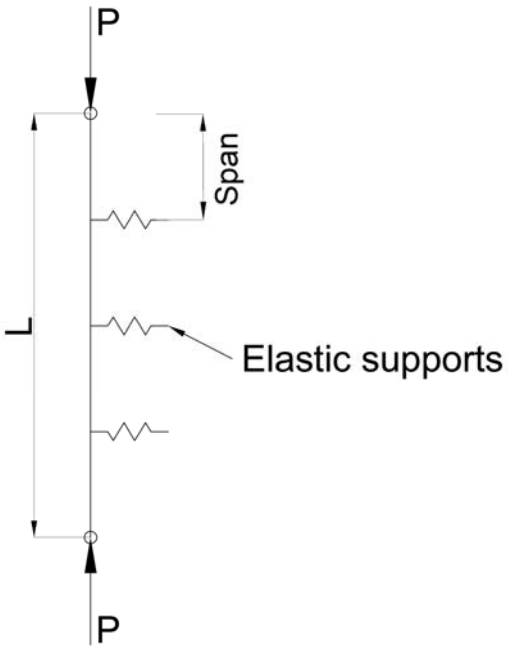

Figure 9.2 Column with elastic restraints

The elastic supports have a stiffness, μ. Initially calculate the minimum value of stiffness of the elastic supports at which they act as though they are rigid using:

$$\mu_{rigid} = \frac{nP_{crit}}{rl}$$

Where: $n =$ number of spans, $r =$ constant dependent upon the number of spans, and,

$$P_{crit} = \frac{n^2 \pi^2 EI}{l^2}$$

Values of r are shown in Table 9.1 for various numbers of spans (n).

Table 9.1 Values of γ for different spans (Timoshenko and Gere, 2009)

n	2	3	4	5	6	7
r	0.500	0.333	0.293	0.276	0.268	0.263

If $\mu_{rigid} > \mu$ the column can be treated as having rigid supports and Euler buckling used to determine buckling load of individual spans.

If $\mu_{rigid} < \mu$ the stiffness of the supports needs to be considered when determining the buckling load of the entire column.

By considering the Euler buckling load (P_E) of the column when $\mu = 0$ and calculating P_{crit} the variation in critical load due to the changing stiffness of the supports can be plotted as shown in Figure 9.3. The curve shown is specific for the 2400mm long 38mm by 89mm C16 stud used for wall type 2 and therefore P_E and l are constant.

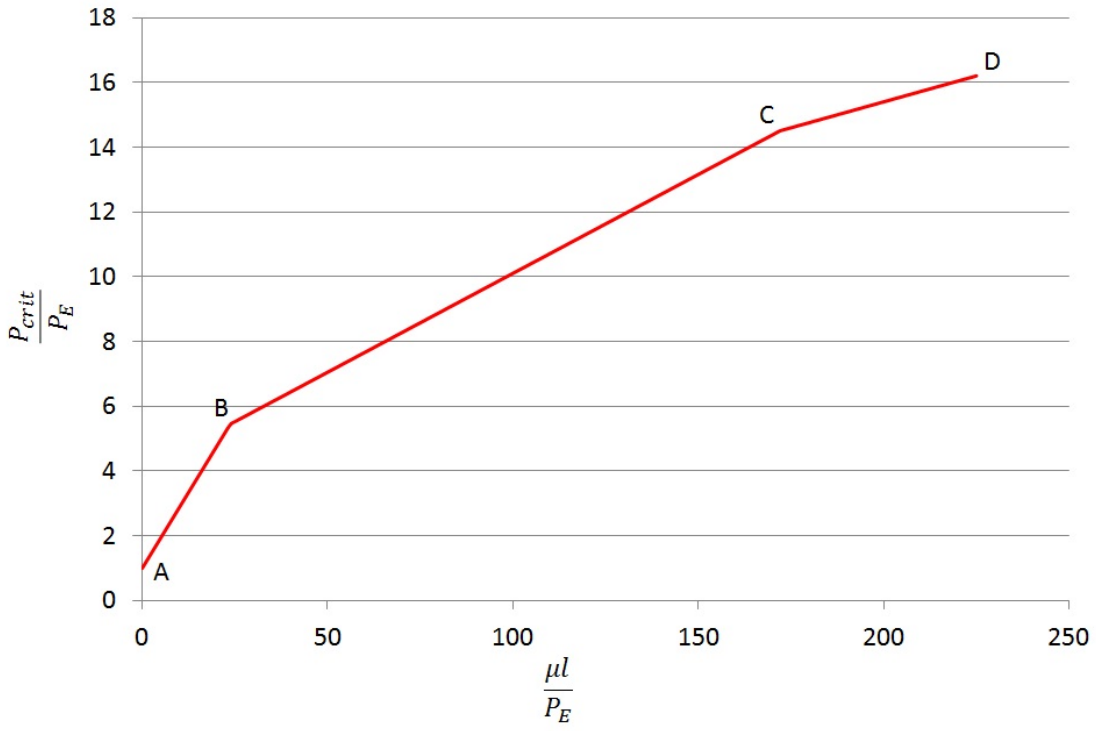

Figure 9.3 Relationship between critical load and support stiffness

From the curve plotted in Figure 9.3 the ratio P_{crit}/P_E for any value of μ can be found and hence P_{crit} can be calculated.

STEP 2: Check the bursting load by finding the cone failure load and assuming a resistance of 2% of the axial load is required to prevent buckling of the stud. This can be carried out in the same way for both Wall type 1 and 2.

Using the bursting geometry outlined in Figure 9.4 calculate the bursting area:

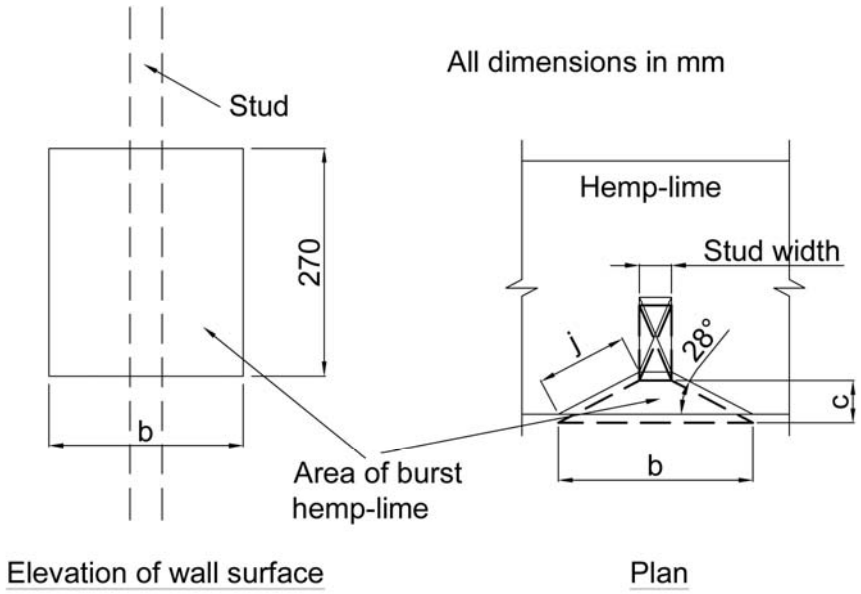

Figure 9.4 Hemp-lime bursting geometry

$$A_{burst} = 2 \times (j \times 270)$$

Then the bursting force assuming the hemp-lime shear strength to be 0.014N/mm^2:

$$F_{burst} = A_{burst} \times 0.014$$

If F_{burst} is less than 2% of the applied axial load, bursting will not occur.

STEP 3: Determine the stud crushing capacity using the correct moisture content for the studs and therefore the appropriate strength. The crushing capacity is calculated from:

$$P_{crushing} = \sigma_{c\,parallel} \times Area$$

STEP 4: Determine the footer and header rail bearing capacity using the correct moisture content for the rails and therefore the appropriate strength. The bearing capacity is calculated from:

$$P_{bearing} = \sigma_{c\,perpendicular} \times Area$$

STEP 5: The design capacity should be taken as the lesser of the above.

Eccentric loading:-

STEP 1: Check the buckling loads as above for concentric loading.

STEP 2: Check the bursting load by finding the cone failure load and assuming a resistance of 2% of the axial load is required to prevent buckling of the stud as above for concentric loading.

STEP 3: Determine the stud crushing capacity using the correct moisture content for the studs and therefore the appropriate strength as above for concentric loading.

STEP 4: Determine the footer and header rail bearing capacity using the correct moisture content for the rails and therefore the appropriate strength as above for concentric loading.

STEP 5: The design capacity should be taken as the lesser of the above.

In-plane racking design checks:

Without sheathing:-

STEP 1: Determine the stiffness of the construction using the theory of a cantilevered column on an elastic restraint (Hetényi, 1946) as shown in Figure 9.5.

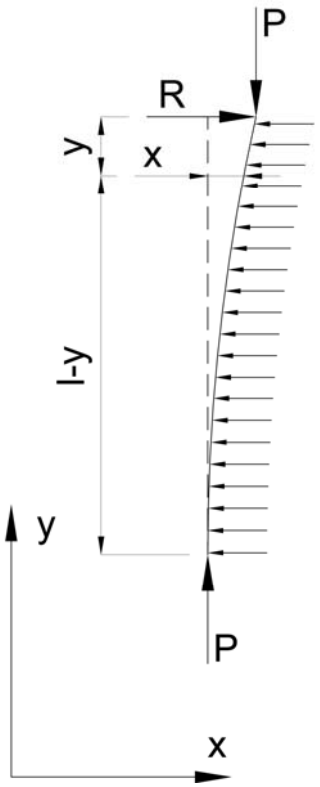

Figure 9.5 Cantilever on elastic foundation

Initially calculate the deflection of the end of the studs in the x direction using:

$$x = \frac{R}{2\lambda^2 EI}\,\frac{1}{H_1 H_2}\,F$$

Where:

$$H_1 = \alpha(3\beta^2 - \alpha^2)\sinh\beta l + \beta(3\alpha^2 - \beta^2)\sin\alpha l$$

$$H_2 = \alpha(3\beta^2 - \alpha^2)\sinh\beta l - \beta(3\alpha^2 - \beta^2)\sin\alpha l$$

$$\begin{aligned} F = \{&\alpha(3\beta^2 - \alpha^2)\sinh\beta l[2\alpha\beta\cos\alpha y\cosh\beta(l-y) \\ &+ (\beta^2 - \alpha^2)\sin\alpha y\sinh\beta(l-y)] \\ &- \beta(3\alpha^2 - \beta^2)\sin\alpha l\,[2\alpha\beta\cosh\beta y\cos\alpha(l-y) \\ &+ (\beta^2 - \alpha^2)\sinh\beta y\sin\alpha(l-y)]\} \end{aligned}$$

$$\lambda = \sqrt[4]{\frac{k}{4EI}}, \qquad \alpha = \sqrt{\sqrt{\frac{k}{4EI}} + \frac{P}{4EI}}, \qquad \beta = \sqrt{\sqrt{\frac{k}{4EI}} - \frac{P}{4EI}}$$

When calculating the deflection at the end of the studs it is important to take into consideration the changing stiffness of the hemp-lime following this the overall deflection at the top of the studwork frame can be calculated. As well as the hemp-lime resisting the racking force, the joints between the studs and the header and footer rails will resist global rotation of the studwork frame. As the footer rail is securely fixed to the foundation, the racking load will cause the rest of the studwork frame to rotate around point A in Figure 9.6 consequently loading the joints.

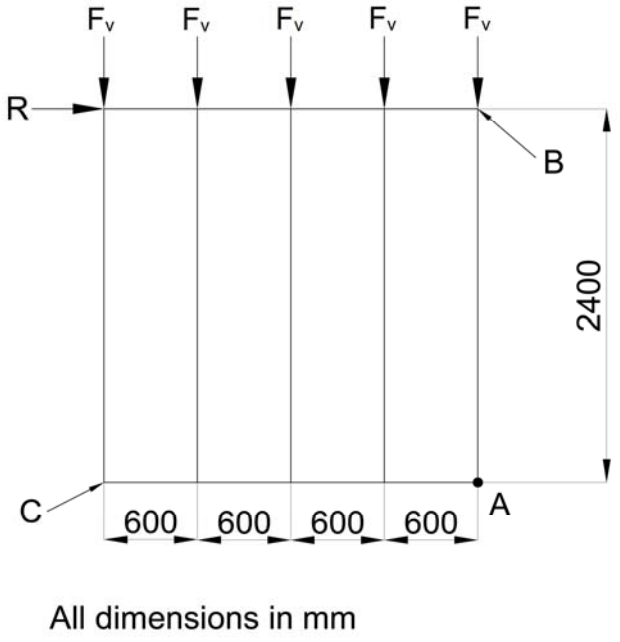

Figure 9.6 Racking wall loading

By taking moments about point A, with constant vertical loads of F_v, the racking load (R_{up}) at which the joint at C will begin to experience a tensile force rather than compressive force can be calculated. When $R<R_{up}$ the equations above are used to calculate the deflections and when $R \geq R_{up}$ the following equation is used:

$$x = \left(\frac{R}{2\lambda^2 EI}\frac{1}{H_1 H_2}F\right) + \left(\frac{R - 12.5kN}{k_{connector}}\right)$$

With this type of construction the panel design will be limited by horizontal deflection. This design approach assumes finishes do not contribute towards stiffness or strength.

With sheathing:-

STEP 1: Calculate the polar modulus of the connector groups fixing the sheathing to the studwork frame:

$$x\ axis\ polar\ modulus = \sum x_i^2$$

$$y\ axis\ polar\ modulus = \sum y_i^2$$

STEP 2: Determine the strength of the wall panel. Once the polar modulus has been calculated the force in the x or y direction for any connector can be found:

$$F_{xi} = \frac{Rhy_i}{\sum y_i^2}$$

$$F_{yi} = \frac{Rhx_i}{\sum x_i^2}$$

Where: $h = height\ of\ panel$, $R = racking\ load$ and
$x_i\ and\ y_i\ is\ the\ distance\ to\ the\ connector\ being\ considered.$

Therefore the total force on a connector is:

$$F_i = \sqrt{F_{xi}^2 + F_{yi}^2}$$

The corner connectors will be most highly loaded and therefore their load can be checked against their strength.

STEP 3: Determine the stiffness of the wall panel using the polar modulus of the connectors. Again by assessing the corner connector the deflection under an applied load can be calculated:

$$\delta = \frac{F_{xi}}{connector\ stiffness}$$

The effects of changing stiffness of the sheathing to stud connections with increased displacement should be included.

This design process assumes that the hemp-lime and other finishes do not contribute towards the strength or stiffness as the sheathing boards are significantly stiffer.

Out-of-plane bending checks:

Without sheathing:-

STEP 1: Calculate the equivalent section made entirely from render to allow the render properties to be applied to the entire cross section. If there is a studwork frame present it should be ignored at this point.

STEP 2: Determine the bending stiffness using the render properties and geometric properties of the equivalent section. Deflections should be calculated assuming that the wall panel is spanning vertically and is simply supported. Both bending and shear deflections should be included. The total deflection:

$$\delta_{total} = \delta_b + \delta_v$$

Where bending deflection:

$$\delta_b = \frac{5wl^4}{384EI}$$

Shear deflection:

$$\delta_v = \int_0^x \frac{qS}{GA} dx$$

STEP 3: Determine the render cracking load from the modulus of rupture of the render by finding the bending moment at the point of rupture from:

$$M = \frac{\sigma_b I}{y}$$

Therefore the load that causes rupture of the render is:

$$w = \frac{8M}{l^2}$$

STEP 4: If there is a studwork frame determine the post crack stiffness and strength from the stud geometric and material properties. Shear deflections can be ignored at this stage due to the slenderness of the studs.

With sheathing:-

STEP 1: Use the partial interaction method set out in Annex B of BS EN 1995 (2004) to find the effective EI of the section.

STEP 2: Determine the bending stiffness using the effective EI. Deflections should be calculated assuming that the wall panel is spanning vertically and is simply supported. Both bending and shear deflections should be included and calculated as above for the wall panel without sheathing.

STEP 3: Determine the initial material failure using the formulas set out in Annex B of BS EN 1995 (2004) to find the element within the wall build-up which will exceed its strength first.

STEP 4: The same method used in **STEP 3** can be repeated to find subsequent elements to fail remembering to take into account the reduced section effective EI due to the first material failure.

9.4 Design example

The following example will show the design process being applied to a larger scale structure. The double height studwork wall shown in Figure 9.7 will be considered. This type of wall may be used in an industrial setting or an atrium type space in a domestic building. The wall height to be designed is 4.8m and the length is 3.6m. A 350mm thick 275kg/m^3 hemp-lime wall will be used and 50mm by 200mm C16 studs at 600mm centres will be checked. The studs will be in the centre of the wall and concentric loads will be assumed. The wall will have 15mm of render on each face. The characteristic material properties shown in Table 9.2 will be used. These are taken from Chapter 3. In the example given below the partial safety factors will be taken as 1.0.

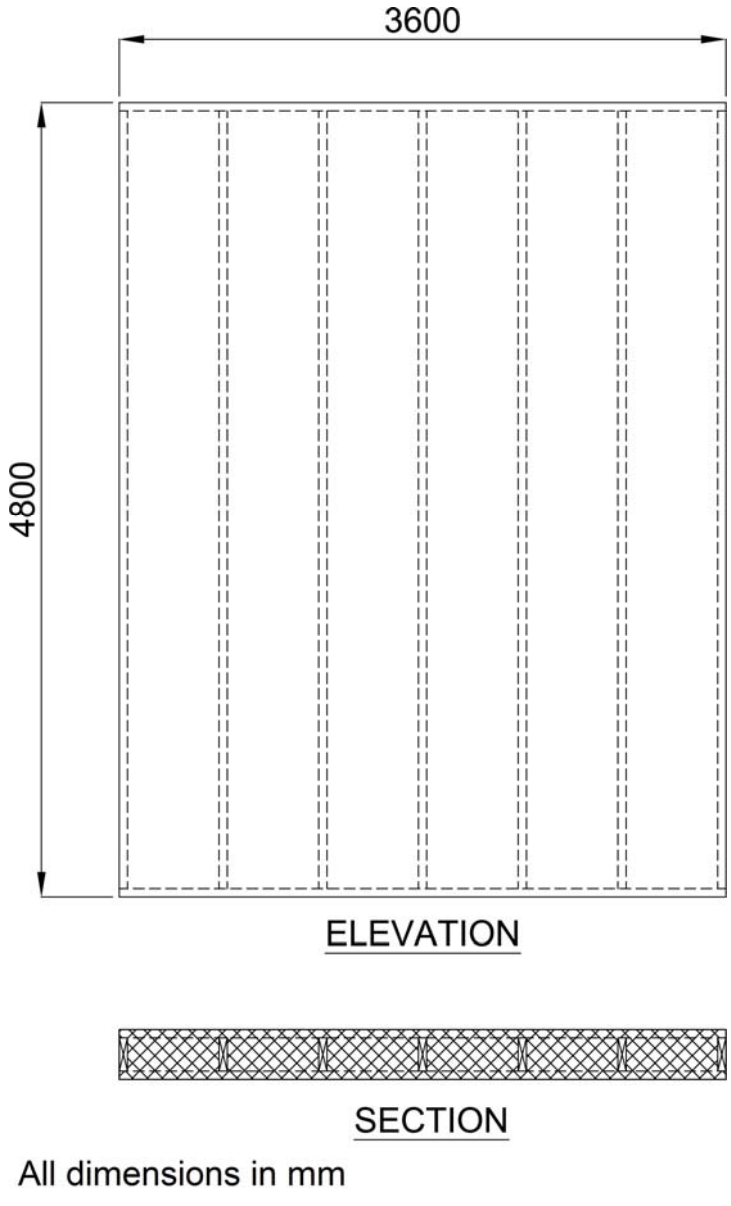

Figure 9.7 Design example wall panel

Table 9.2 Material properties for design example

Property	**Value**
Hemp-lime elastic restraint stiffness	0.007N/mm^2
Hemp-lime shear strength, σ_s	0.014N/mm^2
Hemp-lime elastic modulus, E_{HL}	14.1N/mm^2
Timber compressive strength, $\sigma_{c\ parallel}$ at 20%MC	23.2N/mm^2
Timber bearing strength, σ_b	4.6N/mm^2
Timber elastic modulus, E_T	8738N/mm^2
Render modulus of rupture	0.66N/mm^2
Render elastic modulus, E_R	1573N/mm^2

Compression resistance:

Check buckling load with elastic restraint:

Find ω, the modulus of the elastic restraint:

$\omega_{minor} = 0.007 \times 200 = \underline{1.4N/mm^2}$, $\omega_{major} = 0.007 \times 50 = \underline{0.35N/mm^2}$

Use ω to find m:

$$m^4 = \frac{\omega l^4}{\pi^4 EI}$$

$$\therefore m_{minor} = 5, m_{major} = 2$$

Use m to find P_{bu}:

$$P_{bu} = \frac{2m^2\pi^2 EI}{l^2}$$

$$P_{bu\ minor} = \frac{2 \times 5^2 \times \pi^2 \times 8738 \times 2.08 \times 10^6}{4800^2} = \underline{325.3kN}$$

$$P_{bu\ major} = \frac{2 \times 2^2 \times \pi^2 \times 8738 \times 33.3 \times 10^6}{4800^2} = \underline{703.2kN}$$

Check bursting of hemp-lime:

With 300mm thick wall and 200mm deep studs the cover will be 50mm. Using the geometry shown in STEP 2 of the compression design process above the cone area is 89208mm^2. Therefore the force required to burst the hemp-lime is:

$$F_{burst} = A_{burst} \times 0.014$$
$$F_{burst} = 89208 \times 0.014 = \underline{1249N}$$

Assuming bursting occurs when F_{burst} is equal to 2% of the axial load, the bursting axial load is:

$$P_{burst} = \frac{F_{burst}}{0.02} = \frac{1249}{0.02} = \underline{62.5kN}$$

Check stud crushing capacity:

Assume moisture content of 20% as a worst case. Therefore $\sigma_c = 23.2N/mm^2$.

$$P_{crushing} = \sigma_{c\,parallel} \times Area$$
$$P_{crushing} = (50 \times 200) \times 23.2 = \underline{232.0kN}$$

Check header and footer bearing capacity:

$$P_{bearing} = \sigma_{c\,perpendicular} \times Area$$
$$P_{bearing} = (50 \times 200) \times 4.6 = \underline{46.0kN}$$

Therefore the compression capacity is 46.0kN.

In-plane racking resistance:

Assuming double thread (DT) screw connections and following the process set out above for in-plane racking design the deflection curve shown in Figure 9.8 can be calculated.

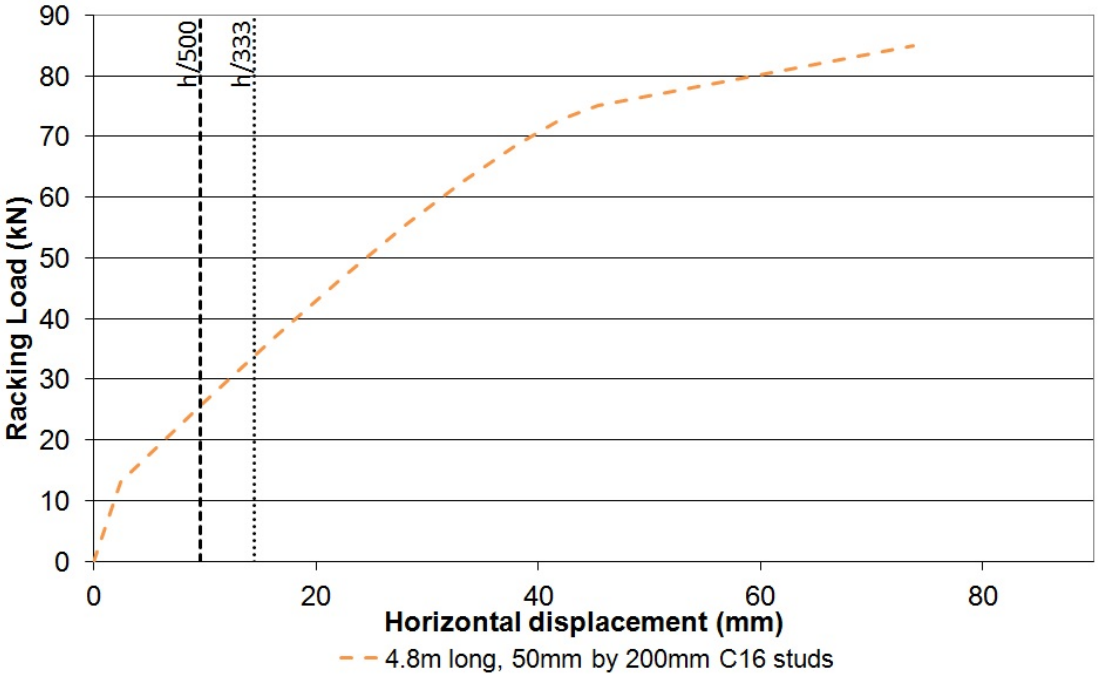

Figure 9.8 Design example racking resistance

From Figure 9.8 the serviceability racking loads are:

- When deflection is h/333 (14.4mm) $R = \underline{33.8kN}$
- When deflection is h/500 (9.6mm) $R = \underline{25.7kN}$

Out-of-plane bending:

Equivalent section second moment of area per m of wall is 765 x 10^6.

Render cracking load:

$$M_{cracking} = \frac{\sigma_{render} I}{y} = \frac{0.66 \times 765 \times 10^6}{(330/2)} = \underline{3.1kNm}$$

$$\therefore w_{cracking} = \frac{8M_{cracking}}{l^2} = \frac{8 \times 3.1}{4.8^2} = \underline{1.1kN/m^2}$$

Deflection at render cracking load:

$$\delta_{total} = \delta_b + \delta_v$$

$$\delta_{total} = \left[\frac{5 \times 1.1 \times 4800^2}{384 \times 1573 \times 802 \times 10^6}\right] + \left[2 \times \left(\frac{1.5 \times (1.1 \times 2400^2 - 2400 \times 1.1)}{18.9 \times 300000} - \frac{1.5 \times (2 \times 0^2 - 0 \times 2)}{18.9 \times 300000}\right)\right]$$

$$\delta_{total} = \underline{7.7mm}$$

$$\therefore initial\ bending\ stiffness = \frac{1.1kN}{7.7mm} = \frac{1100}{7.7} = \underline{143N/mm}$$

Therefore the wall panel shown in Figure 9.7 has the following load capacities:

- Compression – 46.0kN failing by bearing
- In-plane racking – 25.7kN at deflection of h/500
- Out-of-plane bending – Render cracking at 1.1kN/m^2 and deflection of 7.7mm.

9.5 Conclusions

This chapter has given design recommendations for use when specifying composite studwork and hemp-lime walling. The design process that has been set out should be followed during the structural design of such walls. While some of the design processes are long they are currently the most appropriate approach that most accurately matches the actual performance of this type of construction. Further details on the approaches set out in this chapter can be found in Chapter 4.

The design example has shown that the theories presented in Chapter 4 are applicable to different sized wall constructions and can be considered as generalised design methods for this type of walling.

10 Conclusions and further work

10.1 Introduction

In Chapter 1 the aims of this study were set out with the main aim being to establish if by encapsulating studwork framing in hemp-lime the structural capacity can be enhanced. Other aims were to establish theoretical models to predict the performance of the studwork frames when subjected to the three loading conditions, compressive, in-plane racking and out-of-plane bending, and to check these theoretical models against the actual experimental results.

The literature review in Chapter 2 highlighted the limited research that has taken place on hemp-lime as a material and in particular when hemp-lime is used in conjunction with studwork framing. To date there has only been three limited pieces of research on the use of hemp-lime with studwork framing, all of which concentrated on compressive loading. This thesis has increased knowledge of the material properties of hemp-lime and the performance of composite hemp-lime and timber studwork framing. The thesis has further increased the knowledge on compressive loading and created some initial knowledge when in-plane racking and out-of-plane bending loads are applied.

This chapter of the thesis draws together the conclusions made throughout the study. The conclusions will be split into experimental and theoretical sections as with the rest of the study. The possibilities for materials savings are also discussed. Finally recommendations for further work will be made.

10.2 Conclusions

10.2.1 Experimental testing

The experimental study has shown that hemp-lime increases the buckling capacity of studwork framing. When under concentric compressive loading, hemp-lime at a density of 275kg/m^2 prevents minor and major axis buckling of 38mm by 89mm C16 timber studs. Failure occurs by local crushing of the stud, but also the bearing strength of the

footer and header plates may be a limiting factor in design as the compressive strength perpendicular to the grain is lower than parallel to the grain.

The compressive tests have also shown that hemp-lime at a density of 275kg/m^3 prevents buckling of 38mm by 89mm C16 timber studs about their major axis even when subjected to an eccentric load. When the studwork frame is located in the centre of the hemp-lime the timber studs do not buckle about either axis and failure occurred by local crushing of the timber. With the studwork frame located 50mm in from the surface of the hemp-lime, both the hemp-lime and the horizontal rails restrain the studs and increase their buckling load about the major axis. With the studwork frame is on the edge of the hemp-lime, the horizontal rails also restrain the studs about their major axis and increase the buckling load.

When subjected to in-plane racking loads hemp-lime at a target dry density of 275kg/m^2 increases the racking resistance of timber studwork frames. The weakness in the structural system is the leading stud connections. When these are strengthened both the racking stiffness and strength are increased. When hemp-lime is being relied upon to provide in-plane racking resistance in a standard 2.4m long by 2.4m high wall panel with 38mm by 89mm C16 studs, the design racking resistance is equivalent to a Category 2 wall construction as detailed in BS 5268 (1996). The racking stiffness is improved significantly by the use of permanent shuttering that acts as a sheathing board such as Multi-pro boarding. With sheathing the design racking resistance is higher than Category 1 wall constructions as detailed in BS 5268 (1996).

Out-of-plane bending causes the materials in composite hemp-lime and studwork walling to interact in a complex manner. With render on each face of the hemp-lime a timber studwork frame allows continuation of load carrying capacity once the hemp-lime and render have cracked and provides some ductility to the failure of the wall panel. In this situation the hemp-lime and render increase the pre-crack stiffness of the wall and therefore the performance of the wall is reliant upon both materials.

With render on one face and Multi-pro sheathing board on the other face the bending performance of the wall panels varies depending upon the direction of the load. With the render in tension the stiffness is initially high before the render cracks. Post render

failure the stiffness reduces however due to the timber studwork frame the wall can still sustain a high and increasing load. The load increase is a result of the changing interaction between the studwork frame and the sheathing board. With the render in compression the stiffness is initially lower; however this then increases with the load and the interaction between the timber frame, hemp-lime and sheathing board develops and changes. Throughout the UK, design wind loads are generally below 1.0kN/m^2. All of the wall constructions tested are strong enough to resist this force, but care must be taken to check the serviceability criteria as cracking of finishes such as the render may dominate the design.

The main aim of the study set out in Chapter 1 has been met through experimental testing. The level of enhancement hemp-lime provides to the structural capacity of studwork framing and the failure modes for each type of loading have been established.

10.2.2 Theoretical analysis

The theoretical study has shown that the stiffness and strength of composite hemp-lime and studwork frame walls can be predicted when subjected to compressive, in-plane racking and out-of-plane bending loads. When a stud is loaded in compression the buckling load can be predicted by treating the hemp-lime as an elastic foundation. By checking the buckling load in this way and also checking the crushing capacity of the stud and the bearing capacity of the footer rail the failure load can be taken as the lowest of the three.

The study has also shown that under in-plane racking loads the hemp-lime can be treated in a similar manner as an elastic foundation onto which the cantilevering studs deform. The stiffness of a composite hemp-lime and studwork frame wall can be predicted using this theory. The strength cannot be found in this way, however as serviceability deflection will dominate the design limits and the strength is not seen as a problem. When a wall is constructed with a sheathing board the study has shown that both the stiffness and strength can be found by using the polar modulus of the sheathing to stud connection group as this will be revisiting the racking loads.

With applied out-of-plane bending loads the complex interactions between the different materials have been theoretically analysed by considering the slip modulus of the various connections between the materials. The hemp-lime and render can be assumed to fully interact. The sheathing board to stud and the stud to hemp-lime connections are dependent upon the connection stiffness. By considering the different levels of interaction the peak load and stiffness can be predicted. When the wall section is rendered on both faces the transform section can be used and when the wall is rendered on one face and has sheathing board on the other face a combination of transform section and the partial interaction theory in BS EN 1995 (2004) can be used.

The theoretical models for compression loading and out-of-plane bending have been shown to be generalised models that allow the performance to be predicted for any size stud or wall construction. The theoretical models for in-plane racking have also been shown to allow this when there is no sheathing board. The theory used when there is a sheathing board could be applied to larger structures, but sheathing boards are only manufactured at 2400mm high and therefore if these were to be used in a larger structure there would be additional framing required to support all of the edges.

The theoretical models used in this study to predict the performance of the composite wall panels have all predicted the actual stiffness and ultimate failure loads. If these models are to be used for the design of this type of wall structure suitable material and loading factors of safety would need to be applied by the design engineer.

Throughout this study hemp-lime and binder from one manufacturer has been used at one density. The basic principles shown throughout the experimental and theoretical investigations can be applied to any form of studwork framing with any type and density of hemp-lime. However the differences in material properties when using different binders, shiv or density need to be considered if the results of this study are to be applied to different materials.

10.3 Material savings

In Chapter 1 one of the drivers for this study was the possibility of reducing the amount of material used in this type of construction and improving its efficiency. The study has

shown that this can be achieved through the removal of the need for sheathing board as the hemp-lime can provide restraint to the studs under both compressive and in-plane racking loads.

With the necessity for sheathing board removed further material saving are possible. In conventional studwork walling the studs are spaced to allow sheathing boards to be easily attached. Therefore the spacing is limited by the sheathing dimensions, typically 1200mm wide in the UK, and as a result the studs are spaced at 400mm or 600mm centres. With this requirement removed the studs can be spaced at the centres necessary to resist the applied loads, for example at 800mm centres. This would lead to a significant saving of 25% in stud materials.

10.4 Recommendations for further work

This study has shown that hemp-lime does enhance the structural capacity of studwork framing; however there is still further work that could be undertaken. The compressive performance when there is sheathing board fixed to the studs is one area where further research could be undertaken. The sheathing would have a beneficial effect on the minor axis buckling load, however this may not make any difference to the overall performance as this study has shown that the hemp-lime prevents minor axis buckling. Further work is also needed to fully understand the bursting of the hemp-lime when there is limited cover over the studs. While this has been investigated for 50mm cover during this study detailed information about the failure modes are not known or the behaviour when there is a different amount of cover. The addition of a render skin may affect the performance as well.

Further investigation of bursting of the hemp-lime would also require further research on the tensile and shear properties of hemp-lime. These were not established during this study, but they may be critical in understanding the effects of bursting. Due to the low strength and stiffness of hemp-lime these properties could be difficult to obtain with accuracy and may require considerable work in order to do so.

During this study the racking performance has been investigated with and without sheathing boards, however the performance of a completed wall has not been studied. If

the external finish was render then this could enhance the racking performance as it may increase the stiffness of the wall and the render will reduce the deformation in the hemp-lime. Other finishes such as rain screen cladding could be investigated, but they are unlikely to have an effect on the structural performance.

Further investigation is required when a composite wall panel with studwork framing, hemp-lime and sheathing board is subjected to out-of-plane bending and the sheathing board is in tension. Under this load case the interaction between the hemp-lime and studs and the studs and sheathing needs further investigation as the increasing stiffness displayed during the experimental study is not fully understood. Another aspect of out-of-plane bending loading that could potentially be investigated further is when vertical compressive loads are applied as well as out-of-plane loads. The addition of vertical loads could increase the out-of-plane deflections and therefore reduce the apparent out-of-plane stiffness. Different theoretical models would also need to be developed alongside any further experimental work with different wall constructions or load cases.

During this study door and window openings have been largely ignored. As suggested in Chapter 4 these could be considered by simply designing the wall panels adjacent to the openings to resist the loads applied to the opening area. A more thorough approach may result in a more efficient design and this is an area in which further investigations are necessary.

There are some construction issues that could be investigated such as the voids forming around the horizontal rails due to settlement when the hemp-lime is still wet. These not only affect the mechanical performance of the wall panels but will also affect the thermal performance at those locations.

Throughout this study only one specimen of each type of wall construction and each load case has been tested as the size of the specimens and limitations on time did not allow for repeat testing. During construction and testing of the specimens care was taken to minimise the effects of having single specimens and this should not have affected the results. Therefore further work could simply repeat the testing undertaken in this study to establish if the results are consistent and if there is any variation in performance.

References

Arnaud, L. (2000). Mechanical and thermal properties of hemp mortars and wools: experimental and theoretical approaches. *Bioresource Hemp 2000 and other fibre crops.* Wolfsburg. Nova Institut, Hürth, Germany.

Arnaud, L. & Gourlay, E. (2012). Experimental study of parameters influencing mechanical properties of hemp concretes. *Construction and Building Materials,* 28**,** 50-56.

British Lime Association. (2012). *History of Lime* [Online]. Available: http://www.britishlime.org/edu_facts01.php [Accessed 02/03/2012 2012].

Baird, J.A. & Ozelton, E.C. (1984). *Timber designer's manual 2nd ed.,* Oxford: BSP Professional Books.

Bevan, R., Woolley, T., Pritchett, I., Carpenter, R., Walker, P. & Duckett, M. (2008). Hemp Lime Construction: a guide to building with hemp lime composites. IHS BRE Press.

BRE (2002). Final report on the construction of the hemp houses at Haverhill, Suffolk. *In:* Yates (ed.). Watford: Building Research Establishment.

BS 373. (1957). *Methods of testing small clear specimens of timber.* British Standards Institute (BSI)

BS 5268-6.1. (1996). *Structural use of Timber - Part 6: Code of Practice for Timber Frame Walls – Section 6.1: Dwellings not Exceeding Seven Storeys.* British Standards Institute (BSI)

BS 5950-5. (1998). *Structural Use of Steelwork in Buildings - Part 5: Code of Practice for Design of Cold Formed Thin Gauge Sections.* British Standards Institute (BSI)

BS EN 594. (1996). *Timber Structures – Test Methods – Racking strength and stiffness of timber frame wall panels.* British Standards Institute (BSI)

BS EN 594. (2011). *Timber Structures – Test Methods – Racking strength and stiffness of timber frame wall panels.* British Standards Institute (BSI)

BS EN 1015-11. (1999). *Methods of test for mortar for masonry - Part 11: Determination of flexural and compressive strength of hardened mortar.* British standards Institute (BSI)

BS EN 1052-2. (1999). *Methods of test for masonry - Part 2: Determination of flexural strength.* British standards Institute (BSI)

BS EN 1995-1.1. (2004). *Eurocode 5 – Design of timber structures – Part 1-1: General – Common rules and rules for buildings.* British Standards Institute (BSI)

CERAM (2009a). Test Report: Racking tests in accordance with BS EN 594:1996 on 2.4m x 2.4m timber frame panels with Hemcrete In-fill. Stoke-on-Trent.

CERAM (2009b). Test Report: Racking tests in accordance with BS EN 594:1996 on 2.4m x 2.4m timber frame panels with Resistant Multi-Pro Xs sheathing. Stoke-on-Trent.

Cerezo, V. (2005). *Propriétés mécaniques, thermiques et acoustiques d'un matériau à base de particules végétales: approche expérimentale et modélisation théorique.* PhD, Ecole Nationale des Travaux Publics de l'Etat.

Collet, F., Bart, M., Serres, L. & Miriel, J. (2008). Porous structure and water vapour sorption of hemp-based materials. *Construction and Building Materials,* 22**,** 1271-1280.

Department for Business, Enterprise and Regulatory Reform. (2008). *Strategy for sustainable construction.* Department for Business, Enterprise and Regulatory Reform

Department for Communities and Local Government. (2007). *Building a greener furture: policy statement.* Communities and Local Government Publications

de Bruijn, P.B. (2012). *Material properties and full-scale rain exposure of lime-hemp concrete walls.* Doctor of Philosophy, Swedish University of Agricultural Sciences.

de Bruijn, P.B., Jeppsson, K.H., Sandin, K. & Nilsson, C. (2009). Mechanical properties of lime-hemp concrete containing shives and fibres. *Biosystems Engineering,* 103**,** 474-479.

Department for Environment Food and Rural Affairs. (2007). *Consultation on site waste management plans for the construction industry.* Department for Environment Food and Rural Affairs

Department for Environment Food and Rural Affairs. (2012). *Construction and demolition waste, England* [Online]. Available: http://www.defra.gov.uk/statistics/environment/waste/wrfg09-condem/ [Accessed 31/05/2012].

Department for Transport. (2009). *Analytical Annex, The UK Low Carbon Transition Plan.* Department for Transport

Doudak, G. & Smith, I. (2009). Capacities of OSB-sheathed light-frame shear-wall panels with or without perforations. *Journal of Structural Engineering,* 135**,** 326.

Dutton, M. (2009). *Preliminary Analysis of the Structural Benefits on Hempcrete Filled Timber Wall Stud Frames.* Queen's University.

Eires, R. & Jalali, S. (2005). Not conventional materials for a sustainable construction: a bio-construction system reinforced with cellulose fibres. *Portuguese Materials Society Meeting, 12th International Materials Symposium.* Aveiro.

Elfordy, S., Lucas, F., Tancret, F., Scudeller, Y. & Goudet, L. (2008). Mechanical and thermal properties of lime and hemp concrete ("hempcrete") manufactured by a projection process. *Construction and Building Materials.,* 22**,** 2116-2123.

Enjily, V. (2001). The Performance of Timber Structures, Elements and Components. *Cost Action E24.* Denmark.

European Union - Directorate - General for Agriculture and Rural Development. (2012). *Agriculture in the European Union - Statistical and economic information 2011.* European Union - Directorate - General for Agriculture and Rural Development

Eurofortech (1995). *Timber Engineering: STEP 1: Basis of Design, Material Properties, Structural Components and Joints,* Chapters B6 and B13, Almere: Centrum Hout.

Evrard, A. (2002). Hemp concretes - A synthesis of physical properties. *In:* Evrard (ed.). Saint Valérien: French Association Construire en Chanvre.

Evrard, A. (2006). Sorption behaviour of Lime-Hemp Concrete and its relation to indoor comfort and energy demand. *The 23rd Conference on Passive and Low Energy Architecture.* Geneva, Switzerland.

Evrard, A. & De Herde, A. (2005). Bioclimatic envelopes made of Lime and Hemp Concrete. *Proceeding of CISBAT 2005.* Ecole Polytechnique Fédérale de Lausanne, Switzerland.

Evrard, A. & De Herde, A. (2010). Hygrothermal Performance of Lime-Hemp Wall Assemblies. *Journal of Building Physics,* 34**,** 5-25.

Evrard, A., De Herde, A. & Minet, J. (2006). Dynamical interactions between heat and mass flows in Lime-Hemp Concrete. *Third International Building Physics Conference.* Concordia University, Canada and International Association of Building Physics.

Griffiths, D.R. (2010). *RE: (r.griffiths@surrey.ac.uk), 22 July 2010. BS 5268 part 6.1. Email to C. D. Gross (c.d.gross@bath.ac.uk).*

Gross, C., Fovargue, J., Homer, P., Mander, T., Walker, P. & White, C. (2009). Lateral Stability of Prefabricated Straw Bale Housing. *Sustainability in Energy and Buildings***,** 147-154.

Helmich, R. (2008). *The Structural Contribution of Hemp-Lime.* MEng, University of Bath.

Hemp Technology. (2010). *Hemp Technology Ltd: Products – Hemp and Lime Construction* [Online]. Available: www.hemcore.co.uk/hemcrete.htm [Accessed 05/06/2010 2010].

Hendriks, C.A., Worrell, E., De Jager, D., Blok, K. & Riemer, P. (1998). Emission reduction of greenhouse gases from the cement industry. *4th International Conference on Greenhouse Gas Technologies.* Interlaken, Switzerland.

Hetényi, M. (1946). *Beams on elastic foundation - Theory with applications in the fields of civil and mechanical engineering,* London: Oxford University Press.

Hirst, E.A.J. (unpublished). *Characterising hemp-lime composite building materials.* University of Bath.

Hirst, E.A.J., Walker, P., Paine, K.A. & Yates, T. (2012). Characteristics of low-density hemp-lime building materials. *Proceedings of the ICE-Construction Materials,* 165**,** 15-23.

Holmes, S. & Wingate, M. (1997). *Building with lime: a practical introduction*: Intermediate Technology.

Hustache, Y. & Arnaud, L. (2008). Overview of the State of Knowledge of Hemp Concretes and Mortars. France.

IStructE & TRADA (2007). Manual for the design of Timber Building Structures to Eurocode 5. London.

Kallsner, B. & Girhammar, U.A. (2009a). Analysis of fully anchored light-frame timber shear walls-elastic model. *Materials and Structures,* 42**,** 301-320.

Kallsner, B. & Girhammar, U.A. (2009b). Plastic models for analysis of fully anchored light-frame timber shear walls. *Engineering Structures,* 31**,** 2171-2181.

Kermani, A. & Hairstans, R. (2006). Racking performance of structural insulated panels. *Journal of Structural Engineering,* 132**,** 1806.

King, B. (2006). *Design of straw bale buildings: the state of the art*: Green Building Pr.

Lawrence, M. (2009). A Review of the State of the Art of Hemp-lime, Theory, Practice and Current Research. Bath: BRE CICM.

Lawrence, M., Drinkwater, L., Heath, A. & Walker, P. (2009). Racking shear resistance of prefabricated straw-bale panels. *Proceedings of the Institute of Civil Engineers: Construction Materials,* 162**,** 133-138.

Lime Technology. (2010a). *Baumit Fibrous Lightweight Render FL68 Datasheet* [Online]. Available: http://www.limetechnology.co.uk/pdfs/Baumit_FL68_Fibrous_Lightweight_Render.pdf [Accessed 5/04/2012 2012].

Lime Technology. (2010b). *Tradical Hemcrete Product Data Sheet* [Online]. Available: http://www.limetechnology.co.uk/index.htm?pages/hemcrete.php [Accessed 18/06/2010 2010].

Magniont, C., Escadeillas, G., Coutand, M. & Oms-Multon, C. (2012). Use of plant aggregates in building ecomaterials. *European Journal of Environmental and Civil Engineering,* 16**,** S17-S33.

Marxhausen, P.D. & Stalnaker, J.J. (2006). Buckling of conventionally sheathed stud walls. *Journal of structural engineering,* 132**,** 745.

Mukherjee, A. (2012). *Structural benefits of hempcrete infill in timber stud walls.* Master of Applied Science thesis, Queen's University, Kingston, Canada.

Murphy, F., Pavia, S. & Walker, R. (2010). An assessment of some physical properties of lime-hemp concrete. *In:* Nualláin, Walsh, West, Cannon, Caprani & McCabe (eds.) *BCRI Bridge Infrastructure Concrete Research Ireland.* University of Cork.

NA to BS EN 1995-1.1. (2004). *UK National annex to Eurocode 5: Design of timber Structures - Part 1.1: General - Common rules and rules for buildings.* British Standards Institute (BSI)

Nguyen, T., Picandet, V., Amziane, S. & Baley, C. (2009). Influence of compactness and hemp hurd characteristics on the mechanical properties of lime and hemp concrete. *European Journal of Environmental and Civil Engineering,* 13**,** 1039-1050.

Pritchett, I. (2009). Hemp and Lime Composites in Sustainable Construction. *In:* Walker, Ghavami, Paine, Heath, Lawrence & Fodde (eds.) *11th International Conference on Non-conventional Materials and Technologies.* Bath.

Resistant Building Products. (2012). *Resistant Multi-pro XS Datasheet* [Online]. Available: http://www.resistant.co.uk/downloads.php [Accessed 10/04/2012 2012].

Robertson, R.A. & Griffiths, D.R. (1981). Factors Affecting The Racking Resistance of Timber Framed Panels. *Structural Engineer-Part B,* 59**,** 49-63.

Rosowsky, D.V., Yu, G. & Bulleit, W.M. (2005). Reliability of light-frame wall systems subject to combined axial and transverse loads. *Journal of Structural Engineering,* 131**,** 1444.

Shea, A., Lawrence, M. & Walker, P. (2012). Hygrothermal performance of an experimental hemp–lime building. *Construction and Building Materials,* 36**,** 270-275.

Timoshenko, S.P. & Gere, J.M. (2009). *Theory of elastic stability - 2nd ed.,* Mineola: Dover Publications.

United Nations Framework Convention on Climate Change. (2012). *Kyoto Protocol* [Online]. Available: http://unfccc.int/kyoto_protocol/items/2830.php [Accessed 31/08/2012].

Winkel, M. & Smith, I. (2010). Structural behavior of wood light-frame wall segments subjected to in-plane and out-of-plane forces. *Journal of Structural Engineering,* 136**,** 826.

Woolley, T. (Year). The role of low impact building materials in sustainable construction: The potential for hemp. *In:* Sustainable Building Conference, 2004 Stellenbosch, South Africa.

Appendix 1 – Published papers

ICE Construction materials journal paper

Blank page